


This item was submitted to Loughborough University as a PhD thesis by the author and is made available in the Institutional Repository (<https://dspace.lboro.ac.uk/>) under the following Creative Commons Licence conditions.




creative commons
COMMONS DEED


Attribution-NonCommercial-NoDerivs 2.5


You are free:

- to copy, distribute, display, and perform the work

Under the following conditions:

 **Attribution.** You must attribute the work in the manner specified by the author or licensor.


 **Noncommercial.** You may not use this work for commercial purposes.

 **No Derivative Works.** You may not alter, transform, or build upon this work.

- For any reuse or distribution, you must make clear to others the license terms of this work.
- Any of these conditions can be waived if you get permission from the copyright holder.

Your fair use and other rights are in no way affected by the above.

This is a human-readable summary of the [Legal Code \(the full license\)](#).

[Disclaimer](#) 

For the full text of this licence, please go to:
<http://creativecommons.org/licenses/by-nc-nd/2.5/>

BLOSC no:- DX 223247



Pilkington Library

Author/Filing Title SAW

Vol. No. Class Mark T

**Please note that fines are charged on ALL
overdue items.**

OPEN STAFF COPY

FOR REFERENCE ONLY

0402399226



**PHASE INVERSION IN POLYURETHANE
PREPOLYMER-WATER DISPERSIONS**

by


Lin Kiat Saw

A Doctoral Thesis

Submitted in partial fulfilment of the requirements
for the award of Doctor of Philosophy of Loughborough University

August 2000

© by Lin Kiat Saw (2000)

 Loughborough University Public Library
Date Mar 01
Class
Acc No. 040239922

M0003120 LB

Summary

Aqueous polyurethane (PU) colloids, like many other water-borne polymer colloids, have become an increasingly important class of materials in the surface coating industry. Three processing stages, the pre-dispersion, dispersion and post-dispersion stages, are generally involved in the production of aqueous PU colloids. However, existing researches have neglected the importance of the dispersion stage. The present study aims to develop better understanding of the dispersion stage during the production of aqueous PU colloids. Non chain-extendable PU pre-polymer (PUP) is used to enable independent study of the dispersion stage and the phase inversion process is chosen due to its widespread industrial usage.

Valid drop size characterisation techniques and phase inversion detection methods have been developed in this project. Three different dispersion regions have also been identified by changing the ionic group content of PUP. Each dispersion region is associated with a particular dispersion type. Those are (1) Stable aqueous emulsions that contain small PUP-in-water drops. They were produced using PUP with more than 0.2 mmole/g of ionic groups. (2) Aqueous PUP colloids with 0.05 ~ 0.2 mmole/g of ionic groups. These emulsions contain a mixture of drop structures, including simple drops and different multiple drops. (3) Aqueous PUP dispersions containing less than 0.05 mmole/g of ionic groups. These dispersions are not stable and the resultant dispersions separated when agitation was stopped. Modified phase inversion maps are introduced to represent the occurrence of all three dispersion regions. The modified phase inversion maps are partly analogous to those of conventional non-ionic-surfactant-water (nSOW) systems. The three dispersion regions have also been “reproduced” successfully using external surfactants as substitutes for the internal stabilising groups. A new catastrophic phase inversion mechanism is proposed to explain the existence of all three dispersion regions. Other variables studied during this project include different neutralising agents, different amount of carboxylic acid groups, operating temperatures and material addition rates.

In conclusion, this project shows that the phase inversion process is a feasible route for producing aqueous polymer dispersions with little or no added external surfactants. Stable PUP-W dispersions can also be produced below the minimum ionic group content reported in existing literatures.

Acknowledgement

I wish to express my most sincere gratitude to Professor B.W. Brooks for giving me the opportunity to carry out this research, along with his invaluable supervision and proof-readings my less than perfect English. Special thanks are also due to the industrial and academic partners of this project for their useful suggestions and discussions concerning various aspects of this research. Thanks to Professor K.J. Carpenter and Dr. N. George from Zeneca Agrochemicals; Dr. D.V. Keight, Dr. K. Tracey and Dr. T. Annable from Avecia; Professor R.V. Calabrese and Mr. S. Phongikaroon from the Department of Chemical Engineering in the University of Maryland. The financial support by Zeneca is also gratefully appreciated.

My grateful appreciation is also extended to Professor M. Streat, the head of Department of Chemical Engineering in Loughborough University and to Professor B.A. Buffham, my director of research. It is also pleasing to acknowledge the help of the following members of staff: Mr. A. Milne, Mr. F. Page, Mr. S. Graver and Mr. J.S. Bates. My thanks are also due to other technical and administrative staff of the Department of Chemical Engineering for their help throughout the project. The following researchers in the Department of Chemical Engineering, Dr. M. Zerfa, Dr. S. Sajjadi, Dr. S. Hashim and Dr. F. Xie, also deserve a word of thanks for enlightening my knowledge in various aspects of liquid-liquid dispersions and research methodology.

Last, but not least, I would also like to express my grateful thanks to my beloved parents and sisters as well as Chia Ni for their immense mental supports.

Contents

Summary**Acknowledgements**

Contents	i
List of figures and tables	vii
Abbreviations and nomenclatures	xiv
Chapter 1 – Introduction and objectives	1
1.1 General introduction	1
1.2 Introduction to this project	4
1.3 Objectives	4
Chapter 2 – Literature survey	6
<u>“Aqueous polymer colloids”-related literature survey</u>	
2.1 Chemistry of polyurethane (PU) and PU ionomer	6
2.1.1 Building block of PU molecules	6
2.1.2 PU ionomers	7
2.2 Production of aqueous PU ionomer colloids	8
2.2.1 Different manufacturing processes	8
2.2.2 The dispersion stage	9
2.3 Some properties of polymer latices	12
2.3.1 Particle size and its distribution	13
2.3.2 Viscosity of final emulsion products	14
2.3.3 Particle morphology	15
2.3.4 Stability of emulsion	15

2.4	Factors affecting the properties of polymer latex	17
2.5	Chemical factors	18
2.5.1	Stabilising groups	18
2.5.2	Counterions	20
2.5.3	Degree of neutralisation (DN)	21
2.5.4	Molecular weight of polyol	22
2.6	Processing and solution factors	23
2.6.1	Water addition rate	24
2.6.2	Phase inversion temperature	24
2.6.3	Solvent content	24
<u>“Liquid-liquid dispersions”-related literature survey</u>		
2.7	Liquid-liquid dispersion	25
2.8	Direct dispersion	26
2.8.1	Hydrodynamic mechanism and forces controlling drop break-up	26
2.8.2	Kolmogoroff theory of local isotropy	28
2.8.3	Maximum and minimum stable drops in turbulent liquid-liquid dispersions	29
2.8.4	Other aspects of liquid-liquid dispersions in turbulent stirred tank	32
2.9	Phase inversion	34
2.9.1	Transitional phase inversion	36
2.9.2	Catastrophic phase inversion	37
2.9.3	Other aspects of phase inversion	41
2.10	Different type of emulsions and drop structures	43
2.10.1	Different type of emulsions	43
2.10.2	Multiple emulsions	43
Chapter 3 – Experimental apparatus		46
3.1	Dispersion experiments	46
3.1.1	Dispersion section	46
3.1.2	Reservoir section	47

3.2	Droplet characterisations	51
3.2.1	SEM – freeze fracture technique	51
3.2.2	Optical microscope unit	52
3.2.3	LALLS size analyser	53
3.3	Others	53
3.3.1	Viscometer 1	53
3.3.2	Viscometer 2	54
3.3.3	Modified densitometer	54
 Chapter 4 – Materials		59
4.1	Pre-polymers	59
4.1.1	Backbone of PUp samples	60
4.1.2	Amount of functionalised PUp molecules	60
4.1.3	Other physical properties	61
4.2	PUp blends	63
4.3	External surfactants	64
4.3.1	Non-ionic surfactants	64
4.3.2	Anionic surfactants	64
4.4	Others	65
 Chapter 5 - Experimental methods		66
5.1	Dispersion experiments	66
5.1.1	Catastrophic phase inversion experiments	66
5.1.2	Transitional phase inversion experiments	69
5.2	Droplet size measurement	70
5.2.1	Operation of optical microscope unit	71
5.2.2	SEM-freeze fracture technique	71
5.2.3	LALLS size analyser	74

5.3	Method for analysing drop size data	75
5.3.1	Data classification	75
5.3.2	Drop size distribution	76
5.3.3	Mean diameters	77
5.3.4	Useful graphs	78
5.3.5	Error estimation	78
5.3.6	C++ programmes	80
5.3.7	Malvern Mastersizer	82
<u>Specific experimental procedures</u>		
5.4	Methods for the detection of phase inversion points	82
5.5	Effect of ionic group content on PWCPI process	83
5.6	External viscosity measurements	84
5.7	Different types of transitional phase inversion processes	85
5.8	Catastrophic phase inversion mechanism study	86
5.9	Effect of stabilising groups	87
5.9.1	PWCPI experiments	87
5.9.2	Transitional phase inversion experiments	88
5.10	Effect of some processing factors	89
5.10.1	Viscosity of the initial continuous phase	89
5.10.2	Configuration of the dispersion vessel	92
5.11	External surfactant-related studies	93
Chapter 6 - Results and discussion		96
6.1	Preliminary drop size studies	96
6.1.1	Arithmetic progression method vs. Geometric progression method	96
6.1.2	Optimum droplet data	97
6.1.3	Number of bins required	98
6.1.4	Curve fitting using a log-normal distribution function	100
	Conclusions	100

6.2	Methods for the detection of phase inversion points	105
6.2.1	Conductivity graphs	105
6.2.2	Design of conductivity probe(s)	106
6.2.3	Addition of KCl	106
6.2.4	Torque changes graphs	106
	Conclusions	107
6.3	Effect of ionic group content on PWCPI process	108
6.3.1	Catastrophic phase inversion map	108
6.3.2	Region I (RI) – High ionic group content	110
6.3.3	Region II (RII) – Moderate ionic group content	111
6.3.4	Region III (RIII) – Low ionic group content	113
	Conclusions	114
6.4	External viscosity measurements	120
6.4.1	Results	120
6.4.2	Power law	121
6.4.3	Changing rheological properties	122
6.4.4	Using FSTC agitator to detect the phase inversion point	123
	Conclusions	125
6.5	Different types of transitional phase inversion processes	129
6.5.1	Transitional phase inversion points of RIITI process	129
6.5.2	Other features of RIITI process	131
6.5.3	Transitional phase inversion points of RIITI process	135
	Conclusions	138
6.6	Catastrophic phase inversion mechanism	147
6.6.1	Results	147
6.6.2	Zone 1 (Z1) and zone 2 (Z2)	149
6.6.3	At the phase inversion point	150
6.6.4	Zone 3 (Z3)	154
6.6.5	Nomenclature for multiple emulsions	155
6.6.6	Drop size studies	156
	Conclusions	159

6.7	Effect of stabilising groups	169
6.7.1	Carboxylate groups ionised by sodium cations	169
6.7.2	Effect of free carboxylic acid groups	171
	Conclusions	174
6.8	Effect of some processing factors	178
6.8.1	Changing viscosity	178
6.8.2	Configuration of the dispersion vessel	178
	Conclusions	178
6.9	External surfactants-related PUp-W dispersions	180
6.9.1	Non-ionic surfactant – Changing HLB number	180
6.9.2	Non-ionic surfactant – Effect of temperature	182
6.9.3	Different HLB number – operating temperature zone	184
6.9.4	Anionic surfactant	185
	Conclusions	187
	Chapter 7 – General conclusions	191
	Chapter 8 - Future work	194
	Bibliography	198
	Appendixes	208
Appendix I	Viscosity measurements	208
Appendix II	Example calculations	215
Appendix III	Supplement for drop size characterisation	219

List of figures and tables

List of figures

- Figure 2.1. Schematic representation of the pre-polymer mixing process [reproduced from Zeneca (1998)].
- Figure 2.2. Viscosity variation during water additions.
- Figure 2.3. Possible particle morphology of aqueous polymer ionomer colloids.
- Figure 2.4. Particle size and emulsion viscosity as a function of DMPA content.
- Figure 2.5. Specific surface area vs. DMPA concentration [reproduced from Satguru et al.(1994)].
- Figure 2.6. Particle size and emulsion viscosity vs. DN at two MDEA contents [reproduced from Lee and Kim (1995)].
- Figure 2.7. Some of the agitators used in industry.
- Figure 2.8. Phase inversion map for a nSOW system.
- Figure 2.9. Schematic representation of transitional inversion from $W/O_m \rightarrow O/W_m$.
- Figure 2.10. Classification of different multiple drops in multiple emulsions.
- Figure 3.1. Set-up of the dispersion section.
- Figure 3.2. Fittings through the five-neck glass vessel cover.
- Figure 3.3. Schematic diagram of the 4-bladed Rushton type turbine.
- Figure 3.4. Equipment for conductivity measurement: (a) Single sensor probe; (b) Double sensor probe; (c) Electric circuit of the conductivity meter; (d) Schematic diagram of the conductivity meter.
- Figure 3.5. Full view of the SEM machine.
- Figure 3.6. Other equipment of the SEM – freeze fracture technique.
- Figure 3.7. Schematic diagram of the optical microscope.

- Figure 3.8. Full view of the optical microscope unit.
- Figure 3.9. Full view of the LALLS size analyser.
- Figure 3.10. Schematic diagram of equipment set-up for the falling ball method.
- Figure 3.11. Schematic diagram of the modified densitometer.
- Figure 5.1. Flow chart of catastrophic phase inversion experiments.
- Figure 6.1. Number and volumetric distribution curves plotted using different methods.
- Figure 6.2. Determination of N_T required.
- Figure 6.3. Effect of N_T on calculated d_{32} and d_{10} .
- Figure 6.4. Effect of N_T on calculated GSD and δ .
- Figure 6.5. Volumetric distribution curves plotted using different N_T .
- Figure 6.6. Number distribution curves plotted using different N_{bin} .
- Figure 6.7. Volumetric distribution curves plotted using different N_{bin} .
- Figure 6.8. Fitting data using log-normal distribution function [equation (6-1)].
- Figure 6.9. Conductivity graphs of (A) conventional phase inversion processes with transient conductivity response [reproduced from Pacek et al. (1994b)]; (B) experiments EX54/1 to EX54/3.
- Figure 6.10. Torque changes graph of experiment EX54/1.
- Figure 6.11. Catastrophic phase inversion map for PUp-W dispersions.
- Figure 6.12. Torque changes and conductivity graphs of PWCPI experiments.
- Figure 6.13a. Optical microscopic image of emulsions in the RIW region: P_1/W_C drops are too small to be seen clearly.
- Figure 6.13b. SEM image of emulsions in the RIW region: Small P_1/W_C drops.
- Figure 6.14a. Optical microscopic image of emulsions in the RIIW region: A mixture of drop structures can be seen clearly.
- Figure 6.14b. SEM image of emulsions in the RIIW region: Showing the complex multiple drop structures.

- Figure 6.14c. SEM image of emulsions in the RIW region: Showing the existence of small drops $\sim 0.8 \mu\text{m}$.
- Figure 6.15. Different drop structures of emulsions in the RIW region: (a) Simple P_1/W_C drops; (b) Multiple $W_1/P_1/W_C$ drops with (i) large W_1 drops and (ii) small W_1 drops; and (c) Multiple $P_2/W_1/P_1/W_C$ drops.
- Figure 6.16. Optical microscopic image of W_1/P_1 drops in the separated opaque substance of emulsions in the RIW region.
- Figure 6.17. Conductivity and torque changes graphs of EX56/1 and EX56/2.
- Figure 6.18. Viscosity – spindle rotating speed relationship for EX56/1 and EX56/2 (using Brookfield viscometer).
- Figure 6.19. Comparison of measured viscosity (dots) of S3 and S4 of EX56/1 to viscosity predicted using equation (6-3) (lines).
- Figure 6.20. Comparison of measured viscosity (dots) of S3 and S4 of EX56/2 to viscosity predicted using equation (6-3) (lines).
- Figure 6.21. Viscosity – water content relationship at 1 rpm and 500 rpm for EX56/2.
- Figure 6.22. The path of RIIT process.
- Figure 6.23. Torque changes and conductivity graphs of EX57/2.
- Figure 6.24. SEM image of RIIT experiment: After all water addition.
- Figure 6.25. SEM image of RIIT experiment: One aliquot before phase inversion.
- Figure 6.26. SEM image of RIIT experiment: Immediately after phase inversion.
- Figure 6.27. Volumetric distributions at different ionic group contents.
- Figure 6.28. Relationships of d_{32} , δ and a with the ionic group content.
- Figure 6.29a. The path of RIIT process.
- Figure 6.29b. Torque changes and conductivity graphs of EX57/5.
- Figure 6.30. SEM image of RIIT experiment: Before TEA addition.
- Figure 6.31. SEM image of RIIT experiment: Before complete transitional phase inversion.

- Figure 6.32. SEM image of RIITI experiment: After complete transitional phase inversion.
- Figure 6.33. Complete phase inversion map for TEA-neutralised PUp-W dispersions.
- Figure 6.34. Torque changes and conductivity graphs of experiment EX58.
- Figure 6.35. SEM image of sample EX58/S1.
- Figure 6.36. SEM image of sample EX58/S2.
- Figure 6.37. SEM image of sample EX58/S3: (a) pseudo- P_1/W_C drop; (b) pseudo- $W_1/P_1/W_C$ drop; and (c) pseudo- $P_2/W_1/P_1/W_C$ drop.
- Figure 6.38. Enlarged SEM image of sample EX58/S3.
- Figure 6.39. SEM image of sample EX58/S4.
- Figure 6.40. SEM image of sample EX58/S5.
- Figure 6.41. SEM image of sample EX58/S11.
- Figure 6.42. Events occurring during the PWCPI process in the RII region.
- Figure 6.43. The formation of pseudo-simple P_1/W_C drops.
- Figure 6.44. The formation of a pseudo- $W_1/P_1/W_C$ drop.
- Figure 6.45. The formation of a pseudo- $P_2/W_1/P_1/W_C$ drop.
- Figure 6.46. Effect of water content on mean diameters of (a) P_1/W_C and (b) W_1 drops.
- Figure 6.47. SEM image of emulsion sample EX58/S8 analysed 1¼ years later.
- Figure 6.48. SEM image of emulsion sample EX58/S3 analysed 1¼ years later.
- Figure 6.49. Phase inversion maps of NaOH and TEA-neutralised PUp-W dispersions.
- Figure 6.50. The effect of ionic group content on Sauter mean diameter.
- Figure 6.51. SEM image of aqueous PUpB-20/80 emulsions.
- Figure 6.52. SEM image of aqueous PUp2-1.5 emulsions.
- Figure 6.53. Enlarged image of figure 6.52.

- Figure 6.54. Phase inversion maps of PUpB-W and PUp2-7.5-W dispersions.
- Figure 6.55. Phase inversion maps at different operating temperatures.
- Figure 6.56. Phase inversion maps at different configurations of the dispersion vessel.
- Figure 6.57. d_{32} of aqueous emulsions withdrawn from experiments EX510/15 and EX59/12.
- Figure 6.58. Phase inversion map for a non-ionic SPUp-W system at 30 °C.
- Figure 6.59. Cinematography of events leading to the formation of smaller multiple drops in the RII region of the SPUp-W system.
- Figure 6.60. Phase inversion map for a non-ionic SPUp-W system at 60 °C.
- Figure 6.61. Different types of emulsions produced at different HLB number – operating temperature zones.
- Figure 6.62. SEM image of emulsion produced from EX511/9.
- Figure AI.1. Comparison of measured density and viscosity (dots) to values predicted using equations (lines)

List of tables

- Table 2.1. Typical diisocyanates and diols used for the preparation of PU ionomers.
- Table 2.2. Most commonly utilised functional groups.
- Table 2.3. Variables that affect the properties of polymer latices.
- Table 2.4. Some correlation of d_{32} for liquid-liquid dispersion in stirred tanks.
- Table 4.1. Properties of PUp samples.
- Table 4.2. Mole-% of functionalised PUp molecules in the PUp samples.
- Table 4.3. Constants A, B and C of equation (4-3) and the associated errors in representing density-temperature relationship of PUp samples.
- Table 4.4. Constants A, B and C of equation (4-4) and the associated errors in representing viscosity-temperature relationship of PUp samples.
- Table 4.5. Compositions of PUp blends.
- Table 4.6. Constants A, B and C of equation (4-3) and the associated errors in representing density-temperature relationship of PUp blends.
- Table 4.7. Constants A, B and C of equation (4-4) and the associated errors in representing viscosity-temperature relationship of PUp blends.
- Table 4.8. Properties of non-ionic surfactants (Igepal-CO series).
- Table 4.9. Properties of ionic surfactants used.
- Table 5.1. Materials of various phases during catastrophic phase inversion experiments.
- Table 5.2. Experimental details of preliminary experiments.
- Table 5.3. Experimental details of section 5.5.
- Table 5.4. Water contents (wt.-%) at sampling points for EX56/1 and EX56/2.
- Table 5.5. Experimental details of section 5.7.
- Table 5.6. PWCPI experiments designed for studying the effect of stabilising groups.
- Table 5.7. Transitional phase inversion experiments designed for studying the effect of stabilising groups.

- Table 5.8. Summaries of PWCPI experiments carried out at 45 and 80 °C.
- Table 5.9. Details of PWCPI experiments using the new configuration.
- Table 5.10. Details of transitional phase inversion experiments using the new configuration.
- Table 5.11. Details of non-ionic surfactant-related experiments.
- Table 5.12. Details of anionic surfactant-related experiments.
- Table 6.1. d_{10} and d_{32} calculated using arithmetic and geometric progression method.
- Table 6.2. The variations of mean diameters with the number of bins.
- Table 6.3. Characteristics of RI, RII and RIII during the PWCPI process.
- Table 6.4. K and n values of equation (6-3) for samples withdrawn from experiments EX56/1 and EX56/2. (Also includes the extrapolated viscosity at 500 rpm).
- Table 6.5. Various features of samples S1 to S5 and S11 from experiment EX58.
- Table 6.6. Total interfacial area per unit volume, in m^2/m^3 , of the emulsion samples.
- Table 6.7. Effect of time on the emulsion withdrawn at the phase inversion point.
- Table 6.8. Water content at the catastrophic phase inversion points of different PUp ionomer-W dispersions containing same ionic group content.
- Table 6.9. Droplet characteristics of the emulsions produced from experiments EX59/8 and EX59/9.
- Table 6.10. Summaries of experimental results when three different Igepal-CO type non-ionic surfactants were used to produce SPUp-W dispersions at 30 °C.
- Table 6.11. Summaries of experimental results at different operating temperatures.
- Table 6.12. Summaries of experimental results of work involving anionic surfactants.
- Table AI.1. Wall correction factors [reproduced from Sakiadis (1984)].

Abbreviations and nomenclatures

Abbreviations		First appearance (page)
AMM	Aqueous ammonia	8
DMPA	Dimethylol propanoic acid	16
DN	Degree of neutralisation	21
FSTC	Fixed speed, torque changes (agitator)	46
HLB	Hydrophile-lipophile balance	36
LALLS	Low angle laser light scattering	51
MDEA	N-methyl diethanolamine	21
NPE	Polyoxyethylene nonylphenylethers	37
nSOW	Non-ionic surfactant-oil-water	35
O/W	Oil-in-water	35
O-W	Oil-water	38
P ₁ /W ₁ /P _C	Polymer-in-water-in-polymer	131
P ₁ /W _C	Polymer-in-water	25
PIT	Phase inversion temperature	36
PTAd	Polytetramethylene adipate glycol	22
PTHF	Poly(tetrahydrofuran) diol	60
PU	Polyurethane	4
PU _p	Polyurethane pre-polymer	4
PU _p -W	Polyurethane pre-polymer-Water	4
PWCPI	Polymer-continuous to water-continuous catastrophic phase inversion	66

RI, II, III; 'P'	Region I, II and III; polymer-continuous	110
RI, II, III; 'W'	Region I, II and III; water-continuous	110
RIITI	Region III transitional phase inversion	129
RIITI	Region II transitional phase inversion	129
SAD	Surfactant affinity difference	36
SEM	Scanning electron microscope	51
SML	Polyoxyethylene sorbitan monolaurate	7
SOW	Surfactant-oil-water	35
SPUp	Surfactant-polyurethane pre-polymer	93
TEA	Triethylamine	8
TEM	Transmission electron microscope	51
TMA	Trimethylamine	8
TXDI	Tetramethyl xylene diisocyanate	60
VCR	Videocassette recorder	52
W', W''	Two different aqueous phases	196
W/O	Water-in-oil	35
W ₁ /O ₁ /W _C	Water-in-oil-in-water	35
W ₁ /P ₁ /W _C	Water-in-polymer-in-water	112
W ₁ /P _C	Water-in-polymer	25
WPCPI	Water-continuous to polymer-continuous catastrophic phase inversion	66
Z1, 2, 3	Zone 1, 2 and 3	147

Nomenclatures – Symbols

	<u>Descriptions</u>	<u>MLT units</u>
a	Interfacial area per unit volume	$L^2 L^{-3}$
$A - C$	Constants for equations (4-1) and (4-2)	–
$a - d$	Control variables of equation (2-24)	–
$A(h_o)$	Force of adhesion between a colliding droplet pair	MLT^{-2}
a_e	Acceleration due to the external force	LT^{-2}
A_p	Projected particle area in the direction of motion	L^2
$C_1 - C_{16}$	Constants	–
C_D	Fanning drag coefficient	–
C_{DH}	Debye-Hückel constant used in equation (5-20)	$(\text{Mole } L^{-3})^{-1/2}$
d	Drop diameter	L
d_{10}	Arithmetic mean diameter	L
d_{32}	Sauter mean diameter	L
$d_{32,OW}$	d_{32} of the oil-in-water drops	L
$d_{32,OWO}$	d_{32} of the water drops in the multiple O/W/O drops	L
$d_{32,PW}$	d_{32} of the polymer-in-water drops	L
$d_{32,WPEW}$	d_{32} of the polymer drops in the multiple W/P/W drops	L
D_a	Diameter of the agitator	L
D_{avg}	Average diameter of a bin [= $(D_H + D_L)/2$]	L
D_H	Upper drop diameter limit of a bin	L
D_L	Lower drop diameter limit of a bin	L
d_m	Mean diameter of the log-normal distribution	L
d_{nu}	Mean diameter	L
d_N	Number average diameter	L

	<u>Descriptions</u>	<u>MLT units</u>
d_o	d_{32} of an inviscid drop	L
d_{Pol}	Diameter of polymer drops	L
du/dy	Rate of shear (or velocity gradient)	T ⁻¹
$d_{V,xx}$	Particle size correspondent to the xx^{th} percentile of the cumulative volumetric distribution	L
d_w	Weight average diameter	L
d_{Water}	Diameter of water drops	L
e	The negative charges of a dissociation process	-
E_{EV}	External viscous shear stress	ML ⁻¹ T ⁻²
E_{Γ}	Interfacial-tension stress	ML ⁻¹ T ⁻²
E_{IV}	Viscous stress inside the droplet	ML ⁻¹ T ⁻²
E_{PF}	Stress causes by turbulent pressure fluctuations	ML ⁻¹ T ⁻²
F_B	Buoyant force	MLT ⁻²
F_D	Drag force	MLT ⁻²
F_E	External force	MLT ⁻²
$f_{P/W}$	Volume fraction of simple P ₁ /W _C drops	-
g	Acceleration due to gravity	LT ⁻²
$G_{abcd}(x)$	Potential of the butterfly catastrophe	-
GSD	Geometrical standard deviation	-
h_o	Distance between any two drops	L
I	Ionic strength	Mole L ⁻³
k	Constant for equation (2-1)	-
K	Consistency index of equations (6-2) and (6-3)	ML ⁻¹ T ⁽ⁿ⁻²⁾
K_d	Dissociation constant	-

	<u>Descriptions</u>	<u>MLT units</u>
k_w	Correction factors for the wall effect	–
L	Macroscopic length scale of the non-isotropic main flow	L
M_p	Mass of particle	M
N	Agitator speed	T ⁻¹
n	Exponent of equations (6-2) and (6-3)	–
N_A	Total amount of functional group A	–
N_B	Total amount of functional group B	Mole
N_{bin}	Total number of bins used during the analysis	–
$N_{Coalescence}$	Frequency of coalescence	T ⁻¹
$N_{Collision}$	Frequency of collision	T ⁻¹
N_{crit}	The critical number of particles which must be counted to prevent the error from growing catastrophically	–
N_i	Number of droplets in bin i or frequency in bin i	–
N_{lim}	The limited number of particles that must be calculated to obtain marginally acceptable results	–
N_T	Total number of drops calculated ($= \sum N_i$)	–
N_x	Total amount of molecule x	Mole
p	Extent of reaction	–
P_A	Area percentage of a bin	%
pK_I	pK ($=\log K_d$) at a specific ionic strength, I	–
$pK_{I=0}$	pK value when ionic strength is equal to zero	–
P_N	Number percentage of a bin	%
P_V	Volume percentage of a bin	%
r	Functional group ratio ($= N_A/N_B$, for $N_A < N_B$)	Mole
R	Gas constant	ML ² T ⁻² Mole ⁻¹ K ⁻¹

	<u>Descriptions</u>	<u>MLT units</u>
Re	Reynolds number	–
S	Spindle rotating speed	T^{-1}
T	Temperature	K
t	Time	T
$u(z)$	Relative velocity between any two points with z distance apart	LT^{-1}
u_p	Relative velocity of a particle and its surrounding liquid	LT^{-1}
u_t	Terminal (or free-settling) velocity	LT^{-1}
u_t'	Actual terminal velocity, after taken account of the wall effect	LT^{-1}
Vi	Viscosity group	–
Vi'	Dimensionless groups used in table 2.4	–
Vi''	Dimensionless groups used in table 2.4	–
We	Weber number	–
We'	“Generalised” Weber number	–
We'_{crit}	Critical “generalised” Weber number	–
x	State variables of equation (2-24)	–
z	Distance between two points	L
$\overline{u^2(z)}$	Mean square of relative velocity	L^2T^{-2}
$\overline{X_n}$	Number-average degree of polymerisation	–
ΔD	The interval of a bin	L
$(MW)_x$	Molecular weight of component x	M/Mole
$\Delta_r G_T^\circ$	Standard Gibbs energy of formation at temperature T	$ML^2T^{-2}Mole^{-1}$
$[x]$	Mole-% of component x	Mole-%

Nomenclatures – Greek symbols

	<u>Descriptions</u>	<u>MLT units</u>
μ	Viscosity	$ML^{-1}T^{-1}$
ρ	Density	ML^{-3}
ϕ	Volume fraction	–
σ	Interfacial tension	MT^{-2}
τ	External force per unit area	$ML^{-1}T^{-2}$
ν	Kinetic viscosity of fluid	L^2T^{-1}
ε	Local energy dissipation rate per unit mass	L^2T^{-3}
η	Microscopic length scale of turbulence	L
δ	Standard deviation (= ln <i>GSD</i>)	–
β	particle diameter to vessel diameter ratio (= d_p/d_v)	–
$\Delta\rho$	Density difference	ML^{-3}
δ_{LN}	Standard deviation of the log-normal distribution	–

Nomenclatures – Subscripts

	<u>Descriptions</u>		<u>Descriptions</u>
<i>act</i>	Actual	<i>max</i>	Maximum
<i>c</i>	Continuous phase	<i>min</i>	Minimum
<i>d</i>	Dispersed phase	<i>nom</i>	Nominal
<i>f</i>	Final emulsion products	<i>p</i>	Particle
<i>i</i>	Bin number	<i>req</i>	Required
<i>l</i>	Continuous fluid	<i>T</i>	Total
<i>m</i>	Dispersed medium	<i>v</i>	Vessel

CHAPTER 1

Introduction and objectives

This chapter provides a general overview of the manufacturing of aqueous polyurethane colloids. By studying the existing industrial processes and researches, the objectives of this project are clearly identified and outlined in this chapter.

1.1 General introduction

Polymer colloids have found extensive usage as film former. Latex paints first appeared in the market in the 1950s. Now, polymer latices are employed not only in paints industry, but also, for example, in floor coatings, printing inks, adhesives, paper overprint, varnishes, carpet backing and paper making industry. Many industrial grades of polymer colloid are supplied as solvent-based products due to the processibility of dispersing polymer into solvents such as Xylene and n-Methylpyrrolidinone. However, these solvent-borne polymers were found to have detrimental effects on health, safety and the environment. Therefore, under the environmental and legislative pressures, water-borne polymer colloids have become an increasingly important class of material to the surface coatings industry (Oertel (1994); Satguru et al. (1994)).

A polymer colloid is a dispersion of fine particles of polymers in a fluid medium. This is generally formed in either of two ways: (a) by disintegration of larger particles (e.g. by dispersion of pre-formed polymers in water) or (b) by integration of smaller particles, usually molecules (e.g. by emulsion polymerisation) (Fitch (1997)).

The process and products of the later methods have been studied extensively over the past 30 years. A typical process for producing polymer colloids through this idea is the emulsion polymerisation process (Shaw (1992)). In this process, water-

insoluble monomers were first emulsified in water with suitable surfactant(s). A water-soluble free radical initiator was then added and polymerisation could produce a polymer colloid. Examples of polymers produced through this method include acrylic copolymers, vinyl-acrylics, styrene acrylics, and styrene-butadiene. A common feature of these polymers is that they all undergo free radical polymerisation. Latices synthesised through integration of smaller particles, particularly through emulsion polymerisation, is well studied and can offer advantages such as faster reaction rate at lower operating temperature. However, the biggest disadvantage associated with this process is the presence of external emulsifiers or protective colloids. The residual surfactants often contaminate the emulsion products by making them more sensitive to heat and shear stress (Zerfa (1994)). Also, they often cause foam and pinhole formations on the final coating products (Padgett (1994)).

On the other hand, disintegration of larger particles, particularly through secondary dispersions, is a useful method used for preparing aqueous polymer colloids of polymers synthesised by condensation polymerisation (e.g., polyurethane, polyesters and epoxy resins). In this case, polymers were firstly produced in a homogeneous phase, which is usually an organic solution, followed by dispersion into water. If organic solvents were used during the process, they can be distilled off from the emulsions to give water-borne polymer colloids.

Two extreme types of polymers can be classified in terms of their physical appearances when considering latex prepared through disintegration of large particles:

- (1) Highly water soluble polymers over the entire pH range, e.g. polyethylene oxide homopolymer and polyacrylic acid; and
- (2) Highly water-insoluble polymers (or highly hydrophobic polymers).

It is easier to produce water-borne latex from the former group of polymers. When trying to disperse the latter group of polymers into water, the immediate difficulty is that they do not normally form stable solutions in water due to their hydrophobic nature. As a result, large quantities of external emulsifiers are often needed to disperse relatively low molecular weight polymer of this kind under high shear force. Even so, such procedures still often resulted in latices with large particle sizes and poor colloidal stability (Arnoldus (1990); Ellis (1992); Zeneca Resins).

A more elegant approach to make these polymers “dispersible” is to incorporate a suitable amount of hydrophilic ionic groups onto their hydrophobic backbone. These modified polymers can readily be dispersed into water under low shear stress with little or no external emulsifiers. Examples of polymer latices produced by utilising this idea are: hydrophilically modified epoxy resins (Ellis (1992)), cationic epoxy resin latex (Lee and Yang (1992)), water-borne epoxy resin (Yang et al. (1997a)), water-borne polyesters (Kotera and Takahashi (1990)), emulsifier free polyacrylate latex (Schlarb et al. (1995a and 1995b)), water-borne (water-based or aqueous) polyurethane (Rosthauser and Nachtkamp (1986); Arnoldus (1990); Yang et al. (1995); Pinfield (1996); Lee et al. (1997)), polyurethane ionomers dispersions (Dieterich (1981); Kim and Kim (1991a); Kim and Lee (1996); Tharanikkarasu and Kim (1997)), polyurethane cationomers (Lee and Kim (1994); Lee and Kim (1995)), polyurethane anionomers (Chen and Chen (1992); Hourston et al. (1997 and 1998)), and poly(phenylene oxide) ionomer (Gu et al. (2000)).

There are two reasons for using a multistep process. On the one hand, this process allows the preparation of aqueous dispersions from polymers that, traditionally, can not be dispersed into water. Examples of this are stereoregular polymers, polyurethane, polyesters and epoxy resins. On the other hand, this process makes it possible to prepare aqueous polyacrylate dispersion, poly(styrene-acrylate) dispersions, or copolymer of polystyrene and acrylic acid (Puig et al. (1990); Li et al. (1995 and 1997)), which are free of any surfactants and protective colloids. Tharanikkarasu and Kim (1997) summarised the main advantages of applying this concept of self-emulsification as dispersion processes that produce emulsions:

- I. Without requiring strong shear force,
- II. Containing fine particles with improved dispersion stability,
- III. With reduced water sensitivity of the films (after evaporation of water),
- IV. With high resistance to non-polar agents.

Despite having so many advantages, progress in this direction is restricted by inadequate understanding of key phenomena that affect the production, performance and stability of suitable polymer colloids. Consequently, there is a growing need for a more detailed understanding of this relatively new area for the production of aqueous

polymer colloids. This is vital for the identification and characterisation of essential steps in developing any new routes to stabilise high performance polymer colloids.

1.2 Introduction to this project

Polyurethane (PU) has well studied chain extension and dispersion chemistry (Dieterich (1981); Rosthauser and Nachtkamp (1986)). Unlike the aqueous polymer colloids of polyester, epoxy resins and other stereoregular polymers, the studies of aqueous PU colloids are also relatively well documented in the open literature.

Three processing stages are generally involved in the production of aqueous PU colloids. They are: (1) a pre-dispersion stage; (2) a dispersion stage; and (3) a post-dispersion stage (Rosthauser and Nachtkamp (1986)). The pre-dispersion stage includes all processes that produce the PU or PU pre-polymer (PUp). The dispersion stage includes all processes related to the disintegration of large particles into colloidal forms. A common dispersion process employed during this stage is a phase inversion process, and specifically a catastrophic phase inversion process. The last stage of the production normally involves chain-extension of the pre-polymers, which have low or moderate molecular weight, into long polymer chains. In some cases, the post-dispersion stage also involves the removal of solvents.

Most, if not all, existing work on aqueous PU colloids focus on the pre-dispersion chemistry of PU, changes in process factors and the properties of final emulsion products. Although understanding the events occurring during the dispersion process is important, previous studies in this area are relatively sparse. It raises the needs for studying the dispersion stage independently.

1.3 Objectives

The main objective of this project is to develop better understanding of the dispersion stage during the production of aqueous PU colloids. Non chain-extendable PUp is chosen because it enables independent study of the dispersion stage. The phase inversion process is selected due to its widespread industrial usage. For the purpose of this study, it was intended to study the following aspects of phase inversion in PUp-water (PUp-W) dispersions:

- A. Droplet size measurement and analysis technique: Droplet size information is one of the most important parameters in characterising any emulsions. With no exception, the development of a suitable droplet measurement and analysis technique is vital in characterising the PUp-W dispersions properly.
- B. Phase inversion boundaries: This includes developing suitable techniques to follow the phase inversion process and detect the phase inversion loci during the production of PUp-W dispersions. Phase inversion maps, normally used for studying surfactant-oil-water (SOW) dispersions, might provide “standards” against which the behaviour of both internally and externally stabilised PUp-W dispersions can be compared.
- C. Phase inversion mechanism: A better understanding of the phase inversion mechanism during the dispersion stage provides a background against which the effect of any post-dispersion treatments can be compared. This will also affect the choice of post-dispersion process for the preparation of stable aqueous polymer colloids, of small particles ($< 0.2 \mu\text{m}$), from high molecular weight functionalised polymers with minimum amounts of stabilisers and solvent.
- D. Effect of some dispersing conditions: Some dispersing conditions such as the type of stabilising groups, the viscosity of the PUp and the configuration of the dispersion vessel may affect the phase inversion behaviour and/or the qualities of the emulsions. Understanding their effects can lead to more efficient usage of the internal functional groups and suitable design of the dispersion vessel.
- E. Relationship between internal and external stabilisers: This can be done by studying the effect of polymer functionality on phase stability and comparing it with external surfactants. This may lead to more efficient usage of the stabilisers during the production of aqueous PU and PUp colloids.

This thesis consists of eight chapters. A detailed literature survey into subjects related to this project is provided in the next chapter. Then, the experimental apparatus and materials used for this project are shown in chapters 3 and 4 respectively. The details of the relevant experiments are described in chapter 5. The results obtained are described and discussed in the subsequent chapter, chapter 6. This is followed by a general conclusion in chapter 7. Lastly, some probable future work is suggested in chapter 8.

CHAPTER 2

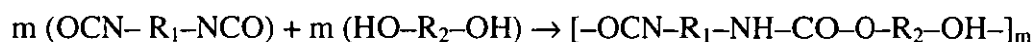
Literature survey

Subjects discussed in this literature survey can be classified into two main categories. They are “aqueous polymer colloids”-related studies and “liquid-liquid dispersions”-related studies. In the first category, focus is placed on literature related to aqueous PU (ionomer) colloids. Subjects discussed under this category include the chemistry of PU, PU colloids’ production methods, properties of polymer latex and factors affecting these properties. In the second category, discussions cover literature related to the direct dispersion processes and phase inversion processes involving the usage of external surfactants. Different types of emulsions and drop structures are also discussed under this category.

2.1 Chemistry of polyurethane (PU) and PU ionomer

2.1.1 Building block of PU molecules

A typical PU is characterised by the occurrence of urethane (-NH-CO-O-) groups in its macromolecular chain. Polyurethane is formed by polyaddition reaction (or condensation polymerisation) between polyisocyanates and polyols (Billmeyer (1984)). The reaction between diisocyanates and equivalent quantities of diols produces a simple linear PU as the following,



Increasing in the diisocyanates-to-diols ratio leads to the formation of isocyanate end-capped polyurethane pre-polymers (PU_p). These pre-polymers can react with chain extenders such as diols and diamines to form high molecular weight

linear PU and urethane-urea copolymer respectively. Alternatively, these pre-polymers can be “de-activated” by reacting with monofunctional amine or alcohol.

Schlack developed the first isocyanate-based dispersion as early as 1943. However, the major breakthrough in obtaining easily water-dispersible PU was only introduced in the late 1960s (Dieterich et al. (1970)). The generally hydrophobic PU is made dispersible by incorporating some internal ionic stabilisation agents (or hydrophilic ionic groups) into its backbone.

2.1.2 PU ionomers

Tharanikkarasu and Kim (1997) defined PU ionomers as PU containing less than 15 mole-% of ionic groups. Almost all raw materials that are used in the synthesis of conventional PU can also be used in the preparation of PU ionomers. Some of the diisocyanates and diols used for this purpose are summarised in table 2.1.

Table 2.1. Typical diisocyanates and diols used for the preparation of PU ionomers,

Diisocyanates	Diols
4,4-Dicyclohexylmethane diisocyanate	Polytetramethylene oxide glycol
Isophorone diisocyanate	Poly(tetramethylene adipate) glycol
1,6-Hexamethylene diisocyanate	Polycaprolactone glycol
Tetramethylxylene diisocyanate	Poly(tetrahydrofuran) diol

The hydrophilic groups are built into the PU chain by replacing a small portion of the aforementioned polyols or polyisocyanates with some special materials that contain, in their molecular structure, some water solubilising functional groups. These special building blocks are often called “hydrophilic monomers” or “internal emulsifiers”. The concentration of such functional groups in the polymer is highly influential in determining the state in which the polymer will exist in an aqueous environment (Padget (1994)). At high concentrations, the polymer may be water soluble; and at lower concentrations, the polymer may be water dispersible if its molecular weight and viscosity are not excessive. At even lower concentrations, the polar group may be capable of only providing charge or steric stabilisation to a dispersion of the polymer in water.

The water solubilising functional groups that are being used commercially can be classified as anionomer, cationomer and non-ionomer. Recently, ionomers with non-ionic segments have also found commercial usage (Arnoldous (1990)). This is made possible because, in the study, non-ionic stabilisers are compatible with ionic groups and can be built into the same PU backbone. The most commonly utilised functional groups conferring water solubility are summarised in table 2.2. In the cases whereby the functional groups are ionisable, the water solubilisation effect is greater when the functional groups are in their ionised (salt) forms (Padget (1994)).

Table 2.2. Most commonly utilised functional groups,

Type	Charge	Functional group	Counterions
Anionomer	Negative	Weak acids (carboxylic acid) Strong acids (sulphonic acid)	Bases, e.g. triamines* and metal hydroxyl oxide
Cationomer	Positive	Weak bases (amine) Strong bases (tertiary and quaternary ammonium compounds)	Alkylation agents, acid or ammonium compounds
Non-ionomer	Neutral	ethylene oxide and vinyl pyrrolidone	N/A

2.2 Production of aqueous PU ionomer colloids

2.2.1 Different manufacturing processes

There are several synthetic processes for producing high molecular weight PU ionomer dispersions (Satguru et al. (1994)). These include the acetone process, melt dispersions process, pre-polymer mixing process, ketimine process and ketazine process. A common feature of all these processes is that the first step, the pre-dispersion stage, involves a conventional PU synthesis in which diols are reacted with diisocyanates. This is followed by dispersing the PU into water (the dispersion stage). The necessary low viscosity of the urethane polymer to enable the dispersion process is achieved by one of the following methods:

* Triamines include Triethylamine (TEA), Trimethylamine (TMA) and Aqueous ammonia (AMM).

- (a) PU pre-polymer (PU_p), which has a low molecular weight is used during the dispersion process. A chain extension process is required at or after the dispersion stage to achieve the required high molecular weight (pre-polymer mixing process, ketimine process and ketazine process)). A schematic representation of the pre-polymer mixing process is shown in figure 2.1;
- (b) PU is dissolved in solvent with low boiling point. In this case, the solvent has to be removed at the post-dispersions stage (acetone process); or
- (c) PU is heated to facilitate the dispersion in water (melt dispersion process).

2.2.2 The dispersion stage

In the presence of solvent, viscosities of PU ionomer solutions drop slightly following the addition of water. Then, solution viscosity starts to rise sharply following further water addition. After reaching a maximum, solution viscosity decreases suddenly. Following this sharp decrease in viscosity, further water addition results in a slow decrease of viscosity and eventually a constant viscosity is reached (Chen and Chen (1992); Yang et al. (1995)), as shown in figure 2.2.

Dieterich et al. (1970) observed that the ionic segments of PU ionomers are brought together by Coulomb forces to form a sort of microionic lattice in the non-aqueous media. The association is greatly reduced or eliminated by the addition of small quantities of water, thereby reducing the viscosity. The subsequent increases in viscosity arise from a relative decrease of solvent content in the polymer phase (Chen and Chen (1992) and Yang et al. (1995)). Hydrophobic polymer segments lose their solvation sheaths following the decreasing solvent content and come together to form hydrophobic associates that are physically cross-linked. Eventually, the associates rearrange into spherocolloids when the solution becomes cloudy and its viscosity decreases considerably. This results in aqueous PU colloids with low viscosity (Chen and Chan (1990); Pinfield (1996)).

According to Dieterich (1981), dispersions produced from organic solutions through water additions can take place by precipitated dispersions or by phase inversions. The transition, from a one-phase into a two-phase system, is completely continuous in the first case (similar to the aforementioned dispersion process in the presence of water-miscible solvent). In the latter case, however, the solvent-free

dispersions are formed via a reverse emulsification of the water-in-polymer mixtures when the addition of water is extended over a longer period of time. This is always the case for a melt dispersion process, and to a certain extent, for the pre-polymer mixing process.

During the “true” phase inversion process, the change in viscosity following water additions is similar to those shown in figure 2.2. However, as mentioned by Dieterich (1981), the dispersion mechanism is different from a system containing water-miscible solvent. Dieterich suggested that the events occurring during the phase inversion process could be described in three distinctive stages. When water is first added during the first stage, PU ionomer absorbs a certain amount of water homogeneously, and thereby reduces the viscosity. Associates formed through the ionic groups, which make PU ionomer more viscous, are now dissolved by the hydration of the ionic groups.

In the second stage, hydrated portions are gradually enlarged with increasing amount of water. Slowly, water extends into the hydrophobic areas and their mobility decreases due to the occurrence of hydrophobic associates in the polymer matrix. At this point discrete water areas are formed in a homogeneous polymer matrix. Their ionic or hydrophilic centres occupy the interface.

In the final stage, the above condition can be made permanent in some cases (e.g., not having enough hydrophilic groups or the occurrence of any unplanned chain extensions during the dispersion process). Additional water is no longer absorbed by the system, but forms a continuous second phase instead. This happens because the water droplets cannot coalesce within the polymer matrix, which is already in its final form. However, the critical condition of maximum viscosity will normally be passed quickly following further water additions. The incorporated water is forced, starting from the dispersed droplets of water, further into the polymer matrix. The polymer-water interfaces then restructure and finally disintegrate into spherical dispersion particles enclosed by a continuous aqueous phase.

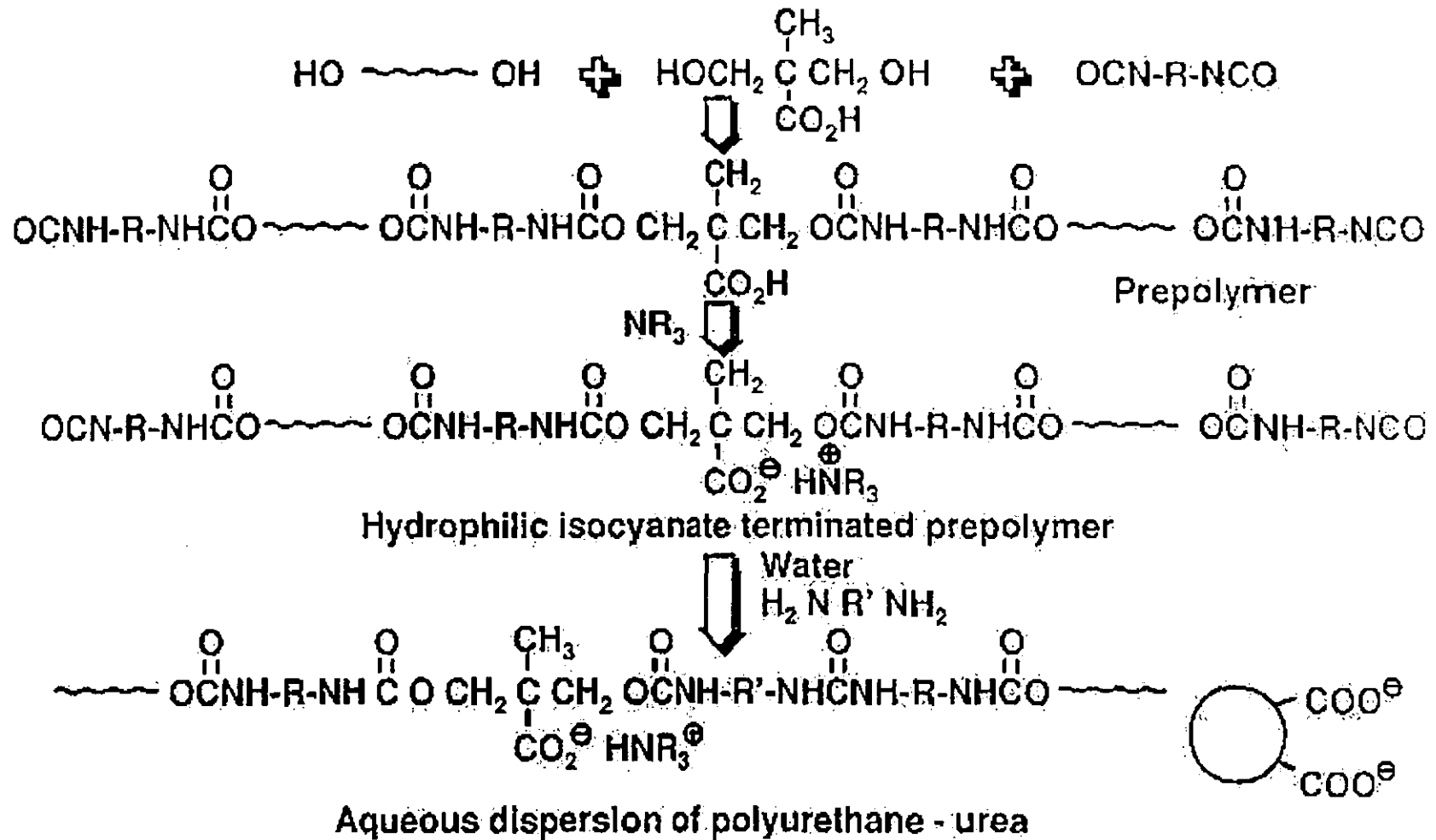


Figure 2.1. Schematic representation of the pre-polymer mixing process [reproduced from Zeneca (1998)]

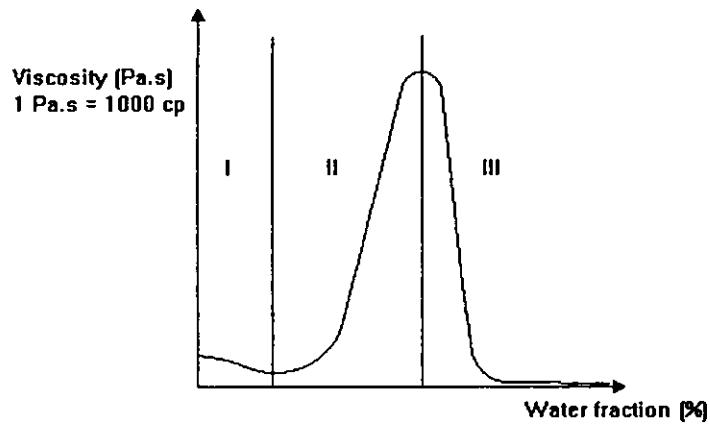


Figure 2.2. Viscosity variation during water additions

2.3 Some properties of polymer latices

Various properties of polymer latices, particularly those of aqueous PU colloids, which have previously been studied by various workers (Chen and Chen (1992); Lee and Yang (1992); Lee and Kim (1994); Yang et al. (1995)) can be grouped as follows:

1. Colloidal properties: Particle (drop) size and particle size distribution, viscosity and stability of colloids;
2. Interfacial properties: Contact angle, surface tension, interfacial tension and Zeta potential;
3. Mechanical properties: Dynamic mechanical properties (or viscoelastic behaviour), tensile properties (tensile strength and elongation at break) and micro-tensile properties (hardness and initial modulus);
4. Thermal properties: Transition temperature and thermogravimetric behaviour;
5. Morphological properties: Internal particle morphology of PU particles and film morphology.

Mechanical and thermal properties are important properties of films cast from the final emulsion products. These properties determine the application of the final emulsion products. According to Zeneca Resin, PU can be made to possess a wide range of properties. Depending on the formulation, they can be made to be hard or soft or tacky, have good chemical resistance, be fast drying, have high compatibility

or low cost. At the same time, all PU will have high impact strength, high abrasion resistance and good tensile strength. The basis of these properties is attributed to the extensive amount of hydrogen bonding between the urethane linkages. The mechanical and thermal properties of PU anionomer and PU cationomer have been studied by Houston et al. (1997 and 1998) and Lee and Kim (1997) respectively. For the purpose of this work, these two properties will not be discussed in greater details since they are not directly relevant to this work. Only the colloidal, interfacial and morphological properties are discussed in more details in the following sub-sections.

Interfacial properties and morphological properties are generally the results of the polymer or pre-polymer preparation. They can be used to describe the physical state of the pre-polymer and polymer prior to their dispersion. Besides that, they can also be used to determine the properties of the final emulsion products. Interfacial properties are also useful in predicting behaviour of polymers or pre-polymers during the dispersion process. Colloidal properties, especially drop size and its distribution, is an important group of properties for both the dispersion process and the final emulsion products. Changes in drop size, and subsequently viscosity, during the process have an effect on colloids stability and can be used to determine the quality of the dispersion process itself. Colloidal properties are also important in determining the stability and processibility of the final products, and have effects on other groups of properties (e.g. mechanical and thermal properties).

2.3.1 Particle size and its distribution

The particle size of aqueous dispersions can vary from about 0.01 to 5 μm . Particles with larger average particle sizes ($> 1 \mu\text{m}$) are generally unstable with respect to sedimentation. Therefore, smaller particle sizes ($< 200 \text{ nm}$) are sought after since such dispersions are storage stable and possess a high surface energy, resulting in a strong driving force for film formation. However, relatively large particles are preferred in many surface coatings to facilitate rapid drying, and relatively small particles are desirable when deep penetration of the dispersion into the substrate is essential. Since the particle diameter lies over several order of magnitudes, the appearance can vary from an opaque translucent solution to a milky white dispersion.

According to Satguru et al. (1994), drop size distribution of aqueous PU dispersions is relatively polydispersed in comparison to most aqueous polyacrylic

polymers. This feature is attributed to (1) the statistical nature of both the step growth polymerisation (or condensation polymerisation) and the chain extension processes which results in a broad distribution of chain lengths and concentrations of stabilising moiety; and (2) the fact that the dispersion is produced by an emulsification process. This relationship between molecular distributions and drop size distributions is a consequence of the specific process studied by Satguru et al. (1994).

2.3.2 Viscosity of the final emulsion products

Viscosity of the final emulsion product is of great importance in practical application and is influenced by the average particle size, particle size distribution, inter-particle interactions and degree of swelling of the particles. Aqueous PU dispersion has relatively low viscosity. The viscosity of typical commercial grades is between 10-700 mPa.s at room temperature, with typical solid content of 30 - 40 %.

Tharanikkarasu and Kim (1997) mentioned that the viscosity of the final emulsion products (μ_f) is directly proportional to the effective volume fraction of dispersed phase (ϕ_d) at low dispersed phase concentration ($\phi_d < 0.02$). At low concentration, the relation between viscosity and dispersed phase volume fraction can be expressed as follows:

$$\frac{\mu_f}{\mu_m} = 1 + k_1 \phi_d^2 + \dots \quad [2-1]$$

where μ_m is the viscosity of dispersed medium and k's are constants. However, concentration dependence will become more pronounced at high ϕ_d .

Since the net solid content of a typical PU dispersion is over 30 wt.-%, higher order terms of equation (2-1) would contribute significantly in a real commercial product. However, the degree of swelling of the PU particles, which generally increases with increasing hydrophilicity of raw materials, contributes to the effective volume fraction of the dispersed phase in the above equation. The electroviscous effect of ionomer dispersion also increases the viscosity. All these factors make it hard to correlate the viscosity of the final emulsion products directly to its emulsion state.

2.3.3 Particle morphology

Particles of PU ionomer have open, water-swollen structures similar to those of polyacrylic acid in aqueous solution, according to Satguru et al. (1994). They proposed that particle of PU ionomer can best be represented by a preliminary model as shown in figure 2.3a. This model is based on a simple spherical surface scattering phenomenon and possesses “water” rich areas within the polyurethane particle. They also proposed that the ability of aqueous polyurethane colloids to combine film formation at low temperature with the ability to give high film hardness is a result of this water-swollen morphology that aids film formation. Chen and Chen (1992) found that factors such as molecular weight, hydrophilicity of the backbone, concentration of stabilising moiety and the concentration of solvent diluent would determine the extent of “openness” of the particle. The openness of PU ionomer particles is a result of the structure of the dispersed particles in the continuous aqueous phase. Dieterich (1981) suggested that PU ionomer particles would contain hydrophobic polymer segments inside its particles, while its outer layer is covered by the hydrophilic stabilising groups.

Recently, Gao et al. (1994) managed to make a similar kind of micelle in water using block copolymers of styrene 4-vinylpyridine methyl iodide. They called this type of particle a “crew-cut” micelle. This micelle consists of a large hydrophobic core (40 ~ 65 nm in diameter) and a relatively thin hydrophilic corona (see figure 2.3b). Li et al. (1995) also managed to disperse polystyrene-based block ionomer containing 3.2 and 8.3 wt-% of sodium carboxylate groups. This micelle also has a hydrophobic core and a hydrophilic corona, which consists of ionomer blocks that swell in aqueous medium.

2.3.4 Stability of emulsion

Ionomeric dispersion

The mechanisms that stabilise ionomeric and non-ionomeric dispersions are different. Tharanikkarasu and Kim (1997) mentioned that ionomeric dispersion is stabilised by the well-known phenomenon of a diffuse double layer (also known as electrical double layers). According to Hunter (1985), the double layer is formed between the ionic constituents (which are chemically bonded to the polymer particle

surface) and their counterions (which migrate into the water phase as far as they are allowed by the attractive forces of the carboxylate ions). This forms a layer with decreasing electrical charge and possesses an electrokinetic or Zeta potential on the surface of shear. The repulsive force by Zeta potential between particles is responsible for the overall stabilisation of the dispersion. Similarly, crew-cut micelles of polystyrene ionomer, in the work of Gao et al. (1994), are stabilised by the strong electrostatic repulsion between soluble ionic blocks of the micelles.

Chen and Chen (1992) mentioned that the aforementioned steric repulsion could be suppressed by addition of inert electrolytes. The electrolyte concentration adequate to induce coagulation is called the critical coagulation concentration. This coagulation happens because the added ions reduce the range of double layer repulsion. Satguru et al. (1994) compared the stability of an anionic PU stabilised by a copolymerised carboxylic acid (such as dimethylol propanoic acid (DMPA)) and an emulsion polymer stabilised by the incorporation of a copolymerisable carboxylic acid (such as acrylic acid and methacrylic acid). In the former case, they discovered an abrupt loss in colloid stability at the pKa of the copolymerised acid, when the pH is reduced from a value above the pKa of the acid. However, in the latter case, no such abrupt loss of colloid stability occurs.

Non-ionomeric dispersion

In non-ionomeric dispersion, the hydrophilic polymer segments are anchored on the surface of the particle and stretch into the water phase. The stabilisation mechanism for this type of particle structure can be explained in terms of entropic repulsion. When the particles approach each other, the freedom of motion of hydrophilic non-ionic chains in the water phase is restricted, and hence leads to a reduction of entropy. This in turn causes repulsion between particles spontaneously. When non-ionic diol was used as the stabiliser for PU dispersion, colloid stability is maintained over a wide range of pH value.

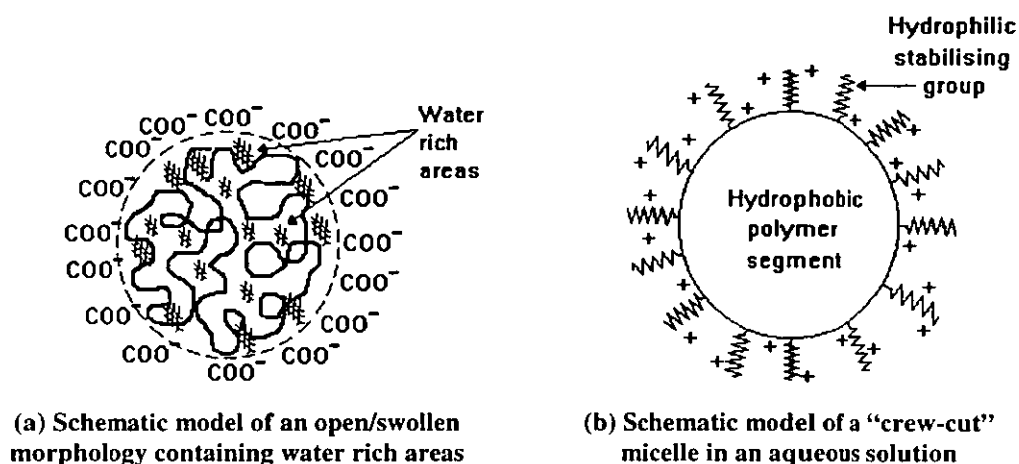


Figure 2.3. Possible particle morphology of aqueous polymer ionomer colloids

2.4 Factors affecting the properties of polymer latex

The precise nature of the aforementioned properties of polymer latex is very dependent on a number of variables, which can generally be classified as chemical factors, processing factors and solution factors. Chemical factors are related to the polymer and pre-polymer chemistry; processing factors are variables related to the synthetic process employed; and solution factors are related to the physical properties of the disperse phase, dispersed medium and emulsion phase. Table 2.3 groups some of the variables that affect properties of polymer latex, particularly aqueous PU colloids, into the aforementioned categories.

Table 2.3. Variables that affect the properties of polymer latices,

Chemical factors	Processing factors	Solution factors
Stabilising groups	Shear condition	PH value
Counterions	Dispersion temperature	Phase volume
Degree of neutralisation	Addition rate of dispersant	Dispersed phase viscosity
Backbone hydrophobicity	Agitation rate	Surfactants content
Extender (functionality)	Dispersion method	Solvents content
Molecular weight		

Lee and Kim (1994) showed that, although the average particle size of aqueous PU colloids is more or less influenced by processing and solution factors, it is mainly governed by the hydrophilicity (i.e., chemical factors) of the PU ionomer.

The effects of some variables, especially those classified as chemical factors, are discussed in more details in the following sections.

2.5 Chemical factors

2.5.1 Stabilising groups

Minimum amount of stabilising groups

A minimum amount of ionic group content is required for the formation of stable PU dispersions and this amount depends on the type of ionic species employed. When DMPA was used to provide anionic groups in a PU dispersion, Chen and Chen (1992) found that the minimum -COOH content required to form a stable dispersion of a fully neutralised PU anionomer is 0.8 wt.-% (17.8 mmole per 100g of PU). Satguru et al. (1994) reported this value as 0.25 mmole/g.

The distribution of anionic stabilising groups

Vijayendran (1979) found that the distribution of acid groups in the carboxylated polystyrene latices (i.e., the relative distribution of acid in the serum phase, the latex surface and the latex core) depends strongly on the nature of the carboxylic monomer used. He showed that itaconic acid, which is very hydrophilic and has poor solubility in styrene, tends to distribute itself in favour of the aqueous serum phase. Acrylic acid, which has limited solubility in styrene and is sufficiently hydrophilic, tends to stay at the particle surface predominantly. Methacrylic acid, which is more hydrophobic and has good solubility in styrene, was shown to be concentrated inside the particle core.

In the case of PU ionomer dispersions, Dieterich (1981) quoted from Lorenz's work to claim that PU latex particles do not contain any embedded ionic groups. It was also suggested that the ions are either located on/at the particle surface or in the aqueous phase.

Anionic stabilising groups vs. Particle size (and its distribution)

When fully neutralised DMPA was used as the anionic centre, Kim and Lee (1996) found that particle size decreases with increasing ionic group content due to the increasing hydrophilicity of PU ionomers. Kim and Kim (1991a) and Lee et al.

(1997) also noted that the particle size of final emulsion product decreases rapidly at low DMPA content (≤ 3.0 wt.-% on total solid), followed by an asymptotic decrease to about $0.1 \mu\text{m}$ (figure 2.4). They therefore suggested that there is a critical concentration of DMPA for particle size reduction. Tharanikkarasu and Kim (1997) explained this phenomenon using the dual effect of ionic centres. That is, particle size decreases due to the increasing hydrophilicity, at the same time it also increases due to the swelling by water, and hence causes an overall asymptotic behaviour. In another work, Satguru et al. (1994) found a linear relationship between specific surface area of particle and DMPA concentration (figure 2.5). Based on this relationship, they suggested the existence of a constant concentration of surface carboxyl groups, irrespective of the particle size. In other words, the particle size obtained is the size that corresponds to a constant surface concentration of acid groups derived from the anionic stabilising groups.

Relationship between particle size distribution and DMPA content is identical with that of average particle size and DMPA content. A smaller particle size is accompanied by a narrower particle size distribution (Kim and Kim (1991b)).

Anionic stabilising groups vs. Emulsion viscosity

Kim and Kim (1991a) and Kim and Lee (1996) observed that emulsion viscosity increases slowly at low DMPA concentration and rapidly at high DMPA concentration (figure 2.4). They explained the results by the fact that the diffusing electrical double layers grow, while the absorption of water into the particle also increases, with increasing hydrophilicity of the PU ionomer. These together augment the hydrodynamic volume of the particles under motion, to which the emulsion viscosity is proportional, linearly at low and non-linearly at high particle concentration. It seems that as the DMPA concentration increases, non-linear terms become significant owing to the increased hydrodynamic volume of the particles. Kim et al. (1991) also observed that smaller particles will lead to larger hydrodynamic volume, and hence increased viscosity, at a fixed total solid content.

Anionic stabilising groups vs. Contact angle

The contact angle of a water droplet on the emulsion-cast film decreases with increasing DMPA content. This is due to the increasing hydrophilicity of the film. At low concentration (≤ 6 wt.-%), this decrease is insignificant, but it becomes

significant at relatively high DMPA contents. This tendency is similar to the relation of particle size and viscosity with increasing DMPA concentration (Kim and Kim (1991a); Kim and Lee (1996)).

Other stabilising groups

The above discussions are based on various aspects of the effect of anionic stabilising groups only. That is because similar effects on particle size (and its distribution), emulsion viscosity and contact angle were reported for polymer cationomer which incorporate N-methyl diethanolamine (MDEA), i.e. a cationic stabilising group, into the PU backbone (Lee and Kim (1994); Lee and Kim (1995)).

When non-ionic hydrophilic segments are used, similar results can again be expected. However, in this case, it is important to carry out reaction and dispersions below the temperature that will cause the loss of hydrophilic sensitivity of the non-ionic segment. Failing to do that will cause particle size and its distribution to be independent of the non-ionic segment contents (Kim and Kim (1991a)). Also, when the non-ionic diol is utilised to attain a given particle size, a larger concentration is required than when DMPA is in use (Satguru et al. (1994)).

2.5.2 Counterions

The dispersity of PU anionomer depends not just on the anionic content of pre-polymer, but also on the type of counterions used (Chen and Chen (1992)). They found that the number (d_N) and weight (d_w) average diameter of particles can be arranged in the order of TEA > TMA > AMM > KOH > LiOH > NaOH (for neutralisation of 90% of the -COOH content). Absolute values of the Zeta potential, however, are in the opposite order. Their results showed that smaller particle sizes are obtained at higher Zeta potential.

Chen and Chen (1992) also found that polydispersities of the dispersions containing alkali metal cations are almost constant ($d_w/d_N = 1.60-1.63$) regardless of the difference in the Zeta potential. Dispersions containing ammonium cations result in a narrower particle-size distribution ($d_w/d_N = 1.32-1.46$). This can be attributed to the sharpening effect of the particle coagulation caused by the low Zeta potential.

According to Schlarb et al. (1995a), surface tension of the emulsion decreases rapidly with salt concentration and levels off at concentrations higher than 20 mmole/l. Dispersions containing alkali metal cations exhibit similar surface tension and show a value of 42 dyne/cm at a concentration of 45 mmole salt groups/l. However, the surface tension of dispersions containing ammonium cations decreases with the alkyl length of the ammonium cations. This means that the surface energy depression of the dispersions depends not only on the concentration of the PU anionomer but also on the surface activity of the counterions.

2.5.3 Degree of neutralisation (DN) (or degree of ionisation)

Many workers have confirmed the importance of neutralisation of the ionisable functional groups. Padget (1994) stated that the water solubilisation effect is greater when the group is in its ionised (salt) form. Lee and Kim (1995) also said that before being neutralised by acid, cationic functional groups (e.g., N-methyl diethanolamine (MDEA)) will simply contribute to the hard segments content of PU ionomer. However, upon neutralisation, it becomes an ionic centre that is inherently hydrophilic. Therefore, in the case of PU ionomer dispersions, ionisation and neutralisation of the ionomeric groups take place at the same time.

B.K. Kim leads a series of works on ionically stabilised aqueous PU dispersion using both anionic stabilising group, e.g., DMPA (Kim and Lee (1996); Lee et al. (1997)) and cationic stabilising groups, e.g., MDEA (Lee and Kim (1994 and 1995)). All these workers observed a similar pattern of changes in various variables following the changes in degree of neutralisation (DN).

Figure 2.6 shows particle size and emulsion viscosity as functions of DN for two MDEA contents (Lee and Kim (1995)). Again, smaller particles are formed at higher DN due to increased hydrophilicity of the PU ionomers. At high DN, the effectiveness of hydrophilicity in decreasing the particle size is largely offset by the increased swelling by water. With more swelling at high DN, the viscosity of the emulsion increases rapidly, driven primarily by the electroviscous effect. At the same DN, emulsions with smaller particles have larger emulsion viscosity (larger effective volume of dispersed phase), and the difference is pronounced at high DN. Due to the increase in hydrophilicity, contact angle of water droplets on film cast from the final

emulsion product was also found to decrease from about 80° at 70% DN to 70° at 100% DN (Lee and Kim (1994)).

The above relationship between DN and particle size of the ionically stabilised PU ionomer dispersion is also applicable to other water-based polymer latices. Ellis (1992) found that the hydrophilicity of epoxy resins is controlled by the DN of pendant acid groups. Li et al. (1997) found that the average particle size of carboxylated polystyrene ionomers also increases with decreasing DN.

2.5.4 Molecular weight of polyol

Lee and Kim (1994) used polytetramethylene adipate glycol (PTAd) as a constituent of PU cationomer dispersions. According to Lee and Kim (1994), as molecular weight of PTAd, $(MW)_{PTAd}$, increases from 600 to 2000, the block length of the soft segments increases while hard segment decreases from 68 to 61 %. Although hydrophilicity of PU cationomer decreases with the length of soft segments supplied by PTAd, particle size was found to decrease asymptotically with $(MW)_{PTAd}$. Therefore, the decrease in particle size in this case is not driven by the hydrophilicity of PU cationomer. Lee and Kim (1994) suggested that the increase in chain flexibility of PU cationomer, which causes the viscosity of the pre-polymer to decrease, is caused by the increasing $(MW)_{PTAd}$. This leads to a finer break-up of dispersed phase during inversion and easier formation of micelle structure in water. A similar relationship between particle size and molecular weight of polyol was found when polypropylene glycol is used to produce PU anionomer dispersion (Kim and Kim (1991c); Kim et al. (1994)).

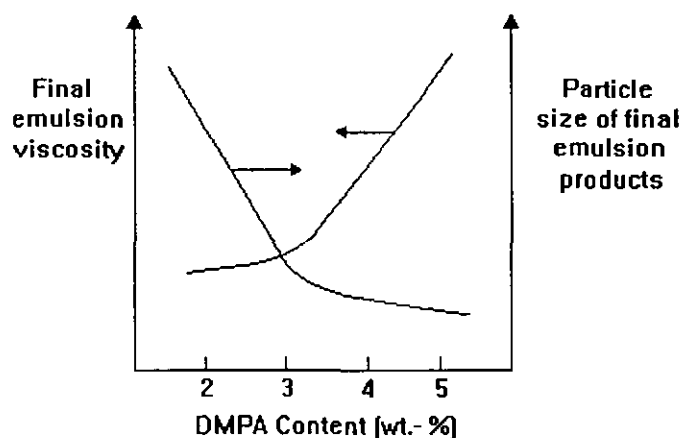


Figure 2.4. Particle size and emulsion viscosity as a function of DMPA content

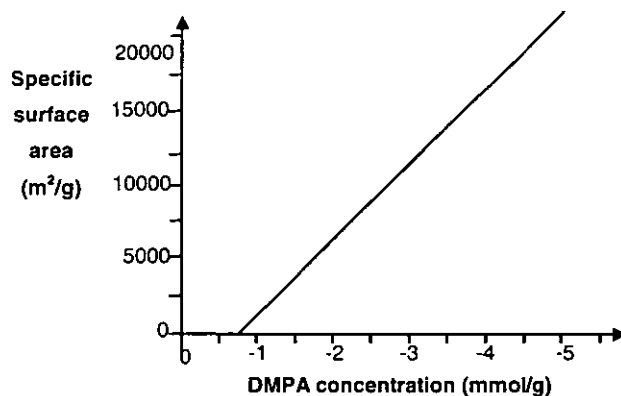


Figure 2.5. Specific surface area vs. DMPA concentration [reproduced from Satguru et al. (1994)]

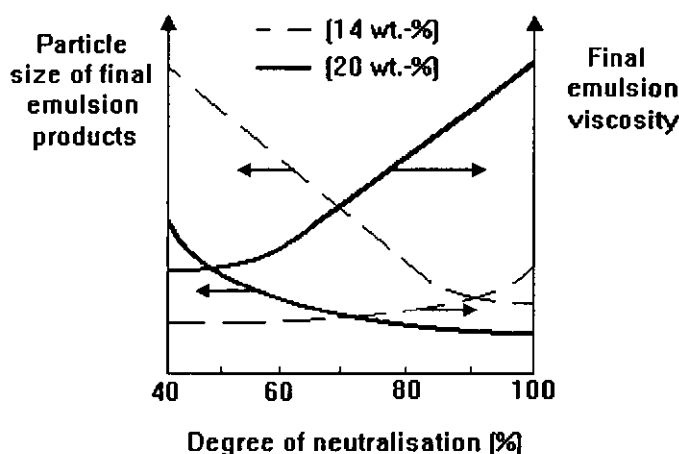


Figure 2.6. Particle size and emulsion viscosity vs. DN at two MDEA contents [reproduced from Lee and Kim (1995)]

2.6 Processing and solution factors

Yang et al. (1995) studied the effect of 5 processing and solution factors: (1) Catalyst concentration; (2) Agitation rate; (3) Phase inversion temperature; (4) Water addition rate; and (5) solvent/PU ratio. From their study, they identified that phase inversion temperature, water addition rate and solvent/PU ratios have significant influences on average particle size of PU ionomer dispersions. They also found that although some variables might not be important on their own, they will have significant influences on average particle size of PU ionomer dispersions when they interact with other variables. Three most significant combinations of variables identified are that of (1) catalyst concentration and phase-inversion temperature; (2)

solvent/PU ratio and phase inversion temperature; and (3) solvent/PU ratio and agitation rate.

2.6.1 Water addition rate

Yang et al. (1995) showed that coagulation of large particles takes place in the aqueous phase at high water addition rate. They attributed this result to the cations that are not uniformly hydrated in aqueous solution at high water addition rate. This local particle coagulation leads to hydrophobic associates that have trouble rearranging to microspheres, and therefore forming larger particles. In their work, drop size of the final emulsion products increased from 100 to 175 nm when water addition rate increased from 2 to 4 ml/minutes.

2.6.2 Phase inversion temperature

Yang et al. (1995) showed that phase-inversion temperature is the dominating factor that affects the average particle size of PU dispersions, compared to those of catalyst addition and solvent/PU ratio. It was found that particle size of the PU ionomer dispersion decreases with increasing phase-inversion temperature. Also, the effects of solvent/PU ratio and catalyst addition are more significant at low temperature.

During the preparation of water-borne, non-ionic, epoxy resin dispersions, Yang et al. (1997a) found that the amount of water required at the phase inversion point decreases with reducing phase inversion temperature. They attributed this result to the increasing water-polymeric emulsifier interaction, which leads to increased hydrophilicity of the polymer.

2.5.3 Solvent content

When considering the combined effect of solvent/PU ratio, phase-inversion temperature, and agitation rate, Yang et al. (1995) found that the effect of phase-inversion temperature on average particle size is significantly greater at a larger solvent/PU ratio. Large particles were obtained at high solvent/PU ratios and low phase inversion temperatures. This was attributed to swelling of polymers in contact

with large amount of solvent and difficulties experienced by the hydrophobic associates in rearranging to microspheres during the dispersion process.

At high solvent/PU ratio, the increase in agitation rate results in increasing average particle size. However, at low solvent/PU ratio, increasing agitation rate causes a decrease in average particle size. Under vigorous agitation, the former result is attributed to polymer swelling, while the latter case was explained in terms of well-dispersed hydrophobic associates readily forming microspheres.

Gu et al. (2000) studied the effect of solvent on the particle size of water-borne sulfonated poly(phenylene oxide) ionomer dispersion. They found that particle sizes of an emulsion using low polarity solvents were larger than those using high polarity solvents. This is because the ion-containing segments of the sulfonated poly(phenylene oxide) are more evenly distributed in the solvent system with high polarity. During the production of cationic epoxy resin latex, Lee and Yang (1992) found that a minimum concentration of organic solvent is required to produce any stable emulsion. The influences of other process and solution factors on particle size during the production of aqueous polymeric nanodispersions using a “reversible salting-out” process were also studied by Allemann et al. (1992).

2.7 Liquid-liquid dispersion

Methods employed for dispersing two immiscible liquids together can generally be classified as either a direct dispersion method or a phase inversion method. When applying these dispersion methods to produce aqueous polymer latices, a direct dispersion method includes those processes which involve dispersing polymer (dispersed phase) into aqueous phase (dispersed medium or continuous phase) directly. On the other hand, a phase inversion method describes dispersion processes that involve a phase change. When a small amount of water is added to an immiscible polymer phase, the water will be dispersed as water-in-polymer drops (W_1/P_C) with a little help from agitation. Further addition of water will cause an ever-increasing water-to-polymer ratio. This eventually creates instability to the system at a certain high concentration of water. Following addition of more water, this instability gives rise to a dispersion of polymer colloids in aqueous phase (P_1/W_C), that is, catastrophic phase inversion occurs. Conversely, starting with a small amount of

polymer in water will eventually lead to the opposite inversion when more polymers are added. The inversion process has not yet found much usage in preparing polymeric emulsions, but has found extensive usage in producing emulsions containing oil and water.

2.8 Direct dispersion

Hinze (1955) described two ways of dispersing one liquid into another immiscible liquid directly. One is by injecting a dispersed phase into the other. In this case, potential energy of the dispersed phase is converted into kinetic energy, and it interacts with the continuous phase at the same time. This interaction generates forces in the dispersed phase and results in its breaking up. Equipment that utilises this concept includes fine clearance valve homogenisers (Davies (1985 and 1987)) and the Kenics static mixer (Berkman and Calabrese (1988)). Another way of dispersing liquids is by inducing turbulence in the continuous phase. In this case, the kinetic energy of the turbulent motion in the continuous phase brings about the break-up of the other dispersed phase. Typical example of this concept is the mixing of immiscible liquids in baffled or non-baffled stirred tanks fitted with some sort of agitator. This method is most commonly used in preparing liquid-liquid dispersions. Figure 2.7 (at the end of the section) shows some of the agitator designs used in the industries (Sinnott (1993)).

2.8.1 Hydrodynamic mechanism and forces controlling drop break-up

In general, the disintegration of dispersed phase during the aforementioned dispersion processes proceeds in stages. Initially, the bulk of dispersed phases break-up into “chunks” of fluids. Then, they disintegrate further through a mechanism described as “the penetration of lamellae and ligaments of one fluid into the other” by Hinze (1955). The ligaments further break-up into globules, which may disintegrate again into smaller drops of different sizes. Hinze (1955) identifies the three basic types of globule deformations that may exist in different flow fields as follows:

Type 1 (Lenticular deformation): - The globules flattened to form oblate ellipsoidal shapes during the initial stage of deformation. Subsequent stages, leading to the break-up of these globules, depend on the magnitude of external forces causing the deformation;

Type 2 (Cigar-shaped deformation): - The globules elongate more and more, forming prolate ellipsoidal shapes. Ultimately, they elongate into long cylindrical threads, which then break-up into droplets.

Type 3 (Bulgy deformation): - Bulges and protuberances occurred as the surfaces of globules are deformed locally. These lead to separations of parts of the globules.

The break-up of globules will occur if the flow pattern, which causes a specific deformation, is large enough to contain the deformed globule and persists long enough (i.e., if there is a sufficient degree of deformation). Whether the break-up can take place depends on the relative magnitude of the external deforming forces and internal restoring forces (Zhou and Kresta (1998a)). In general, the deforming forces are mainly a viscous stress and/or a dynamic pressure due to velocity gradients in the continuous phase surrounding a globule. At the same time, flows in the globules generate viscous stresses and/or dynamic pressures to counteract the deformations (internal restoring forces).

The internal restoring stresses (defined as forces per unit area) are as follows:

(1) The interfacial-tension stress,
$$E_{IT} = \sigma d \quad [2-2],$$

where σ is the interfacial tension (in dyne/cm or kg/s^2) and d is the drop diameter (in cm).

(2) The viscous stress inside the droplet,
$$E_{IV} = \left(\frac{\mu_d}{d} \right) \sqrt{\frac{\tau}{\rho_d}} \quad [2-3].$$

μ_d (in cPs or $\text{kg/m}\cdot\text{s}$) and ρ_d (in kg/m^3) is the viscosity and density of the dispersed phase relatively, and τ is the external force per unit surface area.

The external deforming stresses (defined as forces per unit area) are as follows:

(3) The stress causes by turbulent pressure fluctuations, E_{PF} , can be approximated by,

$$E_{PF} = \rho_c \cdot \overline{u^2(d)} \quad [2-4],$$

where subscript c refers to the continuous phase and, $\overline{u^2(z)}$ is the mean square of relative velocity, $u(z) [= u(z_1) - u(z_2)]$, between any two points with z distance apart.

(4) The external viscous shear stress,
$$E_{EV} = \mu_c \cdot \left(\frac{\partial u}{\partial z} \right) \quad [2-5],$$

where u , z , μ and subscript c carry the same meanings as the aforementioned symbols.

Hinze (1955) suggested two dimensionless groups to account for the force balance between the aforementioned internal restoring force and external deforming force. These dimensionless groups are a “generalised” Weber number,

$$We' = \tau d / \sigma \quad [2-6]$$

and a viscosity group,
$$V_i = \frac{\mu_d}{\sqrt{\rho_d \cdot \sigma_d}} \quad [2-7]$$

Hinze has also shown experimentally that break-up occurs at a critical “generalised” Weber number, We'_{crit} .

2.8.2 Kolmogoroff theory of local isotropy

The Kolmogoroff theory of local isotropy has been reviewed and applied extensively to qualitatively predict the influence of turbulence on both break-up and coalescence of an individual droplet (Shinnar and Church (1960); Shinnar (1961)). Both large and small fluid eddies exist in a turbulent flow field. At high Reynolds number, most of the kinetic energy of the main flow that is contained in the large eddies is transferred to the intermediate eddies, and then to the smallest eddies. The kinetic energy is transferred from the large eddies to the small eddies, in different directions, without energy dissipation. Therefore, when eddies are much smaller than the primary eddies, it is possible to assume that the small eddies are statistically independent of the primary eddies. Hence “the only remaining information received by these small eddies from the primary eddies is the amount of kinetic energy transferred by them to the smaller eddies” (Shinnar (1961)).

If z_1 and z_2 are two points in a small volume of fluids under consideration and z is the radius vector, $z_1 \cdot z_2$, then all eddies much larger than z will contribute little to $\overline{u^2(z)}$. In other words, $\overline{u^2(z)}$ is mainly determined by the small eddies. A local isotropy can therefore exist if the volume under consideration is much smaller than the macroscopic length scale of the non-isotropic main flow, L (i.e., $z \ll L$). Hence,

when $z \ll L$, $\overline{u^2(z)}$ is only a function of the kinetic viscosity of fluid, ν , and of the local energy dissipation rate per unit mass, ε . The local energy dissipation rate per unit mass is defined as,

$$\varepsilon = C_1 N^3 D_a^2 \quad [2-8]$$

where N is the agitator speed (in rps or rpm) and D_a is the diameter of the agitator (in m). Another parameter, the microscopic length scale of turbulence (η) has also been defined by Kolmogoroff as,

$$\eta = \left(\frac{\nu^3}{\varepsilon} \right)^{1/4} \quad [2-9]$$

In stirred tanks, the local isotropy theory is valid when the Reynolds number is above 10^4 . Under the local isotropy condition ($z \ll L$), and when z is much larger than the scale η , ν can be neglected (the inertial sub-range). However, when $z \ll \eta$, ν can no longer be neglected (the viscous sub-range). Under these two conditions, the relationships between $\overline{u^2(z)}$, ε , ν can be written as (Shinnar and Church (1960)),

$$\text{Inertial sub-range } (L \gg z \gg \eta): \quad \overline{u^2(z)} = C_2 (\varepsilon \cdot z)^{2/3} \quad [2-10]$$

$$\text{Viscous sub-range } (z \ll \eta): \quad \overline{u^2(z)} = C_3 \frac{\varepsilon}{\nu} z^2 \quad [2-11]$$

where C_2 and C_3 are universal constants.

2.8.3 Maximum and minimum stable drops in turbulent liquid-liquid dispersions

The performances of heat and mass transfer in many heterogeneous processes depend largely upon the size of dispersed droplets and their interfacial area. During the preparation of liquid-liquid dispersions, break-up and coalescence of droplets occur simultaneously until a dynamic equilibrium is reached.

Maximum drop diameter

As mentioned before, droplets break-up at a certain value of We'_{crit} . Therefore, there exists a maximum drop diameter (d_{max}) above which stable drops cannot exist. By considering the relative influence of internal restoring and external deforming

forces, many workers have derived equations to correlate d_{max} with the geometries of the turbulent stirred tanks and properties of the fluids in the dispersions (Hinze (1955); Shinnar (1961); Sprow (1967a)).

In the inertial sub-range ($L \gg z \gg \eta$), the drops break-up when the ratio of turbulent pressure fluctuation stress to interfacial-tension stress is equal to We'_{crit} . i.e.,

$$\frac{E_{PF}}{E_{IT}} = We'_{crit} \Rightarrow \rho_c \overline{u^2(d)} \cdot \left(\frac{d_{max}}{\sigma} \right) = \text{Constant} \quad [2-12]$$

By substituting equation (2-10) and (2-8) into equation (2-12), Shinnar (1961) derived the following equation for d_{max} in turbulent agitated vessel:

$$\frac{d_{max}}{D} = C_4 \left(\frac{\rho_c N^2 D_a^3}{\sigma} \right)^{-3/5} = C_4 (We)^{-0.6} \quad [2-13]$$

where Weber number, $We = \rho_c N^2 D_a^3 / \sigma$. In the viscous sub-range ($d \ll \eta$), the external viscous shear stress contributed to the break-up of droplets. Sprow (1967a) mentioned that the We'_{crit} in the viscous sub-range is a function of the ratio of dispersed phase viscosity to continuous phase viscosity, $f\left(\frac{\mu_d}{\mu_c}\right)$. Therefore,

$$\frac{E_{EV}}{E_{IT}} = We'_{crit} \Rightarrow \mu_c \left(\frac{\partial u}{\partial r} \right) \cdot \left(\frac{d_{max}}{\sigma} \right) = f\left(\frac{\mu_d}{\mu_c}\right) \quad [2-14]$$

From equation (2-11),

$$\frac{\partial u}{\partial r} = C_5 \left(\frac{\varepsilon}{\nu} \right)^{1/2} \quad [2-15]$$

By substituting equation (2-15) and (2-8) into equation (2-14), Sprow (1967a) also derived the following equation,

$$d_{max} = C_6 \cdot \sigma \cdot \nu_c^{1/2} \cdot \mu_c^{-1} \cdot N^{-3/2} \cdot D_a^{-1} \cdot f\left(\frac{\mu_d}{\mu_c}\right) \quad [2-16]$$

Minimum drop diameter

In agitated liquid-liquid dispersion, coalescence becomes significant and cannot be neglected when the concentration of the dispersed phase is sufficiently large. Coalescence between any colliding droplet pairs depends on the relative magnitude of the external deforming force and the force of adhesion. Shinnar (1961)

defined this force of adhesion between the colliding droplet pair as $A(h_o)$, where h_o is the distance between the two droplets concerned. Since coalescence between droplets is prevented by the turbulent pressure fluctuation force in the inertial sub-range, the minimum drop diameter (d_{min}) can be determined by:

$$\frac{E_{PF} \cdot (area)}{A(h_o)} = \frac{C_7 \cdot \rho_c \cdot \overline{u^2(d)} \cdot d_{min}^2}{A(h_o)} = \text{Constant} \quad [2-17]$$

By substituting equation (2-10) and (2-8), equation can be written as,

$$d_{min} = C_8 \cdot \rho_c^{-3/8} \cdot N^{-0.75} \cdot D_a^{-0.5} \cdot A(h_o)^{3/8} \quad [2-18]$$

Sprow (1967b) applied similar derivation to the viscous sub-range whereby any coalescence between droplets is prevented by the external shear force. In this case, the d_{min} can be determined by:

$$\frac{E_{EV} \cdot (area)}{A(h_o)} = \frac{C_9 \cdot \mu_c \cdot \left(\frac{\partial u}{\partial z}\right) \cdot d_{min}^2}{A(h_o)} = \text{Constant} \quad [2-19]$$

By substituting equation (2-15) and (2-8) into equation (2-19), d_{min} becomes,

$$d_{min} = C_{10} \cdot A(h_o)^{0.5} \cdot \mu_c^{-0.5} \cdot \nu_c^{0.25} \cdot N^{-0.75} \cdot D_a^{-0.5} \quad [2-20]$$

Simultaneous break-up and coalescence

In reality, simultaneous break-up and coalescence of droplets determine the actual drop size distribution in agitated dispersions. Therefore, the diameters defined in previous equations are in fact statistical averages indicating whether drop break-up is most likely to occur [equations (2-13) and (2-16)] or drop coalescence is the dominating factor [equations (2-18) and (2-19)] under specific operating conditions. When drop diameter is proportional to N^{-a} , where a is between 1.2 to 1.5, the dispersions is “break-up controlled”; and when drop diameter is proportional to $N^{-0.75}$, the dispersion is “coalescence controlled” (Shinnar (1961)). Church and Shinnar (1961) showed that the aforementioned relationships between d and N can be combined with that of maximum droplet size in a suspension, $d_{max}(\text{suspension})$, to determine the “area of droplet stability” for turbulence-stabilised dispersions. They proposed that $d_{max}(\text{suspension})$ can be correlated to N as,

$$d_{max}(\text{suspension}) = C_{11} \varepsilon^2 \left(\frac{\rho_c}{\rho_d - \rho_c} \right)^3 f \left(\frac{\phi_d}{\phi_c} \right)$$

$$\Rightarrow d_{max}(\text{suspension}) = C_{11} N^6 D_a^4 \left(\frac{\rho_c}{\rho_d - \rho_c} \right)^3 f \left(\frac{\phi_d}{\phi_c} \right) \quad [2-21]$$

where $f\left(\frac{\phi_d}{\phi_c}\right)$ is an empirical function of the volume ratio of dispersed phase and continuous phase.

2.8.4 Other aspects of liquid-liquid dispersions in turbulent stirred tank

Since Sprow (1967a) started to assume that Sauter mean diameter (d_{32}) is directly proportional to d_{max} (i.e., $d_{32} = C_{12} \cdot d_{max}$), this relationship has been verified experimentally by many researchers. The reported value of C_{12} varied from 0.38 to 0.7 in different liquid-liquid systems studied by workers such as Sprow (1967a), Calabrese et al. (1986a and 1986b) and Zerfa and Brooks (1996). Based on this assumption and some correlations in the form of equation (2-13), many researchers have correlated d_{32} to the properties of the fluids in the dispersions and the geometries of the turbulent stirred tanks. Some of the vast amounts of correlations that have been reported in literature are summarised in table 2.4.

In table 2.4, d_o is d_{32} of an inviscid drop, $V_i' = [(\rho_c/\rho_d)^{0.5} \cdot \mu_d \varepsilon^{1/3} \cdot d_{32}^{1/3}] / \sigma$, $Re = \rho_c \cdot N \cdot D_a^2 / \mu_c$ and $V_i'' = (\mu_d \cdot N \cdot D_a / \sigma) \cdot (\rho_c/\rho_d)^{0.5}$. A more detailed review of similar correlation has been published by Zerfa (1994) and Zhou and Kresta (1998a). Despite all this well-developed usage, the linear relationship between d_{32} and d_{max} has recently been questioned by Pacek et al. (1998) and Zhou and Kresta (1998a). By considering a normal drop size distribution, Pacek et al. (1998) derived an equation to show that d_{32} depends non-linearly on both d_{max} and d_{min} . Based on some experimental work, Zhou and Kresta (1998a) showed that $d_{32} = C_{12} \cdot d_{max}$ becomes invalid when operating conditions change dramatically. They followed through to suggest that d_{32} is better correlated using the maximum energy dissipation rate.

Table 2.4. Some correlation of d_{32} for liquid-liquid dispersion in stirred tanks,

Investigators	Correlations	ϕ_d	N (rps)	Impeller type	Dispersed / Continuous phase
Sprow (1967a)	$d_{32}/D_a = 0.0524 We^{-0.6}$	< 0.015	4.2 ~ 33.4	6-bladed turbine	Iso-Octane / NaCl Solution
Chen and Middleman (1967)	$d_{32}/D_a = 0.053 We^{-0.6}$	0.001 ~ 0.005	1.33 ~ 1.67	6-bladed turbine	14 oil phases / water
Calabrese et al. (1986a)	$d_{32}/d_o = (1 + 11.5 Vi')^{5/3}$ (for moderate μ_d) $d_{32}/D_a = 2.1 (\mu_d/\mu_c)^{3/8} Re^{-3/4}$ (for high μ_d)	< 0.015	0.93 ~ 5.95	6-bladed Rushton type turbine	Silicone oil / Water
Wang and Calabrese (1986)	$d_{32}/D_a = 0.053 We^{-0.6} (1 + 0.97 Vi'^{0.79})^{0.6}$	< 0.002	1.4 ~ 4.7	6-bladed Rushton type turbine	Silicone oil / Methanol solution
Zerfa and Brook (1996)	$d_{32}/D_a = 0.027 (1 + 3.1 \phi_d) We^{-0.6}$	0.01 ~ 0.4	4.16 ~ 13.33	6-bladed turbine	Vinyl Chloride / Water + Poly(Vinyl Alcohol)
Pacek et al. (1998)	$d_{32}/D_a = 0.022 (1 + 23.3 \phi_d) We^{-0.43}$	0.005 ~ 0.1	3 ~ 8	6-bladed disc turbine	Chlorobenzene / water or NaCl solution

In a later work, Zhou and Kresta (1998b) recorded the occurrence of four different types of drop size distributions that evolved with increasing agitator speed. These are identified as the long tail, double peak, skew and skew normal distributions. Pacek et al. (1998) also observed the transition of a bimodal distribution to a monomodal distribution as agitator speed increases. Due to these observations, Zhou and Kresta (1998b) proposed a new scaling-up parameter to define the transitions amongst the four types of distributions. The suggested parameter is the product of average power input per unit mass and $N \cdot D_a^2$.

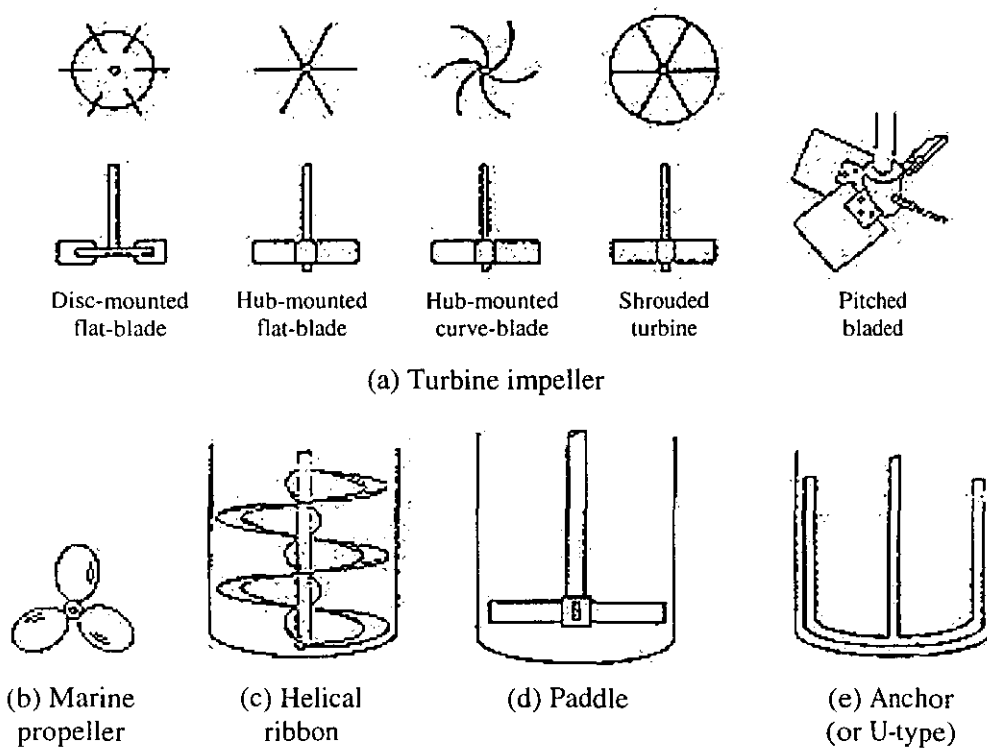


Figure 2.7. Some of the agitators used in industry

2.9 Phase inversion

In general, phase inversion refers to the phenomenon that occurs when an agitated emulsion of, for instance, oil droplets in water, changes its morphology and becomes an emulsion of water droplets in oil, or vice versa. For a “clean” system, it is customary to use the terms “oil phase” and “aqueous phase” to describe the emulsion. In practice, a third component, external stabiliser, is usually present at the phase interface. Brooks and Richmond (1991) and Zerfa et al. (1999) showed that either of the two phases in an oil-water system containing non-ionic surfactant can become the

continuous phase, depending on the system's composition and processing history. In a non-ionic surfactant-oil-water (nSOW) system, phase inversion can normally be induced by altering the surfactant's affinity for the oil and water phases (transitional phase inversion) or by changing the water phase to oil phase ratio (catastrophic phase inversion). Without changing the overall phase composition or phase ratio at the inversion step, Akay (1998) has recently managed to bring about the phase inversion by using equipment that provides high deformation rate (flow-induced phase inversion).

Due to the complexity of phase inversion, and the use of multicomponent surfactants, Brooks and Richmond (1991) argued that it is inappropriate to use conventional triangular phase diagrams to describe phase changes in a nSOW system. The solution they put forward is to use a phase inversion "map" to represent the dynamics of changes in the dispersions. A typical phase inversion map for a nSOW system is shown in figure 2.8 (at the end of this section).

Salager (1988) assigned a SOW mixture to one of the three groups defined using Winsor's concept of interaction energies. For a Winsor Type 1 mixture, the affinity of the surfactant for the aqueous phase exceeds its affinity for the oil phase and surfactant micelles can form in the aqueous phase. One or two phases can exist at equilibrium. In the two-phase region, an oil phase coexists with a surfactant-rich aqueous microemulsion. The oil phase contains dissolved water and surfactant at the critical micelle concentration. Therefore, agitation of Type 1 mixtures is expected to produce oil-in-(micelle-containing) water (O/W_m) emulsion. For a Winsor Type 2 mixture, micelles can form in the oil phase. Again, one or two phases can exist at equilibrium. In the two-phase region, an aqueous phase coexists with an oleic microemulsion. As a result, agitation of this type of mixtures is expected to produce water-in-(micelle-containing) oil (W/O_m) emulsions. For a Winsor Type 3 mixture, surfactant affinity for both phases is approximately equal and mixtures can form one, two or three phases. In the three-phase region, there is an oil phase and an aqueous phase. Both phases contain dissolved surfactant at (but not above) their respective critical micelle concentrations. The third phase (or a surfactant phase or middle phase) contains most of the surfactant together with solubilised oil and water. The microemulsion phase for a Type 3 mixture can be an oleic microemulsion (M_o), an aqueous microemulsion (M_w) or a surfactant phase (M_s).

The concept of interaction energies is similar to surfactant affinity difference (SAD), which is applied to the phase inversion map shown in figure 2.8. SAD is equal to zero at the occurrence of “optimum formulation”, i.e. when a Winsor Type 3 system occurs. With positive SAD, Winsor Type 2 phase behaviour can be observed. With negative SAD, Winsor Type 1 phase behaviour can be observed.

Phase inversion maps can be represented equally well by replacing SAD with hydrophile-lipophile balance (HLB) values. In this case, Type 3 phase behaviour will occur, again, close to the lines where $SAD = 0$. Then, Type 2 behaviour will occur when HLB values are lower than those required for $SAD = 0$ and Type 1 behaviour occurs when HLB values are higher than those required for $SAD = 0$. According to Brooks and Richmond (1991), the advantage of the phase inversion map is that, the result of changing HLB and water fraction in a particular system can be predicted from the path on the inversion map (providing that the starting condition is known).

2.9.1 Transitional phase inversion

As mentioned earlier, transitional inversion is brought about by changing the surfactant's affinity for the oil and water phases. By changing SAD across the region where $SAD = 0$, a transitional inversion will happen (Salager (1988)). As SAD is a function of surfactant hydrophile-lipophile balance (HLB), temperature, oil type and salt concentration, a transitional inversion can be induced using the idea of phase inversion temperature (PIT) (Shinoda and Friberg (1986)) or by altering the HLB at constant temperature (Brooks and Richmond (1994a-c)). Brooks and Richmond (1991) showed that five stages are involved during the transitional inversion process across the $SAD = 0$ line. The phases at each stage across the transition are shown schematically in figure 2.9.

In a later study, Brooks and Richmond (1994c) confirmed this mechanism through the drop size analysis of emulsions at different stages during the transition from SAD^+ to SAD^- . They found that, for Winsor Type 1 and 2 emulsions, drop size decreases and emulsification rate increases as SAD approaches zero value. This result was attributed to the change of interfacial tension across the phase transition. They found that the drop sizes of Winsor Type 3 emulsions are not affected by agitation conditions (for a low-viscosity oil phase system) and are only dependent on the surfactant type and its concentration. They also shown that the drop sizes of Winsor

Type 3 emulsions are controlled by the maximum area of coverage of interfacial surfactant in the system.

The advantage of transitional phase inversion is that it can produce extremely fine emulsions with low energy input and, therefore, provides a more attractive emulsification route than direct emulsification. Brooks and Richmond (1994c) also found that the “finest” O/W_m emulsion that can be produced by this method is through inversion from an O/M_w state. They suggested that when the system has a high oil phase viscosity, the transitional inversion point should be approached with inviscid water as the initial continuous phase to produce a fine emulsion.

By considering the partitioning of non-ionic surfactants between the three phases of Winsor Type 3 emulsions, Brooks and Richmond (1994a) derived a model that can be applied to isothermal transitional phase inversion process. They used the model to consider the effect of surfactant concentration. The surfactant and the two oil phases used in their study are polyoxyethylene nonylphenylethers (NPE), cyclohexane and toluene respectively. Based on the same model, Brooks and Richmond (1994b) showed that isothermal transitional phase inversion of NPE-oil-water systems occur at a specific Gibbs free energy, irrespective of the oil type.

The continuity of transitional phase inversion lines and drop size reductions at the transitional phase inversion points were questioned by some recent work. Zerfa et al. (1999) discovered that transitional phase inversion occurs at either low or high water volume fraction when polyoxyethylene sorbitan monolaurate (SML) surfactants was used to stabilise *p*-xylene-water emulsions. The gap, in the middle range of water volume fraction where inversion did not occur, was found to reduce with increasing SML concentrations. In a later work, Zerfa et al. (2000) showed that multiple water-in-oil-in-water (W/O/W) drops were present during the transitional phase inversion process for the production of SML-polyisobutene-water emulsions. They attributed the lack of drop reduction at the transitional phase inversion point of the SML-polyisobutene-water system to the presence of the multiple emulsions.

2.9.2 Catastrophic phase inversion

As mentioned before, catastrophic inversion can be obtained by altering the system's water-to-oil ratio. In contrast to transitional phase inversion, where the

solution factors dominate the phase inversion characteristics and dampen the effect of other processing factors, catastrophic inversion depends mainly on other processing factors. These include the type and strength of flows (Akay (1998)), the viscosity of both phases (Brooks and Richmond (1994e); Norato et al. (1998)), the configuration of the vessel (Gilchrist et al. (1989)), the agitator speed (Brooks and Richmond (1994d)), the wetting characteristic of the impeller (Kumar et al. (1991)) and the nature (composition) of the initial continuous phase (Pacek et al. (1994a)).

As early as 1910, Ostwald proposed that catastrophic phase inversion occurs as a result of the complete coalescence of the unstable dispersed phases at a closest packing arrangement of the drops (Brooks and Richmond (1994e)). For a clean oil-water (O-W) system (i.e., in the absence of external surfactants), there is an “ambivalence” region in which either phase can be dispersed. By assuming that phase inversion takes place when coalescence occurs at every collision, Arashmid and Jeffrey (1980) derived a model to predict the phase inversion loci and the ambivalence region. The model correlates the dispersed phase hold-up to the agitator speed and the physical properties of the systems using the following equation,

$$\frac{N_{Coalescence}}{N_{Collision}} = \frac{C_{13}}{\phi_d \cdot d_{32}^2 \cdot N^{0.46}} \quad [2-22]$$

where $N_{Coalescence}$ and $N_{Collision}$ are the frequencies of coalescence and collision respectively. Catastrophic phase inversion occurs when $N_{Coalescence}/N_{Collision} = 1.0$, in which case, ϕ_d can be treated as the volume fraction of dispersed phase at the phase inversion point. C_{13} is a characteristic constant for specific O-W systems and agitator designs. d_{32} was related to the physical properties of the systems by,

$$d_{32} = C_{14} \left(\frac{\mu_c^3}{\rho_c^2 \cdot g} \right) \left(\frac{\rho_c \cdot \sigma^3}{\mu_c^4 \cdot g} \right)^{0.14} \left(\frac{\rho_c}{\mu_c \cdot g^4} \right)^{-0.32} N^{-2.88} + C_{15} \left(\frac{\sigma}{\mu_c^2 \cdot g} \right) \left(\frac{\Delta\rho \cdot \sigma^3}{\mu_c^4 \cdot g} \right)^{-0.62} \left(\frac{\Delta\rho}{\rho_c} \right)^{0.05} \phi_d \quad [2-23]$$

where $\Delta\rho$ is the density difference and the other symbols bear the same meanings as in other previously-mentioned equations.

One short fall of this model is that it fails to account for the occurrence of multiple drops during some catastrophic phase inversion process. When the initial dispersed phase is water, Pacek et al. (1994 a and b) presented evidence of multiple drops leading to the phase inversion. Conversely, for initially aqueous-continuous dispersions, no multiple drops were found before the inversion. They subsequently demonstrated that there is no delay time during the water-to-oil continuous inversion; but that delay times were present during the oil-to-water continuous inversions. The effective dispersed phase volume fraction in the latter case is greater than the actual dispersed phase volume fraction due to the incorporation of continuous phase as small droplets in the dispersed phase. This droplet incorporation process delays the inversion process, since inversions can occur when sufficient effective dispersed phase volume fraction was obtained.

Gilchrist et al. (1989) argued that the growth of droplets during the delay period is controlled by the relative rate of droplet break-up and coalescence. They followed on to show that any effects favouring droplet break-up will prolong the delay time and effects favouring droplet coalescence will reduce the delay time. The delay times reported by Gilchrist et al. (1989) are between 5 to 1,500 seconds. This phase inversion mechanism has recently been confirmed by Groeneweg et al. (1998) and Norato et al. (1998). Besides the coalescence that takes place in the quiescent region and in the impeller vortices (Gilchrist et al. (1989)), Kumar et al. (1991) have also shown that coalescence of drops can occur on the impeller. This phenomenon is caused by the wetting characteristic of the impeller and, according to Kumar et al. (1991), should also be incorporated into the phase inversion mechanism.

For a nSOW system, there are four ways to induce the catastrophic phase inversions (figure 2.8). Zerfa et al. (2000) classified these catastrophic phase inversion routes into two categories:

1. "Stable" catastrophic phase inversion (lines 'a' and 'b'): This is carried out by either adding a water phase to the surfactant-containing oil phase at low HLB (line 'a') or adding an oil phase to the surfactant-containing water phase at high HLB (line 'b'). No multiple drops are formed en-route to the phase inversion; and
2. "Unstable" catastrophic phase inversion (lines 'c' and 'd'): This is carried out by either adding a water phase (containing the same surfactant type) to the oil phase

(line 'c') or adding an oil phase (containing the same surfactant type) into the water phase (line 'd'). Multiple drops are formed before the inversion and they disappear after the phase inversion has taken place.

Considering oil phase as the initial continuous phase, Brooks and Richmond (1994d) proposed that the inverted O/W_m drops of the "unstable" catastrophic inversion can be produced by one of the following four mechanisms:

- (i) Surfactant gel-phase microemulsions mechanism: The smallest oil drops are formed from the dissolution of surfactant gel into the water drops at equilibrium. This process takes place at the presence of low water content;
- (ii) Emulsification at drop surface mechanism: Small oil drops are incorporated into the W_m/O drops due to the tendency of the surfactant to form concave interfaces towards the oil phase at the O-W interface. The size of the oil drops depends on the turbulent eddies and is comparable to drops produced by direct emulsification;
- (iii) Localised catastrophe mechanism: Oil drops are trapped between localised coalescing water drops. Hence, the size of the oil drops (in the $O/W_m/O$ drops) depends on the size of the W_m/O drops, which increases as the volume fraction of water phase increases;
- (iv) Catastrophic inversion point mechanism: Similar to the localised catastrophe mechanism, but concerns oil drops formed at the final catastrophic inversion point. The oil drops formed by this mechanism are much larger than those formed by other mechanisms.

Brooks and Richmond (1994d) also showed that d_{32} of O/W_m drops ($d_{32,ow}$) is greatly affected by catastrophic mechanism [(iii) and (iv)]. For SML-cyclohexane-water system, where little multiple drops are formed before phase inversion, O/W_m drops are mainly produced by mechanism (iv). They also showed that d_{32} of the water drops in the $O/W_m/O$ drops ($d_{32,owo}$) is proportional to $N^{-1.2}$ (i.e., the process is break-up control). In a later paper, Brooks and Richmond (1994e) showed that $d_{32,owo}$ of a SML-polyisobutene/cyclohexane-water dispersion is proportional to $N^{-0.8}$ (i.e., the process is coalescence control). Both works reveals a linear relationship between $d_{32,owo}$ and $d_{32,ow}$. Using this relationship, Brooks and Richmond (1994e) devised a method that can be used to predict the "unstable" catastrophic phase inversion point

for a nSOW system. In a recent work, Zerfa et al. (1999) showed that the reduction in drop size could also occur during the “stable” catastrophic phase inversion process.

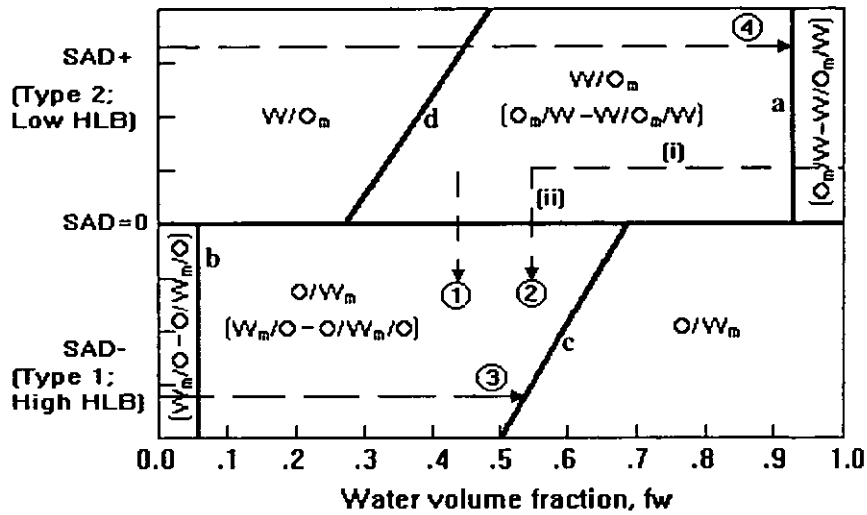
2.9.3 Other aspects of phase inversion

Poston and Stewart (1978) mentioned that discontinuities in the behaviours of natural phenomena might be interpreted, at least locally, by one of the seven elementary catastrophe models laid down by Thom. Later, Dickinson (1981) suggested that various aspects of a catastrophic phase inversion process, such as bimodality of emulsion mixtures and hysteresis of the dynamic process, could be modelled using this catastrophe theory. By using the second elementary (or Cusp) catastrophe, Dickinson (1981) demonstrated that both phase behaviours and emulsion inversion could be interpreted by means of the same state and control variables. Dickinson’s work revealed the hidden thermodynamic characteristic of emulsion formation and inversion process. However, the Cusp catastrophe model (being of fourth degree and only have two minimum states) cannot be used to explain the occurrence of three phases of a Winsor Type 3 mixture.

Salager (1985) solved this problem by adapting the fourth elementary (or Butterfly) catastrophe to model the behaviour of SOW systems. Gibbs free energy of SOW systems can be represented by the potential of the butterfly catastrophe as,

$$G_{abcd}(x) = \frac{1}{6}x^6 + \frac{a}{4}x^4 + \frac{b}{3}x^3 + \frac{c}{2}x^2 + dx \quad [2-24]$$

where x is the state variable (which is taken as the phase density in Salager’s work) and a, b, c, d are four control (or observable or measurable) variables. It was shown that phase behaviour represented on the bifurcation (c, d) plane of the butterfly catastrophe matches with the classical Winsor type III ternary diagram. Salager (1985) also suggested that the four control variables are surfactant concentration, water-to-oil ratio, deviation from optimum formulation and a parameter characterising the “quality” of the SOW system. Salager (1988) presented a detailed usage of the butterfly catastrophe in modelling both catastrophic and transitional phase inversion processes.



Applications of the phase inversion map,

Path	Start condition	Path condition (Inversion method [*])	End condition
1	W/O _m	W/M _o → (O+W)/M _s → O/M _w (T)	O/W _m
2 (i)	W	O _m /W + W/O _m /W (C)	-
2 (ii)	O _m /W + W/O _m /W	W/M _o /W → (O+W)/M _s → O/M _w (T)	O/W _m
3	O	W _m /O + O/W _m /O (C)	O/W _m
4	O	W/O _m (C)	W/O _m /W

Figure 2.8. Phase inversion map for a nSOW system

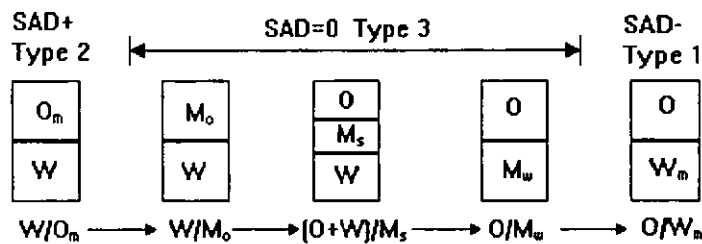


Figure 2.9. Schematic representation of transitional inversion from W/O_m → O/W_m[†]

^{*} T refers to the transitional inversion; C refers to the catastrophic inversion.

[†] (O+W)/M_s in figure 2.9 represents oil and water drops in a continuous surfactant phase.

2.10 Different type of emulsions and drop structures

2.10.1 Different type of emulsions

The aforementioned liquid-liquid dispersion processes can be used to produce different type of emulsions. Based on different known dispersion behaviours, Zeneca (1998) proposed the classification of any emulsion product into one of the following five categories:

Type 1 emulsion: (“Does not disperse”) The dispersed phase stays as a lump throughout the process;

Type 2 emulsion: (“Temporary dispersion”) The dispersed phase breaks-up to form big lumps of a few tens of microns during the dispersion process and coalesce as soon as the dispersion condition has stopped;

Type 3 emulsion: (“Unstable coarse emulsions”) The dispersed phase breaks-up to form droplets of a few microns. However, the emulsions and droplets produced are unstable;

Type 4 emulsion: (“Stable coarse emulsions”) The dispersed phase breaks-up to form droplets of a few microns. The emulsions and droplets produced are stable over a few hours; and

Type 5 emulsion: (“Stable emulsions”) The dispersed phase breaks-up to form nanosize droplets. The emulsions produced are stable over several hours or days.

2.10.2 Multiple emulsions

It was shown in section 2.9 that multiple emulsions (i.e., emulsions containing multiple drops) can be produced before and after catastrophic phase inversion processes. However, multiple emulsions produced using this method cannot be controlled easily. To solve this problem, Matsumoto et al. (1976) developed a two-step emulsification process for the production of stable and reproducible multiple emulsions. During the preparation of a multiple W/O/W emulsion, the first step of the process involves the production of a W/O emulsion using an organophilic emulsifying agent. The W/O emulsion is subsequently emulsified into an aqueous phase containing a hydrophilic emulsifying agent to produce the W/O/W emulsion. This

production method has been employed in scientific studies by other researchers (Davis and Burbage (1977); Florence and Whitehill (1981 and 1982)).

By using Glucose as a marker, Matsumoto et al. (1976) managed to study the yield of W/O/W emulsions under various processing conditions. It was shown that the ratio of the organophilic surfactant (in the oil phase) to the hydrophilic surfactant (in the aqueous phase) has a significant effect on the yield of W/O/W emulsions. Matsumoto et al. (1976) also found that a higher organophilic surfactant-to-hydrophilic surfactant ratio results in more multiple drops in the final emulsion product.

Florence and Whitehill (1981) managed to prepare three different types of multiple droplets by changing the type of surfactants used during the second step of the emulsification process. These three different types of multiple W/O/W drops can be classified as follows (figure 2.10):

Type A multiple drops: The O/W drops encapsulate only one large internal water drop (figure 2.10a);

Type B multiple drops: The O/W drops contain several small and well separated internal water drops (figure 2.10b);

Type C multiple drops: The O/W drops contain vast amount of small internal water drops that are arranged in close proximity (figure 2.10c).

According to Florence and Whitehill (1981), the aforementioned multiple drops did not exist exclusively in any emulsions produced in their study. However, the emulsions studied were always dominated by the existence of one of the three types of multiple drops. Therefore, three different types of multiple emulsions (A, B and C) were classified according to the predominant multiple droplet structures that existed in the emulsion of concern. Florence and Whitehill (1981 and 1982) also studied the breakdown pathway and stability of the multiple emulsions in great details.

For systems as complex as multiple emulsions, Myers (1988) highlighted the needs to employ a clear and consistent system of nomenclature. A future section of this thesis, section 6.6.5, discusses the shortfalls of various existing nomenclature systems for multiple emulsions. It is shown in the same section that a suitable nomenclature system should be based on the "location" of the different phases in the

multiple droplets. This nomenclature system is adopted throughout this thesis. Further details about this nomenclature system are shown in section 6.6.5 to avoid duplication of efforts by the readers.

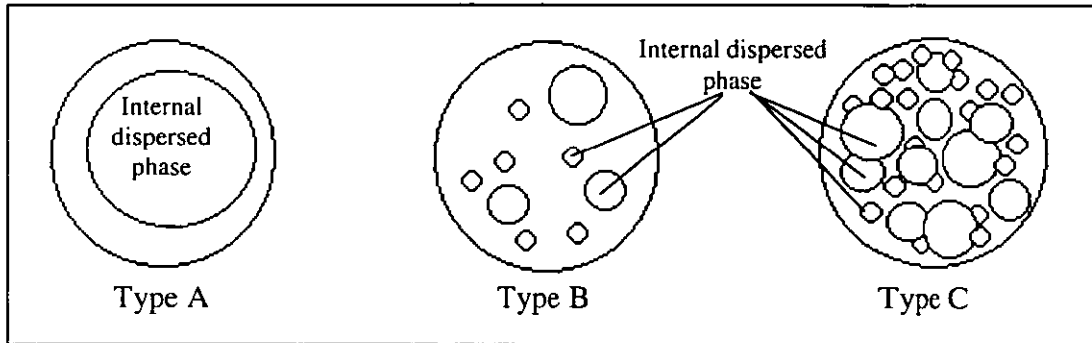


Figure 2.10. Classification of different multiple drops in multiple emulsions

CHAPTER 3

Experimental apparatus

This chapter describes equipment and experimental set-up used for this work. The first section refers to those used for various dispersion experiments. This is followed by descriptions of apparatus used for obtaining droplet information. Set-ups for viscosity and density measurements are also included in this chapter.

3.1 Dispersion experiments

Dispersion experiments carried out in this work can be grouped as catastrophic phase inversion and transitional phase inversion. This section describes the experimental set-ups for these experiments.

3.1.1 Dispersion section

Figure 3.1 shows a typical set-up used for the dispersion section. A glass water bath with a temperature controller was used to maintain a constant temperature throughout the dispersion process. The dispersion itself was carried out using a 700-ml round bottom glass vessel (dispersion vessel). Baffles were put into the dispersion vessel before a glass vessel cover was clamped onto the vessel using a flask clip. A turbine was then inserted through a stirrer gland into the centre of the dispersion vessel. Agitation was provided by an overhead fixed speed, torque changes (FSTC) agitator. A temperature indicator, connected to a thermocouple in the vessel, was used to show the actual temperature in the reactor during the dispersion process. Conductivity probe(s) was (were) connected to a conductivity meter to record the conductivity readings during the dispersion experiments. Initial dispersed phase was added through either a 20-ml syringe or a pipette.

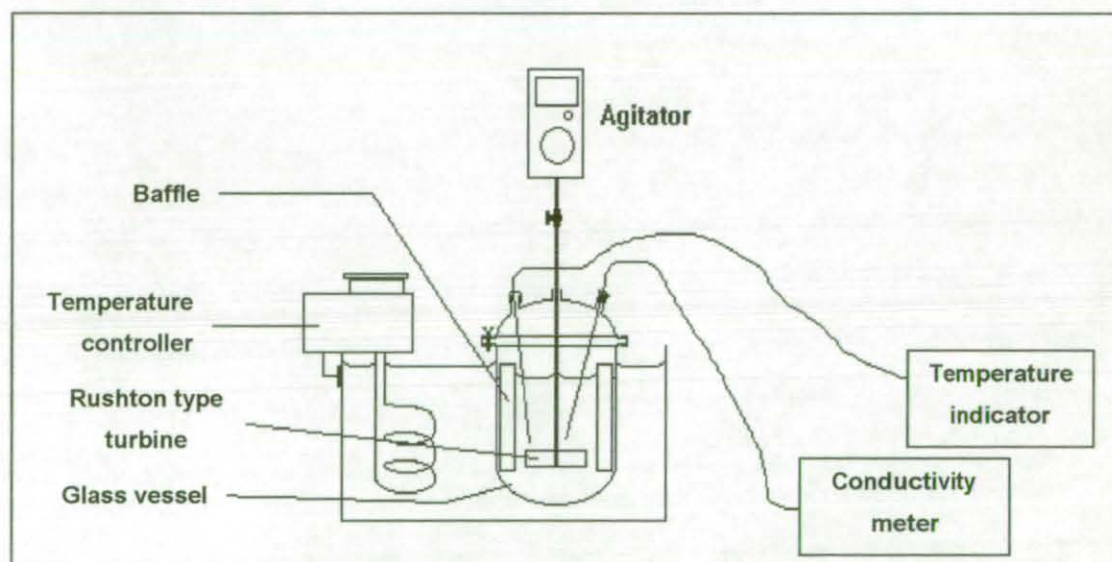
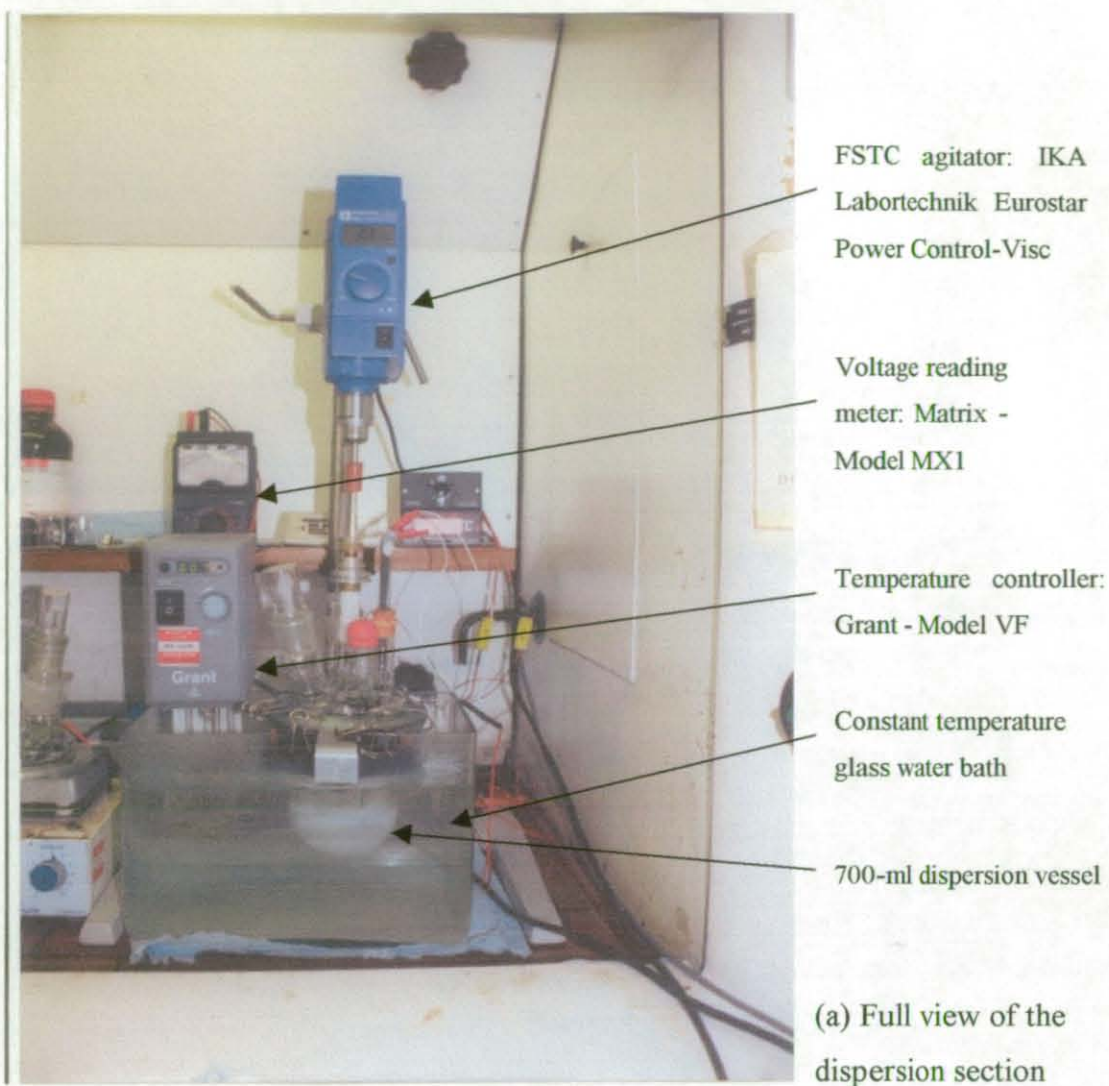
Specifications and models of some of the equipment used were as follows:

- Glass water bath.
- Temperature controller: Grant (Cambridge, UK) - Model VF, ± 0.1 °C stability.
- Baffles^{*}: Two 3-sided baffles were used. Widths of baffles 1 and 2 were 10.5 mm and 5 mm respectively. Both baffles have a thickness of 1 mm.
- Five-neck glass vessel cover: Fittings as shown in figure 3.2.
- Turbines^{*}: Two 4-flat-bladed turbines were used. Length and width of turbine 1 were 3.7 cm and 1.2 cm respectively; Length and width of turbine 2 were 4.9 cm and 1 cm respectively. Both turbines have a thickness of 1 mm (figure 3.3).
- Fixed speed, torque changes (FSTC) agitator: IKA Labortechnik (Germany) Eurostar Power Control-Visc. This agitator has a function that allows users to record relative changes in torque while agitation is maintained at a fixed speed.
- Temperature indicator: Digitron Instrumentation Ltd. (UK)– Model 3900.
- Conductivity probes^{*}: Two types of probes were used. Figures 3.4a and 3.4b show the schematic diagrams of the single and double sensor probes respectively.
- Conductivity meter^{*}: Electric circuit and schematic diagram of the conductivity meter are shown in figures 3.4c and 3.4d.
- Voltage reading meter: Matrix (UK) - Model MX1.

3.1.2 Reservoir section

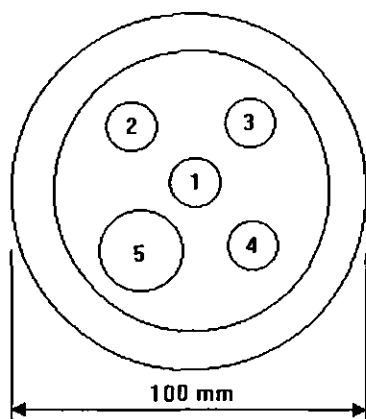
A reservoir section was needed to pre-treat the initial dispersed phase that was added to the initial continuous phase in the dispersion vessel. There were two different set-ups for this purpose, depending on the amount of pre-treatment needed. When little pre-treatment was needed, a 400-ml glass beaker was used as the reservoir vessel. It was submerged in a glass water bath that was being heated by a magnetic stirrer hotplate (Stuart Scientific UK – Model SM3). A thermocouple was placed in the reservoir vessel to measure its temperature. Adjustment to the heating of the hotplate can then be made to warm the initial dispersed phase up to the operating temperature.

^{*} All equipment with ‘*’ was made in the workshop of the Department of Chemical Engineering in Loughborough University.



(b) Schematic set-up diagram of dispersion section

Figure 3.1. Set-up of the dispersion section



	Name	Angle ; size	Purpose
1	Centre Socket	0° ; 19/26	Inlet of agitator
2	Parallel Socket	0° ; 19/26	Inlet of conductivity probe
3	5° Socket	5° ; 19/26	Second inlet of conductivity probe
4	10° Socket	10° ; 19/26	Inlet of thermocouple
5	15° Socket	15° ; 34/35	Inlet of initial dispersed phase and sampling point

Figure 3.2. Fittings through the five-neck glass vessel cover

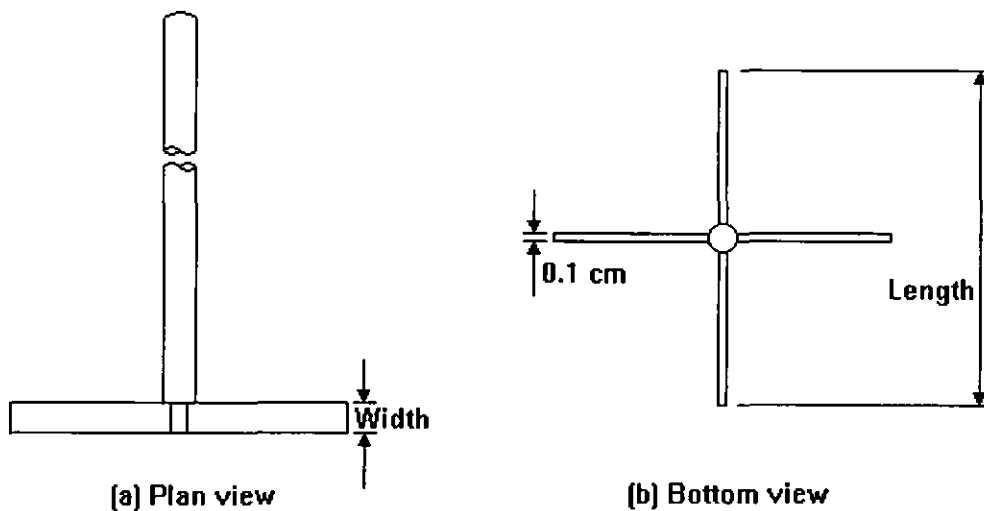
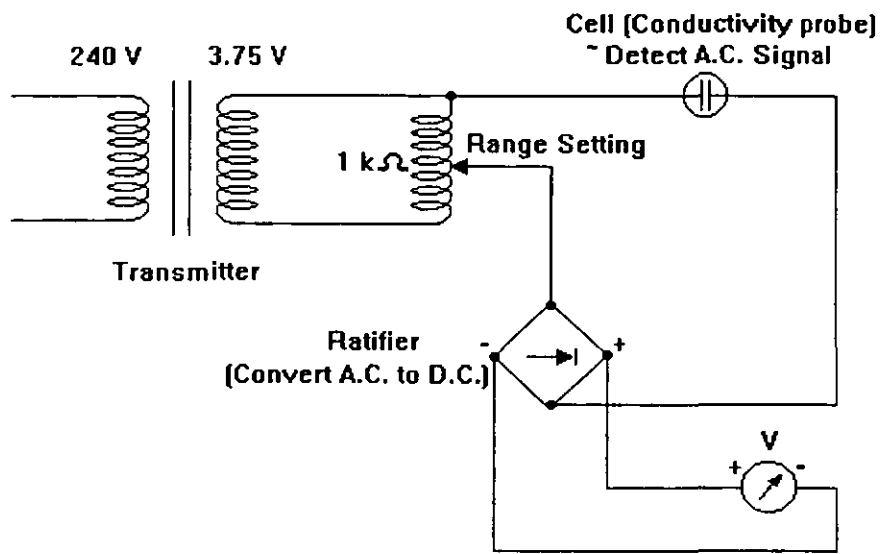
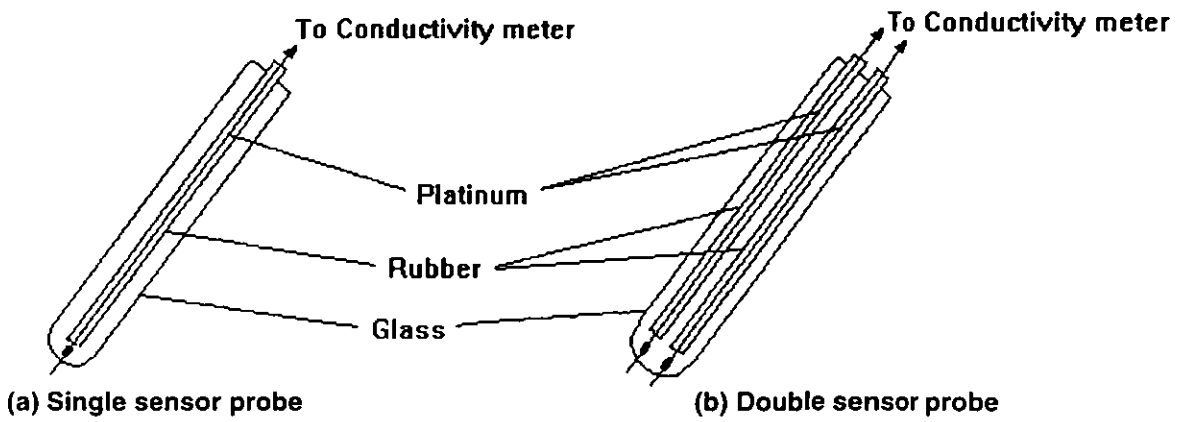
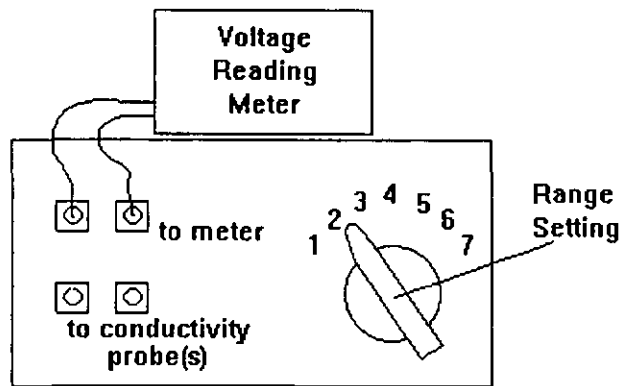


Figure 3.3. Schematic diagram of the 4-flat-bladed turbine



(c) Electric circuit of the conductivity meter



(d) Schematic diagram of the conductivity meter

Figure 3.4. Equipment for conductivity measurement: (a) Single sensor probe; (b) Double sensor probe; (c) Electric circuit of the conductivity meter; (d) Schematic diagram of the conductivity meter

PUp containing internal stabilising groups sometimes needed to be pre-neutralised before being added as initial dispersed phase. In this case, a more complicated reservoir set-up was required. The set-up was similar to the dispersion section but without the conductivity probe. An overhead fixed speed agitator (IKA Labortechnik, Germany - Eurostar digital) was used to provide the agitation.

3.2 Droplet characterisations

The equipment used to characterise droplet information of PUp-W dispersions in this study includes scanning electron microscope (SEM), optical microscope and low angle laser light scattering (LALLS) size analyser. This section describes the models and set-up of these apparatus. It is also worth pointing out that some efforts have been put into characterising emulsions using the transmission electron microscope (TEM) machine, but had been fruitless. This is because PUp droplets are very soft and form film-like structure on the TEM specimen grid. The problem remained even after the emulsions were stained using methods described by Kay (1965) and Wischnitzer (1981). Staining agents used include Silver Nitrate, Ammonium Molybdate, Sodium Dihydrogen Phosphate and Sodium Tungstate. Due to these unsuccessful attempts, TEM usage was limited to the preliminary stage of this work.

3.2.1 SEM – freeze fracture technique

The following equipment was used for the SEM – freeze fracture technique:

- Scanning electron microscope (SEM): Cambridge Stereo Scan, UK – Model S360 (shown in figure 3.5). The SEM machine was fitted with a cold stage.
- Cryogenic preparation system: Oxford instrument (Oxford, UK) – Model CT1500 (shown in figure 3.5). This system keeps samples frozen during the “fracturing” and gold-coating processes.
- SEM sample holder: Holds the frozen rivets for examinations in the SEM machine.
- Rivets: Oxford instrument (Oxford, UK) – Model HCR0113. As ‘A’ of figure 3.6.
- Rivets holder: As ‘B’ of figure 3.6, holds up to 8 different frozen samples at a time.

- Holder transfer rod: As 'C' of figure 3.6.
- Polypropylene vials: Nalgene (Milton Keynes, UK) cryogenic vials – Model 5000-0020. As 'D' of figure 3.6. They were used to store the frozen samples.
- Aluminium vial holder: Nalgene (Milton Keynes, UK) cryocane – Model 5015-0002. As 'E' of figure 3.6, holds up to 6 vials.
- Vacuum pump: Balston UK – Model 9955-12.
- Polypropylene desiccators: Kartell UK.
- Cryogenic storage vessel: Taylor-Wharton (USA) – Model 10XTA.
- Liquid nitrogen and liquid propane containers.
- Polystyrene cups: Used for transferring liquid nitrogen.
- Rubber tube.
- Brass tube coil.

3.2.2 Optical microscope unit

The following was apparatus used for the optical microscope technique:

- Optical microscope: Leica (New York, USA) – Model ATC 2000.
- Colour video camera: JVC (Japan) – Model TK-C1381.
- Colour video title generator: Video Tech. (UK) – Model VTG 228 Plus.
- SVHS videocassette recorder (VCR): Panasonic (Japan) – Model AG 4700.
- Colour video monitor: JVC (UK)– Model TM-14 EKD.
- Video graphic printer: Sony (Tokyo, Japan) – Model UP-890CE.
- SVHS videocassette: Sony (Tokyo, Japan) – Model SE-180.
- Microscope slide with cavities.
- Cover glass.

A schematic diagram of the set-up of optical microscope is shown in figure 3.7, and a photograph of this unit is shown in figure 3.8. This set of equipment consists of an optical microscope capable of amplifying images by up to 1000 fold and allows detection of droplets as small as 0.7 μm . A 10 \times eyepiece was used to focus

on droplet images of the emulsion. The focused images can then be captured by colour video camera fitted on the microscope. A high-resolution video camera recorder was used to transmit these captured images to a colour video monitor and a SVHS VCR. A colour video title generator was used to create title on the graphic picture while the video graphic printer printed the images that were shown on the monitor. Printed drop size images can then be analysed manually. The images were also stored in the SVHS videocassette for future usage.

3.2.3 LALLS size analyser

This unit was supplied by Malvern instrument. Figure 3.9 shows a picture of the LALLS size analyser. The unit comprises of the size analyser (Malvern Instrument, Worcestershire, UK - Mastersizer Model S), a small volume sample dispersion unit and a dispersion unit controller. Data collected from the size analyser was analysed using computer system, Vigler VigIII/LS. Pre-dilution of emulsion samples were carried out using 20-ml glass sample tubes (Merck UK Ltd.).

3.3 Others

Two sets of equipment were used for viscosity measurements. One was for measuring viscosity of PUP samples and the other was for measuring viscosity of PUP-W dispersions. A modified densitometer was used to measure density of PUP samples.

3.3.1 Viscometer 1

A falling ball method, as will be described in appendix I, was used to measure viscosity of PUP samples. Apparatus used for this purpose was as follows:

- Glass tube: Length was 18 cm and internal diameter was 1.6 cm.
- 30 cm long transparent ruler.
- Stainless steel ball bearings: Diameter was 1.6 mm and density was $7,572 \text{ kg/m}^3$.
- Stands and clamps.
- Glass water bath.

- Temperature controller: Grant, UK – Model VF, gives ± 0.1 °C stability.

A schematic diagram of equipment set-up for this method was shown in figure 3.10. The ruler was strapped to the glass tube. Both of them were then clamped and immersed into the water bath. The temperature controller was used to maintain the water bath at a suitable measuring temperature.

3.3.2 Viscometer 2

A Brookfield viscometer was used to measure the viscosity of PUp-W dispersions. Equipment used for this purpose was as follows:

- Brookfield (Massachusetts, USA) - Synchro-lectric viscometer: RV models.
- Spindle number 4 of Brookfield viscometer: Diameter of the spindle was 28 mm.
- 100-ml sample bottle: Fisher scientific (Loughborough, UK) – Model BTF-600-070R. Height of bottle (with cap) was 91mm and outside diameter was 50 mm.
- Glass water bath.
- Magnetic stirrer hotplate: Stuart Scientific UK – Model SM3.

3.3.3 Modified densitometer

The densitometer used for this purpose has a tube shape as shown in figure 3.11. The purpose of this design was to allow any entrapped air bubbles in the viscous PUp samples to ‘escape’ easily. Other pieces of apparatus used included glass water bath, temperature controller (Grant, UK – Model VF), a stand and a few clamps.

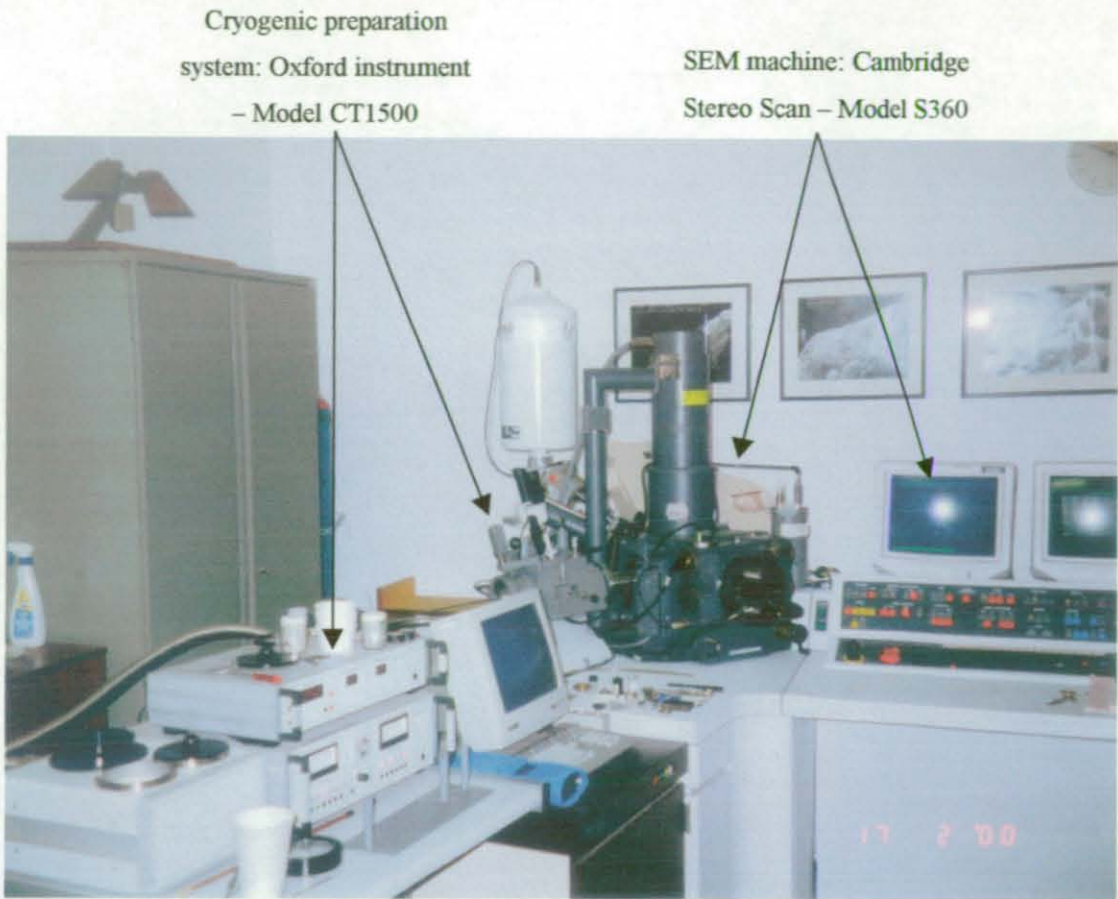


Figure 3.5. Full view of the SEM machine

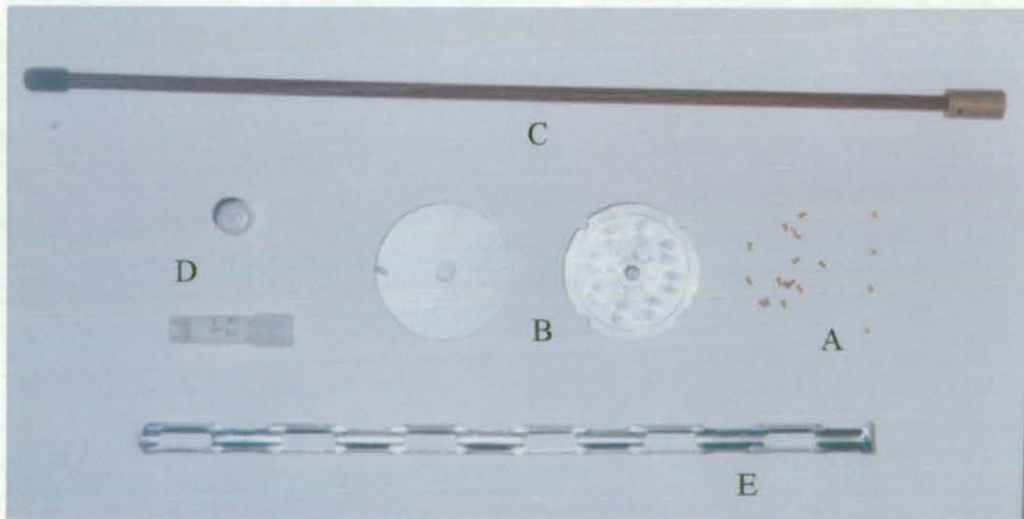


Figure 3.6. Other equipment of the SEM – freeze fracture technique

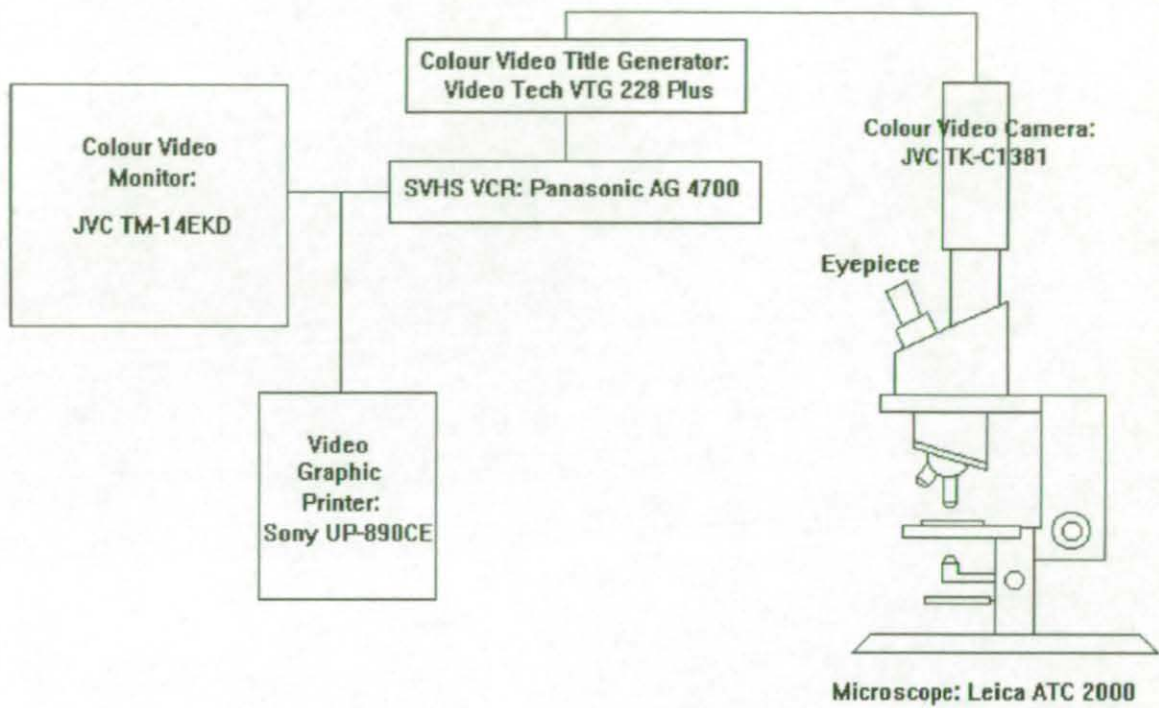


Figure 3.7. Schematic diagram of the optical microscope

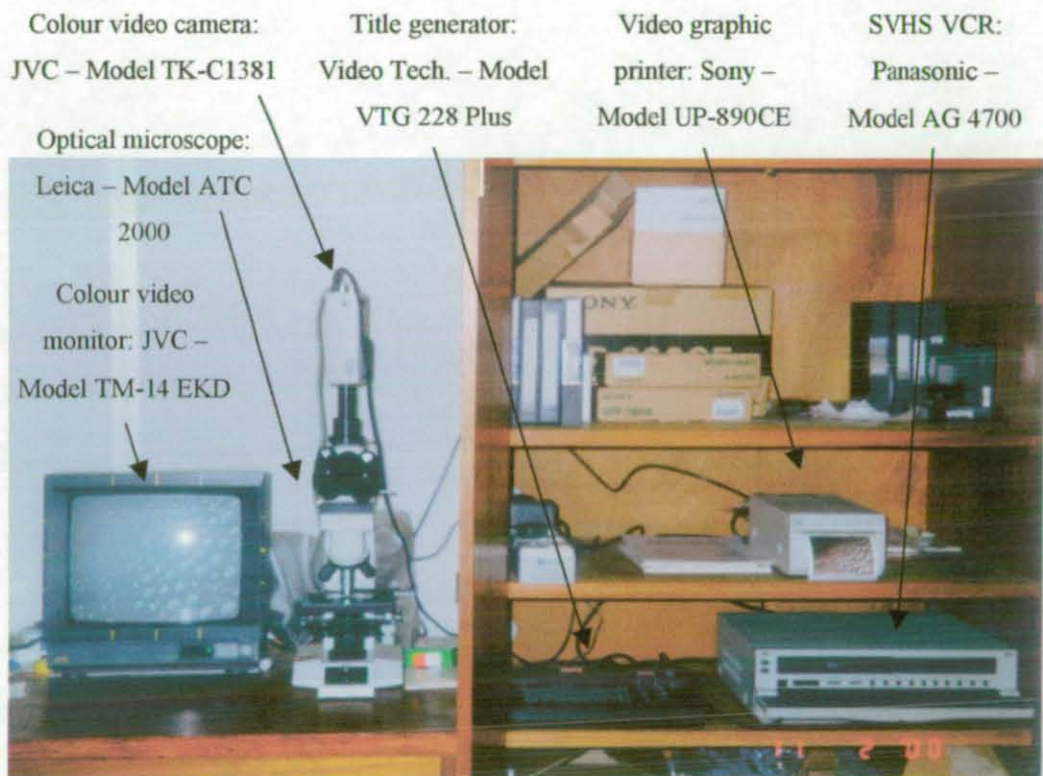


Figure 3.8. Full view of the optical microscope unit

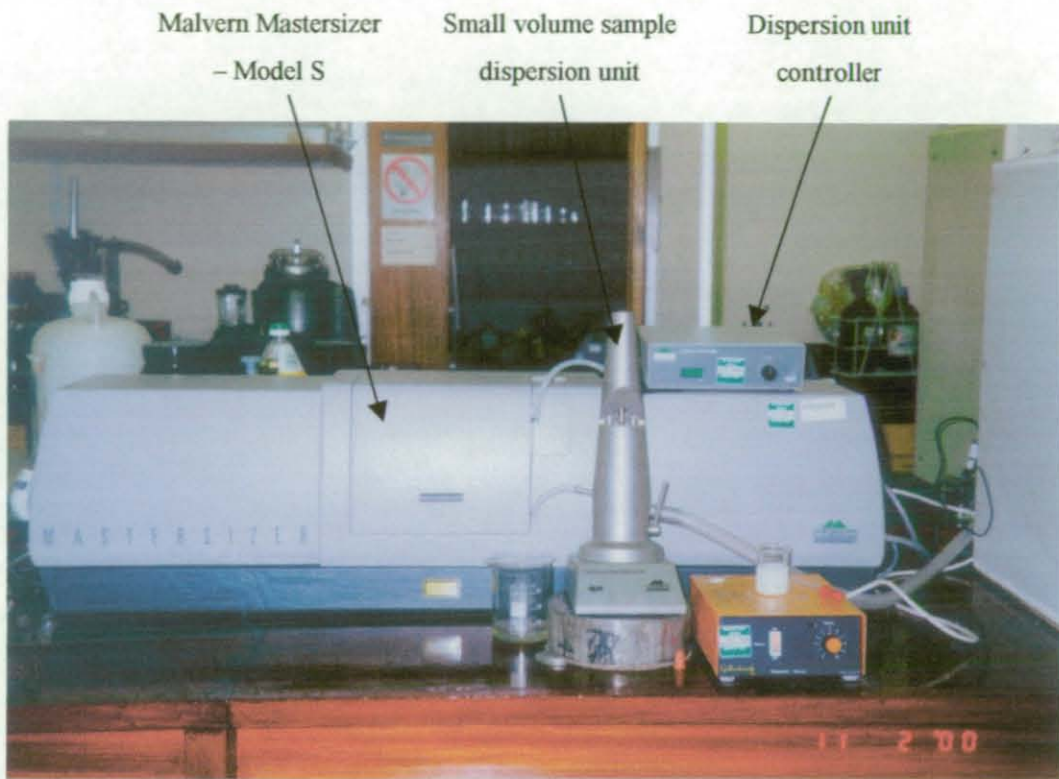


Figure 3.9. Full view of the LALLS size analyser

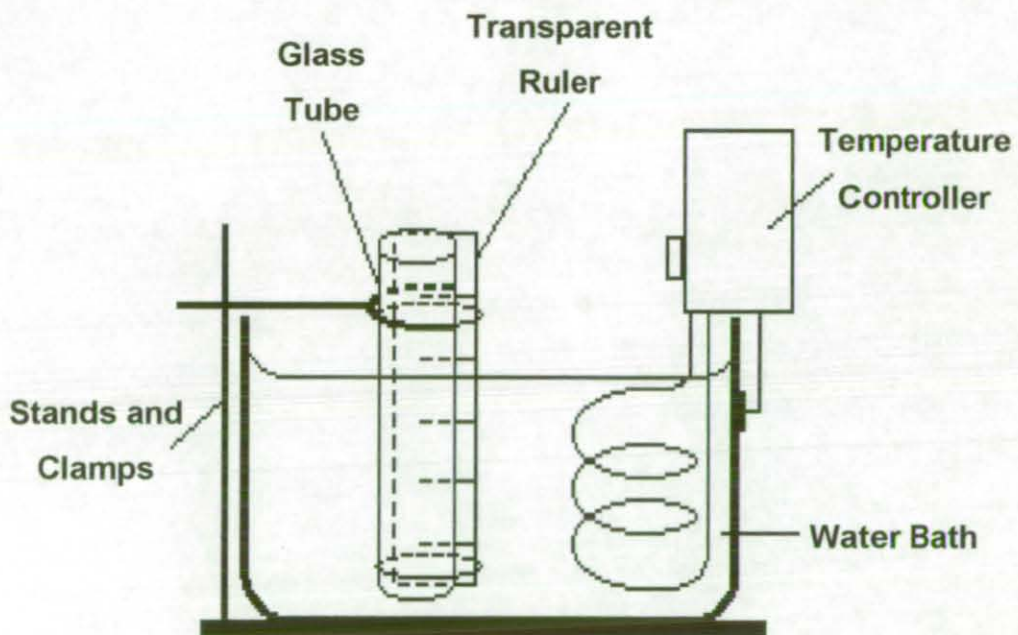


Figure 3.10. Schematic diagram of equipment set-up for the falling ball method

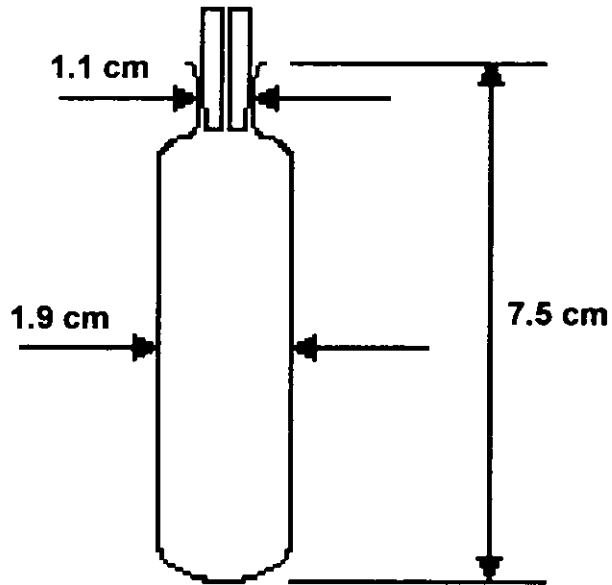


Figure 3.11. Schematic diagram of the modified densitometer

CHAPTER 4

Materials

This chapter describes materials used in this work. The first section describes the properties of the pre-polymers. The second section includes physical properties of the surfactants and the final section introduces other materials used.

4.1 Pre-polymers

After careful consideration, the following specifications of pre-polymers were listed for the purpose of this work:

1. No chain extension ability: Chain extension of pre-polymers is an important part of the industrial process during the production of polymer latex. However, the aim of this project is to understand the dispersion stage during the production of pre-polymer-water dispersions. Therefore, it is vital to prevent chain extension from happening.
2. End groups do not contribute to hydrophilicity of the pre-polymer: One way of preventing any unwanted chain extension from happening is to end-cap the PUp chain. However, some end-cap compounds could possess hydrophilic properties. Therefore, suitable hydrophobic end-cap compounds are chosen so that hydrophilicity of the PUp chain is provided solely by internal stabilising groups.
3. Solvent-free and/or dissoluble in water-immiscible solvent: This property enables study of the dispersion mechanism of the pre-polymer without being confused by any freely moving, water miscible solvent. As mentioned in section 2.2.2, a “true” phase inversion can only be obtained in the absence of water-miscible solvent.

4.1.1 Backbone of PUp samples

Avecia* supplied PUp ionomer (also known as functionalised PUp or ionically modified PUp) made to the above mentioned specifications. The monomer units of the PUp samples supplied are poly(tetrahydrofuran) diol (PTHF), tetramethyl xylene diisocyanate (TXDI) and dimethylol propanoic acid (DMPA). The DMPA provided -COOH side groups on the PUp chains. The NCO/OH ratio of all PUp supplied is equal to 2. These PUp chains are end-capped with n-propanol and were supplied free of solvents. The difference between the PUp samples is their DMPA group contents. These are summarised in table 4.1.

Table 4.1. Properties of PUp samples,

Sample	PUp2-7.5	PUp2-3.75	PUp2-2.5	PUp2-1.5	PUp2-0
DMPA content (wt.-%)	7.5	3.75	2.5	1.5	0

4.1.2 Amount of functionalised PUp molecules

Some of the PUp samples consist of a mixture of functionalised PUp molecules (PUp containing DMPA groups) and non-functionalised PUp molecules (PUp without any DMPA groups).

According to Billmeyer (1984), the number of structural units (or monomer molecules) on condensation polymers, such as PUp, can be predicted from the reactants' functional groups ratio and extent of reaction. Consider a case when only bifunctional reactants are present and when two types of group (designated A and B) are initially present in number $N_A < N_B$ with ratio $r = N_A/N_B$. Then, the total number of monomers present is $\frac{1}{2} (N_A + N_B) = \frac{1}{2} N_A (1 + 1/r)$. At extent of reaction, p (defined for A group; for B groups extent of reaction = rp), the total number of chain ends is $N_A (1-p) + N_B (1-rp) = N_A [1-p+(1-rp)/r]/2$. Therefore, the number-average degree of polymerisation (or the number of structural units on each polymer molecules), \overline{X}_n , can be represented as,

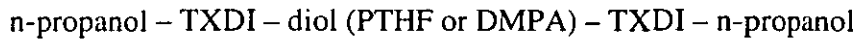
$$\overline{X}_n = \frac{N_A(1+1/r)/2}{N_A[1-p+(1-rp)/r]/2} = \frac{1+r}{1+r-2rp} \quad [4-1]$$

* Previously known as the speciality branch of Zeneca.

When sufficient reaction time is given, the functional groups deficient in amount, i.e., type A groups in this case, are completely used up. All chain ends will consist of the groups present in excess. As $N_A \rightarrow 0$, then $p \rightarrow 1$, and hence equation (4-1) can be simplified to

$$\overline{X}_n = \frac{1+r}{1-r} \quad [4-2]$$

For PUp samples with NCO/OH ratio of 2, $r = 0.5$. From equation (4-2), $\overline{X}_n = 3$, with the chain ends being isocyanate groups. Since n-propanol is used to end-cap these active pre-polymers, average PUp molecules of the samples supplied have the following structure:



Based on the molecular weight of the monomer used, these PUp samples have a number average molecular weight of about 1,500 g/mole. Since we know the amount of DMPA used in the reactant mixture, the amount of functionalised PUp molecules can also be calculated. Details of these calculations are shown in appendix II and the results are summarised in table 4.2.

Table 4.2. Mole-% of functionalised PUp molecules in the PUp samples,

Sample	PUp2-7.5	PUp2-3.75	PUp2-2.5	PUp2-1.5	PUp2-0
Functionalised molecules	56.08	33.51	23.89	15.18	0

4.1.3 Other physical properties

Density and viscosity of PUp samples were measured using methods that will be mentioned in appendix I. As will be shown in appendix I, the density-temperature and viscosity-temperature relationships of all PUp samples can be represented by the following equations:

$$\text{Density-temperature relationship:} \quad \rho = A + BT - CT^2 \quad [4-3]$$

$$\text{Viscosity-temperature relationship:} \quad \ln \mu = A + B/(T+C) \quad [4-4]$$

Where ρ is density, μ is viscosity, T is temperature, A , B and C are constants for the equations. A , B and C values (for the PUp samples) of equations (4-3) and (4-4) are shown in tables 4.3 and 4.4 respectively. These constants are determined from

this work, as mentioned in appendix I. Errors of the density and viscosity values predicted using these constants are also shown in the same tables.

Table 4.3. Constants A, B and C* of equation (4-3) and the associated errors in representing density-temperature relationship of PUp samples,

Sample	A	B	C	Errors
PUp2-7.5	1057.5	0.623	0.0106	± 0.10 %
PUp2-3.75	1088.9	-1.271	-0.0055	± 0.05 %
PUp2-1.5	1068.8	-1.062	-0.0038	± 0.02 %
PUp2-0	1054.6	-0.762	-0.0007	± 0.02 %

Table 4.4. Constants A, B and C† of equation (4-4) and the associated errors in representing viscosity-temperature relationship of PUp samples,

Sample	A	B	C	Errors
PUp2-7.5	-3.10	1724.69	69.73	± 0.31 %
PUp2-3.75	-4.68	2369.01	111.74	± 2.00 %
PUp2-1.5	-2.65	1815.38	102.23	± 1.85 %
PUp2-0	-3.78	2146.56	121.61	± 0.86 %

In a preliminary work, water was carefully laid on top of PUp2-7.5 samples with different DN values. The mixtures were left untouched for a few days. It was noticed that the neutralised PUp2-7.5 shows a self-dispersing behaviour when it comes in contact with water, i.e., it dispersed into water without additional external force. The self-dispersing behaviour was observed for PUp2-7.5 with DN as low as 10 %. This self-dispersing behaviour of neutralised PUp2-7.5 was also observed by Phongikaroon and Calabrese (2000) recently. Phongikaroon and Calabrese (2000) also used a pendent drop method to measure the interfacial tensions of PUp2-7.5 at 12.5 % DN and at 50 % DN. The measured interfacial tensions were between 118.8×10^{-4} N/m (at DN = 12.5 %) and 5.23×10^{-4} N/m (at DN = 50 %).

* Using these constant values, density calculated is in kg/m^3 and temperature used is in $^{\circ}\text{C}$.

† Using these constant values, viscosity calculated is in cPs and temperature used is in $^{\circ}\text{C}$.

4.2 PUp blends

Some PUp blends were prepared using mixtures of PUp2-7.5 and PUp2-0. Measured amounts of both PUp samples were carefully poured into 500-ml sampling bottles. They were then heated in an oven maintained at about 50 °C. The bottles were turned upside down every few hours. This process continued over a few days until the mixtures were well blended. Table 4.5 shows the compositions of PUp2-7.5 and PUp2-0 in the blends prepared.

Density and viscosity of some of the blends were measured. Their density-temperature and viscosity-temperature relationship can, again, be represented using equations (4-3) and (4-4). Tables 4.6 and 4.7 show the A, B and C values of equations (4-3) and (4-4) respectively. The associated errors are also shown in these tables.

Table 4.5. Compositions of PUp blends,

Sample	PUp2-7.5 (wt.-%)	PUp2-0 (wt.-%)	DMPA (wt.-%)
PUpB-20/80	20.2	79.8	1.52
PUpB-32/68	32.0	68.0	2.40
PUpB-50/50	50.3	49.7	3.77
PUpB-75/25	75.0	25.0	5.62

Table 4.6. Constants A, B and C^{*} of equation (4-3) and the associated errors in representing density-temperature relationship of PUp blends,

Sample	A	B	C	Errors
PUpB-20/80	1056.1	-0.065	0.0050	± 0.03 %
PUpB-50/50	1062.3	-0.165	0.0054	± 0.05 %

Table 4.7. Constants A, B and C[†] of equation (4-4) and the associated errors in representing viscosity-temperature relationship of PUp blends,

Sample	A	B	C	Errors
PUpB-20/80	1.26	751.20	49.69	± 1.10 %
PUpB-50/50	-0.97	1266.81	67.25	± 1.75 %

* Using these constant values, density calculated is in kg/m³ and temperature used is in °C.

† Using these constant values, viscosity calculated is in cPs and temperature used is in °C.

4.3 External surfactants

4.3.1 Non-ionic surfactants

Non-ionic surfactants used were the Igepal-CO series (supplied by Aldrich chemical). These were used without further purification. Properties of these surfactants are shown in table 4.8.

Table 4.8. Properties of non-ionic surfactants (Igepal-CO series),

Igepal CO	CO-210	CO-520	CO-720	CO-890	CO-990
n[*]	1	4	16	39	99
Formula weight	308.47	440.63	749.00	1982.50	4625.72
Specific gravity	0.96	0.997	1.053	N/A	N/A
Melting point (°C)	N/A	N/A	N/A	46 ~ 47	57 ~ 58
HLB number[†]	4.6	10	14.2	17.8	19

4.3.2 Anionic surfactants

Two types of anionic surfactants were also used. Both of them contain free carboxylic acid group. These were chosen to allow direct comparison with the built-in stabilising groups provided by DMPA on the PUp ionomer backbone. Properties of these anionic surfactants are shown in table 4.9.

Table 4.9. Properties of ionic surfactants used,

Ionic surfactant	Lauric acid	Stearic acid
Supplier	Sigma Chemical	Aldrich chemical
Purity	99-100 % pure	95% pure
Molecular formula	CH ₃ (CH ₂) ₁₀ COOH	CH ₃ (CH ₂) ₁₆ COOH
Formula weight	200.3	284.48
Melting point (°C)	44 ~ 46	67 ~ 69
Specific gravity	0.883	N/A
HLB number at 25°C[‡]	16	17

* Molecular formula of Igepal-CO series is 4-(C₉H₁₉)C₆H₄O(CH₂CH₂O)_nCH₂CH₂OH.

† HLB number at 25 °C. (Reference: Ash and Ash (1989)).

‡ HLB number of the non-neutralised ionic surfactants at 25 °C. (Reference: Myers (1988)).

4.4 Others

Other materials used in this project included:

1. Distilled water.
2. Potassium Chloride (KCl): To make the distilled water conductive. [Fisons Scientific Apparatus; 99.8% pure; molecular weight = 74.56].
3. Triethylamine (TEA): To ionise -COOH groups [ACROS chemical; 99% pure; molecular formula is $(C_2H_5)_3N$; formula weight = 101.19; specific gravity = 0.7280; flash point = $-11^\circ C$].
4. Sodium hydroxide (NaOH) solution: To ionise -COOH groups [Aldrich chemical; 50 % solution in water; specific gravity = 1.515].
5. Liquid Nitrogen: For SEM - freeze fracture experiment. [Liquid range* = $-209.86^\circ C \sim -195.8^\circ C$; heat capacity† = $0.475 \text{ cal/g } ^\circ C$; latent heat of vaporisation† = $1,336 \text{ cal/mole}$ at atmospheric pressure]
6. Propane gas: For SEM - freeze fracture experiment. [Boiling point* = $-42^\circ C$; latent heat of vaporisation† = $4,500 \text{ cal/mole}$ at atmospheric pressure]
7. Decon90: For cleaning purpose [Decon Laboratories Limited].
8. Coulter latex standard: For validation of Malvern Mastersizer. The standard is Polydivinyl Benzene latex with a volume mean diameter, $d_{v,50}$, of $2.22 \mu m$. [Coulter electronics Ltd.]

* Reference: - Weast (1973).

† Reference: - Perry and Green (1984).

CHAPTER 5

Experimental methods

This chapter gives details of various experiments involved during this work. The first few sections describe the general procedures of experiments. These are followed by details of experiments designed for specific studies.

5.1 Dispersion experiments

Two types of dispersion processes were studied in this work. General procedures of these processes are described in this section.

5.1.1 Catastrophic phase inversion experiments

During a catastrophic phase inversion experiment, the initial dispersed phase was firstly dispersed into the initial continuous phase. As more initial dispersed phase was added, the proportion of this phase in the mixtures kept increasing until catastrophic phase inversion occurred. After phase inversion had happened, the initial dispersed phase became the final continuous phase and the initial continuous phase became the final dispersed phase. Further addition of the initial dispersed phase served to dilute the final emulsions.

Two types of catastrophic phase inversion processes were studied in this work: (1) polymer-continuous to water-continuous catastrophic phase inversion process (PWCPI); and (2) water-continuous to polymer-continuous catastrophic phase inversion process (WPCPI). Materials of various phases during these processes are shown in Table 5.1. In order to avoid duplication of efforts, procedures described in this (and the following) section(s) will only refer to the initial/final

dispersed/continuous of the phases and not specific materials. A flow chart of catastrophic phase inversion experiments is shown in figure 5.1.

Table 5.1. Materials of various phases during catastrophic phase inversion experiments,

	PWCPI	WPCPI
Initial dispersed phase	Water	Polymer
Initial continuous phase	Polymer	Water
Final dispersed phase	Polymer	Water
Final continuous phase	Water	Polymer

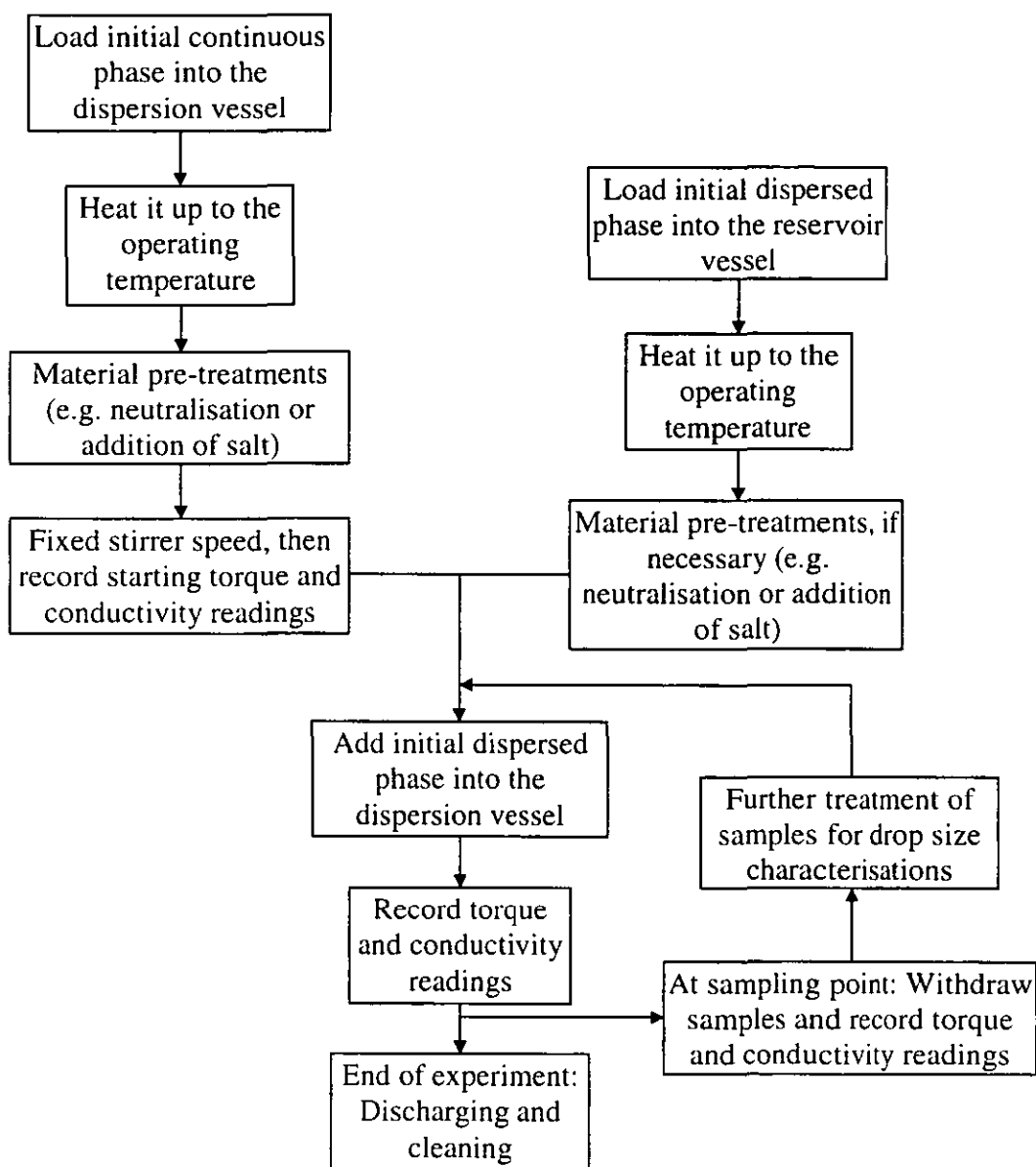


Figure 5.1. Flow chart of catastrophic phase inversion experiments

Charging and pre-treatment of sample

Firstly, a measured amount of initial continuous phase was poured into the dispersion vessel. Suitable baffle and agitator were then placed into the dispersion vessel. After clamping the vessel cover onto the dispersion vessel, thermocouple and conductivity probe(s) were inserted through appropriate sockets of the cover (as shown in figure 3.2). When this was done, the initial continuous phase (together with the capped vessel) was heated in the water bath to the operating temperature. Pre-treatment of the material was then carried out at the operating temperature. Pre-treatment varied depending on the material used as the initial continuous phase. When water was used, about 0.5 wt.-% of KCl was sometimes dissolved into it.

When PUp was the initial continuous phase, one of several pre-treatment methods was used depending on the requirements of the studies. Those were (1) Adding calculated amount of counterions (TEA or NaOH) into the dispersion vessel to neutralise a predetermined amount of the free carboxylic acid groups on the PUp ionomer backbone. The mixture was left stirring at operating agitator speed for 1 ~ 2 hours to complete the ionisation and/or homogenisation of the mixture (as suggested by Chen and Chen (1992) and Kim and Lee (1996)). (2) Blending calculated amount of external surfactants into the PUp. When anionic surfactants were used, a calculated amount of TEA was subsequently added to neutralise 98% of the carboxylic acid groups in the surfactant-PUp mixtures and stirring was maintained at 50 ~ 100 rpm for 1 hour. When non-ionic surfactants with high melting point were used, the mixtures were heated to the melting point of the surfactants and stirred at 50 ~ 100 rpm until all surfactants were completely melted. When other non-ionic surfactants were used, the mixtures were stirred at the operating agitator speed for 10 minutes.

Initial dispersed phase was pre-treated in the reservoir vessel, in parallel to the above-mentioned processes. The procedure was similar to those mentioned above except that water was pre-treated in a 400-ml glass beaker and PUp was normally pre-treated in a 700-ml round bottom glass vessel.

Dispersion and sampling

Dispersions took place after all sample pre-treatments had been completed. About 15 minutes before the first aliquot of initial dispersed phase was added, the FSTC agitator was switched over to record the relative torque changes in the

dispersion vessel at a fixed operating agitator speed. The first torque and conductivity readings were recorded at about 1 to 2 minutes before the addition of initial dispersed phase. Then, a fixed amount of the initial dispersed phase was added into the initial continuous phase over a fixed time interval. Torque changes and conductivity readings were made at about 1 to 2 minutes before each addition of initial dispersed phase.

At the sampling points, torque changes and conductivity readings were made before and after samples were withdrawn. Subsequent additions of initial dispersed phase were carried out at a rate that depends on the requirement of the studies. The withdrawn emulsion samples were further treated, and subsequently characterised, using methods that will be mentioned in sections 5.2 and 5.3.

Discharging and cleaning

Experiments ended when the PUp-W mixtures reached a pre-determined composition or when there was no initial dispersed phase left. The emulsions produced, and any PUp left, were discharged into waste glass bottles and disposed according to regulations of the Loughborough University. Equipment was cleaned using warm soapy water. In some cases, equipment containing pure PUp samples or PUp-W mixtures was exceptionally difficult to clean. In those cases, the equipment was soaked in Decon90 over a few days until they could be cleaned readily with warm soapy water. After cleaning with the soapy water, the equipment was rinsed twice with cold tap water and once using distilled water. They were left to air dried over night.

5.1.2 Transitional phase inversion experiments

Transitional phase inversion was brought about by changing the hydrophilicity of ionically modified PUp, and hence the interaction energies between PUp and water, at a fixed PUp-W ratio. Hydrophilicity of PUp can be improved by increasing the amount of ionic group content. There are two ways to achieve this: (1) adding counterion to a non-neutralised, or poorly neutralised, PUp ionomer; or (2) adding highly neutralised PUp ionomer to poorly neutralised PUp ionomer or PUp without any free carboxylic acid groups.

During the experiment, the initial continuous phase was firstly charged into the dispersion vessel in a similar way to those mentioned in the previous section. In all transitional phase inversion experiments, the initial continuous phase used was PUp. PUp was pre-treated by adding calculated amount of counterions (TEA or NaOH) to neutralise a predetermined amount of free $-\text{COOH}$ on the PUp ionomer backbone. The mixture was again left to stir at the operating agitator speed for 1 ~ 2 hours to complete the ionisation and/or homogenisation of the mixture.

Before transitional phase inversion took place, water at the operating temperature was added at a fixed rate to the initial continuous phase until it reached a predetermined PUp-W ratio. The PUp-W ratio was chosen to ensure that catastrophic phase inversion does not take place. Torque changes and conductivity readings were recorded 1 to 2 minutes before each water addition to confirm that no unwanted phase inversion had taken place.

If highly neutralised PUp ionomer was used during the experiment, it was pre-treated in the reservoir section, in parallel to the above-mentioned process. The procedure was similar to those mentioned above, except that no water was added at all. Water was heated up in glass beaker separately. The counterions were used without further treatment.

Dispersions took place after all sample pre-treatments had been completed. The procedure was similar to that given in sub-section 5.1.1 on “dispersion and sampling”. The difference was that counterions or highly neutralised PUp ionomers were added instead of the initial dispersed phase. Water was subsequently added to balance the chosen PUp-W ratio.

Experiments ended when the mixture reached the pre-determined ionic group content. In most case, this was after the initial dispersed phase, water, had become the final continuous phase.

5.2 Droplet size measurement

Non-diluted emulsion samples were firstly examined using the optical microscope technique. This technique was successfully used for measurement of droplet diameters larger than $0.7\ \mu\text{m}$ for emulsions with a relatively low disperse

phase volume fraction. For emulsions with a high disperse phase content or with droplets smaller than $0.7\ \mu\text{m}$, other techniques were used. The SEM-freeze fracture technique was used extensively to capture images of droplet with size from as small as $60\ \text{nm}$ to a few tens of μm . This technique was also used to examine the drop structures of emulsions in detail. The LALLS size analyser served as a quick quantification method for emulsions containing only polymer-in-water (P_1/W_C) drops larger than $0.05\ \mu\text{m}$. Methods used for the analysis of droplet data will be discussed in section 5.3.

5.2.1 Operation of optical microscope unit

A small drop of the non-diluted emulsion samples was carefully placed onto the cavity of the microscope slide. The sample was then contained using a cover glass just before being examined on the sample stage of the optical microscope. In all experiments, the $10\times$ eyepiece was used, together with the $20\times$, $40\times$ or $100\times$ objectives. Images were firstly focused using the $20\times$ objective. For smaller droplets, objectives with higher magnifying power were subsequently used. This method cannot be used to detect droplets that are smaller than $0.7\ \mu\text{m}$. The focused images were stored in SVHS videocassettes and printed optical microscope images were analysed manually.

5.2.2 SEM-freeze fracture technique

The freeze fracture technique is a method developed to freeze emulsion samples so that they are suitable to be analysed under cold vacuum condition in a SEM machine. By doing this, the physical states of emulsions can be analysed closer to their real states because neither dilutions nor other sample treatments are needed. For most emulsion samples, liquid propane was primarily used as the cooling medium in order to freeze emulsion samples fast enough so that distortion of the physical state of the emulsion was minimised. For some of the stable emulsion samples, sub-cooled liquid nitrogen was also used as an alternatively cooling medium. As mentioned earlier, this technique is suitable for analysing highly concentrated emulsions without dilution and for measurements of droplets that are as small as $80\ \text{nm}$ in diameter.

Preparation of cooling mediums

Liquid propane was prepared from propane gas, which was supplied in a pressurised container. A rubber tube was tightly connected to the container and a brass coil was connected to the other end of the rubber tube. A large section of the coil was then immersed into liquid nitrogen to cool the coil down. The coil was cooled down completely when the liquid nitrogen stopped boiling off. Then, with the coil still immersed in the liquid nitrogen, propane gas was released from the container through the rubber tube and brass coil connection. Propane gas was cooled down and become liquid propane as it passed through the cold brass coil. Liquid propane was collected in a liquid-propane container placed at the other end of the brass coil. In order to conserve the liquid propane for as long as possible, the filled-up liquid-propane container was immersed into liquid nitrogen. Liquid propane was now ready for use.

Due to the lengthy preparation process needed for making liquid propane, some stable emulsions were frozen using “cold” liquid nitrogen (liquid nitrogen at its freezing point). Although cold liquid nitrogen has a smaller heat capacity compared to liquid propane and took a longer time to freeze emulsion samples, it was easier to prepare and has larger heat capacity than liquid nitrogen at its boiling point. Cold liquid nitrogen was prepared by first pouring liquid nitrogen into a container that was placed inside a polypropylene desiccator. A plastic tube was connected to the desiccator outlet; the other end of the tube was connected to a vacuum pump. The pump was switched on and ran for a few minutes until nitrogen slush started to form in the container. The pump was switched off and the plastic tube removed. Vacuum in the desiccator was slowly released through the pinhole valve at its outlet. When the desiccator reached atmospheric pressure, its cover could be removed and the cold liquid nitrogen was ready for use.

However, it should be noted that the freshly prepared cold liquid nitrogen could generally be used to freeze 3 to 5 samples only. After that, liquid nitrogen starts boiling off as soon as samples were immersed into it, indicating that the liquid nitrogen was no longer close to its freezing point. Therefore, the cold liquid nitrogen was always prepared immediately before its use.

Sample preparation

A small drop of emulsion sample was first rested on a rivet using a pipette. The sample was then contained by placing another rivet, upside-down, on top of the first rivet. The rivets were then carefully transferred into liquid propane, or cold liquid nitrogen, in order to freeze the emulsion sample. The sample was left in liquid propane, or cold liquid nitrogen, for more than 15 seconds before it was quickly transferred into a rivet holder that was submerged in liquid nitrogen.

At least 3 frozen samples of each emulsion sample were made to allow for any possible damages that may happen during further treatments. After all the samples were frozen and transferred to the rivet holder, the samples were transferred into polypropylene vials containing liquid nitrogen. After covering the vials, the vials were put onto aluminium cranes that held up to 6 vials. The samples, together with the vials and cranes, were then stored in the cryogenic storage vessel until the SEM machine was available. Prior to being analysed by the SEM machine, the frozen samples were transferred from the vials to the rivet holder to enable easier operational usage.

Operation of the SEM machine

The SEM machine used was fitted with a cryogenic preparation system. When using it, samples prepared using the methods mentioned above were first transferred to a SEM sample holder, which held the bottom rivets firmly. Then, this sample was placed into the cryogenic preparation system that was kept at about $-160\text{ }^{\circ}\text{C}$ to $-198\text{ }^{\circ}\text{C}$. The top section of the rivet was knocked off in the cryogenic preparation system before the sample was transferred into a cold stage fitted in the SEM machine. Temperature of the cold stage was also kept at about $-160\text{ }^{\circ}\text{C}$ to $-198\text{ }^{\circ}\text{C}$. From experience, when the continuous phase is aqueous, best images can be obtained after the frozen sample was 'etched'. This etching process was carried out by heating the cold stage to $-90\text{ }^{\circ}\text{C}$ and maintaining that temperature for 1 ~ 1½ minutes. Since the cold stage was under vacuum, water crystals sublimed from the surface of the frozen sample at $-90\text{ }^{\circ}\text{C}$ to yield more distinct images.

After the etching process, the SEM sample holder was put back into the cryogenic preparation system. While the cold stage was being cooled back to $-160\text{ }^{\circ}\text{C}$ to $-198\text{ }^{\circ}\text{C}$, the vacuum of the cryogenic preparation system was adjusted to 0.2 mbar. Under this vacuum condition, a sputter device was switched on to coat the sample

surface with a thin layer of gold. This thin gold layer served to pick up minute surface details of the fractured sample. After the coating process, the SEM sample holder was replaced into the cold stage that was now cold enough. After all these steps, the image of the frozen sample can be examined using the SEM machine. Focused images of the frozen samples were taken using a camera. Negatives were developed into photographs, and these photographic images can be analysed manually.

5.2.3 LALLS size analyser

A LALLS size analyser was used to quantify emulsions containing only P_1/W_C drops. When using the size analyser, heavy dilutions of emulsions were required. Therefore, its usage was limited for stable P_1/W_C emulsions only.

Sample preparation

10 to 15 g of distilled water were heated up to the operating temperature in a 20-ml glass sample tube. 3 to 5 g of water-continuous emulsion samples were then injected into the warm water. The bottle was covered and hand-shaken to dilute the mixture homogeneously. The diluted sample was then ready for analysis.

Sample analysis

The 300RF lens of the Malvern Mastersizer, which measures droplets ranging from 50 nm to 900 μm , was used. The analysis model chosen was a 'polydisperse' model. The refractive index value used was 1.33 for the continuous phase (i.e., water phase); and 1.55 for the disperse phase (i.e., PU particles). According to Malvern Instruments, polyurethane has a refractive index of 1.50 ~ 1.60, and degree of light absorption of the disperse phase was 0.01.

After the machine had been set up, according to above-mentioned condition, the lens was properly aligned and a background measurement was taken. The sample was then added to the small volume sample dispersion unit that was filled with distilled water. The sample dispersion unit was connected to the sample cell in the size analyser. Flows were driven by the dispersion unit controller, which maintained the agitation at 1100 rpm. Sample was added to give a concentration that brought about 10 % to 30 % light obscuration. Lower concentrations generated insufficient data and higher concentrations caused 'multiple scattering'. Multiple scattering

occurred when light bounced off more than one particle before reaching the detectors and that led to inaccurate results.

5.3 Method for analysing drop size data

Droplet data obtained from optical microscope and SEM images were characterised using methods described in this section. Due to the large amount of calculations involved, two C++ programmes were written to aid the characterisation of droplet data. The last section validates the use of Malvern Mastersizer.

5.3.1 Data classification

The very first task in analysing drop size data is to arrange the measured values into a number of intervals and to record the numbers of drops that fall within each interval. Each interval is termed a class (or a bin), and the droplet diameter limits (lower limit, D_L to upper limit, D_H) of each class are known as class boundaries (or bin size). The choice of bin size is very important and there are many methods to choose these boundaries. Phongikaroon and Calabrese (1998) described a method that utilises a three interlaced Fibonacci series to define the bin size. Orr (1983) described two common methods for defining bin size, an arithmetic progression method and a geometric progression method.

Bin size

Both of the bin size characterisation methods described by Orr were investigated and compared in section 6.1. The arithmetic progression method is usually adequate for systems with a narrow drop size distribution. When using this method, the size of all the class boundaries is equal. In other word, the differences between D_H and D_L are constant for all the bins. The interval of bin i , ΔD_i , for an arithmetic progression method can be represented as,

$$\Delta D_i = \frac{(D_{\max} - D_{\min})}{N_{bin}} \quad [5-1]$$

where D_{\max} and D_{\min} are the maximum and minimum drop diameter found in the population respectively, and N_{bin} is the total number of bins used during analysis.

As shown in appendix III, the lower drop diameter limit of bin i , $D_{L,i}$, can be expressed as,

$$D_{L,i} = D_{\min} + (i - 1) \cdot \Delta D_i \quad [5-2]$$

The upper drop diameter of bin i , $D_{H,i}$, can be expressed as,

$$D_{H,i} = D_{\min} + i \cdot \Delta D_i \quad [5-3]$$

The geometric progression method is needed for systems with a wider drop size distribution, where droplet diameters may be logarithmically distributed. In this method, differences between the logarithms of D_H and D_L are equal for all bins. As shown in appendix III, $D_{L,i}$ for the geometric progression method can be expressed as,

$$D_{L,i} = D_{\min}^{(1-(i-1)/N_{bin})} \cdot D_{\max}^{((i-1)/N_{bin})} \quad [5-4]$$

and $D_{H,i}$ can be expressed as,

$$D_{H,i} = D_{\min}^{(1-i/N_{bin})} \cdot D_{\max}^{(i/N_{bin})} \quad [5-5]$$

Number of bins

Orr (1983) suggested to use 10 ~ 20 bins for drop size characterisation, since fewer can result in the discarding of valuable information and more creates excessive computation. However, an example shown in section 6.1 shows that the number of bins chosen also depends on the spreading of the drop size data and is also limited by the choice of bin size for the smaller droplets.

5.3.2 Drop size distribution

The number of droplets in each bin, i , is called the frequency N_i . The total number of drops calculated is N_T ($= \sum N_i$). Therefore, the number percentage of a specific bin, $P_{N,i}$, is defined as,

$$P_{N,i} = \frac{N_i}{N_T} \times 100 \% \quad [5-6]$$

$P_{N,i}$ is a very important variable as it can be used as well as actual numbers, N_i , in most cases. It is particularly useful for converting number distribution data to area and volumetric distribution data using the following equations:

$$\text{Area percentage of bin } i, \quad P_{A,i} = \frac{P_{N,i} \cdot D_{avg,i}^2}{\sum_i P_{N,i} \cdot D_{avg,i}^2} \times 100 \% \quad [5-7]$$

$$\text{Volumetric percentage of bin } i, \quad P_{v,i} = \frac{P_{N,i} \cdot D_{avg,i}^3}{\sum_i P_{N,i} \cdot D_{avg,i}^3} \times 100 \% \quad [5-8]$$

where $D_{avg,i}$ is the average diameter of bin i [$= (D_{H,i} + D_{L,i})/2$].

Derivation of equations (5-7) and (5-8) are shown in appendix III. $P_{N,i}$ can also be used for the calculation of mean diameters.

5.3.3 Mean diameters

There are many advantages in using mean diameters to represent systems containing unequal drop sizes (Orr (1983)) Firstly, use of mean diameters provides a mechanism for reducing a mass of data to a conveniently handled form. This is because mean diameters can be used to focus on particular parameters from among those of number, length, area, and volume (or mass). Secondly, they serve as a guide for property correlation. Finally, use of mean diameters permits direct computation of product quantities. In general, mean diameter can be defined by the following equation:

$$d_{mn} = \left[\frac{\sum_i N_i \cdot D_{avg,i}^m}{\sum_i N_i \cdot D_{avg,i}^n} \right]^{1/(m-n)} \quad [5-9]$$

where $m = 1,2,3$; $n = 0,1,2$; and m is always larger than n .

The two mean diameters used are arithmetic mean diameter, d_{10} , and Sauter mean diameter, d_{32} . As shown in appendix III, they can be related to $P_{N,i}$ and $D_{avg,i}$ by,

$$d_{10} = \frac{\sum_i P_{N,i} \cdot D_{avg,i}}{\sum_i P_{N,i}} \quad [5-10]$$

and,

$$d_{32} = \frac{\sum_i P_{N,i} \cdot D_{avg,i}^3}{\sum_i P_{N,i} \cdot D_{avg,i}^2} \quad [5-11]$$

Interfacial area per unit volume can be related to d_{32} by,

$$a = 6 \cdot \phi_d / d_{32} \quad [5-12]$$

where ϕ_d is the volume fraction of the disperse phase.

5.3.4 Useful graphs

Both the distribution curve and the cumulative distribution curve were used during this work. The distribution curve is drawn by plotting $P_{N,i}$, $P_{A,i}$ or $P_{V,i}$ against $D_{avg,i}$. This type of graph shows how droplets are distributed in terms of number, surface area, volume or mass*.

Data from some of the emulsions produced during this work can be fitted using a log-normal distribution function suggested by Orr (1983), which takes the form of

$$\frac{dP_{N,i}}{d(\log D_{avg,i})} = \frac{100}{\log \delta_{LN} \cdot \sqrt{2\pi}} \cdot \exp\left(-\frac{(\log D_{avg,i} - \log d_m)^2}{2 \cdot \log^2 \delta_{LN}}\right) \quad [5-13]$$

where δ_{LN} is the standard deviation of the log-normal distribution and d_m is the mean diameter of the log-normal distribution. The curve fitting was performed using the *solver* function of *Microsoft Excel97*.

Cumulative distribution curves are used to show percentage of droplets (in terms of number, surface area or volume) equal to and less than, or equal to and greater than, the corresponding diameter. The first one is plotted using accumulated percentages against the lower value of each bin; and the second one is plotted using the upper value of each diameter interval.

5.3.5 Error estimation

Due to the limitation of droplet measurement using microscopic images, drop size distribution parameters often have to be inferred from a limited number of drops. Paine (1993) shows that errors of drop size information can grow catastrophically when sampling is inadequate and he concludes that one must sample at least a certain

* Volumetric and mass distribution are convertible between each other since density = mass/volume.

number of particles. This number is not evident *a priori*, but must be established after an initial measurement of geometrical standard deviation, GSD , defined as,

$$GSD = (d_{V,84}/d_{V,16})^{1/2} \quad [5-14]^*$$

Two parameters have also been defined in Paine (1993):

1. The critical number of particles which must be counted to prevent the error from growing catastrophically, N_{crit} . If number of droplets counted is larger than N_{crit} , the droplet distribution parameters obtained are considered reliable. Standard deviation, δ , can be defined as

$$\delta = \ln GSD \quad [5-15]$$

and N_{crit} is related to standard deviation by

$$N_{crit} = \exp[1.5 + 5.5\delta + 7.5\delta^2] \quad [5-16]$$

2. The limited number of particles that must be calculated to obtain marginally acceptable results, N_{lim} . When the number of droplets counted lies between N_{crit} and N_{lim} , errors in some of the distribution parameters estimated can be smaller than 20%[†]. N_{lim} is related to δ by

$$N_{lim} = \exp[0.5 + 7\delta + 3.5\delta^2] \quad [5-17]$$

Both N_{crit} and N_{lim} were used in this work to evaluate the amount of droplet samples needed to avoid either obtaining poorly estimated droplet distribution parameters or excessive time consumption. Although Paine's work is based on the assumption of log-normally distributed particles, these two parameters still serve well for the purpose of this work.

* $d_{V,16}$ and $d_{V,84}$ are particle sizes correspondent to the 16th and 84th percentile of the cumulative volumetric distributions respectively.

† In his work, Paine (1993) shows that the $d_{V,50}$ estimated can have an error of smaller than 10% if GSD is smaller than 1.2. However, the error increases with larger GSD values. When $GSD = 2.3$, the error in estimated $d_{V,50}$ value is smaller than 20.6%.

5.3.6 C⁺⁺ programmes

Due to the large amount of calculations involved, two C⁺⁺ programmes were written to aid the drop size characterisation. One programme was used for characterising simple drop systems and the other for characterisation of multiple drop systems. Both full programmes are shown in appendix III.

Simple drop system

This C⁺⁺ programme was written for characterisation of emulsions consisting of mainly P_1/W_C or W_1/P_C drops. Equations (5-1) to (5-12) and (5-14) to (5-17) were incorporated into this programme. The followings are important features of this programme:

- Demands the user to input name of the source file that contains the droplet data. The source file must be a text (.txt) file.
- Scans the data bank for the number of drops in it, the maximum drop diameter and the minimum drop diameter.
- Allows the user to input or modify relevant data for calculation. These data include maximum and minimum drop diameter, number of drops to be counted and the number of bins to be used.
- Allows the user to choose the calculation methods. Two calculation methods, an arithmetic progression method and a geometric progression method, have been included in this programme.
- Performs calculations and displays the results. These include the number percentage, area percentage, volume percentage, cumulative data, mean diameters and standard deviations. Reliability of the result is estimated using equations (5-16) and (5-17) and then comparing it with the number of drops counted.
- Allows the user to write the results into a specific file in a text format. The file can later be retrieved and retreated using a spreadsheet programme (such as *Microsoft Excel97*).

Multiple drop system

Another C⁺⁺ programme has been written to characterise droplet information for emulsions consisting of a mixture of drop structures. Some emulsions produced

during this project contain a mixture of drop structures, which include simple drops, and type A, B and C multiple drops*. This new programme can handle all the drop structures mentioned and performed separate calculations for each type of drop whenever it is necessary. In addition to the features of the aforementioned programme, this programme also performs the following functions:

- Calculates the number of each type of drop in the data bank. Data in the source file must have a text (.txt) format and must be input in the following pattern:

$$\phi_d$$

$$d_{Pol} \quad d_{Water} \quad d_{Pol} \quad d_{Water} \quad d_{Pol} \quad d_{Water} \quad \dots$$

where ϕ_d is the volume fraction of the disperse phase, d_{Pol} and d_{Water} are the diameters of polymer and water drops respectively. For a simple drop, $d_{Water} = 0$ following a d_{Pol} value, indicating that the polymer drop contains no water drop at all. For type A multiple drops, each d_{Pol} is followed by a corresponding d_{Water} value, indicating that each polymer drop contains one water drop. For type B and C drops, each polymer drop contains more than one water drop. The d_{Pol} value only has to be input once; the subsequent d_{Pol} values are input as zero, each with an associated d_{Water} value. For example, a 10- μm polymer drop that contains three water drops of sizes 1, 2 and 3 μm should be stored in the source file as

$$10 \quad 1 \quad 0 \quad 2 \quad 0 \quad 3.$$

- Identifies the maximum and minimum diameters of each type of drops.
- Performs separate drop size characterisation for: (1) simple polymer drops; (2) multiple polymer drops; (3) equivalent multiple polymer drops[†]; (4) internal water drops; (5) Combined simple polymer drops and equivalent multiple polymer drops; (6) Combined equivalent multiple polymer drops and internal water drops; and (7) Combined simple polymer drops and multiple polymer drops.

* Nomenclatures of multiple drops are same as those mentioned in section 2.10.2.

[†] Equivalent multiple drop diameters are the diameters of the multiple polymer drops if they do not contain any internal water drops. In other words, equivalent multiple drop diameters are calculated after the volumes of internal water drops occupying the multiple polymer drops have been deducted.

- Generates data for the study of relationships between the multiple polymer drops and their internal water drops.
- Calculates the volume fraction of simple drops vs. multiple drops vs. water drops.
- Calculates the interfacial area per unit volume value for different polymer-water interfaces.

5.3.7 Malvern Mastersizer

A typical Malvern analysis report contains many drop size distribution parameters. However, only a few were abstracted for usage during this work. These include d_{10} , d_{30} , d_{32} , $d_{V,50}$, δ^* , the number (cumulative) distribution data and volumetric (cumulative) distribution data.

Coulter latex standard, $d_{V,50} = 2.22 \mu\text{m}$, was used to validate the Malvern Mastersizer. Its analysis report is included in appendix III. The Malvern measured $d_{V,50}$ value is $2.20 \mu\text{m}$, less than 1% error compared with the quoted value.

5.4 Methods for the detection of phase inversion points

This section describes details of experiments performed to aid the development of valid phase inversion detection methods.

Some PWCPI experiments were carried out using PUp2-2.5 as the initial continuous phase and distilled water (with or without KCl) as the initial dispersed phase. Operating temperature and agitator speed for these experiments were 60°C and 500 rpm respectively. Water was added at an average rate of 10 ml every 10 minutes. TEA was used as the neutralising agent in these experiments. Other experimental details are shown in table 5.2. The purposes of these experiments are to assess: (1) the effect of the design of conductivity probe(s); (2) the need of salt addition to aid the detection of phase inversion points; and (3) the combined usage of conductivity and torque change measurements to detect phase inversion points.

* δ was calculated using equations (5-14) and (5-15). $d_{V,16}$ and $d_{V,84}$ were obtained from volumetric cumulative distribution data.

Table 5.2. Experimental details of preliminary experiments,

Experiment code	Conductivity probe	Amount of KCl in water	Degree of neutralisation
EX54/1	1 × double sensor probe	0.5 wt.-%	98%
EX54/2	2 × single sensor probe	0.5 wt.-%	98%
EX54/3	1 × double sensor probe	None	98%

5.5 Effect of ionic group content on PWCPI process

A series of experiments was carried out to study the effect of ionic group content on PWCPI process during the production of PUP-W dispersions. There are two ways to change the ionic group content: (1) use fully neutralised PUP that contains different amount of free carboxylic acid groups; and (2) change the DN of PUP that contains a fixed amount of free carboxylic acid groups. The later method was chosen for this study. The experimental procedure was similar to those mentioned in section 5.1.1. PUP2-7.5 was used as the initial continuous phase and TEA was used as the neutralising agent. In all experiments, PUP2-7.5 was initially added to the dispersion vessel. The amount of TEA required was then calculated, based on the amount of PUP used and on the chosen nominal DN. The calculations involved are shown in appendix II. Table 5.3 shows the amount of PUP2-7.5 and TEA added, the nominal and actual DN values and the actual ionic group content of each experiment.

Table 5.3. Experimental details of section 5.5,

Experiment code	Amount of PUP2-7.5	Nominal DN	Actual TEA	Actual DN	Ionic group content (mmole/g)
EX55/1	141.9 g	98 %	7.947 g	98.05 %	0.548
EX55/2	144.7 g	75 %	6.201 g	75.00 %	0.419
EX55/3	149.3 g	60 %	5.125 g	60.06 %	0.336
EX55/4	146.5 g	50 %	4.178 g	49.90 %	0.279
EX55/5	147.8 g	31.8 %	2.670 g	31.84 %	0.178
EX55/6	148.5 g	20 %	1.702 g	20.05 %	0.112
EX55/7	149.7 g	5 %	0.432 g	5.05 %	0.028
EX55/8	149.2 g	0 %	N/A	0 %	0

All experiments were carried out using turbine 1 and baffle 1. Operating temperature and agitator speed were 60 °C and 500 rpm respectively. Distilled water, heated to the operating temperature, was added at a rate of 10 ml per 10 minutes using a syringe. No KCl was added into the water for experiments with DN larger than 20 %; for EX55/7 and EX55/8, 0.5 wt.-% of KCl was added into the water. The double sensor probe and FSTC agitator were used to monitor the changes in conductivity and torque respectively. Samples were withdrawn from time to time for drop size analysis. Experiments ended when the PUp-W mixture contained about 60 wt.-% of water.

5.6 External viscosity measurements

Annable (1999) mentioned that rheological properties of aqueous based coatings could vary during a drying process. Coatings can behave as non-Newtonian or Newtonian fluids depending on the polymer-water (P-W) ratio at various stages of the drying process. The change in P-W ratio during a catastrophic phase inversion process is in the opposite direction to the drying of an aqueous base coating. By analogy, P-W mixtures should also experience some rheological changes during a catastrophic phase inversion process. The successful use of the FSTC agitator to measure phase inversion point, therefore, depends on a thorough understanding of possible rheological changes during the phase inversion process. It is relatively straightforward if the P-W mixture behaves as a Newtonian fluid throughout the process. However, it is necessary to assess what might happen otherwise.

Two catastrophic phase inversion experiments were carried out for the purpose of this study. The experimental procedure was similar to that shown in section 5.1.1. However, 450 g (± 20 g) of PUp2-7.5 was used during each experiment to allow for the withdrawals of samples that were large enough for external viscosity measurements. Operating temperature and agitator speed for both experiments were 60 °C and 500 rpm respectively. Both experiments were carried out using TEA as the neutralising agent. The degree of neutralisation was 50 % and 30 % for experiments EX56/1 and EX56/2 respectively. Neutralisation time was increased to 1½ hours. Distilled water, heated to 62 °C (± 2 °C), was added to the vessel at a rate of 20 ml every 30 minutes when sampling was not required. When sampling occurred, the

subsequent water addition was delayed. Water was added after 42.5 minutes (± 7.5 minutes) for EX56/1 and after 40 minutes for EX56/2. Conductivity and torque change readings were recorded immediately before and after samples were withdrawn.

About 80 ml of samples were transferred to the 100-ml sampling bottles that were located in a water bath maintained at 60 °C. Spindle number four (#4) of the Brookfield Synchro-Lectric RV type viscometer was then immersed into the samples, up to the “immersion point” of the spindle. Dial readings were then recorded at rotating speeds of 0.5, 1, 2.5, 5, 10, 20, 50 and 100 rpm for all samples. Depending on the viscosity of the samples, measurements at the high rotating speeds were not always possible. Experiments ended when the PUp-W mixtures contained 53 wt.-% and 47 wt.-% of water for EX56/1 and EX56/2 respectively. Table 5.4 shows water contents at the sampling points for both experiments.

Table 5.4. Water contents (wt.-%) at sampling points for EX56/1 and EX56/2,

Samples	S1	S2	S3	S4	S5	S6
EX56/1	7.94	15.86	20.00	24.64	29.96	41.50
EX56/2	12.13	19.86	27.59	31.69	36.38	46.48

5.7 Different types of transitional phase inversion processes

A few transitional phase inversion experiments were carried out using about 150 g of PUp2-7.5 as the initial continuous phase and TEA as the neutralising agent. For all experiments in this study, the operating temperature was 60 °C and the operating agitation speed was 500 rpm. Baffle 1 and turbine 1 were also used. Some of the experiments were started with DN of about 29 % and the others without any neutralisation at all. Water, heated to 60 °C, was added at a rate of 10 ml every 10 minutes to obtain a pre-determined PUp-W ratio before TEA or highly neutralised PUp ionomer was added. Details of transitional phase inversion experiments were already mentioned in section 5.1.2.

Table 5.5 summarises the initial DN and ionic group content, initial water content, addition methods employed to induce the transitional phase inversion, water content maintained throughout the experiments and the DN and ionic group content at the end of the transitional phase inversion experiments.

For EX57/1 and EX57/5, water was added into the PUp-W mixtures, at rates of 40 ml and 10 ml every 10 minutes respectively, after the final DN were obtained. The SEM-freeze fracture technique was used to characterise droplet structures at various DN during experiments EX57/2 and EX57/5. The SEM images were also used to aid the explanation of events that occurred during the transitional phase inversion processes. After transitional phase inversion had occurred in EX57/3, some emulsion samples were withdrawn for drop size analysis using the LALLS size analyser as mentioned in section 5.2.3. Instantly pre-diluted samples were analysed within 5 hours after the samples were withdrawn (same day); and the non-diluted samples were diluted and analysed again 1½ months later (1½ months).

Table 5.5. Experimental details of section 5.7,

Experiment code	Initial DN*	Initial	Addition methods	Maintained	Final DN*
		water content		water content	
EX57/1	28.02 % (0.157)	28.72 wt.-%	10.6 (± 0.8) g/20 min. of PUp2-7.5 at DN = 91.46 %	28.72 (± 0) wt.-%	41.61 % (0.233)
EX57/2	29.94 % (0.167)	25.21 wt.-%	0.15 (± 0.02) g/10 min. of TEA	25.31 (± 0.1) wt.-%	45.88 % (0.257)
EX57/3	29.03 % (0.162)	28.66 wt.-%	0.15 (± 0.03) g/10 min. of TEA	28.58 (± 0.1) wt.-%	44.36 % (0.248)
EX57/4	0 % (0)	28.77 wt.-%	0.3 (± 0.01) g/10 min. of TEA	28.73 (±0.07) wt.-%	77.57 % (0.434)
EX57/5	0 % (0)	28.67 wt.-%	0.4 (± 0.02) g/10 min. of TEA	28.61 (±0.06) wt.-%	100 % (0.559)

5.8 Catastrophic phase inversion mechanism study

A catastrophic phase inversion experiment (EX58), as mentioned in section 5.1.1, was carried out using 148.4 g of PUp2-7.5 as the initial continuous phase. TEA was used as the neutralising agent and the DN was 20.08 % (corresponding to an ionic

* Numbers shown in bracket are the ionic group content, in mmole/g.

group content of 0.112 mmole/g). Operating temperature for this experiment was 60 °C and the speed of the agitator was maintained at 500 rpm. 10 ml of pure distilled water was added every 10 minutes when no samples were taken. Torque and conductivity readings were made at the 8th and 9th minutes after each addition of water. When sampling was needed, it was done after the torque and conductivity readings were recorded. The subsequent water addition, after the sample withdrawal, was made immediately at the 10th minutes; albeit, the next water addition was delayed from 10 minutes to 20 minutes.

It was known that the rate of water addition changes the phase inversion point during a catastrophic phase inversion process (Brooks and Richmond (1991)). However, the purpose of this experiment is to trace the events that occurred during the catastrophic phase inversion process; therefore, it is more important to preserve the real physical state of the samples than to fix the water addition rate. The emulsion samples were treated, using the SEM-freeze fracture technique mentioned in section 5.2.2, as soon as they were withdrawn in order to conserve their real physical state. Since it took about 12 to 15 minutes to prepare samples for freezing, the interval for water addition has to be adjusted accordingly.

Water content (in wt.-%) for seven of the samples withdrawn for SEM-freeze fracture analysis are as follows: S1 ~ 6.29; S2 ~ 17.03; S3 ~ 25.91; S4 ~ 29.87; S5 ~ 33.66; S8 ~ 49.08; and S11 ~ 58.29. Emulsion samples S1 ~ S5 and S11 were frozen immediately after being withdrawn. Emulsion S3 was frozen again 3 months and 1¼ years later. After 1¼ years, the separated sample S8 was hand-shaken to recreate the emulsion before being frozen again. All frozen samples were analysed using the SEM-freeze fracture technique mentioned earlier.

5.9 Effect of stabilising groups

5.9.1 PWCPI experiments

Baffle 1 and turbine 1 were used in the dispersion vessel for all experiments in this study. The same operating temperature and operating agitator speed were also used throughout this study, those were 60 °C and 500 rpm respectively. All PWCPI experiments started with about 150 g of PUp ionomers as the initial continuous phase. The PUp ionomers in use include PUp2-7.5, PUp2-3.75, PUp2-1.5, PUpB-20/80,

PU_pB-32/68, PU_pB-50/50 and PU_pB-75/25. Either TEA or NaOH solution was used as the neutralising agent depending on the purpose of specific experiment. Water was pre-heated to 60 °C and was added at a rate of 10 ml every 10 minutes for all PWCPI experiments. Detailed procedure of PWCPI experiments were already mentioned in section 5.1.1. Table 5.6 summarises the component of the initial continuous phase, the neutralising agent used, the nominal DN, the real DN and its resultant ionic group content. Drop size measurements and analysis methods as those mentioned in sections 5.2 and 5.3 were also used to characterise some of the aqueous emulsions produced.

Table 5.6. PWCPI experiments designed for studying the effect of stabilising groups,

Experiment code	Initial	Neutralising agent	Nominal	Ionic group	
	continuous phase		DN	Real DN	content (mmole/g)
EX59/1	PU _p 2-7.5	NaOH solution	20 %	21.53 %	0.120
EX59/2	PU _p 2-7.5	NaOH solution	30 %	29.54 %	0.165
EX59/3	PU _p 2-7.5	NaOH solution	50 %	50.86 %	0.284
EX59/4	PU _p 2-7.5	NaOH solution	60 %	60.65 %	0.339
EX59/5	PU _p 2-7.5	NaOH solution	98 %	98.14 %	0.549
EX59/6	PU _p 2-1.5	TEA	98 %	98.17 %	0.110
EX59/7	PU _p 2-3.75	TEA	98 %	98.65 %	0.276
EX59/8	PU _p B-20/80	TEA	98 %	98.20 %	0.111
EX59/9	PU _p B-32/68	TEA	98 %	97.98 %	0.175
EX59/10	PU _p B-50/50	TEA	98 %	100 %	0.281
EX59/11	PU _p B-75/25	TEA	98 %	97.99 %	0.411

5.9.2 Transitional phase inversion experiments

Some transitional phase inversion experiments were carried out under similar operating conditions as the aforementioned experiments. Baffle 1 and turbine 1 were used in the dispersion vessel; operating temperature and operating agitator speed were 60 °C and 500 rpm respectively. The calculated amount of NaOH solution was firstly added to neutralise about 0.17 mmole/g of ionic groups. After one hour, water at 60 °C was dispersed into the initial continuous phase at a rate of 10 ml every 10 minutes to attain a pre-determined PU_p-W ratio. NaOH solution was subsequently

added into the PUp-W mixture at a rate of 0.167 g (± 0.066 g) every 10 minutes. This is equivalent to an increment in ionic group content at a rate of 0.0145 mmole/g (± 0.0055 mmole/g) every 10 minutes.

After the final ionic group content was obtained, a few aliquots of warm water (at 60 °C) were added into the PUp-W mixture at a rate of 10 ml every 10 minutes. Again, details of the transitional experiments were already mentioned in section 5.1.2. Table 5.7 summarises the initial ionic group and water contents, the water content maintained throughout the transitional inversion experiments and the final ionic group content. Drop size measurements and analysis methods as those mentioned in sections 5.2 and 5.3 were again used to characterise some of the aqueous emulsions produced.

Table 5.7. Transitional phase inversion experiments designed for studying the effect of stabilising groups,

Experiment code	Initial ionic group content (mmole/g)	Initial water content (wt.-%)	Maintained water content (wt.-%)	Final ionic group content (mmole/g)
EX59/12	0.167	25.53	25.58 (± 0.05)	0.243
EX59/13	0.168	29.09	29.13 (± 0.04)	0.232
EX59/14	0.170	32.36	32.40 (± 0.04)	0.251

5.10 Effect of some processing factors

Two sets of PWCPI experiments have been carried out to study the effect of the viscosity of the initial continuous phase and configuration of the dispersion vessel on phase inversion process.

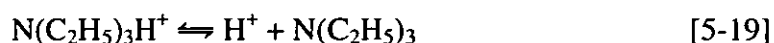
5.10.1 Viscosity of the initial continuous phase

Suitability of modifying viscosity through changing temperature

In order to avoid any complication caused by using solvents, the change in viscosity was intended to be done by varying the operating temperature. However, Dieterich et al. (1970) has shown that ionised and non-ionised PU ionomers could have different viscosities. It is also well known that temperature might have a significant effect on the dissociation of ions in water. The effect of temperature on the equilibrium constant can be represented by the equation,

$$\Delta_r G_T^\circ = -RT \ln K_d \quad [5-18]$$

Where $\Delta_r G_T^\circ$ is the standard Gibbs energy of formation (in J/mole) at the reaction temperature, T (in Kelvin), R is the gas constant (in J/mole·K) and K_d is the dimensionless equilibrium constant. The dissociation process of TEA ion in water is,



For the dissociation process, K_d of equation (5-18) can then be treated as a dissociation constant. Depending on the magnitude of the effect of temperature on the dissociation process, the de-ionisation of the TEA ion might overshadow the effect of temperature on viscosity alone. When this happens, any changes in temperature would not modify the viscosity of the ionised PUp ionomer independently.

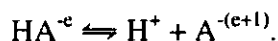
Although thermodynamic values for the dissociation of the TEA ion are not available, it is possible to predict the effect of its dissociation using recorded values for the Trimethylammonium (TMA) ion. From the work by Alberty and Silbey (1995), the $\Delta_r G_{25}^\circ$ value for the TMA ion in a zero ionic strength environment at 25 °C is 55.89 kJ/mole. By substituting this value into equation (5-18) and assuming that a zero ionic strength environment exists, the calculated dissociation constant of a TMA ion at 80 °C is about 2×10^{-9} . Although this is not the true dissociation constant value for a TEA neutralised PUp ionomer in a higher ionic strength system, the calculated constant is the highest possible K_d value of the TEA neutralised PUp ionomer in this work. There are three reasons for this:

1. Alberty and Silbey (1995) recorded thermodynamic values for both the Ammonium ion and the TMA ion. Using the recorded values for calculations, the K_d values decrease with increasing amount of methyl substituents at an isothermal condition. Therefore, the TEA ionised PUp ionomers should have a smaller K_d value.
2. According to Lewis and Randall (1961) and Alberty (1987), pK ($= \log K_d$) at a specific ionic strength, I , can be written as,

$$pK_I = pK_{I=0} - \frac{(2e+1)C_{DH}I^{1/2}}{(1+C_{I5}I^{1/2})} \quad [5-20]$$

where $pK_{I=0}$ is the pK value when ionic strength is equal to zero. C_{DH} is the Debye-Hückel constant, which is always positive, and C_{I5} is a constant often

taken as $1 \text{ (mole/l)}^{-1/2}$. e is taken from the dissociation process with e negative charges:



For a TEA ion-related dissociation process, e can be taken as -1. Therefore, equation (5-20) can be rewritten as,

$$pK_I = pK_{I=0} + \frac{C_{DH} I^{1/2}}{(1 + C_{IS} I^{1/2})} \quad [5-21]$$

as a result, when ionic strength is taken into account, pK_I will have higher values and hence lower K_d values.

3. According to equation (5-18), the K_d value increases exponentially with increasing temperature. Operating temperatures for any dispersion process involved in this study ranged from 45* to 80 °C. Therefore, the largest amount of dissociation will take place at 80 °C.

Having made the above analysis, it is not unreasonable to assume that the dissociation constant of TEA neutralised PUP ionomer is smaller than 2×10^{-9} for all dispersion processes to be studied in this work. This value is small enough to be neglected. Therefore, the viscosity of TEA neutralised PUP (i.e., the initial continuous phase) can be modified independently by changing the operating temperature.

Experiments

Some PWCPI experiments (as mentioned in section 5.1.1) were carried out at 45 and 80 °C. Results from these experiments can be compared with PWCPI experiments mentioned in section 5.5, which were carried out at 60 °C. At these operating temperatures, 45, 60 and 80 °C, the viscosity of the initial continuous phase are 150,000 (± 150) cPs, 27,000 (± 27) cPs and 4,530 (± 4) cPs respectively. These viscosities are calculated using equation (4-4) and constants shown in table 4.4. As with experiments mentioned in section 5.5, PUP2-7.5 and TEA were used as the initial continuous phase and the neutralising agent respectively. Turbine 1 and baffle 1 were used in all experiments and distilled water, heated to the operating temperature, was added at a rate of 10 ml every 10 minutes. Agitator speed was maintained at 500 rpm. The double sensor probe and FSTC agitator were also used to trace the

* The calculated K_d value for TMA ion at 45 °C is 0.5×10^{-9} .

changes in conductivity and torque readings. Table 5.8 summarises the amount of PUp2-7.5 used, the nominal and actual DN, the amount of TEA added and the resultant ionic group content.

Table 5.8. Summaries of PWCPI experiments carried out at 45 and 80 °C,

Experiment code	Nominal DN (%)	Amount of PUp2-7.5 (g)	Amount of TEA added (g)	Actual DN (%)	Ionic group content (mmole/g)
At 45 °C,					
EX510/1	20	148.3	1.70	20.00	0.112
EX510/2	50	145.8	4.14	50.03	0.280
EX510/3	75	143.5	6.14	74.91	0.419
EX510/4	98	142.1	7.95	97.94	0.548
At 80 °C,					
EX510/5	20	148.9	1.72	20.17	0.113
EX510/6	30	148.2	2.56	30.22	0.169
EX510/7	50	146.5	4.19	50.00	0.280
EX510/8	75	142.6	6.12	75.06	0.420
EX510/9	98	141.9	7.94	97.88	0.547

5.10.2 Configuration of the dispersion vessel

Some PWCPI and transitional phase inversion experiments were carried out using turbine 2 (diameter = 4.9 cm) and baffle 2 (width = 5 mm) in the dispersion vessel. These experiments used PUp2-7.5 as the initial continuous phase and NaOH solution as the neutralising agent. All experiments were carried out at operating temperature and agitator speed of 60 °C and 500 rpm respectively. These experiments are similar to EX59/1 ~ EX59/5 and EX59/12 ~ EX59/14 mentioned in section 5.9, which employed turbine 1 (diameter = 3.7 cm) and baffle 1 (width = 10.5 mm) in the dispersion vessel. Results from these two sets of experiments were combined to study the effect of the configuration of dispersion vessel on the phase inversion processes. Table 5.9 and 5.10 show some details of the PWCPI and transitional phase inversion experiments respectively.

Table 5.9. Details of PWCPI experiments using the new configuration,

Experiment code	Nominal DN (%)	Amount of PUp2-7.5 (g)	Amount of NaOH solution added (g)	Actual DN (%)	Ionic group content (mmole/g)
EX510/10	20	149.0	1.57	23.58	0.132
EX510/11	30	147.8	2.05	30.96	0.173
EX510/12	60	147.7	3.99	60.39	0.338
EX510/13	75	147.4	4.94	75.03	0.419
EX510/14	98	147.2	6.58	99.96	0.559

Table 5.10. Details of transitional phase inversion experiments using the new configuration,

Experiment code	Initial ionic group content (mmole/g)	Initial water content (wt.-%)	Maintained water content (wt.-%)	Final ionic group content (mmole/g)
EX510/15	0.168	25.55	25.61 (± 0.05)	0.2396
EX510/16	0.170	32.48	32.51 (± 0.03)	0.2202

After transitional phase inversion has taken place during EX510/15, aqueous emulsions were withdrawn, diluted instantly and analysed using the Malvern Mastersizer on the same day as their production.

5.11 External surfactant-related studies

Various external non-ionic and anionic surfactants, as mentioned in section 4.3, have been used to disperse PUp2-0 (i.e., PUp without any DMPA groups) into water via the PWCPI process. The pre-treatments of the surfactant-PUp2-0 blends were already mentioned in section 5.1.1. The amounts of non-ionic surfactants ('Igepal-CO' series) used were kept at about 7.5 wt.-% of the surfactant-PUp (SPUp) blend; and the amounts of anionic surfactants used were maintained at about 0.559 mmole (of free carboxylic acid groups)/g of SPUp blend, except for EX511/11. These amounts of surfactants were chosen to allow direct comparison with PUp2-7.5, which contained 7.5 wt.-% of DMPA groups (also equivalent to 0.559 mmole of free carboxylic acid groups/g of PUp).

After the pre-treatments, about 150 g of SPUp blends were used as the initial continuous phase. Distilled water, heated to the operating temperature, was added into the dispersion vessel at a rate of 5 ml or 10 ml every 10 minutes. About 0.5 wt.-% of KCl was pre-dissolved into the distilled water when non-ionic SPUp blends were used during the experiments. However, no KCl was added when anionic SPUp blends were used. Water (with or without KCl) was added until a predetermined SPUp-water ratio was obtained. Turbine 2 and baffle 2 were used in all experiments except EX511/10 and EX511/12, which used turbine 1 and baffle 1. The agitator speed was maintained at 500 rpm for all experiments, but operating temperatures were chosen as 30 °C, 45 °C or 60 °C depending on specific requirements of each experiment. The double sensor probe and FSTC agitator were, again, used to trace the changes in conductivity and torque readings.

Table 5.11 shows details of PWCPI experiments involving the use of non-ionic surfactants. The variables shown include the type of 'Igepal-CO' non-ionic surfactant used, the actual weight percentage of surfactant in the SPUp blends, the operating temperature and the water addition rate. For the anionic surfactant-related experiments, the water addition rate was maintained at 10 ml every 10 minutes and TEA was used as the neutralising agent. Further details of these anionic surfactant-related experiments are shown in table 5.12. The variables shown include the type of surfactant, the actual concentration of free carboxylic acid groups per g of SPUp blends, the degree of neutralisation of the anionic surfactant (using TEA as the neutralising agent) and the operating agitator speed.

Several aqueous emulsion samples were withdrawn from EX511/7, EX511/9, EX511/10, EX511/11 and EX511/12. These samples were diluted instantly and analysed using the Malvern Mastersizer on the same day as their production. A non-diluted aqueous emulsion obtained from EX511/9 was also analysed using the SEM-freeze fracture technique. This particular emulsion sample contains about 52 wt.-% of water.

Table 5.11. Details of non-ionic surfactant-related experiments,

Experiment code	Type of surfactant	Wt.-% of surfactant	Operating temperature	Water addition rate
EX511/1	CO-210	7.50 wt.-%	60 °C	10 ml/10 min.
EX511/2	CO-210	7.51 wt.-%	30 °C	10 ml/10 min.
EX511/3	CO-520	7.56 wt.-%	60 °C	10 ml/10 min.
EX511/4	CO-520	7.62 wt.-%	30 °C	10 ml/10 min.
EX511/5	CO-720	7.52 wt.-%	60 °C	10 ml/10 min.
EX511/6	CO-720	7.76 wt.-%	45 °C	5 ml/10 min.
EX511/7	CO-720	7.57 wt.-%	30 °C	5 ml/10 min.
EX511/8	CO-890	7.51 wt.-%	60 °C	5 ml/10 min.
EX511/9	CO-990	7.50 wt.-%	60 °C	5 ml/10 min.

Table 5.12 Details of anionic surfactant-related experiments,

Experiment code	Type of surfactant	Actual concentration of -COOH group	Degree of neutralisation	Agitator speed
EX511/10	Lauric acid	0.559 mmole/g of blend	98.1 %	500 rpm
EX511/11	Lauric acid	1.116 mmole/g of blend	98.2 %	600 rpm
EX511/12	Stearic acid	0.553 mmole/g of blend	99.0 %	500 rpm

CHAPTER 6

Results and discussion

This chapter presents and discusses the results of experiments described in chapter 5. This chapter begins with discussing the development of methods used for the detection of phase inversion points. New phase inversion maps are then developed to describe PUp-W dispersions. Effects of various process variables are also studied and discussed separately. The use of external surfactant to produce PUp-W dispersions, via catastrophic phase inversion route, is investigated in the last section.

6.1 Preliminary drop size studies

This section investigates how the choice of variables for drop size characterisation, as those mentioned in section 5.3, affects the results. These studies include (1) Comparing the arithmetic progression method with the geometric progression method; (2) Determining the optimum droplet data required; (3) Determining the number of bins needed; and (4) Fitting results using a log-normal distribution function. These studies are based on sample S2 of EX58 (mentioned in section 5.8). Data obtained from both SEM and optical microscopic images of the sample were analysed using the C⁺⁺ programme mentioned in section 5.3.6.

6.1.1 Arithmetic progression method vs. Geometric progression method

For the purpose of this study, 10 bins were used and all 843 drops calculated in the data bank were analysed. Figure 6.1 shows both the number and volumetric distribution curves plotted by using (a) the arithmetic progression method and (b) the geometric progression method.

The number distribution curve is generally biased towards the smaller drops of a droplet size distribution. When comparing the number distribution curves of figures 6.1a and 6.1b, it is seen that the arithmetic progression method enhances the bias towards small drops and creates a larger skew towards the left of the curve. Therefore, an arithmetic progression method is more suitable when comparison between smaller drop sizes is important.

On the other hand, the volumetric distribution curve places more emphasis on larger droplets. When comparing figures 6.1a and 6.1b, it is noticed that the geometric progression method enhances this property of the volumetric distribution curve. Also, the multimodal characteristic of the volumetric distribution curve, which appeared in figure 6.1a, is almost eliminated from figure 6.1b. Since the volumetric distribution of W_1/P_C drops in the experiment is unlikely to be multimodal, a geometric progression method is suitable for comparisons that emphasise the larger drops.

Table 6.1. d_{10} and d_{32} calculated using arithmetic and geometric progression method,

Method of calculation	d_{10}	d_{32}
Arithmetic progression method	1.74 μm	4.62 μm
Geometric progression method	2.00 μm	4.94 μm

Table 6.1 shows values of both d_{10} and d_{32} calculated from the arithmetic progression method and the geometric progression method. As predicted, the mean diameter values calculated from the geometric progression method are larger than that calculated from the arithmetic progression method (in this case, 0.3 μm). This result agrees with the above argument that the geometric progression method gives more emphasis on larger drop sizes. Unless otherwise specified, the geometric progression method is primarily used for the purpose of this work.

6.1.2 Optimum droplet data

One problem that arises during drop size characterisation is the uncertainty about the amount of data needed. Using too little data can result in losing some valuable information; using too much data requires excessive computation and is time consuming. This sub-section discusses the strategy used to determine the optimum

number of droplet data. Methodology mentioned in section 5.3.5 was used and data were analysed using geometric progression method.

The GSD , N_{crit} and N_{lim} values change when different amount of droplet data is used. When $N_T/N_{crit} \geq 1$, the amount of drops counted are enough to prevent the error from growing catastrophically (Paine (1993)). From figure 6.2, the absolute N_{crit} value is about 425. Paine (1993) also suggested that marginally acceptable results can be obtained between $N_T/N_{lim} \geq 1$ and $N_T/N_{crit} \leq 1$. From figure 6.2, this is between N_T of 140 to 425. However, it is noticeable that the N_T/N_{lim} value could also be larger than 1 when N_T is smaller than 150, giving a pseudo- N_{lim} value. Unfortunately, the pseudo- N_{lim} and actual N_{lim} value can only be distinguished by counting more drops than would otherwise be needed. On the safe side, when N_{crit} is very large and unobtainable, the minimum number of drops that must be counted to obtain marginally acceptable results should be when $N_T/N_{lim} = 2$ (in this case, $N_T = 280$).

Figures 6.3 and 6.4 show that d_{32} , d_{10} , GSD and δ are almost constant when $N_T \geq N_{crit}$. These values are 4.94 μm , 2.02 μm , 1.60 and 0.47 for d_{32} , d_{10} , GSD and δ respectively. Generally, the errors of these variables increase as N_T decreases. However, the errors are negligible when $N_T \geq N_{crit}$. When N_T/N_{lim} equals to 2, i.e., when N_T is about 280, the calculated error of d_{32} are about 14 % and the errors for the other variables are less than 5 %. At N_{lim} ($N_T \approx 140$), the calculated error of d_{32} is as large as 20 % and are slightly less than 10 % for the other variables.

Figure 6.5 shows six volumetric distribution curves plotted using 75, 150, 300, 500, 600 and all 843 droplets respectively. When less than 400 droplets were used (i.e., below N_{crit}), inconsistency in the distribution curves can be clearly identified. However, when more than 500 droplets (i.e., above N_{crit}) were used, the distribution curves show little difference. In other words, distribution curves can only be plotted with confidence when $N_T \geq N_{crit}$.

6.1.3 Number of bins required

As mentioned in section 5.3.1, choosing the number of bins is also important. Figures 6.6 and 6.7 show how distribution curves change when different numbers of

bins are used during the drop size characterisation. Analysis was performed using the geometric progression method with 650 droplet data.

It is noticed in figure 6.6 that the number of bins chosen affects the number distribution curve considerably. When more than 8 bins are used, the number distribution curves show bimodal characteristic (when $N_{bin} = 8$) or even multimodal characteristic (when $N_{bin} = 10$ and 15). However, when only 7 bins are used, the resulting number distribution curve has a monomodal characteristic.

These differences can be attributed to the fact that the geometric progression method tends to require smaller bin size at a small droplet range and larger bin size at a large droplet range. As a result, the geometric progression method works well only when the small drops can be characterised as accurately as the larger drops. This is not difficult if the smallest drop in a group of widely distributed droplets is a few microns in diameter, or if droplets are narrowly distributed in the sub-micron range. In the case studied, the W_1/P_C drops appear as both sub-micron drops and large drops of about 14 μm . It is therefore difficult to characterise the small drops in this type of system precisely, when the information from the larger drops is to be preserved at the same time. Hence, the number of bins used has to be chosen carefully in order to avoid creating too many bins at the sub-micron ranges. In this case, 7 bins have to be used, in favour of 10 to 20 bins suggested by Orr (1983).

Similar results are found in figure 6.7 which shows how volumetric distribution curves are affected by the number of bins used. Table 6.2 shows that both d_{10} and d_{32} values are only slightly affected by the number of bins chosen. The errors of d_{10} obtained are less than 2 % from the average value; and error of d_{32} obtained is less than 4 % from the average value.

Table 6.2. The variations of mean diameters with the number of bins,

Number of bins	d_{10}	d_{32}
7	2.01 μm	4.91 μm
8	2.05 μm	4.63 μm
10	2.02 μm	4.96 μm
15	2.07 μm	4.61 μm
Average	2.04 μm	4.78 μm

6.1.4 Curve fitting using a log-normal distribution function

The number drop size distribution of this sample can be fitted using a log-normal distribution function as shown in equation (5-13). The best-fit curve is obtained using the *solver* function of *Microsoft Excel97*. For analysis using $N_{bin} = 7$, $N_T = 650$ and the geometric progression method, the number distribution can be fitted using equation (6-1),

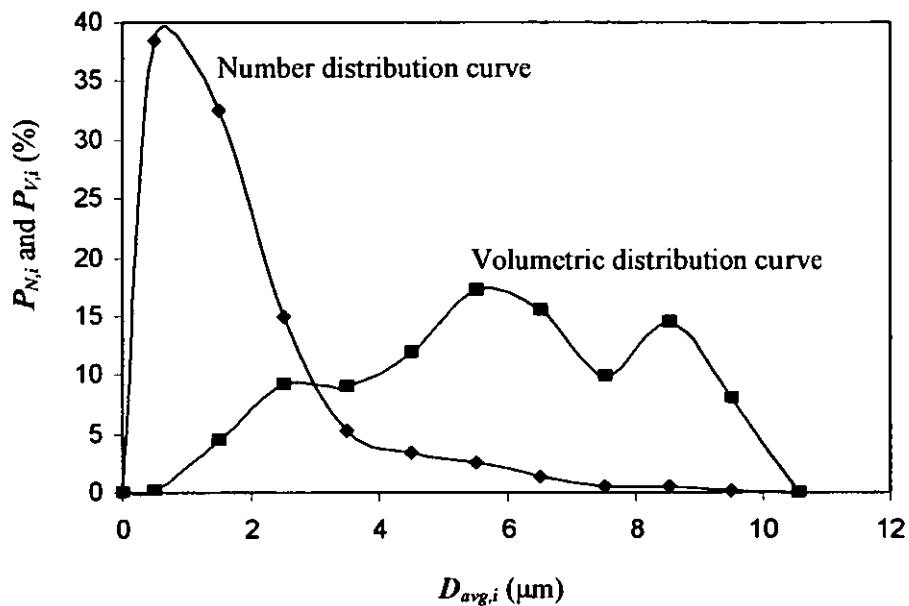
$$\frac{dP_{N,i}}{d(\log D_{avg,i})} = \frac{100}{\log 1.87 \cdot \sqrt{2\pi}} \cdot \exp\left(-\frac{(\log D_{avg,i} - \log 1.40)^2}{2 \cdot \log^2 1.87}\right) \quad [6-1]$$

where the fitted value are $\delta_{LN} = 1.87$ and $d_m = 1.40$.

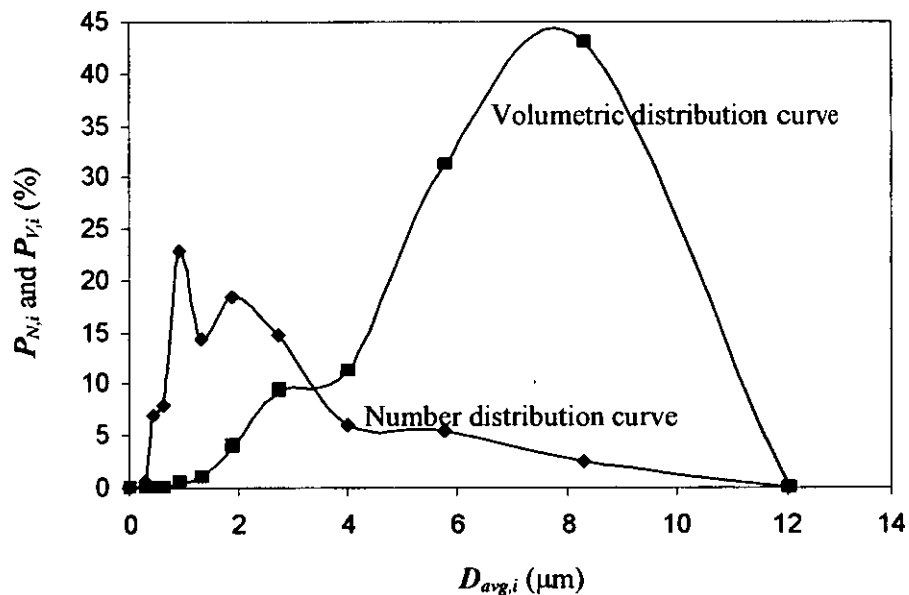
$P_{N,i}/(\Delta \log D_{avg,i})$ is plotted against $\log D_{avg,i}$ in figure 6.8. All points are calculated values and the smooth line is drawn using equation (6-1). The average curve fitting error is about 9%.

Conclusions

Droplet data in this work are analysed using geometric progression method primarily. Various parameters of droplet size distribution (such as d_{32} , d_{10} , GSD and δ) are reliable when $N_T/N_{crit} \geq 1$. Marginally acceptable results are obtainable between $N_T/N_{lim} \geq 2$ and $N_T/N_{crit} < 1$. Distribution curves can only become reproducible when $N_T \geq N_{crit}$. The number of bins that should be used in an analysis can only be determined by trial and error, with some prior estimations of the type of distribution. Also, the number of bins is not necessary confines to 10 ~ 20 bins, as suggested by other researchers. The log-normal distribution function, in the form of equation (5-13), can be used to represent some of the number drop size distribution results.



(a) Arithmetic progression method



(b) Geometric progression method

Figure 6.1. Number and volumetric distribution curves plotted using different methods

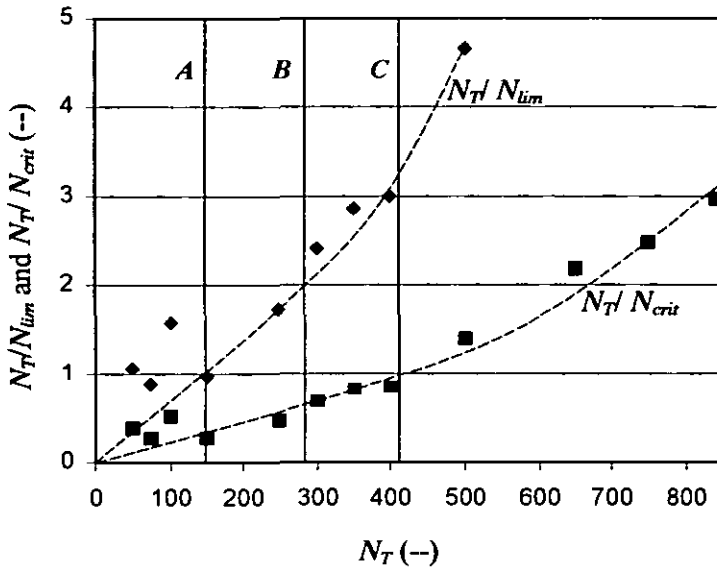


Figure 6.2. Determination of N_T required. (Line 'A': $N_T/N_{lim} = 1$; Line 'B': $N_T/N_{lim} = 2$; Line 'C': $N_T/N_{crit} = 1$)

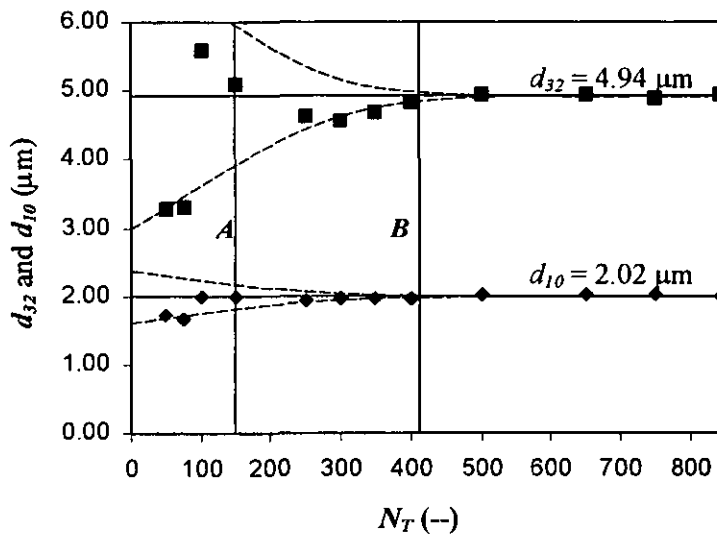


Figure 6.3. Effect of N_T on calculated d_{32} and d_{10} . (Line 'A': $N_T = N_{lim} = 140$; Line 'B': $N_T = N_{crit} = 425$)

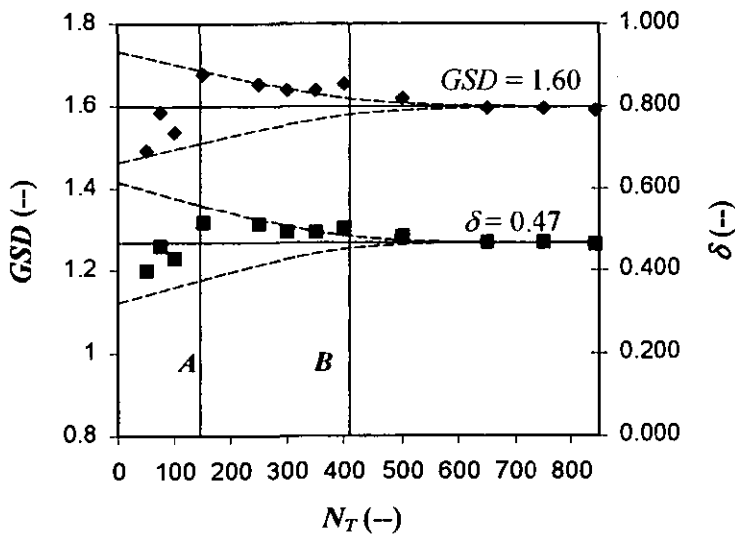


Figure 6.4. Effect of N_T on calculated GSD and δ . (Line 'A': $N_T = N_{lim} = 140$; Line 'B': $N_T = N_{crit} = 425$)

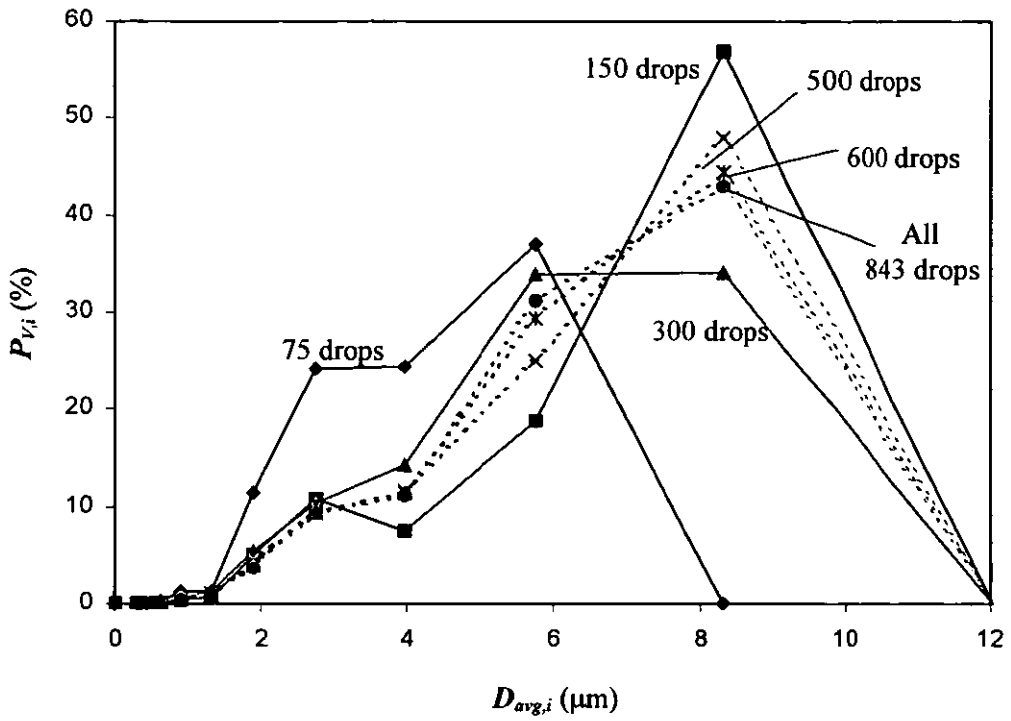


Figure 6.5. Volumetric distribution curves plotted using different N_T

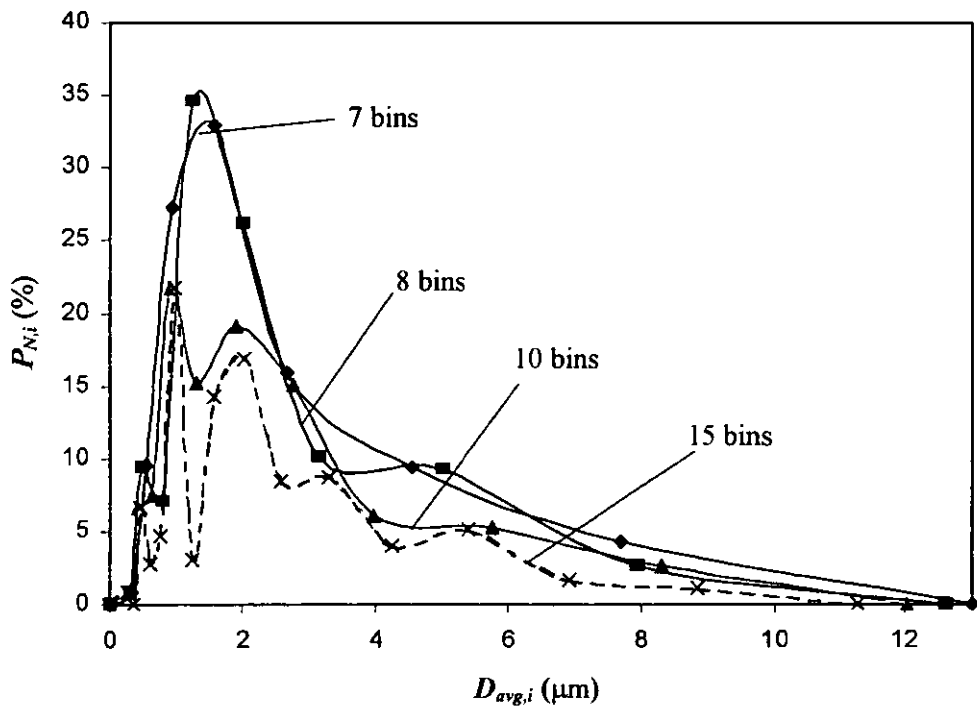


Figure 6.6. Number distribution curves plotted using different N_{bin}

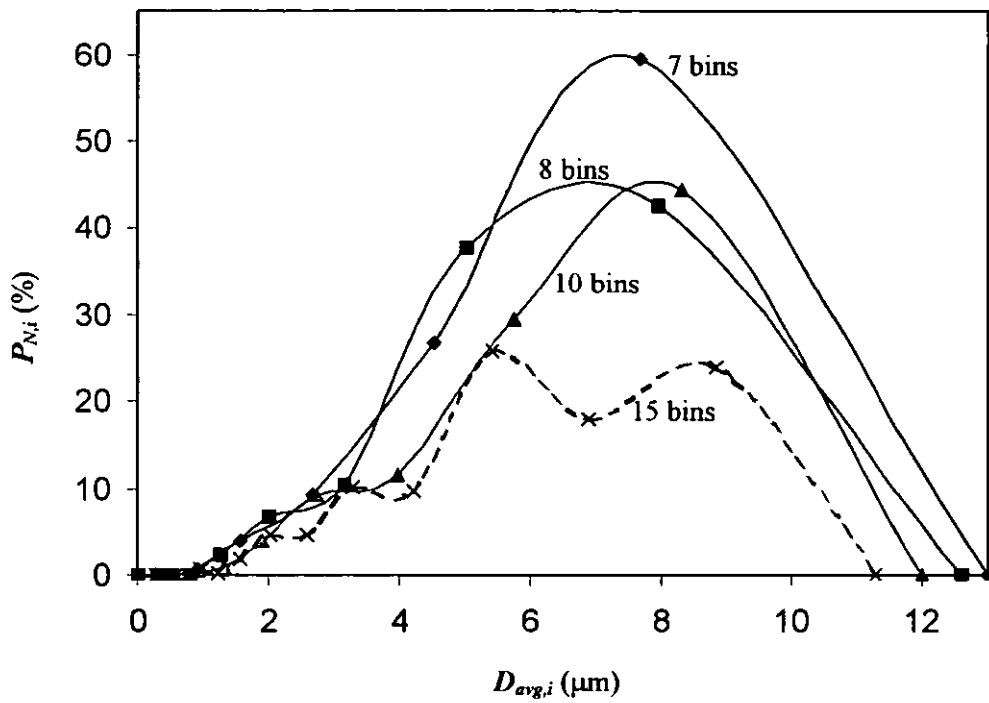


Figure 6.7. Volumetric distribution curves plotted using different N_{bin}

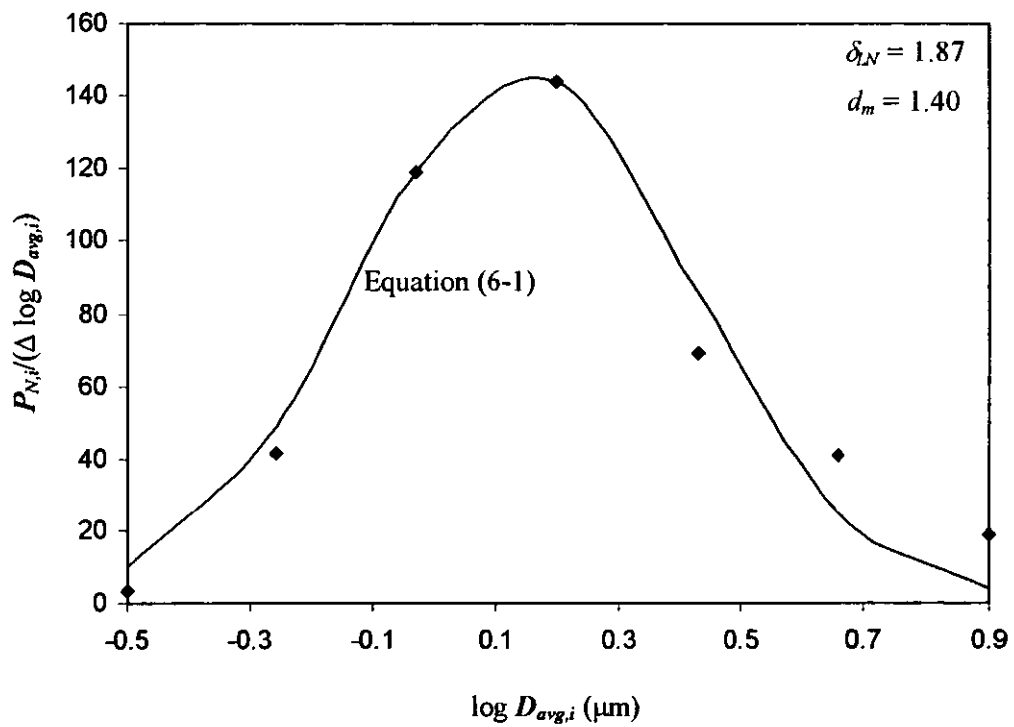


Figure 6.8. Fitting data using log-normal distribution function [equation (6-1)]

6.2 Methods for the detection of phase inversion points

Many researchers have used conductivity measurements (Salager (1988); Gilchrist et al. (1989); Brooks and Richmond (1991, 1994d); Zerfa et al. (1999)) and torque (or viscosity) measurements (Chen and Chen (1992); Yang et al. (1995); Akay (1998)) to detect the phase inversion points. This section assesses the possibility of using both methods to detect the phase inversion points in this work.

6.2.1 Conductivity graphs

During a catastrophic phase inversion experiment, a conductivity graph is plotted using conductivity as the ordinate and weight percentage of water in the emulsions as the abscissa (as shown in figure 6.9).

Line 'A' in figure 6.9 represents a conventional conductivity graph of a catastrophic phase inversion process where the emulsions are stabilised by external emulsifiers, or when no surfactants are used at all. In those cases, low conductivity readings indicate that polymer or oil phase is the continuous phase. The aqueous phase is normally distilled water in which some salts, such as potassium chloride and sodium chloride, are dissolved to improve the conductivity of the aqueous phase. Therefore, high conductivity readings indicate that the aqueous phase is the continuous phase. Phase inversion in those cases could be identified by a transient response in conductivity that took place over a few seconds (Pacek et al. (1994b)). Line 'A' shows that the system changes from oil or polymer-continuous to aqueous-continuous at a specific water fraction. The phase inversion point in those cases can therefore be identified easily.

Line 'B' in figure 6.9 represents the conductivity graph obtained from experiment EX54/1. Conductivity starts increasing at a water content as low as 10 wt.-% and the increase only becomes smaller at water content greater than 50 wt.-%. The conductivity readings increase continuously and this shows that the phase inversion route taken by a PUp-W system is different from those stabilised by external emulsifiers. There must be more interactions between water and the polymer than that in the previous case. Therefore, the use of conductivity as the sole mean to detect phase inversion points is unsatisfactory for producing phase inversion maps of PUp-W systems.

6.2.2 Design of conductivity probe(s)

The above-mentioned experiment used only one double sensor probe to measure the changes in conductivity. It was suspected that the above-mentioned abnormal conductivity graph could be caused by the deficiency of the double sensor probe in measuring the conductivity. For example, the conductivity meter may give a faulty reading of the system if large dispersed drops stretch across the two sensor heads and do not move away for a prolonged period of time.

Experiment EX54/2 is similar to EX54/1, except that two single sensor probes were used apart in the vessel. The conductivity graph obtained from this modified experiment is similar to that shown in figure 6.9. Therefore, the lack of sharp change in conductivity is a property of the PUp-W systems studied and not an artefact. In other words, both probes can be used with confidence. For practical reasons, only the double sensor probes will be used in future studies.

6.2.3 Addition of KCl

Experiment EX54/3 is similar to EX54/1, except that no KCl was added to the aqueous phase. It was found that the conductivity graph obtained from EX54/3 is similar to EX54/1. This finding indicates that it is unnecessary to add any salt to aid the conductivity measurements. This is because the neutralised PUp ionomer alone can make the aqueous phase conductive. Therefore, addition of KCl is only needed for PUp-W systems that use poorly neutralised, or non-neutralised, PUp ionomer.

6.2.4 Torque changes graphs

It is now clear that conductivity measurements alone can not be used to detect the phase inversion points of all PUp-W systems. Another way of identifying inversion points is by measuring the viscosity changes during the phase inversion processes. For Newtonian fluids in the laminar flow region, changes in torque at a fixed agitation speed are proportional to the changes in viscosity. Under the process conditions studied in this work, the pure polymers were being agitated at Reynolds numbers smaller than 0.79 (i.e., in the laminar flow region). Although it is hard to predict the changes in Reynolds numbers throughout the phase inversion processes, it is not unreasonable to assume that the polymer-continuous dispersions will be

agitated in the laminar flow region at least up to the phase inversion points. In addition to this, assume that the PUp-W mixtures behave as Newtonian fluids throughout the phase inversion process, it should then be possible to use a FSTC agitator to monitor the torque (and hence viscosity) changes experienced by the PUp-W mixtures during the process.

In this work, torque changes can be plotted using relative torque changes as the Y-axis and water content as the X-axis. Figure 6.10 shows a torque changes graph plotted from experiment EX54/1. It resembles closely to the viscosity variation of a phase inversion process during the production of PUp-W dispersions (as studied by other researchers, see figure 2.2 of section 2.2.2). As mentioned in section 2.2.2, a phase inversion point can be identified as the point when viscosity just passes its maximum. Since torque is proportional to viscosity, the phase inversion point can be identified from figure 6.10 as the point when the torque just passes its maximum value. In this case, phase inversion takes place at about 30 wt.-% of water.

Conclusions

Only torque change measurements can be used to detect phase inversion points for the experiments mentioned so far. However, the sensitivity of torque changes measurement is not as distinct as in cases when conductivity measurements are effective. Therefore, both methods are used together for the detection of phase inversion points during the production of PUp-W dispersions.

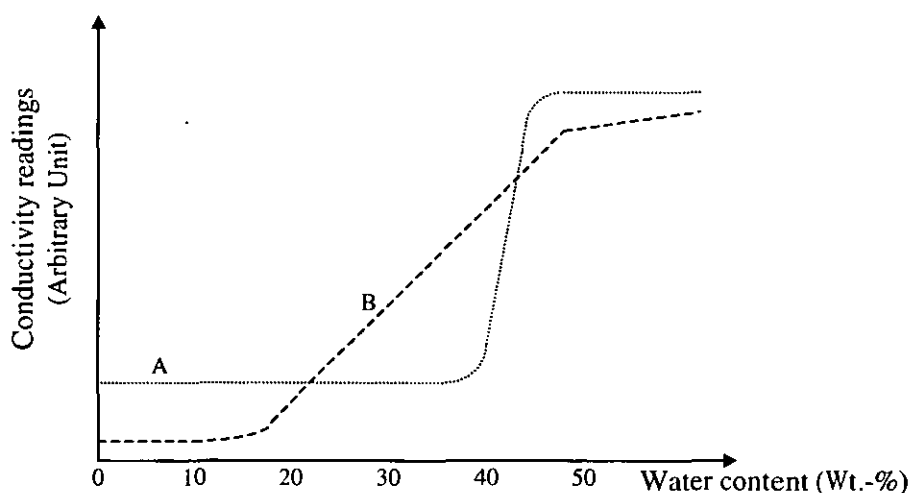


Figure 6.9. Conductivity graphs of (A) conventional phase inversion processes with transient conductivity response [reproduced from Pacek et al. (1994b)]; (B) experiments EX54/1 to EX54/3

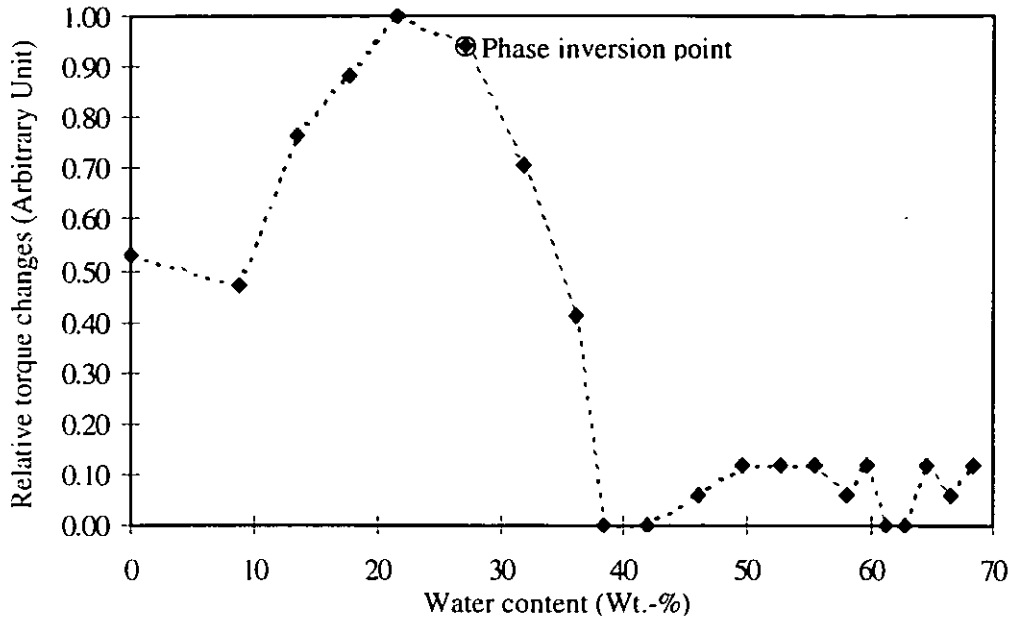


Figure 6.10. Torque changes graph of experiment EX54/1

6.3 Effect of ionic group content on PWCPi process

Depending on the DN, and hence the ionic group content, three distinctive types of dispersion behaviours have been identified for PUp-W systems (Brooks and Saw (1999)). These dispersion regions can be represented using a catastrophic phase inversion map proposed in this section. Differences in various behaviours amongst all three dispersion regions are also discussed here.

6.3.1 Catastrophic phase inversion map

Concept

As mentioned in section 2.9, the dynamics of changes in the dispersion of external surfactant stabilised oil-water (O-W) systems is best described by a phase inversion map (Brooks and Richmond (1991)). Typical phase inversion maps for non-ionic surfactant-oil-water (nSOW) systems are plotted using either SAD or HLB value as the ordinate and O-W ratio as the abscissa (as figure 2.8 of section 2.9).

Whether it is HLB or SAD, the ordinates of the phase inversion maps reflect Winsor's concept of interaction energies, which assigns a SOW mixture to one of

three different groups*. Agitation of Type 1 and Type 2 mixtures is expected to produce oil-in-water (O_1/W_C) and water-in-oil (W_1/O_C) emulsions respectively. For Type 3 mixtures, surfactant affinity for both phases is approximately equal and a mixture can form one, two or three phases. According to Salager (1988), Type 3 system is obtained when $SAD = 0$, at the occurrence of “optimum formulation”. In essence, half of the phase inversion map represents external stabilised O-W mixtures that are more likely to be water-continuous and the other half represents mixtures that are more likely to be oil-continuous; the central line (often horizontal) represents the transition between these two states.

Modified application

Padget (1994) showed that the hydrophilicity of hydrophobic polymers can be modified using water-solubilising groups, such as materials containing carboxylic acids, as the co-monomers. Depending on the ratio of hydrophobic co-monomer to hydrophilic co-monomer, the polymer can change from highly water-insoluble to highly water-soluble. Similarly, the hydrophilicity of PUp containing a fixed amount of carboxylic acid group can be modified by changing the DN, as shown in this study. As DN increases, a water-indispersible polymer becomes readily water-dispersible. In essence, the interaction energies between PUp and water change in a similar fashion to the ordinate of the traditional phase inversion maps. During a PWCPI process, the PUp-W ratio changes at a fixed DN, similar to the abscissa of a traditional phase inversion map. Therefore, a phase inversion map can be plotted to describe the dynamics of changes in the dispersion of ionically modified PUp-W system.

Catastrophic phase inversion map

Based on this idea, figure 6.11 shows a new phase inversion map plotted using the amount of ionic groups (DN can be used equally well) as the ordinate and water content (PUp-W ratio can be used equally well) as the abscissa. This map is not complete because the transitional phase inversion line(s) have not yet been located. Since it only shows the phase inversion loci of PWCPI process, the term “catastrophic phase inversion map” is used to describe figure 6.11. This map is plotted using results obtained from experiments EX55/1 to EX55/8 mentioned in section 5.5.

* Details of Winsor’s concept of interaction energies have been mentioned in section 2.9.

From figure 6.11, different dispersion “regions” are revealed as the amount of ionic groups increases. This is a surprising result, when compared with previous researches, in at least two ways:

1. As mentioned before, only two regions are identifiable in a traditional phase inversion map for externally stabilised O-W dispersions. Therefore, the internal functional groups might contribute to the existence of the extra region in the PUP-W dispersions; and
2. Literature on the production of aqueous PU ionomer colloids shows that a minimum ionic group concentration is required to form stable PU ionomer dispersions and no dispersion can be formed below that minimum concentration (Chen and Chen (1992); Satguru et al. (1994)). In other words, a phase inversion map for PU ionomer – water dispersions should only have two regions. Unlike those studies, the present study concerns the dispersion of pre-polymer. Therefore, it is possible that typical chain extension process following the creation of aqueous PUP dispersions (as used in industry and previous researches) will eliminate one of the dispersion regions obtained from PUP-W dispersions.

In figure 6.11, the three dispersion regions are identified as RI, RII and RIII. The last letter “P” or “W” indicates whether an emulsion is polymer or water-continuous. Properties of these regions are discussed in the following sub-sections. Table 6.3 summarises various characteristics of all three dispersion regions.

6.3.2 Region I (RI) – High ionic group content

Ionic group content in this region is more than about 0.2 mmole/g of neutralised –COOH groups. Typical conductivity and torque changes graphs in this region are shown in figure 6.12a. It can be seen that transition points of the two curves do not match with each other.

It is believed that this disagreement on transition point is a direct result of the swelling of ionically modified PUP in the presence of dispersed water. The extent of swelling increases with increasing amount of ionic group content. It is possible that, above a certain neutralised -COOH content, the swelling is so intense that the polymer-continuous dispersion actually “conducts”. This can happen if the continuous polymer phase can expand, or swell, enough to create a “channel” to provide free

movement to the dispersed water. With the creation of these channels, the dispersed water can move freely between the continuous phase and sends a false signal to the conductivity meter. For this reason, together with reasons mentioned in section 6.2.4, the torque changes measurement is a better method to detect a phase inversion point in this region.

As shown in table 6.3, emulsions produced in this region are stable. These emulsions contain simple P_1/W_C drops in the sub-micron range. Due to the small drop size, these drops cannot be detected using the optical microscope unit, as shown in figure 6.13a. The SEM-freeze fracture technique can be used instead. A typical SEM image of water-continuous emulsions in the RI region is shown in figure 6.13b. Aqueous emulsions in this region were also characterised using the LALLS technique.

Emulsions produced in this region are stable for periods of time from one week to more than a year. This result is expected since ionic group content in this region is above the reported minimum requirement for the production of stable aqueous PU dispersions.

6.3.3 Region II (RII) – Moderate ionic group content

Ionic group content in this region is between about 0.05 to 0.2 mmole/g of neutralised $-\text{COOH}$ groups. Typical conductivity and torque change graphs in this region are shown in figure 6.12b. It can be seen that the transition points of both curves match with each other nicely. This matching in transition point shows that torque-change detection is a valid method in identifying phase inversion points, although it might not be as sensitive as using the conductivity measurement. Although the FSTC agitator cannot be calibrated to detect viscosity changes directly, its ability to detect the relative changes in torque is sensitive enough to identify the phase inversion points of PUp-W systems.

The matching of transition points in both graphs also supports the previous argument that excessive swelling of PUp ionomer caused the pre-polymer to “conduct” when it is still the continuous phase in the RI region. In the RII region, the pre-polymer does not swell enough to “conduct” when pre-polymer is the continuous phase. Therefore, the abrupt increase in conductivity corresponds to the phase inversion point when water becomes the continuous phase.

Table 6.3. Characteristics of RI, RII and RIII during the PWCPI process,

Region	RI	RII	RIII
Ionic group content	High (> 0.2 mmole/g)	Moderate (0.05 ~ 0.2 mmole/g)	Low (< 0.05 mmole/g)
Catastrophic phase inversion route*	$W_1/P_C \rightarrow P_1/W_C$ (Small)	$W_1/P_C \rightarrow P_2/W_1/P_1/W_C + W_1/P_1/W_C + P_1/W_C$ (Small and Large)	$W_1/P_C \rightarrow (W_1/P_1)/W_C$
Detection method†	T only	T and C	T (and possibly C)
PWCPI loci (figure 6.11)	As shown along line 'CRI'.	As shown along line 'CRII'.	As shown along line 'CRIII'.
Dispersion behaviour‡	Stable emulsion (Type 5 emulsion)	Stable coarse emulsion (Type 4 emulsion)	Temporary dispersion (Type 2 emulsion)
Sedimentation	Stable for one week to more than a year.	Stable for ½ ~ 3 days. Separated emulsions can easily be recreated.	Separation occurs as soon as agitation has stopped.
Drop structure	Small simple P_1/W_C drops in the sub-micron range.	Mixture of drop structures (Figure 6.15).	Opaque W_1/P_1 lumps in continuous water phase.

As shown in table 6.3, stable coarse emulsion that is stable for half to three days can be produced in this region. Figures 6.14 and 6.15 illustrate the drop structures of an emulsion in this region. This emulsion is produced using 32 %

* W_1/P_C ~ Water drops in a polymer-continuous phase. P_1/W_C ~ Polymer drops in a water-continuous phase. $W_1/P_1/W_C$ ~ Water drops in polymer drops which are dispersed in the water-continuous phase. $(W_1/P_1)/W_C$ ~ Not a true emulsion, a water-continuous phase surrounds polymer-continuous lumps which contain water drops in them. (Small) ~ small drops. (Large) ~ Large drops.

† T stands for torque changes detection method and C stands for conductivity detection method.

‡ Nomenclature for the type of emulsion produced has already been mentioned in section 2.10.1.

neutralised PUp2-7.5* through the PWCPI process and this sample contains 60 wt.-% of water. From figure 6.14, it is not difficult to notice the complex structures of drops. These drop structures include: (1) Simple P_1/W_C drops in the sub-micron range and drops as large as a few microns (figures 6.14 and 6.15a); (2) Multiple drops in the form of water-in-polymer-in-water ($W_1/P_1/W_C$, figures 6.14a, 6.14b and 6.15b); and (3) Multiple drops in the form of polymer-in-water-in-polymer-in-water ($P_2/W_1/P_1/W_C$, figures 6.14b, 6.14c and 6.15c). Also, the primary water drops (W_1) can appear as both large drops, which fill almost the entire primary polymer drops (P_1), and small drops, which only fill a small proportion of the P_1 drops. The sizes of these P_1 drops range from a few microns to as large as 25 μm .

The separated emulsions can be recreated with very low energy input, for example, this can be done by shaking the sample bottle with hand. When these recreated emulsions were examined under the optical microscope, the drops still appeared in their original structures. These well-preserved drop structures suggest that the neutralised -COOH content is sufficient to prevent coalescence of aqueous PUp drops from happening. Therefore, the unstable emulsions contain stable droplets.

In other works, Chen and Chen (1992) and Satguru et al. (1994) reported that the minimum ionic group content required to form a stable dispersion of PU anionomer is between 0.178 mmole/g to 0.25 mmole/g of neutralised -COOH groups. RII contains about 0.05 to 0.2 mmole/g of neutralised -COOH groups, and its emulsion is, therefore, expected to separate after a few days or even after a few hours. However, it has never been reported that this unstable emulsion is caused by the dual factors of the presence of larger drops and a mixture of drops' structures in the water-continuous emulsion. Also, it has not been reported that unstable emulsions containing stable droplets can be produced below the "minimum" ionic group content.

6.3.4 Region III (RIII) - Low ionic group content

Ionic group content in this region is below about 0.05 mmole/g of neutralised -COOH groups. Typical conductivity and torque changes graphs in this region are shown in figure 6.12c. Due to the low ionic group content, water used in this region

* Equivalent to 0.178 mmole/g of neutralised -COOH content.

was added with 0.5 wt.-% of KCl to increase the conductivity. This aqueous solution was then adjusted to show a reading of 40 on the conductivity meter. It is interesting to notice that, when water has become the continuous phase (judging by both the torque changes graph and visual inspection), conductivity measured by the meter is still very low. Apart from this low conductivity reading (maximum average reading of about 12), the conductivity readings also fluctuate a lot. This abnormal conductivity graph shows that the dispersion is very unstable. Pre-polymer “lumps” constantly break-up and coalesce to send the fluctuating signal to the conductivity meter.

Emulsions obtained in this region are temporary. They separate as soon as agitation has stopped. After the separation, two layers were obtained - a clear water layer and an opaque layer. Under the microscope, the opaque layer contains W_1/P_1 drops. These water drops are believed to have been entrained within the polymer phase before inversion occurs (figure 6.16).

According to Dieterich (1981), when there are not enough hydrophilic groups, excess water can no longer be absorbed by the polymer-continuous phase and is forced to form a continuous second phase instead. Based on this inversion mechanism, when there are insufficient ionic groups as in this case, PWCPI takes place when water is refused its entrance to the polymer-continuous phase. Therefore, unstable simple $(W_1/P_1)/W_C$ emulsion is created as has happened in the RIII region.

Conclusions

Depending on the ionic group content, three different dispersion regions have been discovered when a catastrophic phase inversion process is used for the preparation of aqueous ionically modified PUp colloids. Valid phase inversion detection methods have been developed for all three regions and characteristics of these regions have been studied. Stable emulsions containing small P_1/W_C drops are produced in RI; Stable coarse emulsions containing a mixture of stable drop structures are produced in RII; and only temporary dispersions can be produced in RIII. The existence of these dispersion regions during the PWCPI process can also be described using a modified catastrophic phase inversion map.

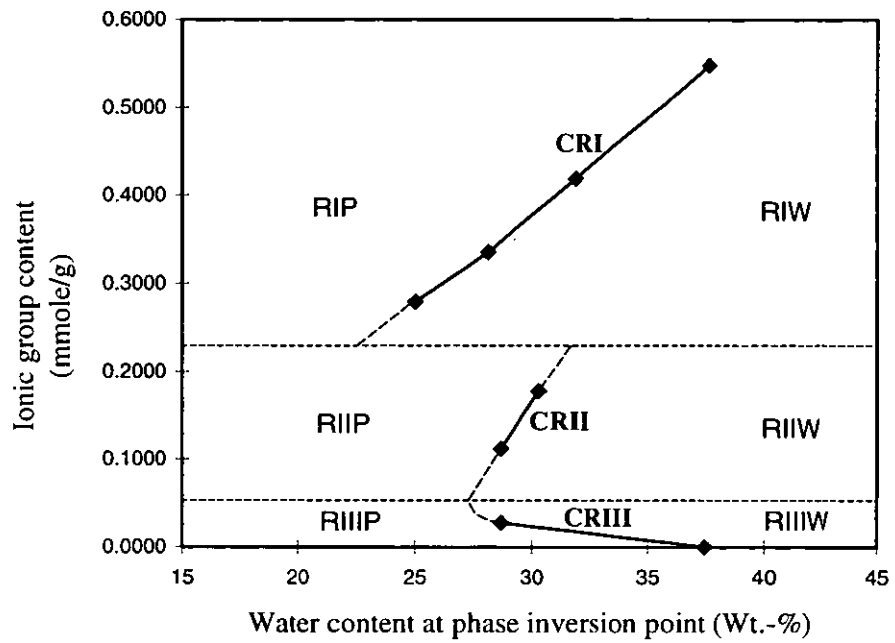
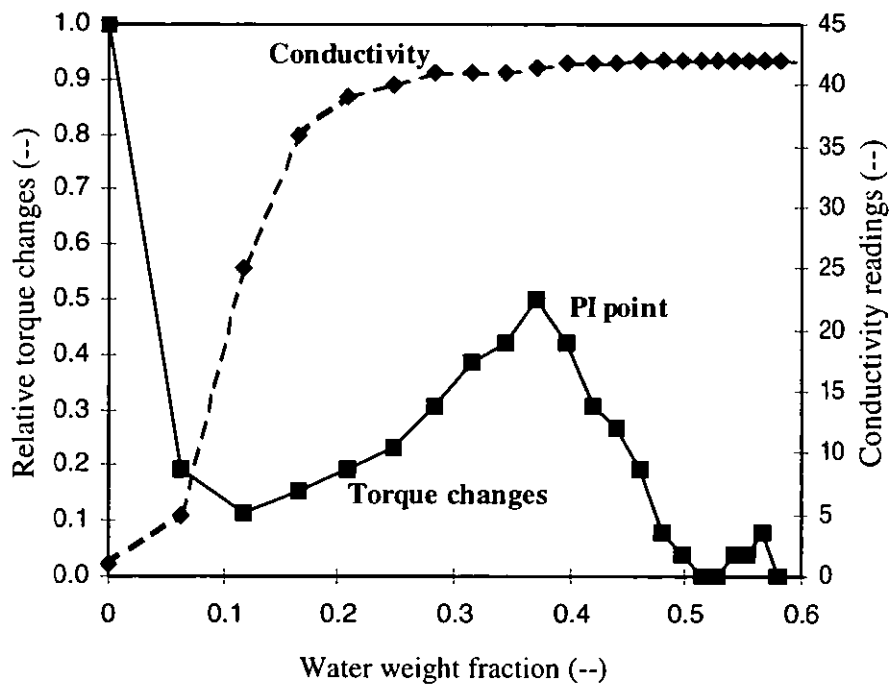
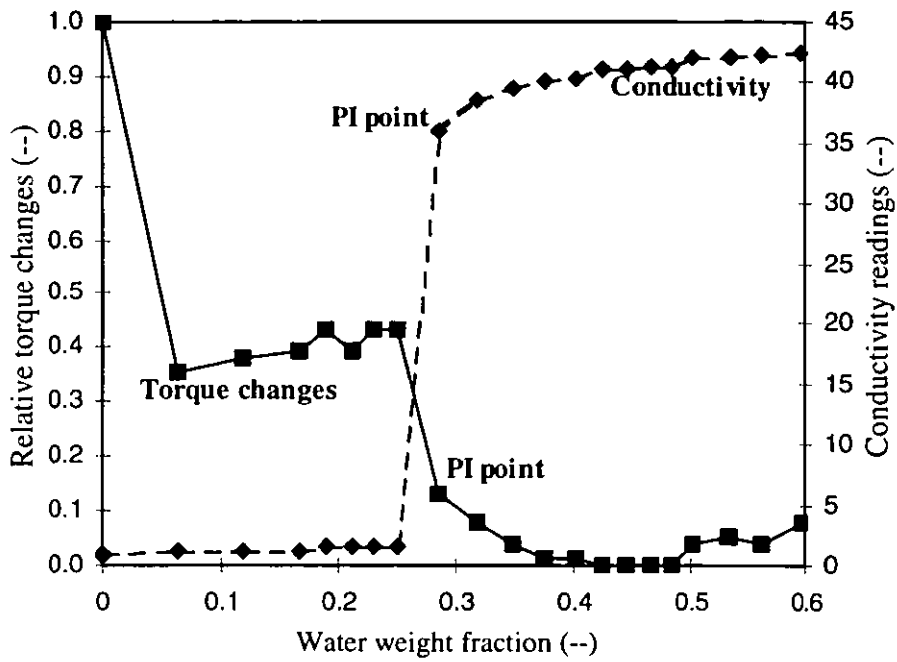


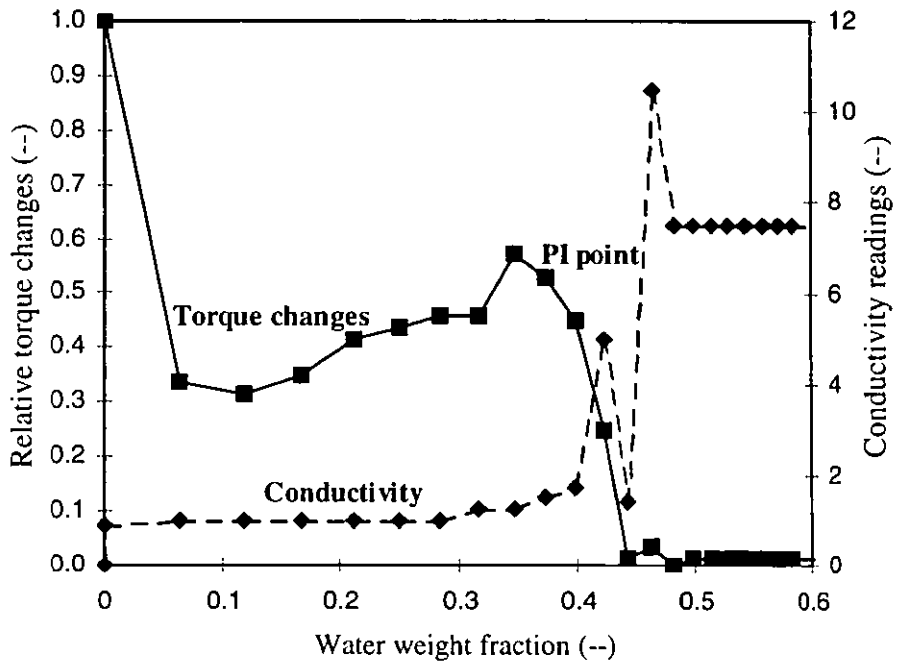
Figure 6.11. Catastrophic phase inversion map for PUp-W dispersions (The horizontal lines are tentative boundaries between RI-RII and RII-RIII)



(a) Region I (RI)



(b) Region II (RII)



(c) Region III (RIII)

Figure 6.12. Torque changes and conductivity graphs of PWCPI experiments

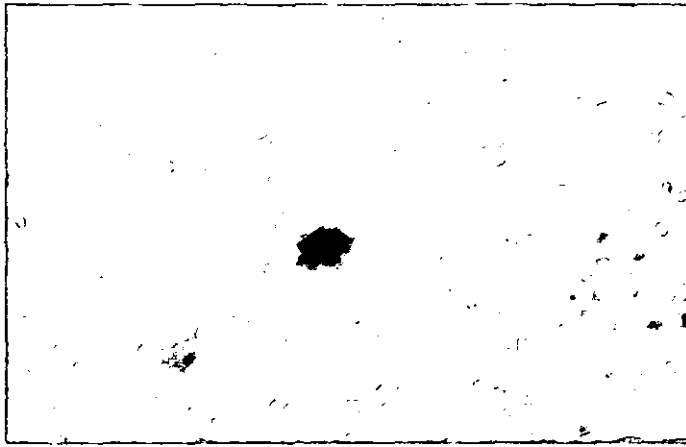


Figure 6.13a. Optical microscopic image of emulsions in the RIW region: P_1/W_C drops are too small to be seen clearly

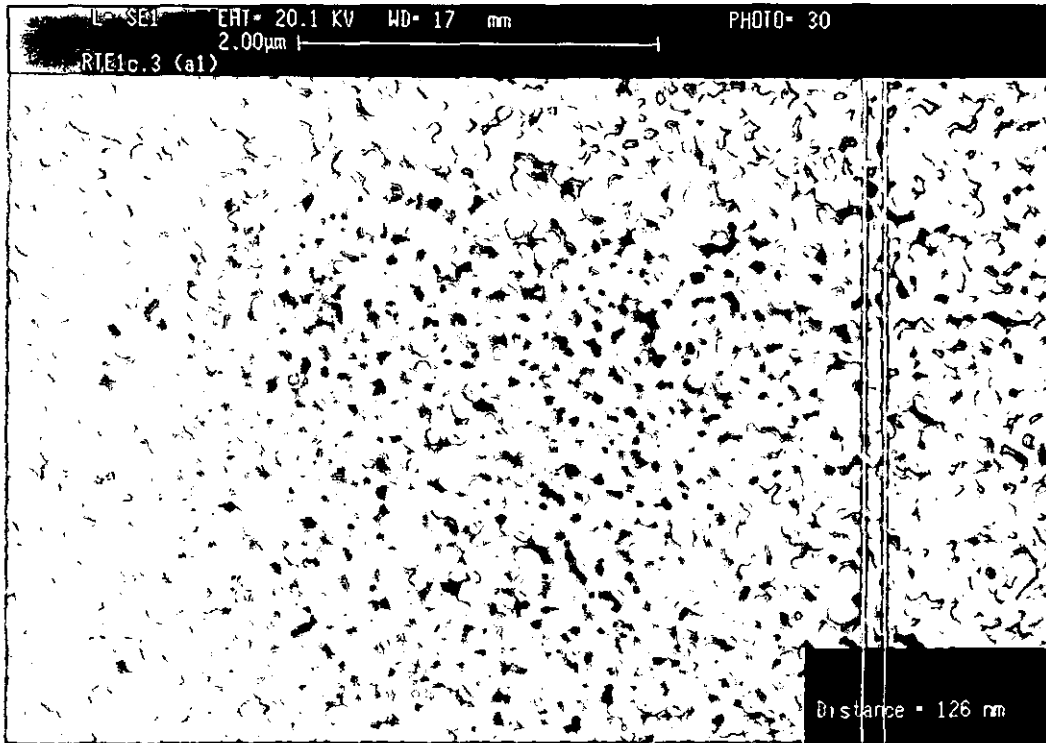


Figure 6.13b. SEM image of emulsions in the RIW region: Small P_1/W_C drops

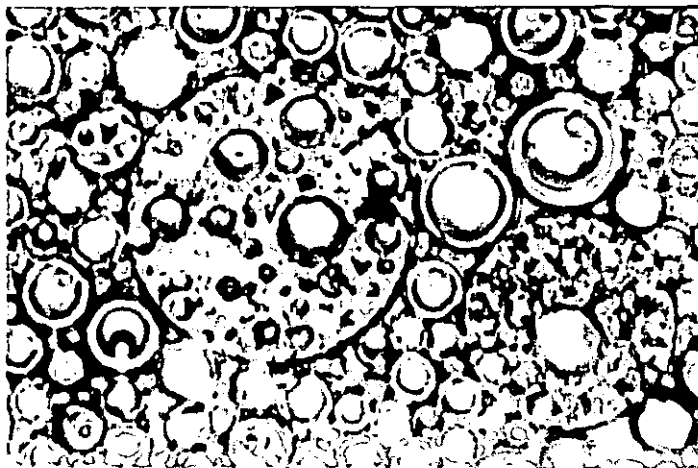
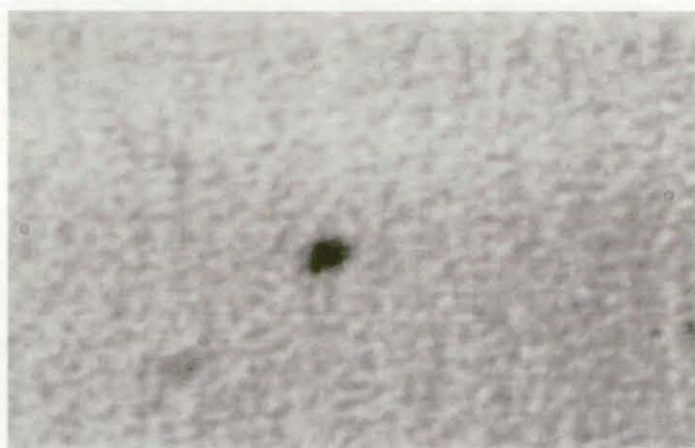


Figure 6.14a. Optical microscopic image of emulsions in the RIW region: A mixture of drop structures can be seen clearly



10 μm

Figure 6.13a. Optical microscopic image of emulsions in the RIW region: P_1/W_C drops are too small to be seen clearly

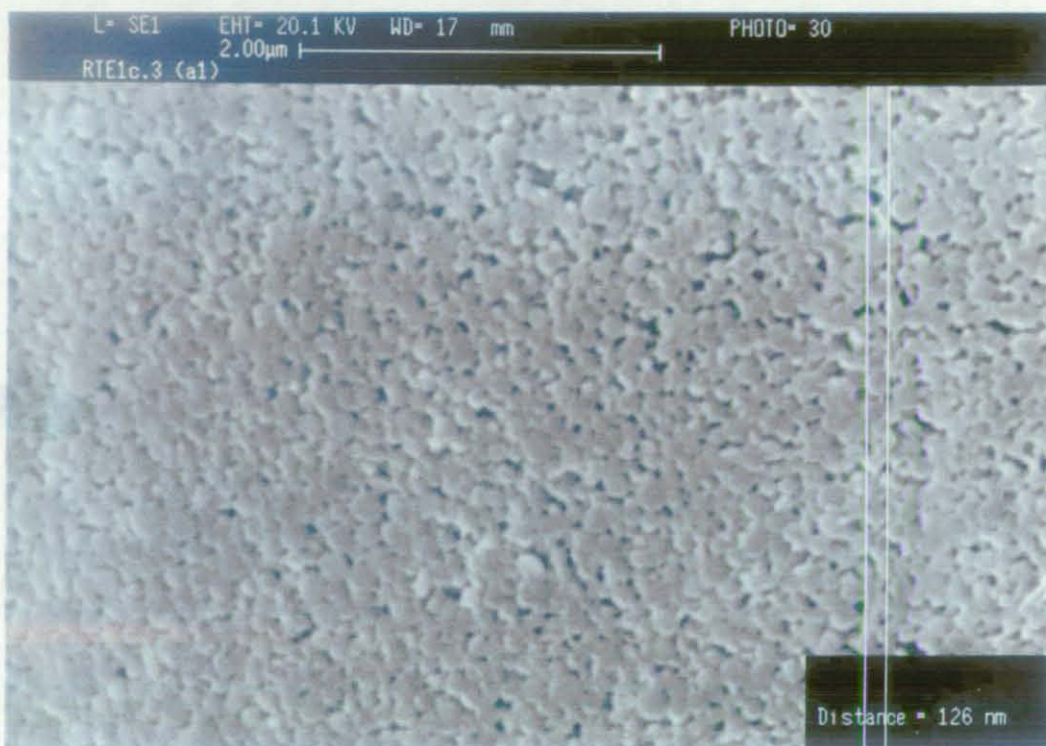
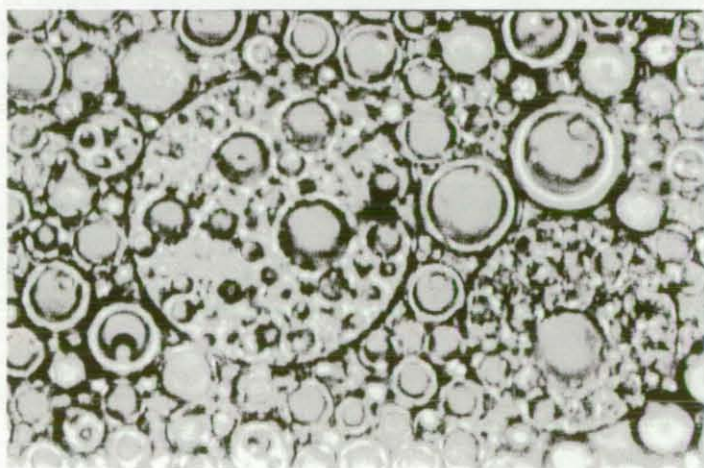


Figure 6.13b. SEM image of emulsions in the RIW region: Small P_1/W_C drops



10 μm

Figure 6.14a. Optical microscopic image of emulsions in the RIIW region: A mixture of drop structures can be seen clearly

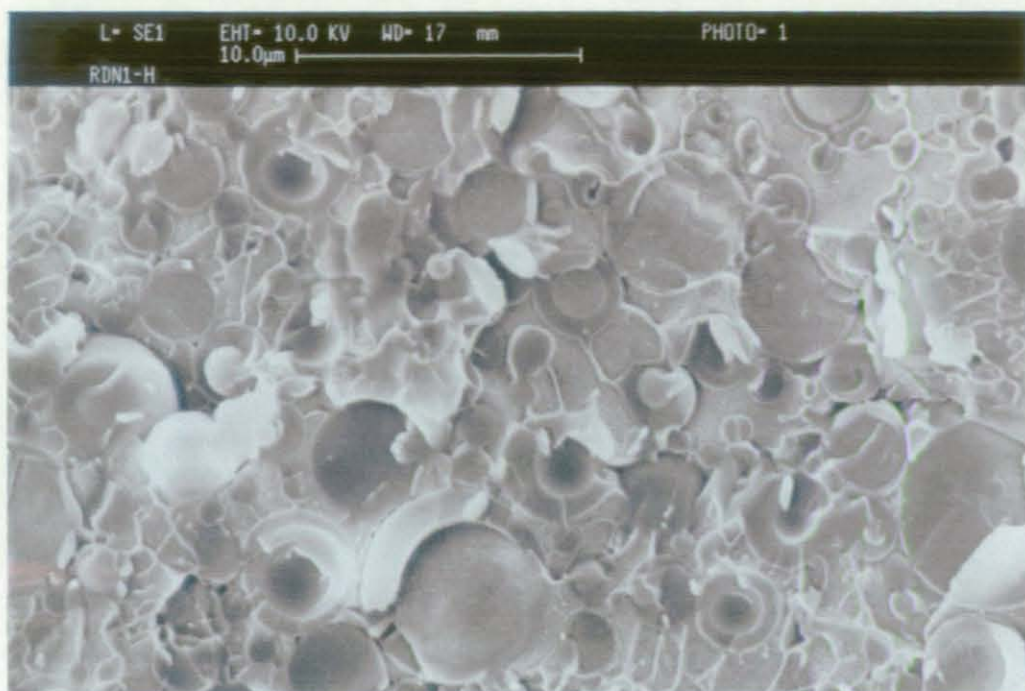


Figure 6.14b. SEM image of emulsions in the RIIW region: Showing the complex multiple drop structures



Figure 6.14c. SEM image of emulsions in the RIIW region: Showing the existence of small drops $\sim 0.8 \mu\text{m}$

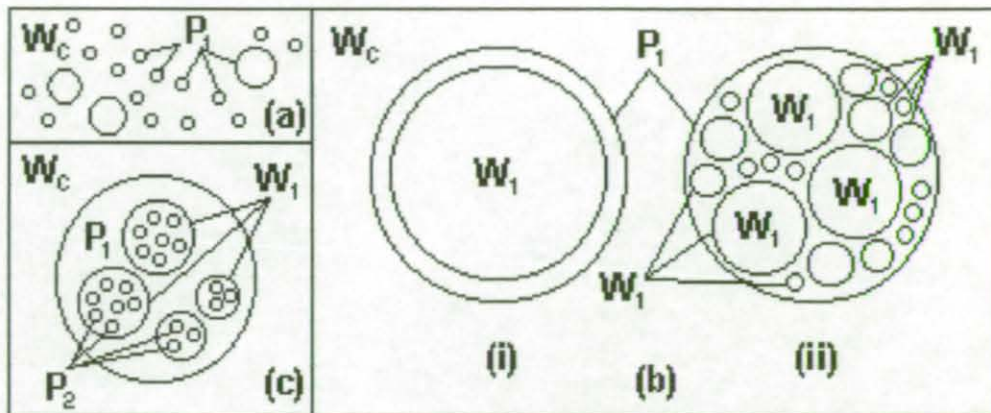


Figure 6.15. Different drop structures of emulsions in the RIIW region: (a) Simple P_1/W_C drops; (b) Multiple $W_1/P_1/W_C$ drops with (i) large W_1 drops and (ii) small W_1 drops; and (c) Multiple $P_2/W_1/P_1/W_C$ drops

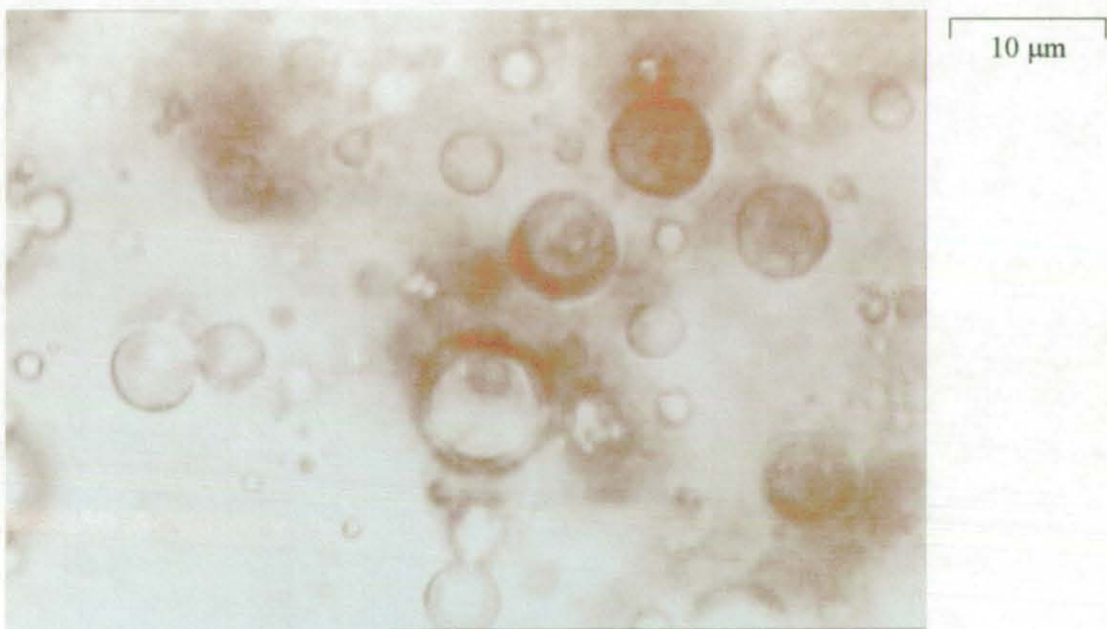


Figure 6.16 Optical microscopic image of W_1/P_1 drops in the separated opaque substance of emulsions in the RIIIW region

6.4 External viscosity measurements

As mentioned in section 5.6, some rheological changes might take place during a catastrophic phase inversion process. The successful usage of the FSTC agitator to detect phase inversion points, therefore, depends on a thorough understanding of rheological changes during the phase inversion process.

6.4.1 Results

Figure 6.17 shows the conductivity and torque changes graphs of experiments EX56/1 and EX56/2 mentioned in section 5.6. Based on the chosen DN, the amount of ionic groups in EX56/1 and EX56/2 are 0.280 and 0.168 mmole/g respectively; from figure 6.11, these should produce RI and RII dispersions respectively. Similar to other PWCPI process in the RI region, rises of conductivity in figure 6.17a cannot be used to determine the phase inversion point of EX56/1. For EX56/1, torque changes start dropping when water content is close to 24.64 wt.-% (S4). In figure 6.17b, both the rise in conductivity and the drop in torque changes reading take place when the mixture contains about 31.69 wt.-% of water (S4). For reasons mentioned in section 6.3, this is the catastrophic phase inversion point when the PUp-W mixture changes from polymer-continuous to water-continuous.

Figure 6.18 shows how viscosity changes with spindle rotating speed for all 6 samples withdrawn from both experiments. At low water content (< 15.86 wt.-% of water), figure 6.18a shows that S1 and S2 of EX56/1 have a Newtonian behaviour. At 20.00 wt.-% of water, S3 starts to show a pseudo-plastic (or shear thinning) behaviour. S4 and S5 have very distinct pseudo-plastic behaviours. Also, the viscosity of both samples decrease sharply as spindle rotating speed increases. When water content increases above 24.64 wt.-% (S4), viscosity decreases at all rotating speeds.

For EX56/2, figure 6.18b shows that S1 (12.13 wt.-% of water) has a slightly pseudo-plastic behaviour. As water content increases, S2 and S3 show more significant pseudo-plastic behaviours and both samples have similar viscosity. Again, S4 and S5 show distinct pseudo-plastic behaviours. Once more, as water content increases above 31.69 wt.-% (S4), viscosity decreases regardless of spindles rotating speeds. Figure 6.18b also shows that the viscosities of S4 and S5 are significantly higher than S3 at spindle rotating speeds below 5 and 2 rpm respectively. However, at higher spindle rotating speeds, S4 and S5 are less viscous compared to S3.

6.4.2 Power law

The viscosity of non-Newtonian fluids such as pseudo-plastic and dilatant material can generally be represented using a power-law. Sakiadis (1984) mentioned one form of power-law by correlating viscosity to shear rate:

$$\mu = C_{16} \cdot K \left| \frac{du}{dy} \right|^{n-1} \quad [6-2]$$

where μ is viscosity, in Pa.s; C_{16} is a dimensional constant; K is a consistency index, in $N.s^n/m^2$; du/dy is the rate of shear (or velocity gradient); and n is an exponent, dimensionless.

According to Brookfield engineering laboratories, the rate of shear of a non-Newtonian fluid depends on the spindle rotating speed, and to a lesser extent, on the shape of the spindle. For a series of measurements at different speeds using the same spindle, the rate of shear is directly proportional to the spindle rotating speed, S (rpm). Therefore, equation (6-2) can be re-written, for this study, as,

$$\mu = K(S)^{n-1} \quad [6-3]$$

where μ is viscosity, in cPs; K is consistency index, in $cPs.rpm^{(1-n)}$; S is the spindle rotating speed, in rpm; and n is an exponent, dimensionless.

Table 6.4. K and n values of equation (6-3) for samples withdrawn from experiments EX56/1 and EX56/2. (Also includes the extrapolated viscosity at 500 rpm),

Experiment	Sample	K value	n value	Viscosity at 500rpm (cPs)
EX56/1	S3	30,000	0.54	1,530 ± 4%
EX56/1	S4	77,000	0.34	1,300 ± 4%
EX56/1	S5	69,000	0.26	820 ± 4%
EX56/1	S6	15,000	0.31	190 ± 2%
EX56/2	S2	16,000	0.71	2,610 ± 4%
EX56/2	S3	16,000	0.69	2,320 ± 6%
EX56/2	S4	29,000	0.41	760 ± 6%
EX56/2	S5	18,000	0.42	480 ± 6%
EX56/2	S6	4,100	0.48	160 ± 7%

Figures 6.19 and 6.20 compare the measured viscosity, of S3 and S4 for both experiments, to the viscosity correlated using equation (6-3). Normal-normal and log-log plots are shown in figures 6.19 and 6.20 respectively. It can be seen that the measured viscosity can be estimated, to an error smaller than 7 %, using equation (6-3). In other words, these samples are all power-law non-Newtonian fluids. More specifically, they are power-law pseudo-plastic materials. Equation (6-3) can also be used to correlate the viscosity – spindle rotating speed relationship of other samples withdrawn from the experiments. Table 6.4 lists the K and n values (obtained by curve fitting using the *solver* function of *Microsoft Excel97*) for other samples taken from experiments EX56/1 and EX56/2. Based on the K and n values, table 6.4 also shows extrapolated viscosity for the samples at 500 rpm*.

6.4.3 Changing rheological properties

It is now clear that rheological properties of PUp-W mixtures do change during a catastrophic phase inversion process. The starting material, PUp, is Newtonian. At the beginning of the PWCPI process, the PUp-W mixture behaves as a Newtonian fluid up to 15 wt.-% and 12 wt.-% of water for EX56/1 and EX56/2 respectively. This is probably due to the ability of neutralised PUp to swell up with water to form a homogeneous continuous phase. Therefore, at low water content, the homogeneous PUp-W mixtures behave rheologically as the starting material. As water droplets start forming after further addition of water, the mixtures show some pseudo-plastic behaviour. This pseudo-plastic behaviour of the PUp-W mixture can exist in both the polymer-continuous mixture and the water-continuous emulsions. Therefore, it is impossible to identify the phase inversion points by using the rheological change of the PUp-W mixture alone. The later sub-section, 6.4.4, will discuss how the phase inversion point can be identified.

* Predicting viscosity at 500 rpm using viscosity measured at a range of 0.5 to 100 rpm will undoubtedly incur large errors to the predicted results. However, the purpose of this exercise is to estimate what might happen at high rotating speed, which we can not assess using the existing equipment. Therefore, while the predicted viscosity serves well for qualitative comparison purposes (as in this study), the value should not be taken as absolute viscosity of the PUp-W mixtures.

As for now, let's assume that sample S4 of both experiments are at the phase inversion points (as will be shown in the next sub-section). It can then be noticed that viscosity starts decreasing regardless of the rotating speed after phase inversion has occurred. The n value in Table 6.4 can be used as a guideline of how "pseudo-plastic" a material is. Lower n values correspond to more significant pseudo-plastic behaviours. It can be seen that n values of both experiments reached a minimum before they start to increase again. These minimum n values are obtained in S5 and S4 of EX56/1 and EX56/2 respectively. The increasing n values imply that the pseudo-plastic behaviour of aqueous emulsions starts to diminish. Therefore, after phase inversion, viscosity decreases and pseudo-plastic behaviour diminishes until the aqueous emulsion becomes inviscid and behaves as a Newtonian fluid (like pure water). Yang et al. (1997b) also observed similar changes in rheological properties at the phase inversion point during the production of water-borne epoxy resins.

6.4.4 Using the FSTC agitator to detect the phase inversion point

Viscosity changes have long been used as a means to identify the phase inversion points during the production of aqueous PU colloids (Dieterich (1981); Chen and Chen (1992); Yang et al. (1995)). However, these researchers have never discussed the changes of rheological properties during catastrophic phase inversion processes. In those studies, the precise location of the phase inversion point was not important. Hence, it was suitable to assume that phase inversion took place after the PU-W mixture passes through the maximum viscosity.

Figure 6.21 shows two lines plotted using viscosity against water content of EX56/2 at two different spindle rotating speeds. At low spindle speed (1 rpm), S4 which contains 31.69 wt.-% of water lies at the maximum of the plot. Viscosity drops as water content increases. At high spindle rotating speed (500 rpm), S4 lies at the point when viscosity drops sharply from > 2000 cPs to about 750 cPs. Therefore, both rheological properties and viscosity have to be taken into account when a catastrophic phase inversion point is to be identified using a viscosity-related measurement method. When a Brookfield Synchro-Lectric viscometer is being used, the spindle rotating speed plays an important role. At low spindle rotating speed, the maximum of a viscosity – water content graph is where the phase inversion took place; at high spindle rotating speed, viscosity drops sharply at the phase inversion point.

As mentioned in section 6.3.3, conductivity can be used to measure the catastrophic phase inversion point of RII dispersions accurately. For EX56/2, phase inversion took place at S4 (as in figure 6.17b). This can be related to a sharp change in pseudo-plastic behaviour of the PUp-W mixtures as shown in figure 6.18b and table 6.4. This sharp rise in pseudo-plastic behaviour could be explained by the fact that a highly concentrated water-continuous emulsion has been produced from a relatively diluted polymer-continuous emulsion. The decrease in overall viscosity of mixture, following addition of more water, confirms that water has become the continuous phase. Since the FSTC agitator is operated at 500 rpm, the torque change graph closely resembles line 'B' of figure 6.21. Therefore, the sharp drops in torque changes reading during the RII PWCPI processes correspond to the inversion points.

Similar arguments can be applied to the RI catastrophic phase inversion process. As shown in the previous paragraph, two pieces of information are required to identify the phase inversion point:

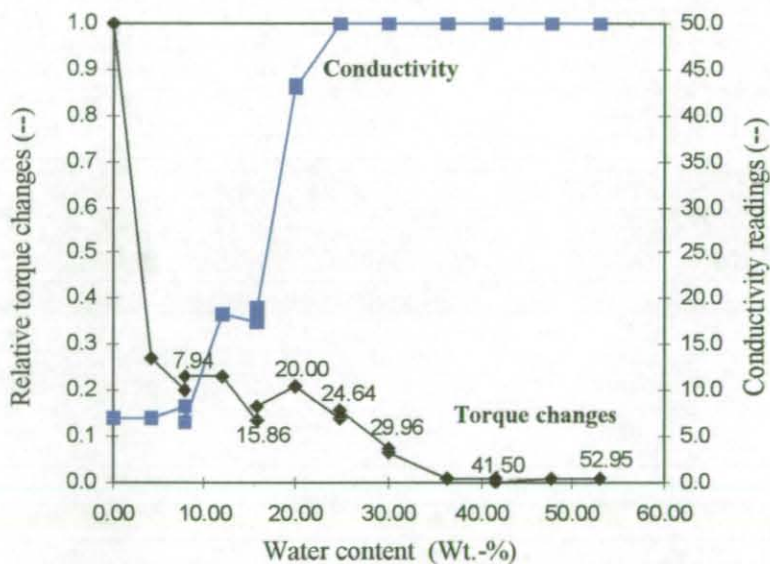
1. Sharp rise in pseudo-plastic behaviour in the vicinity of the catastrophic phase inversion point. This can be identified by a sharp drop in n values; and
2. Viscosity continues to drop, regardless of its rotating speed, when more water is added into the PUp-W mixture after PWCPI has taken place.

Table 6.4 shows that both S4 and S5 have a lower n value when compared to their previous samples. However, at a similar increment in water content, the n value of S4 drops more sharply than that of S5*. In figure 6.18a, viscosity reaches a maximum at S4. Both S5 and S6 have a lower viscosity compared to S4 at all spindle rotating speed. Combining evidence from changes in rheological property and viscosity, S4 is the phase inversion point. Within the measurable speed range of figure 6.18a for EX56/1, viscosities of both S4 and S5 are higher than that of S3. Therefore, a viscosity – water content graph within this speed range is similar to line 'A' of figure 6.21. However, at 500 rpm, figure 6.21 and table 6.4 show that the viscosities of S4, S5 and S6 are all smaller than that of S3. In other words, the catastrophic phase inversion point is the point at which viscosity start dropping for RI dispersions carried out at high spindle rotating speed (as the torque change graph in figure 6.17a).

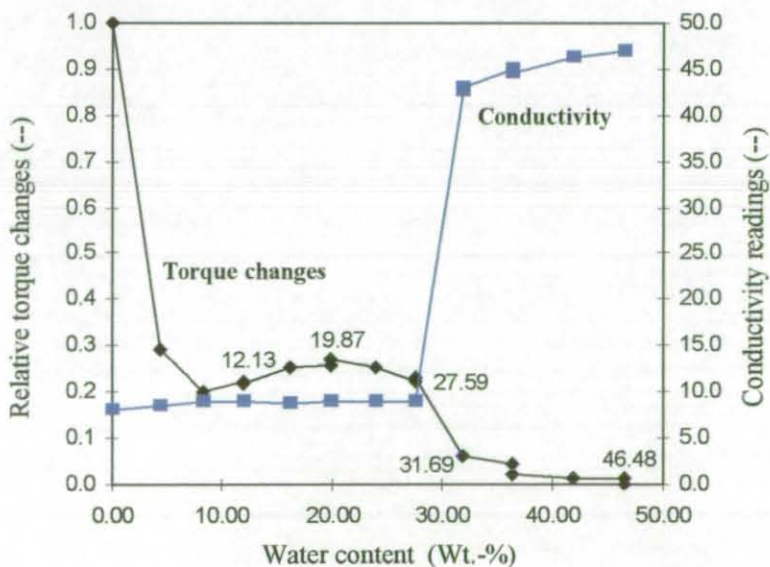
* From S3 to S4: Change in water content is 4.1 wt.-% and drop in n value is 0.193. From S4 to S5: Change in water content is 4.7 wt.-% and drop in n value is 0.08

Conclusions

This study confirms that there are rheological changes during the catastrophic phase inversion process in the production of PUP-W dispersions. Although the initial continuous phase is a Newtonian fluid, PUP-W mixtures containing more than 20 wt.-% of water behave as power-law pseudo-plastic fluids both before and after phase inversion. Based on the new findings, it is demonstrated that the FSTC agitator can be used to detect the phase inversion points fairly accurately. At high spindle or agitator rotating speeds, phase inversion points can be identified from the torque change graphs as the point when torque starts to drop and/or when the torque drops sharply. Errors involved in detecting the phase inversion points are attributed mainly to the step-increments of water content.



(a) EX56/1



(b) EX56/2

Figure 6.17. Conductivity and torque changes graphs of EX56/1 and EX56/2

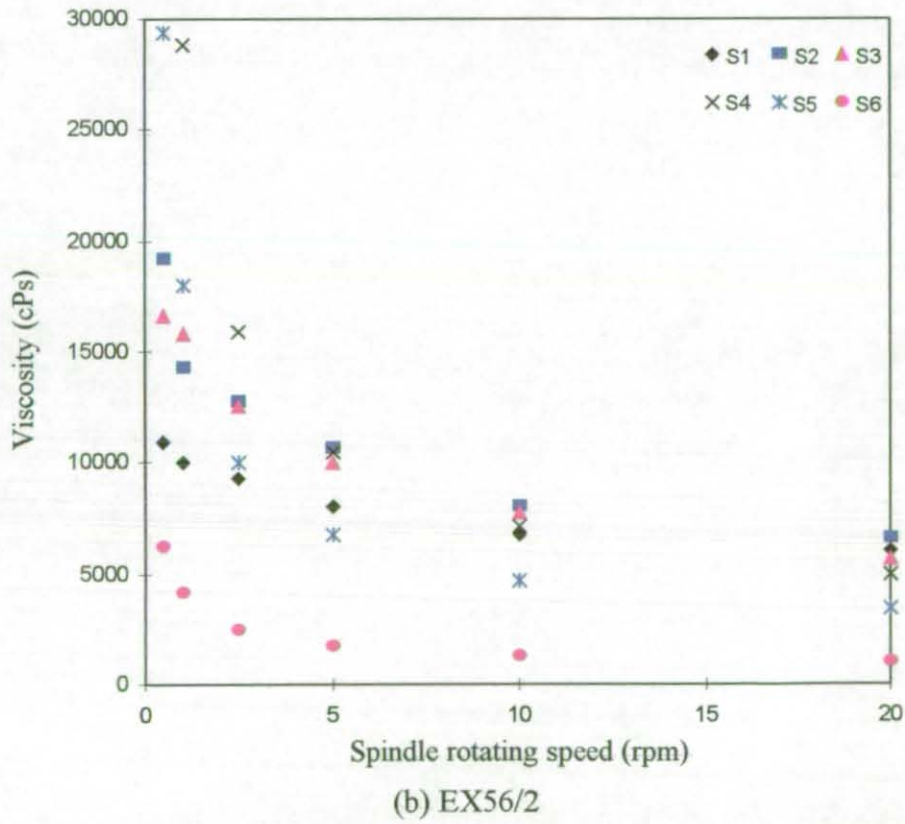
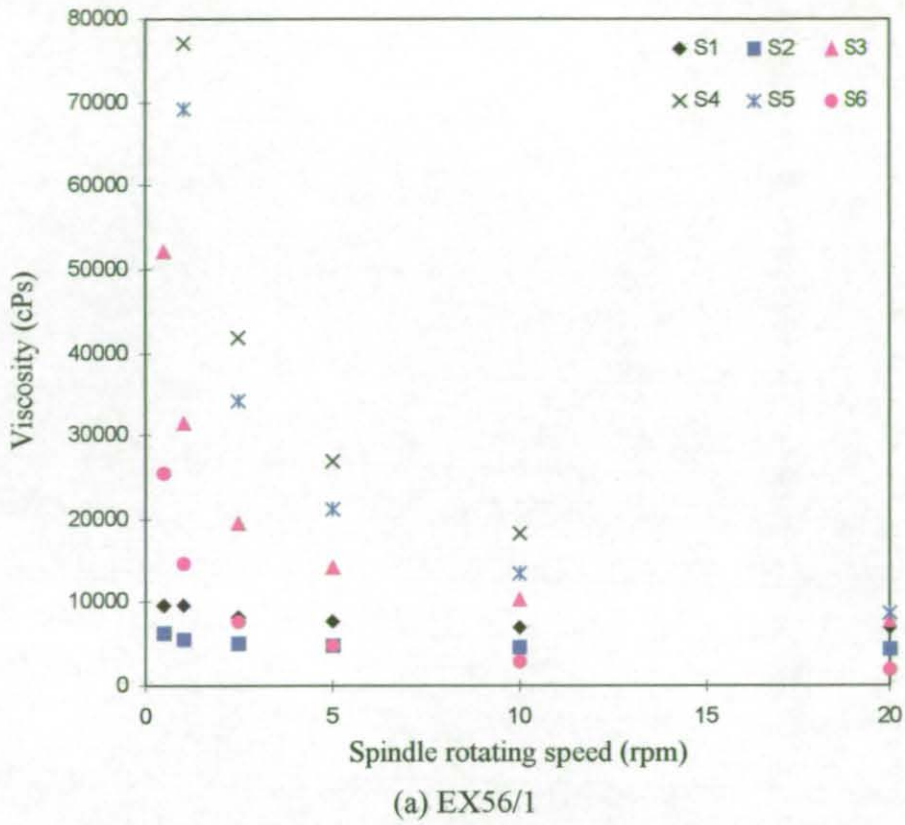
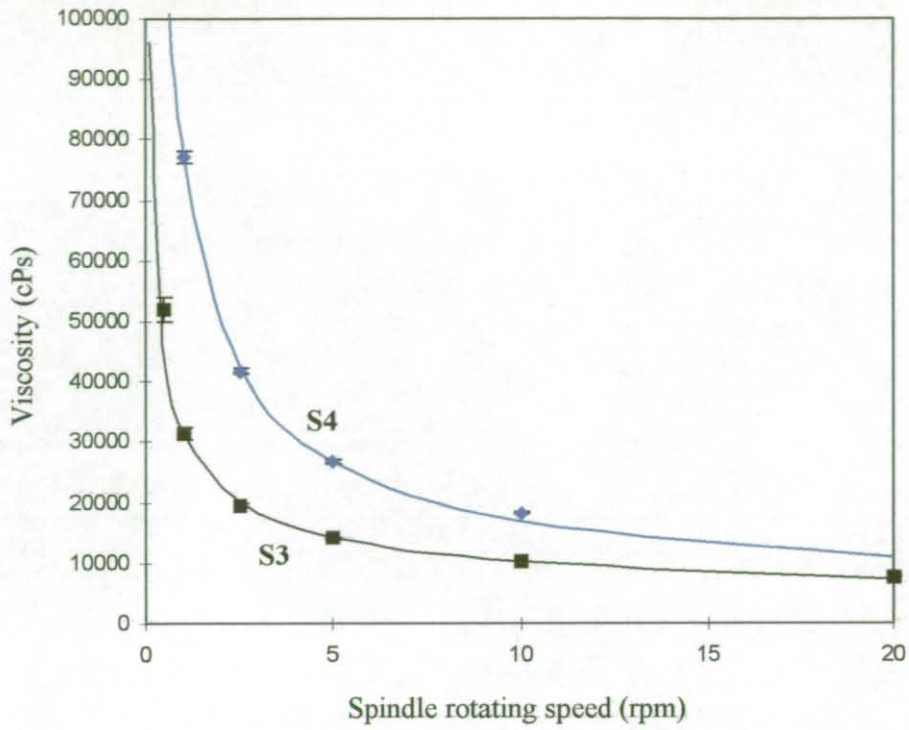
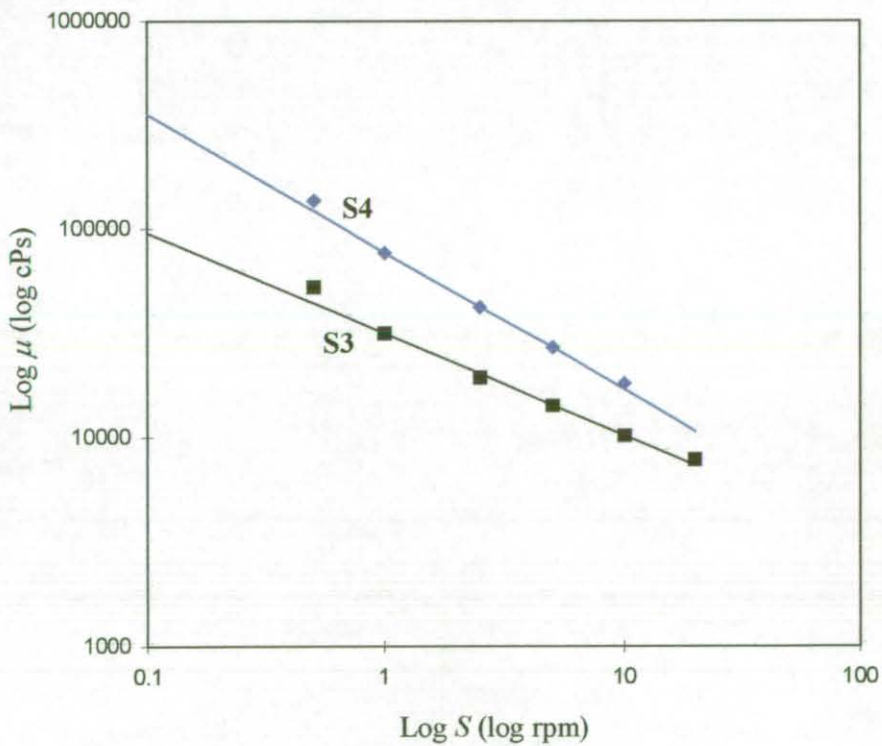


Figure 6.18. Viscosity – spindle rotating speed relationship for EX56/1 and EX56/2 (using Brookfield viscometer)

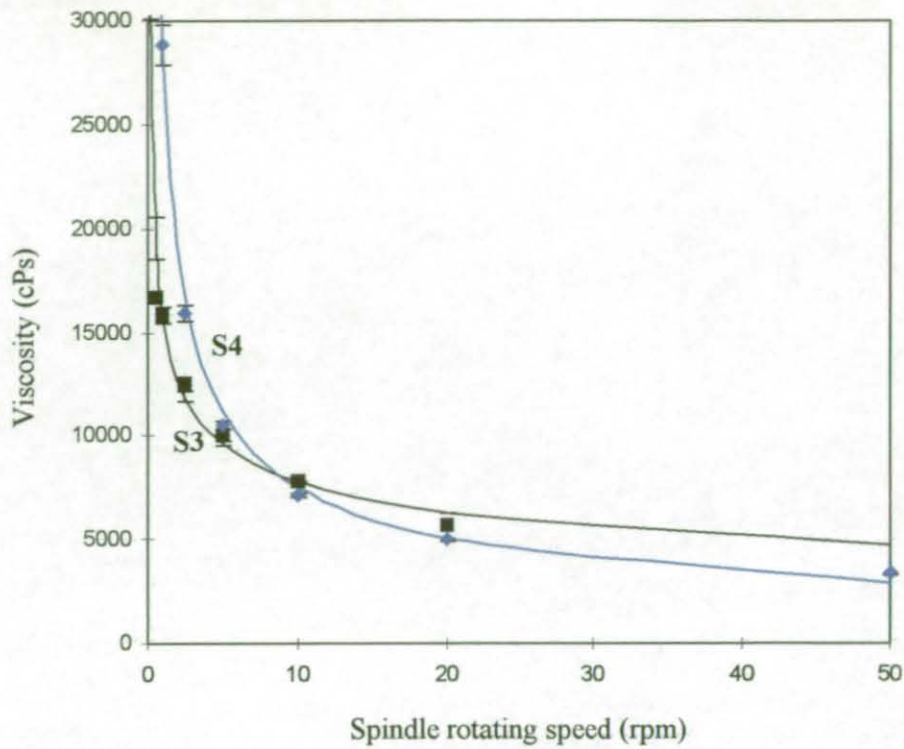


(a) Normal-normal plot

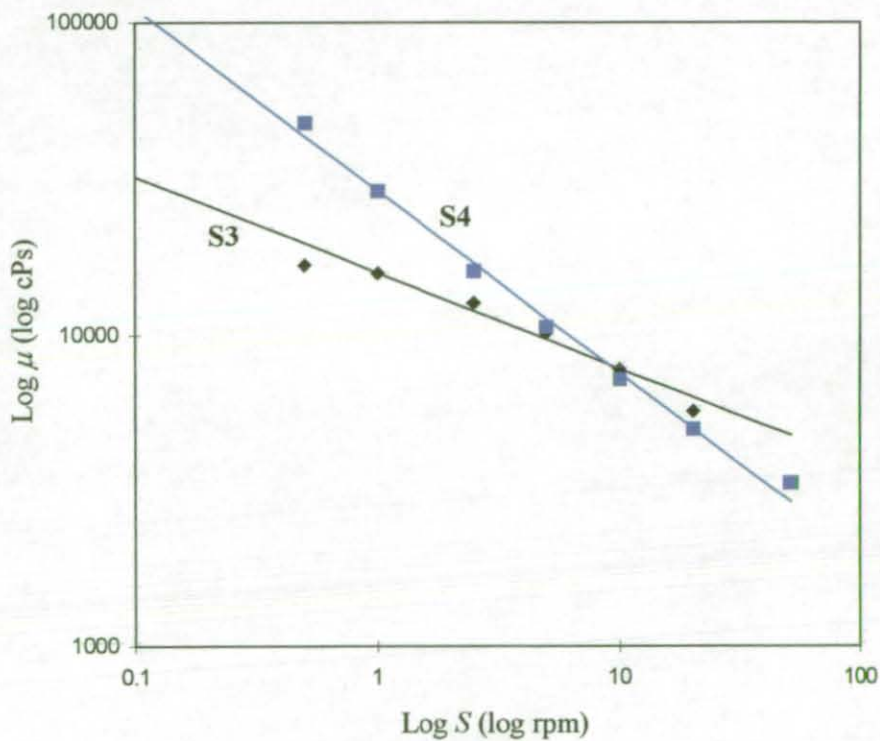


(b) Log-log plot

Figure 6.19. Comparison of measured viscosity (dots) of S3 and S4 of EX56/1 to viscosity predicted using equation (6-3) (lines)



(a) Normal-normal plot



(b) Log-log plot

Figure 6.20. Comparison of measured viscosity (dots) of S3 and S4 of EX56/2 to viscosity predicted using equation (6-3) (lines)

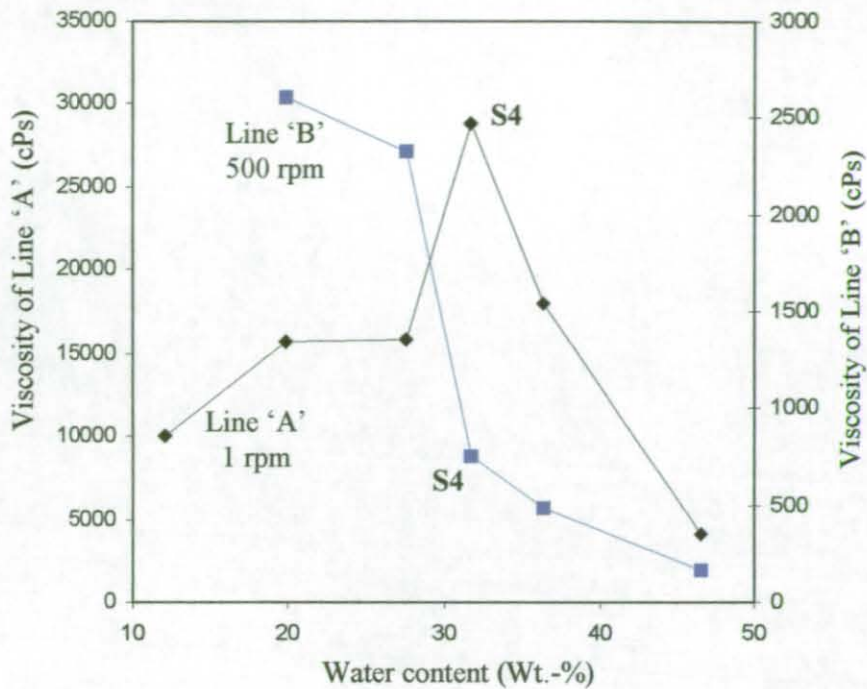


Figure 6.21. Viscosity – water content relationship at 1 rpm and 500 rpm for EX56/2

6.5 Different types of transitional phase inversion processes

By referring to the catastrophic phase inversion map shown in figure 6.11, it is obvious that at least two types of transitional phase inversion processes can be used to produce PUP-W dispersions. This section confirms that transitional phase inversion processes initiated from RIIP behave differently from those initiated from RIIP. They are called region II transitional phase inversion (RIITI) and region III transitional phase inversion (RIITI) processes respectively. The detection of transitional phase inversion points and possible changes of events during both processes are discussed here. Effects of ionic groups' addition methods on RIITI process and effects of the TEA addition rate on RIITI process are also investigated.

6.5.1 Transitional phase inversion points of RIITI process

Judging by the initial DN and ionic group content shown in table 5.5 (of section 5.7), EX57/1, EX57/2 and EX57/3 are all RIITI processes. Figure 6.22 shows the path of the RIITI process with reference to the catastrophic phase inversion map.

Torque changes and conductivity graphs

Torque changes and conductivity graphs of all RIITI experiments are similar. Figure 6.23 shows the torque changes and conductivity graphs of EX57/2: (a) during

the water addition and (b) during the TEA addition (and hence, changing ionic group content). Conductivity readings, shown in figure 6.23a, stay constant throughout the water addition process (line 'A' of figure 6.22). Torque readings drop sharply after the first aliquot of water (due to the break down of associations between ionic groups as will be shown in section 6.6) and then increase slowly following subsequent water additions. This graph shows the characteristics of PWCPI process in RII before phase inversion takes place and confirms that the mixture is still polymer-continuous.

Ionic group content in the PUp-W mixture increases as TEA was added at a fixed PUp-W ratio (line 'B' of figure 6.22). In figure 6.23b, an abrupt rise in conductivity (> 40) correspondences to a sharp drop in the relative torque changes reading (about 0.7) when there is 0.220 mmole/g (± 0.006 mmole/g) of ionic groups. Similar to the RII PWCPI process, the transient responds of the torque changes and conductivity readings correspond to the transitional phase inversion points.

An extra exercise was carried out for EX57/1, more water was added into the postulated water-continuous emulsions (line 'C' of figure 6.22). No sharp transitions in either torque changes or conductivity readings can be observed even when water content is as high as 60 wt.-%. This simple exercise verifies that the emulsion is water-continuous.

SEM images

SEM images of PUp-W mixtures withdrawn from RIITI experiments are shown in figures 6.24 to 6.26. Figure 6.24 is the image of the mixture after all water additions, but before any alterations of ionic group contents take place. Figure 6.25 is the emulsion sample withdrawn one aliquot before there are any rigorous transitions in torque or conductivity readings. Figure 6.26 is the sample withdrawn immediately after the torque and conductivity readings show some major changes.

It is obvious that figure 6.24 and 6.25 have similar drop structures, and are distinctly different to figure 6.26. This confirms that the abrupt transitions in the torque changes and conductivity graphs do, in fact, correspondence to a phase change in the mixture. After all water is added, figure 6.24 shows that the mixtures consist of mainly W_1/P_C drops in the range of 0.13 μm to 1.2 μm . Just before phase inversion takes place, the distribution of W_1/P_C drops narrows down to 0.13 μm \sim 0.93 μm . It is also interesting to notice that small polymer drops are formed inside the W_1/P_C drops

to produce the polymer-in-water-in-polymer ($P_1/W_1/P_C$) structures. Since PUp ionomers with high ionic group contents are self-dispersible, the P_1 drops can form thermodynamically at the ionic-centre-rich PUp-W interfaces. After the phase inversion has happened, highly concentrated aqueous PUp emulsions with solid contents as high as 70 ~ 75 wt.-% are produced. The closely packed aqueous PUp emulsions can be identified in figure 6.26*. Immediately after the phase inversion, the emulsion consists of mainly simple P_1/W_C drops with just a few $W_1/P_1/W_C$ drops.

6.5.2 Other features of RIITI process

Ionic groups' addition method

EX57/1 and EX57/3 are used to compare the effect of ionic groups' addition method on RIITI process. Both experiments have similar initial DN and water content. Transitional phase inversion of EX57/1 occurs at a DN of 36.93 % (± 1.48 %), which is equivalent to ionic group content of 0.207 mmole/g (± 0.008 mmole/g). Transitional phase inversion of EX57/3 occurs at a DN of 34.13 % (± 1.03 %), which is equivalent to ionic group content of 0.191 mmole/g (± 0.006 mmole/g).

The result shows that transitional phase inversion takes place earlier if counterion is added instead of highly neutralised PUp ionomer. This is because the counterion molecules are smaller and should diffuse through the polymer matrix faster than the ionised PUp molecules. Therefore, by adding counterion, the ionised and non-ionised PUp mixture is blended together more homogeneously. As a result, less ionic groups are needed.

PUp-W ratio

EX57/2 and EX57/3 have similar initial DN (about 29.5 %) but different initial water content (25.21 wt.-% and 28.66 wt.-% respectively). Transitional phase inversion points for the two experiments are at DN = 39.33 % (± 1 %) and

* Unfortunately, contrast between the drops and the background is not obvious and only some poor images of the droplets can be seen in figure 6.26. It is not possible to improve the image using the existing technique due to the high concentration of the emulsion and that the PUp drops are too "soft" for further SEM treatments.

DN = 34.13 % (\pm 1.03 %) respectively. The result shows that less ionic groups are needed to engender the transitional phase inversion at higher water content.

Brooks and Richmond (1994a) and Zerfa et al. (1999) observed that a lower overall HLB is required to engender the transitional phase inversion at a lower water fraction. They attribute the result to the high solubility of lipophilic surfactant in the oil phase. They also showed that the actual HLB at the oil-water interface is the same at transitional phase inversion points when the preferred solubilisation of lipophilic surfactants does not exist. Using Salager's terminology, one could say that SAD is 0 at the transitional phase inversion points.

It might be assumed that, for PUp-W systems, the actual ionic group content at the PUp-W interface is the same at transitional phase inversion points since a preferred solubilisation of ionic groups does not exist. Then, in the presence of more PUp-W interface (as in systems with higher water content), more ionic groups will lie at the PUp-W interface at a fixed ionic group content. Hence, lower overall ionic group content is required to induce the transitional phase inversion.

Another possible explanation is based on the occurrence of $P_1/W_1/P_C$ drops prior to transitional phase inversion (as shown in figure 6.25). The effective volume fraction of the dispersed phase increases as more P_1 drops are formed inside the W_1/P_C drops; and the amount of P_1 drops is likely to be proportional to the amount of counterions added. The dispersed phase becomes more closely packed together and a "catastrophic phase inversion" -like transitional phase inversion takes place when a certain dispersed phase to continuous phase ratio is obtained. Therefore, the transitional phase inversion takes place at a lower overall ionic group content when the amount of initial dispersed water phase is higher.

Drop size studies -- Results

Figure 6.27 shows the volumetric distributions of the PUp ionomer particles at different ionic group contents (based on inverted water-continuous emulsions withdrawn from EX57/3). Figure 6.27a is based on instantly pre-diluted samples measured on the same day as their production; and figure 6.27b is based on non-diluted samples that are pre-diluted immediately prior to new measurements 1½ months later. The relationships between d_{32} , standard deviation of diameter, δ , and

external interfacial area per unit volume, a , and the ionic group contents of emulsions withdrawn from EX57/3 are shown in figure 6.28.

From figure 6.27, it is obvious that the PUp drops become smaller as ionic group content increases. An asymptotic decrease in drop size with increasing ionic group content is observed for both sets of samples shown in figure 6.28a. The asymptotic behaviour is more pronounced for samples measured on the same day. The two curves intersect at about 0.205 mmole/g of ionic group content; below which d_{32} is lower and above which d_{32} is higher after 1½ months.

Figure 6.28b shows that standard deviation of diameters, δ , for both sets of measurements behave differently. For samples measured on the same day, δ increases to a maximum before it decreases again. For samples measured 1½ months later, δ is almost constant with a slight increase from 0.37 to 0.47 when ionic group content increases from 0.197 mmole/g to 0.248 mmole/g. An asymptotic increase in external interfacial area per unit volume with ionic group content is also observed in figure 6.28c for both sets of samples; smaller increases in a at low ionic group content and larger increases at higher ionic group content.

Drop size studies -- Discussion

Hydrophilicity of PUp ionomers increases with increasing ionic group content and leads to smaller particle size (as seen in figure 6.27). Tharanikkarasu and Kim (1997) attributed the asymptotic decrement of drop size with increasing ionic group content (seen in figure 6.28a) to the dual effect of ionic centres (as mentioned in section 2.5.1). For internally, and anionically, stabilised polystyrene latices, Goodwin et al. (1973) found a linear log-log relationship between particle diameter and ionic strength. Since ionic strength is proportional to ionic group content, similar relationships between particle size and ionic group content should also exist. Kim and Lee (1996) showed that average particle size of PU ionomer dispersions is mainly governed by the concentration of the solubilising groups (i.e., the ionic groups, viz. the carboxylate anions). Therefore, the size reduction of PUp particles with ionic group content should also follow the linear log-log relationship. This reasoning should be treated with care because the formation of polystyrene dispersions is likely to be different from those of PUp dispersions. On the other hand, Dieterich (1981) described qualitatively that the degree of swelling of PU ionomer particles increases

with increasing ionic group contents. These two counteracting effects on particle size may offer more quantitative explanations for the asymptotic behaviour mentioned earlier.

It is apparent that the above arguments are insufficient to explain the decreasing particle size at low ionic group content and, simultaneously, increasing particle size at high ionic group content over 1½ months. Also, the simultaneous decrease and increase in particle size over time cannot be explained using some long-term degradation processes such as coagulation or flocculation of particles (which will lead to overall increment in particle size). It is difficult to be precise about the rate of changes in particle size due to the time interval between the two measurements. However, the measurements made on the same day will represent the dynamic events following counterion additions after the transitional phase inversion has taken place; and measurements made after 1½ months represent the thermodynamic state of the emulsions (assuming that the emulsions had achieved their equilibrium conditions). One probable explanation is provided by studying the relationship between standard deviation and ionic group contents.

As shown in figure 6.28b, particle size distribution grows wider and reaches a maximum before it reduces again following counterion addition at the dynamic condition (line “same day”). Since overall particle size reduces at the same time, the smaller drop must break-up faster than the bigger drops to result in the growing particle size distributions at the early stage of counterion addition. Eventually, most of the free acid groups in the small particles would have been ionised and would provide stability to the smaller particles formed afterwards. After that, the bigger drops would break-up faster and result in narrower particle size distribution. Due to this droplets’ break-up sequence, not all ionised ionomer can be “effective”; some may be trapped inside big PUp drops while the others stay at the surface of small drops locally. Dieterich (1981) shows that the swollen PU ionomer particles do not contain any embedded ionic groups. Therefore, at equilibrium (line “1½ months”), all ionised groups would have been redistributed to the particle surface and produce the thermodynamically stable emulsions. These thermodynamically stable emulsions have a narrow size distribution, with δ between 0.37 to 0.47 (as shown in figure 6.28b).

It is now clear that there is a third element, the “effectiveness” of ionic groups, in controlling the particle formation following counterion additions. It is probable that

the simultaneous tendencies to decrease and increase in particle size over time are caused by the difference between the dynamic and equilibrium conditions. As the ionic groups redistributed to form the thermodynamically stable emulsions, the final particle size reduces due to the dual effect of ionic centres as mentioned earlier. Below 0.205 mmole/g of ionic group content (the left side of the intersection point in figure 6.28a), drop size reduction over time is governed by the increasing hydrophilicity (ionic-strength control). Above 0.205 mmole/g of ionic group content (the right side of the intersection point in figure 6.28a), the drop size increase over time is governed by the swelling of particles (swelling control).

According to Satguru et al. (1994), linear plots of specific surface area versus ionic group content are to be expected (as mentioned in section 2.5.1). However, the plot in figure 6.28c shows asymptotic increases of external interfacial area per unit volume with ionic group content. Direct comparisons between the two results are complicated by at least two factors. First of all, the emulsions studied by Satguru et al. are chain-extended. Secondly, only outer PUp-W interfacial area was calculated in the current study (overall PUp-W interfacial area is not obtained due to unknown degree of swelling of PUp particles).

6.5.3 Transitional phase inversion points of RIITI process

Both experiments EX57/4 and EX57/5, mentioned in section 5.7, are RIITI processes. The path of the RIITI process is shown in figure 6.29a. Water was firstly dispersed into the non-neutralised PUp until the mixture contained about 28.5 wt.-% of water. This mixture lies in the RIII region of the catastrophic phase inversion map and is polymer-continuous (line 'A' of figure 6.29a). Torque changes and conductivity graphs during this process are similar to those in figure 6.23a.

Torque changes and conductivity graph

Judging from the catastrophic phase inversion map, one may expect to see four inversions as ionic group content increases at a fixed PUp-W ratio. The four inversions expected are (1) a polymer-to-water continuous inversion occurs near to the 'CRIII' line^{*}; (2) a water-to-polymer continuous inversion occurs near to the

^{*} 'CRI', 'CRII' and 'CRIII' lines are the PWCPI loci of the RI and RII and RIII regions respectively.

'CRII' line; (3) a polymer-to-water continuous inversion as detected from the RIITI process; and (4) a final water-to-polymer continuous inversion occurs near to the 'CRI' line. However, figure 6.29b shows that only two inversion points were detected as ionic group content increases at a fixed PUp-W ratio (line 'B' of figure 6.29a). Figure 6.29b shows the torque changes and conductivity graphs during the counterion addition process. The graphs are plotted based on results of experiment EX57/5. EX57/4 has a similar graph, but with different inversion points. The two inversion points of both experiments are shown in figure 6.29a as 'a' and 'b' for EX57/5; and 'c' and 'd' for EX57/4.

The first inversion is a polymer-to-water continuous inversion which occurs within the RII region of the catastrophic phase inversion map (points 'a' and 'c'). Before the first inversion, a serious "rod-climbing" effect is observed; PUp-W mixtures formed an inverse cone shape around the agitator shaft. After the first inversion, the rod-climbing effect is replaced by a "hollowing" effect; PUp-W mixtures form a small vortex around the agitator shaft. The above observation is a direct result of the reduced viscosity after the first inversion has taken place.

The second inversion is a water-to-polymer continuous inversion which lies in the RI region of the catastrophic phase inversion map (points 'b' and 'd'). After the second inversion has taken place in EX57/4, water was added into the polymer continuous dispersions (line 'C' of figure 6.29a) to simulate a PWCPI process. The torque changes and conductivity graph during this process is similar to those mentioned in section 6.3.2 and, as expected, the polymer-to-water continuous inversion lies on the same PWCPI locus.

SEM images

Three samples were withdrawn during EX57/5 for examinations using the SEM-freeze fracture technique. These are emulsion samples at 0 %, 19.5 % and 33.3 % DN and are identified as S1, S2 and S3 in figure 6.29b respectively. At 0 % DN, the mixture consists of only W_1/P_C drops ranging from 1.5 to 24 μm (figure 6.30). At 19.5 % DN, the polymer-continuous mixture consists of W_1/P_C drops, in the range of 0.6 to 4.6 μm , and large regional water-continuous phases. As shown in figure 6.31, the regional water-continuous phase contains $W_1/P_1/W_C$ drops. The size of the P_1 drops are about 1.1 to 25.5 μm in diameters and the W_1 drops are in

the range of 2.6 to 4.6 μm . It is possible that the large W_1/P_C drops, as seen in figure 6.30, have contributed to the formation of the regional water-continuous phases. Their existence results in a slow decline in torque readings (or viscosity). After the phase inversion has taken place, at 33.3 % DN, the emulsion produced contains a mixture of P_1/W_C drops and $W_1/P_1/W_C$ drops (figure 6.32). The image of this closely packed emulsion confirms that water is the continuous phase and the emulsion contains over 70 wt.-% of the disperse phase. The P_1 drops are smaller than 4.7 μm and W_1 drops are between 0.28 to 3.6 μm .

Possible causes for second inversion during the RIITI process

Although no emulsion was analysed after the first inversion, the second water-to-polymer continuous inversion might be explained using the variation of standard deviation during the dynamic RIITI process as shown in figure 6.28b. Rumpf (1990) mentioned that the largest packing density of regularly packed mono-size, spherical solid, particle is 0.74. Therefore, this must be the limiting volume fraction of disperse phase for emulsions containing rigid spherical particles that are distributed in a mono-modal fashion. For emulsions with wider distributions, the maximum packing density increases because the smaller particles can slip between the voids of the larger particles.

As more counterions are added into the water-continuous emulsions, standard deviation decreases as ionic group content increases beyond 0.22 mmole/g (the peak of figure 6.28b). Hence, droplets approach mono-modal distribution and the limiting volume fractions of disperse PUP phase decrease as ionic group content increases. In other words, at a fixed PUP-W composition, the mixture become closer packed as ionic group content increases. Eventually, during the RIITI process, the second water-to-polymer continuous inversion may occur when the highest attainable packing of PUP particles exists in the emulsion mixtures.

Effect of counterion addition rate

The first and second phase inversion points of EX57/4 and EX57/5 are located in figure 6.29a. When TEA is added at a rate of 0.4 g (\pm 0.02 g)/ 10 minutes (EX57/5), the first transitional phase inversion takes place at an ionic group content of about 0.199 mmole/g (\pm 0.13 mmole/g). When TEA is added at a rate of 0.3 g (\pm 0.01 g)/ 10 minutes (EX57/4), only 0.148 mmole/g (\pm 0.01 mmole/g) of ionic

groups are needed to induce the transitional phase inversion. In other words, higher ionic group content is required to induce the first transitional phase inversion if TEA addition rate is higher. However, the second transitional phase inversions of the experiments take place at about the same ionic group content (~ 0.4 mmole/g).

When polymer is the continuous phase, the counterion ionised the PUp ionomer molecules first. After that, the time it takes for the ionised molecules to migrate to the PUp-W interface determines the occurrence of the first transitional phase inversion (i.e., mass-transfer-controlled process). As a result, less ionic groups are needed when counterion is added slowly. However, when water is the continuous phase, the counterion moves to the PUp-W interface first and ionisation of PUp ionomer takes place subsequently. Since the transfer rate of counterion to the PUp-W surface is relatively fast, the second phase inversion process does not depend on the counterion addition rate (i.e., reaction-controlled process).

Conclusions

Two different transitional phase inversion processes, RIITI process and RIITI process, can be used to prepare PUp-W dispersions. Both conductivity and torque changes measurements can be used to detect the inversion point of the RIITI process and the first polymer-to-water continuous inversion of the RIITI process; the second water-to-polymer inversion of the RIITI process can only be detected using the torque changes measurement. For the RIITI process, inversion takes place at a lower ionic group content when counterion is added instead of highly neutralised PUp ionomer. For the RIITI process, two possible transitional phase inversion routes are suggested: (1) the inversion takes place when a certain amount of the ionic groups has occupied the PUp-W interface; (2) a “catastrophic phase inversion”-like transitional phase inversion takes place when a certain disperse phase to continuous phase ratio is obtained. Both probable inversion routes support the results, which show that less overall ionic groups are required to induce the inversion at high water content.

During the dynamic conditions after phase inversion has taken place in a RII process, the asymptotic decrease of drop size with ionic groups is due to the dual effect of ionic centres and the “effectiveness” of ionic groups. Ionic groups redistributed to produce thermodynamically stable emulsions, which contain droplets

with sizes governed solely by the dual effect of ionic centres. Below 0.205 mmole/g of ionic groups, the particle size reduction is ionic-strength controlled; above 0.205 mmole/g of ionic groups, the particle size increment is swelling controlled.

Two inversion points were detected for the RIITI process. The first inversion lies in the RII region of the catastrophic phase inversion map and is caused by coalescence of large water drops in the polymer matrix. This inversion is a mass-transfer-controlled process and is affected by the counterion addition rate. The second inversion lies in the RI region of the catastrophic phase inversion map and takes place when the highest attainable packing of PUP particles exists in the emulsion mixtures. This inversion is a reaction-controlled process and is independent of the counterion addition rate.

It becomes clear that transitional phase inversion of the RIITI process might take place near to a condition when $SAD = 0$, (i.e., at the "true" transitional phase inversion condition). On the other hand, phase inversions of the RIITI process do not necessarily take place at $SAD = 0$. Therefore, only the transitional phase inversion loci obtained from the RIITI process are to be shown in the phase inversion map. A completed phase inversion map for TEA-neutralised PUP-W dispersions is shown in figure 6.33. It includes the definite location of the transitional phase inversion loci.

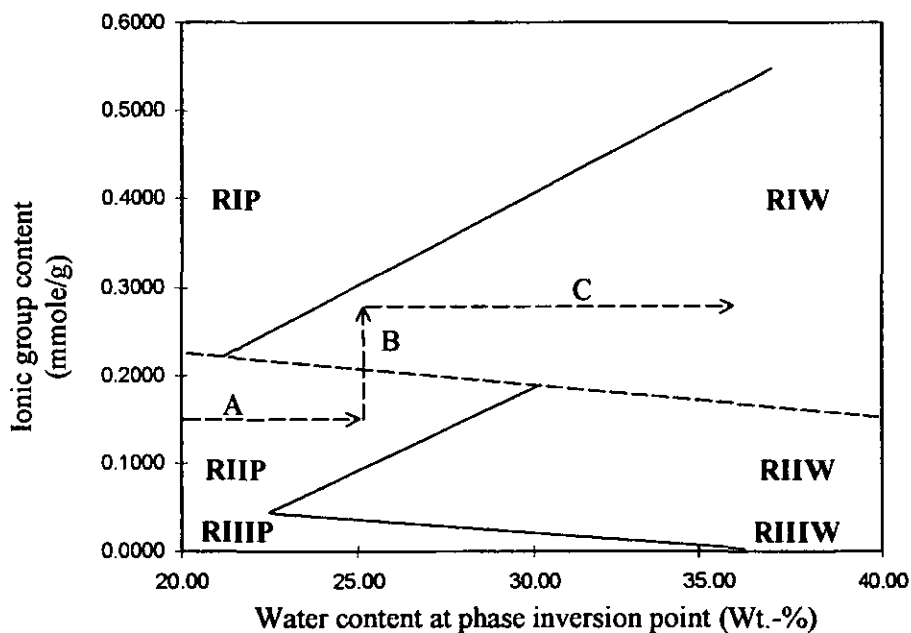
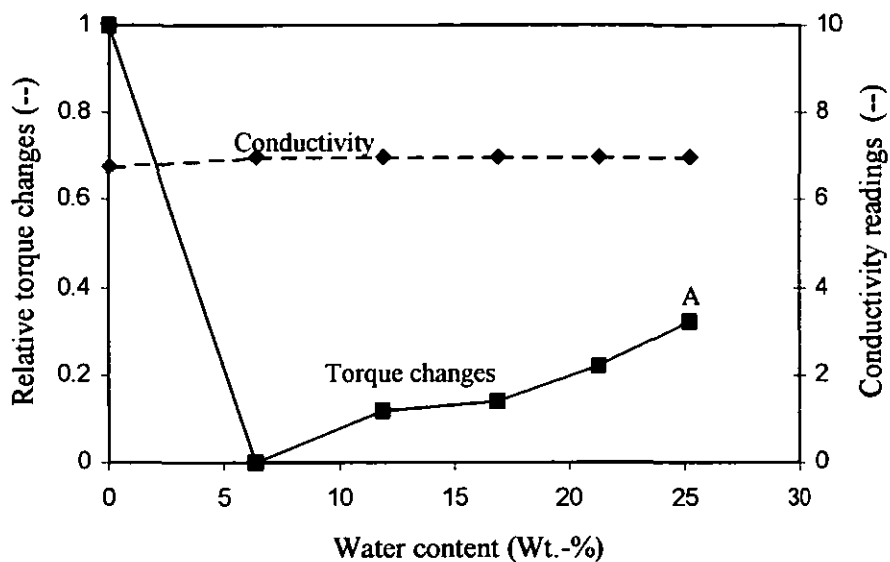
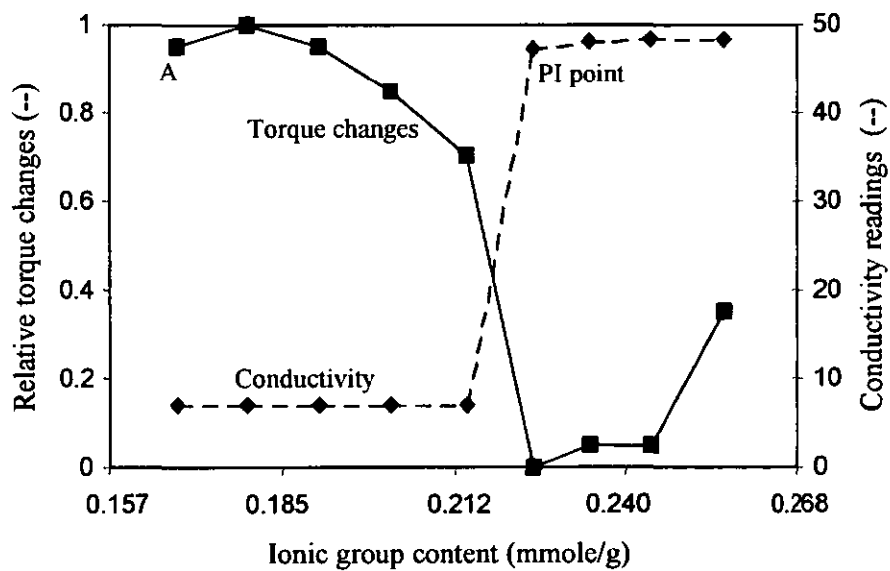


Figure 6.22. The path of RIITI process (black line is polymer-continuous emulsions and blue line is water-continuous emulsions)



(a) During water addition



(b) During TEA addition

Figure 6.23. Torque changes and conductivity graphs of EX57/2

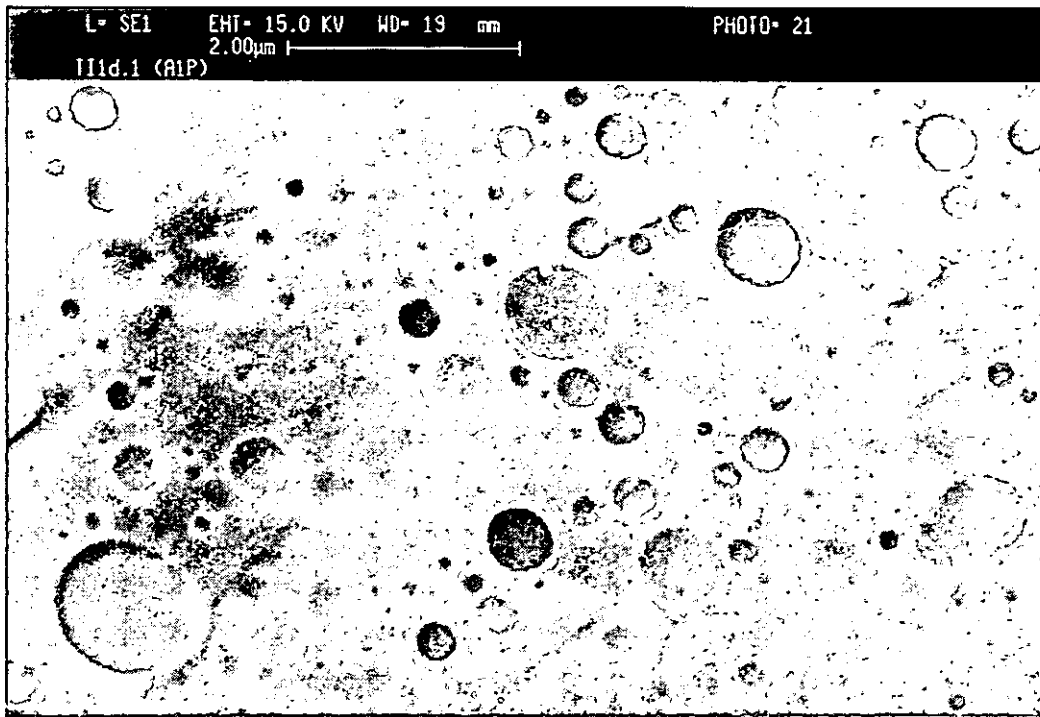


Figure 6.24. SEM image of RIITI experiment: After all water addition

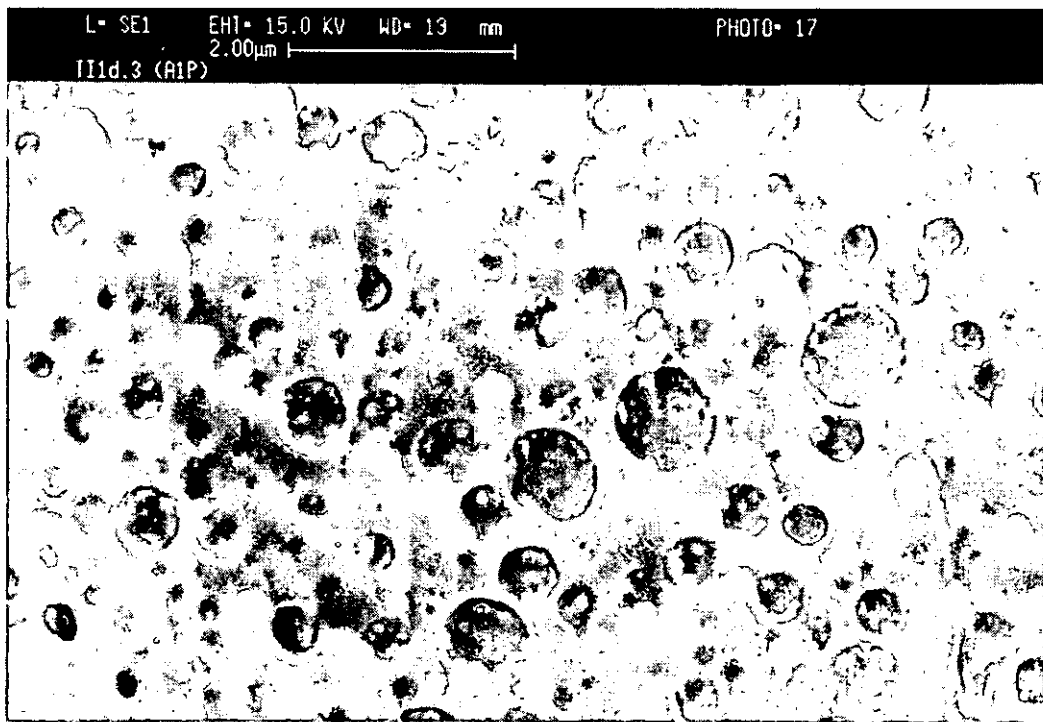
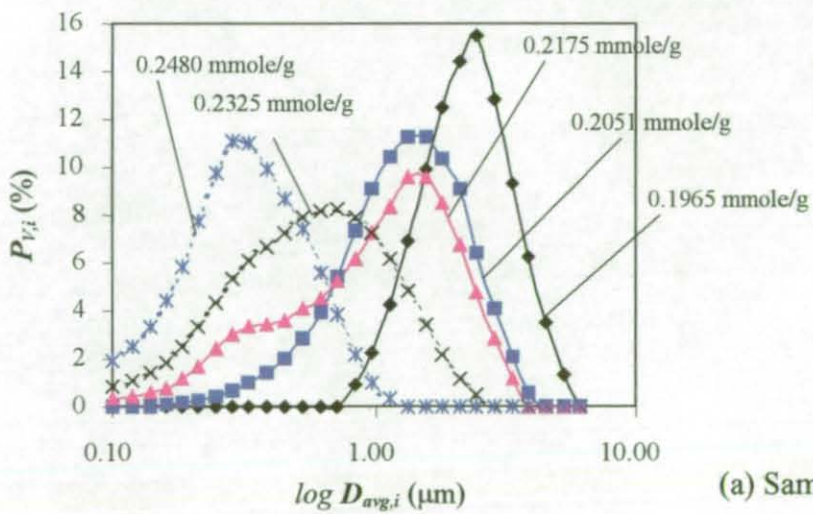


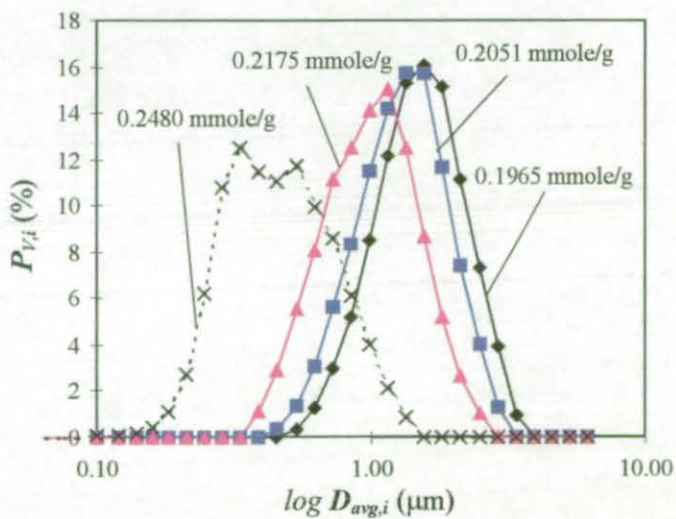
Figure 6.25. SEM image of RIITI experiment: One aliquot before phase inversion



Figure 6.26. SEM image of RIITI experiment: Immediately after phase inversion



(a) Same day



(b) 1½ months

Figure 6.27. Volumetric distributions at different ionic group contents

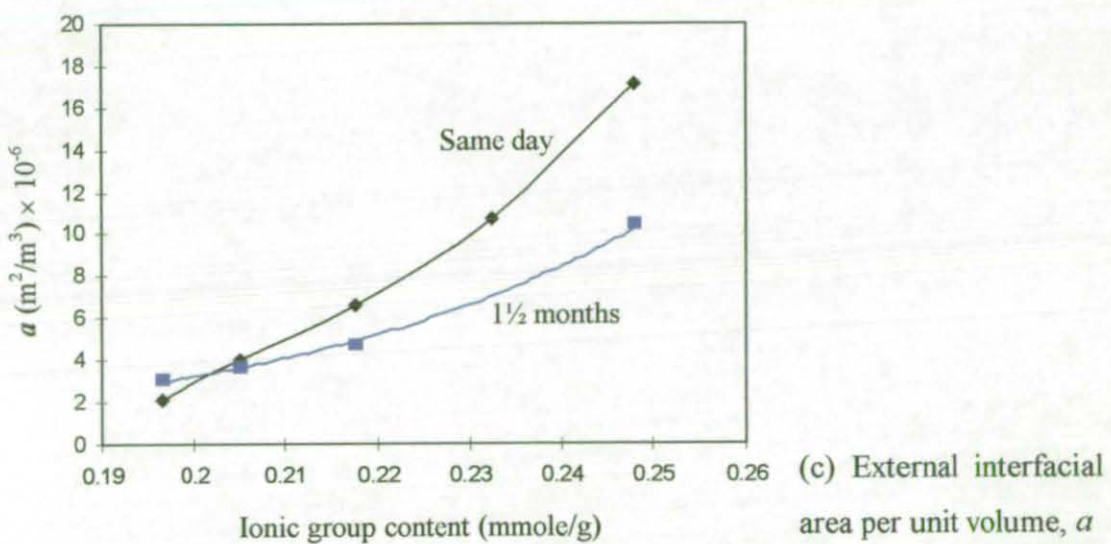
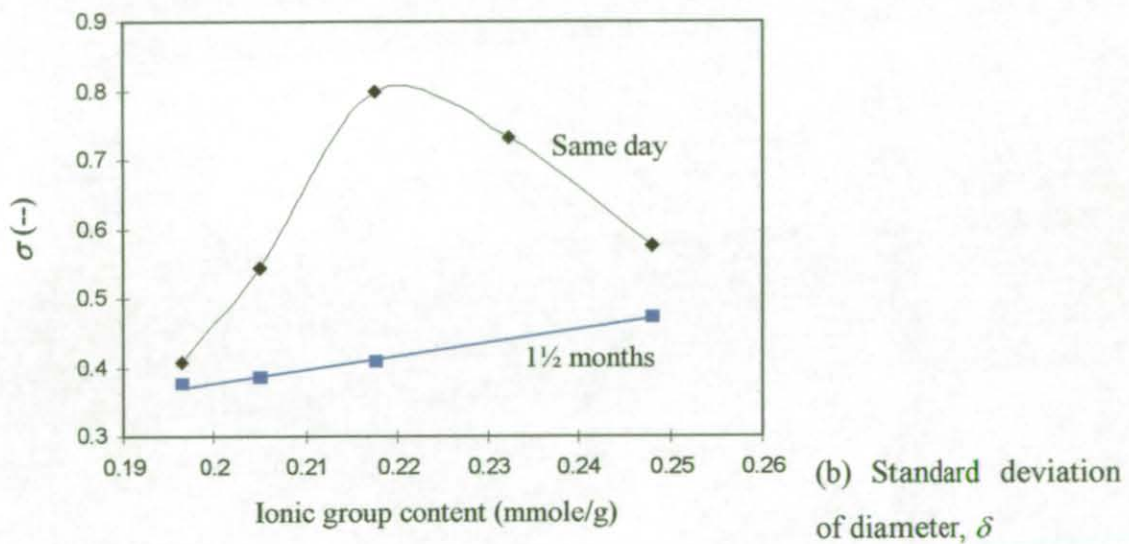
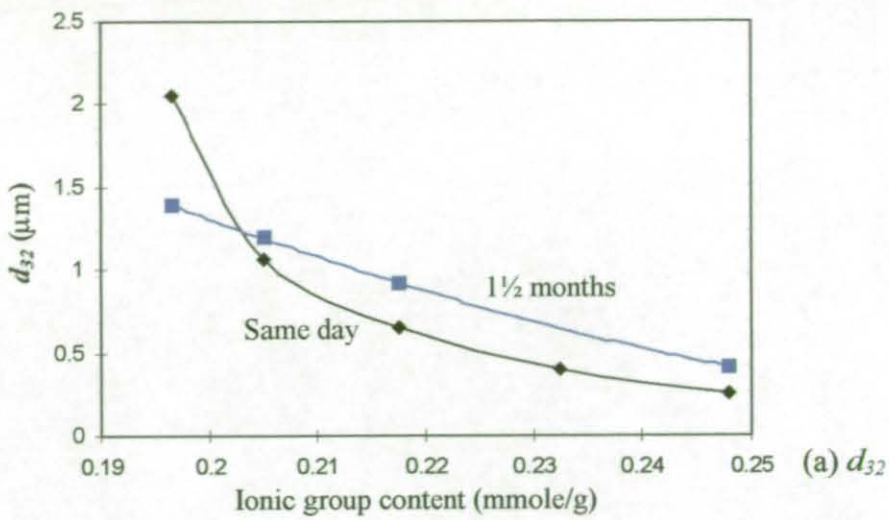


Figure 6.28. Relationships of d_{32} , δ and a with the ionic group content

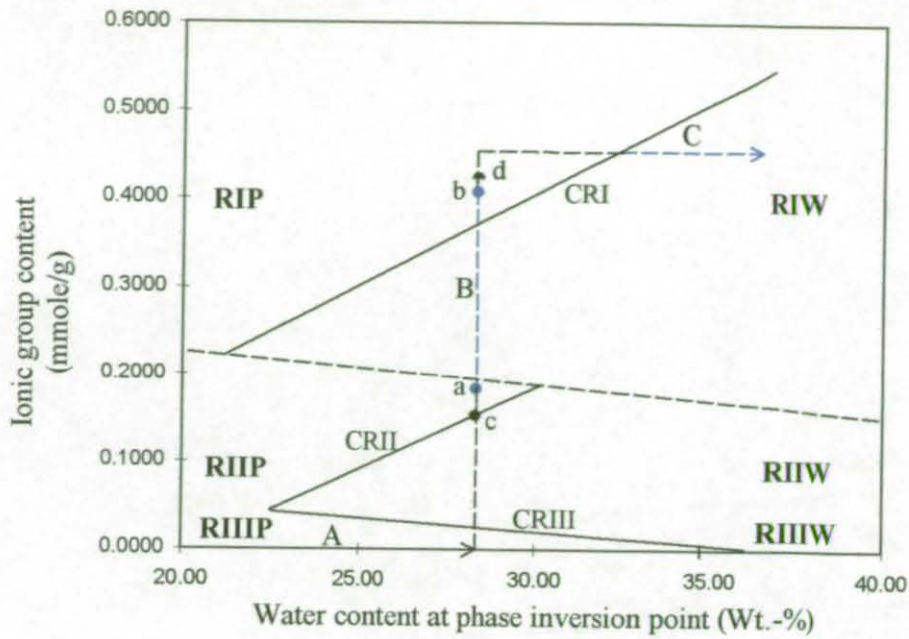


Figure 6.29a. The path of RIITI process (black line is polymer-continuous emulsions and blue line is water-continuous emulsions)

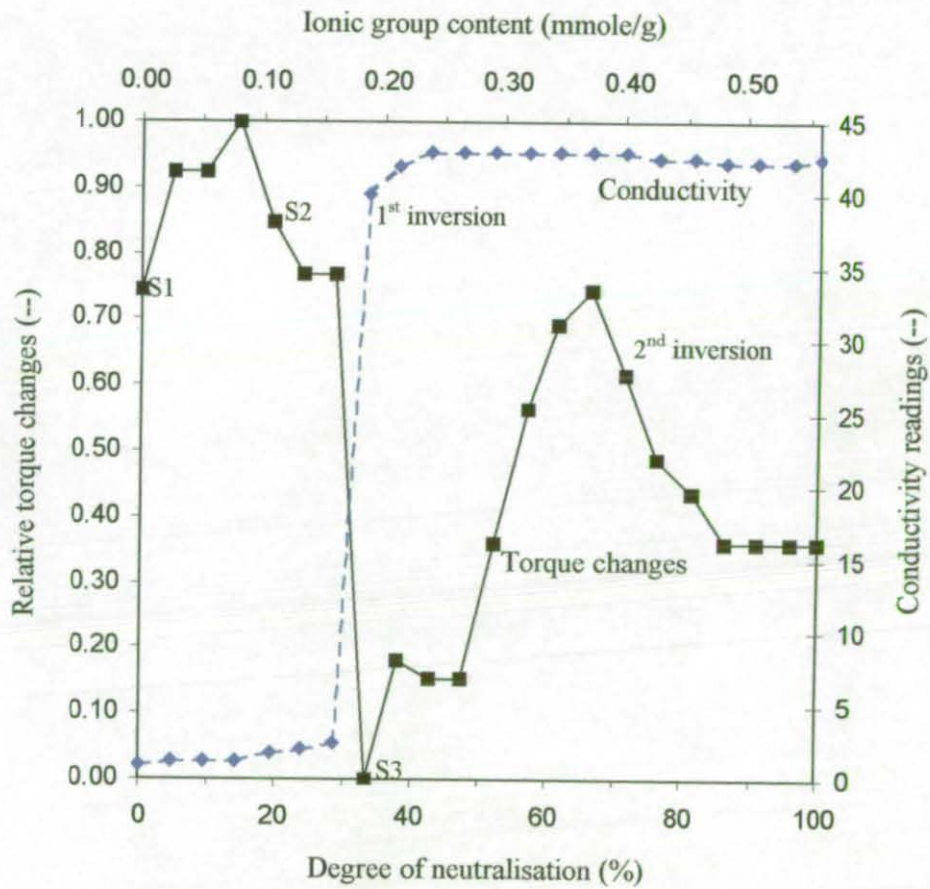


Figure 6.29b. Torque changes and conductivity graphs of EX57/5

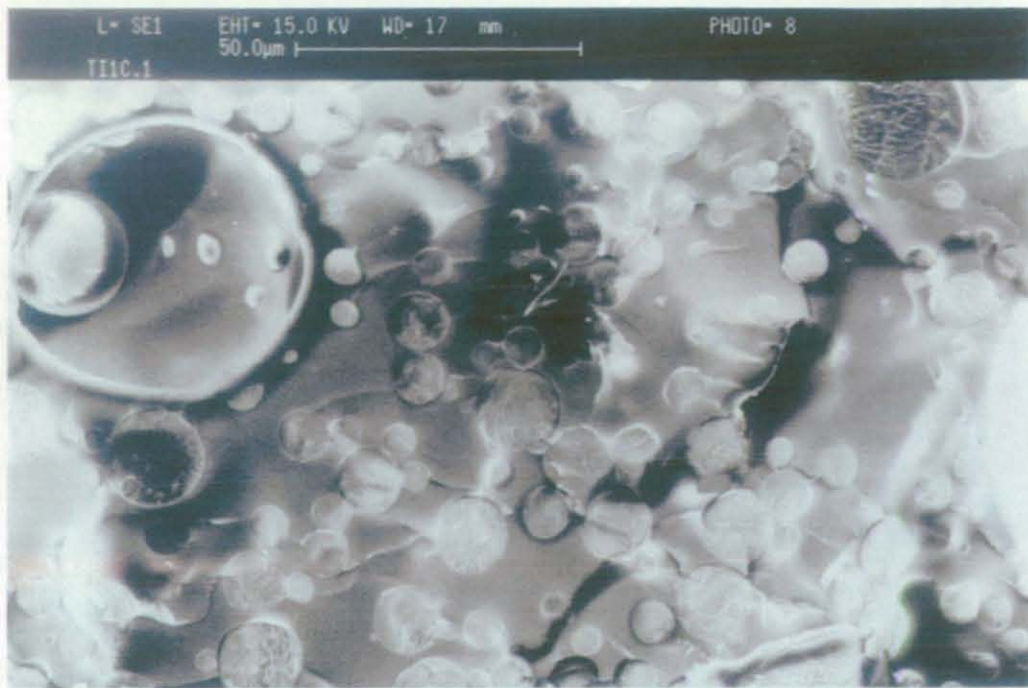


Figure 6.30. SEM image of RIITI experiment: Before TEA addition



Figure 6.31. SEM image of RIITI experiment: Before complete transitional phase inversion

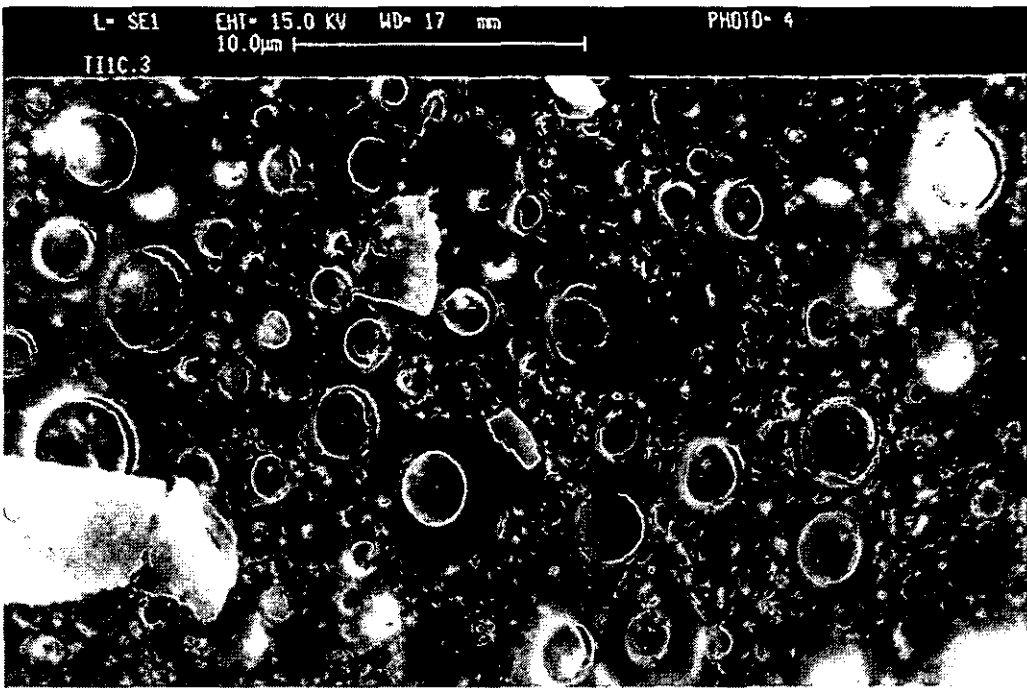


Figure 6.32. SEM image of RIITI experiment: After complete transitional phase inversion

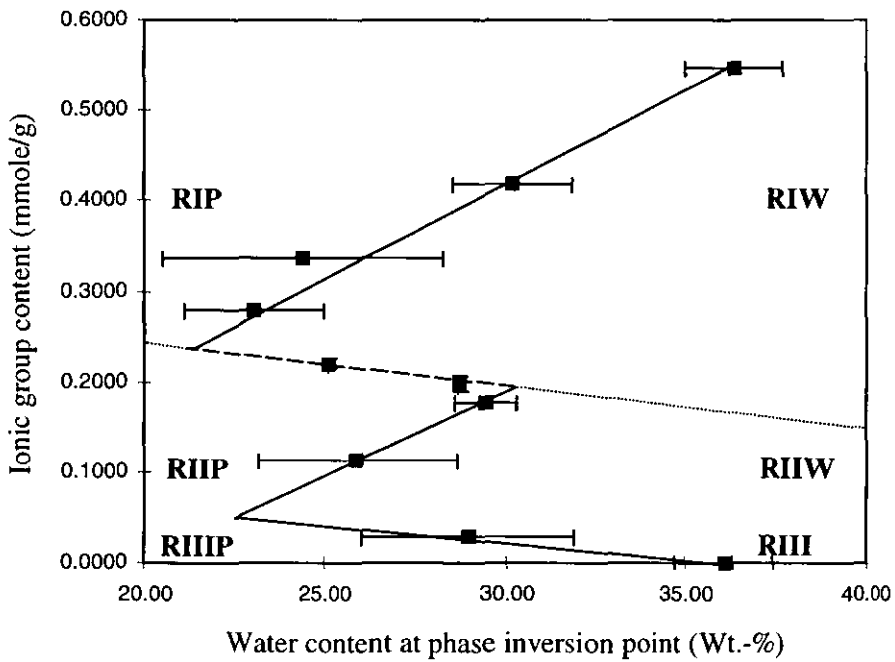


Figure 6.33. Complete phase inversion map for TEA-neutralised PUp-W dispersions

6.6 Catastrophic phase inversion mechanism

Due to the absence of solvent, the phase inversion processes studied in this work are essentially the dispersion stage of a pre-polymer mixing process or a melt dispersion process. Dieterich (1981) suggested a phase inversion mechanism for this dispersion process during the production of aqueous PU colloids (details of this mechanism are shown in section 2.2.2). The suggested mechanism is sufficient to describe the existence of the RI and RIII regions of the phase inversion map but cannot explain the newly discovered RII region. Based on results obtained from experiment EX58, mentioned in section 5.8, a modified phase inversion mechanism is proposed for the PWCPI process during the production of PUp-W dispersions.

6.6.1 Results

Torque changes and conductivity graphs

Figure 6.34 shows the torque changes and conductivity graphs of experiment EX58. The sampling points are marked on the graph as S1 ... S5, S8 and S11. Three different zones, Z1, Z2 and Z3, are identified on figure 6.34 with reference to the torque changes line. The location of the phase inversion point, at a water content of 25.91 wt.-%, is also shown in figure 6.34.

SEM images

Figure 6.35 to figure 6.41 are the SEM-freeze fractured images of samples S1, S2, S3, S4, S5 and S11. These pictures can be used to understand the mechanism of the catastrophic phase inversion process in the RII region. Important features of these samples are described in this sub-section.

- S1: This sample contains 6.29 wt.-% of water in a polymer-continuous phase. The viscous mixture is semitransparent in colour and contains entrapped air bubbles. No water drops were observed from its SEM image (figure 6.35).
- S2: This sample contains 17.03 wt.-% of water. Again, the mixture is polymer-continuous as identified from the torque changes and conductivity graphs. This sample is viscous and is semitransparent to milky white in colour. The mixture consists of simple W_1/P_C drops with a wide drop size distribution (figure 6.36).
- S3: This sample contains 25.91 wt.-% of water. As shown in figure 6.34, this is the phase inversion point. The emulsion appears to be milky white in colour and is

still viscous. It was noticed that this emulsion is stable and no separation has occurred even after 1¼ years. SEM images of its frozen samples revealed peculiar drop appearances. First of all, the drop structures of this emulsion can barely be identified due to the very high polymer content (~ 74 wt.-%). When examined carefully, a mixture of “pseudo-drop” structures can be identified in figure 6.37. The term “pseudo-drop” is used to describe a local region that consists of small P_1/W_C drops and does not have clear-cut boundaries within itself and its surrounding. These pseudo-drop structures include (1) simple P_1/W_C drops of a few microns (figure 6.37a); (2) multiple drops in the form of $W_1/P_1/W_C$ (figure 6.37b); and (3) multiple drops in the form of $P_2/W_1/P_1/W_C$ (figure 6.37c). Figure 6.38 shows an enlarged image of the same sample. It is noticeable that the pseudo-drop structures are made out of small P_1/W_C drops, which are about 140 nm in diameter.

S4: This sample contains 29.87 wt.-% of water and is water-continuous. This emulsion is less viscous than the previous sample, but is still milky white in colour. Separation was observed after three days. The mixture of drop structures inherited from the previous sample is easily identifiable from the SEM image (figure 6.39). Again, these structures include P_1/W_C drops, $W_1/P_1/W_C$ drops and $P_2/W_1/P_1/W_C$ drops. The P_1 drops have a broad size distribution; and the W_1 phase can appear as both large drops (which fill almost the entire P_1 drops) and small drops (which only fill a small portion of the P_1 drops). The nano-scale P_1/W_C drops that appeared in S3 no longer exist in this sample.

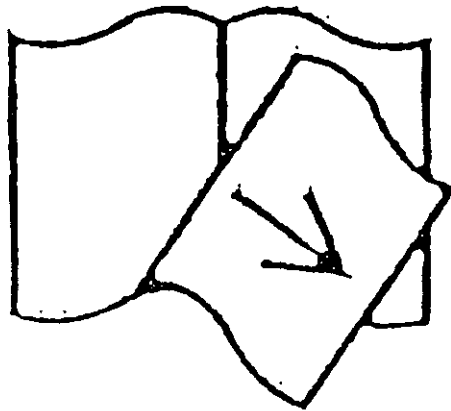
S5: This sample contains 33.66 wt.-% of water. The appearance and SEM image of this sample are similar to S4 (figure 6.40).

S11: This sample contains 58.29 wt.-% of water. It is very inviscid and is milky white in colour. After three days, the emulsion separates into a clear water layer at the top and a milky white bottom layer. Similar to samples mentioned in section 6.3.3, this separated emulsion can be recreated by simply shaking the sample bottle with hand. Figure 6.41 shows a mixture of drop structures similar to S4.

Table 6.5 summarises the condition of the emulsions, their visual appearance and important features of the SEM images of the aforementioned samples. The following sub-sections use a modified catastrophic phase inversion mechanism to explain the results obtained.

Pages
Missing
not
Available

149.



decreased because they are surrounded by hydrophobic regions that have experienced less hydration. Water drops also start forming independently in the hydrophobic portions of the polymer matrix. At this point, discrete water areas are all entrained in a homogeneous polymer matrix (figure 6.42d). The overall PUp-W mixture only has a moderate ionic group content. Therefore, some water drops would be fully surrounded by the ionic or hydrophilic centres of the partially neutralised PUp ionomer; some water drops would be partly surrounded by ionic centres; and some water drops would not be surrounded by any ionic centre.

6.6.3 At the phase inversion point

The phase inversion took place when the emulsion contained about 26 wt.-% of water (i.e., 74 wt.-% of polymer). According to the inversion mechanism suggested by Dieterich (1981), water addition must cause only one of the following two situations to occur at the phase inversion point:

- (1) Additional water forms a continuous second phase because the water droplets can neither be absorbed by the system nor coalesce within the polymer matrix. When this happens, the RIII phase inversion that has been observed in this work would occur.
- (2) Starting from the dispersed water droplets, the incorporated water is forced further into the polymer matrix. Then, the PUp-water interface starts to restructure and the PUp ionomer disintegrates into spherical dispersion particles enclosed by a continuous aqueous phase. When this happens, the RI phase inversion that has been observed in this work would occur.

However, in order to explain the occurrence of sample S3 (which contains both small PUp ionomer drops and undisturbed water drops), both of the events suggested by Dieterich must occur simultaneously. This situation occurred because the moderate amounts of ionic centres present in RII mixtures inhibit the coalescence of some water drops within the polymer matrix (as for RIII mixtures). At the same time, the ionic centres allow the restructuring of the PUp-water interface to form small PUp ionomer drops (as for RI mixtures).

At the phase inversion point, restructuring of the PUp-water interface will be initiated from the ionic centres-rich interfaces. Locally, the PUp ionomer restructures

and disintegrates into small spherical particles that disperse in a continuous aqueous phase. This process of restructuring will continue to take place and quickly extends towards the bulk of polymer matrix and the PUp-water interfaces without any ionic centres. Water movement from any isolated water drops, into the newly formed continuous aqueous phase, is prevented by the closely packed PUp ionomer drops surrounding it. These isolated water drops will eventually become the primary water (W_1) phase of a multiple $W_1/P_1/W_C$ drop. Figure 6.42e shows how PUp ionomer molecules coil together to form small PUp ionomer drops and 6.42f shows the mixture of pseudo-drop structures that developed from the small PUp ionomer drops.

The stabilisation of the small PUp ionomer drops

The minimum ionic group content required to form stable dispersions containing small P_1/W_C drops in the TEA neutralised PUp-W system studied is about 0.2 mmole/g, as shown in the phase inversion map (figure 6.33). Below this minimum requirement, it is well known that the ionic groups present will not be enough to stabilise the dispersed particles (Chen and Chen (1992); Satguru et al. (1994)). In this work, however, small P_1/W_C drops are found at the phase inversion point (sample S3) even though the mixture contains only 0.112 mmole/g of ionic groups. It is also worth pointing out that these small drops do not exist in samples following subsequent water addition. Therefore, the fact that these small PUp drops only appear at the phase inversion point suggested that there must be a mechanism that only stabilised closely packed* emulsions containing small PUp ionomer particles.

Satguru et al. (1994) also mentioned that emulsions stabilised by the incorporation of copolymerisable carboxylic acids, such as acrylic acid, possess better stability over a broad pH range (further details are shown in section 2.3.4). They attribute this property to the fact that acid-rich chains with adjacent acid groups at the particle surface are produced when acrylic acid is employed in emulsion polymerisation. With the presence of these acid-rich chains, ionisation at one acid group affects its neighbouring acid groups in the polymer chain. Therefore, acidification of such latex does not lead to abrupt loss of colloid stability.

* It is already mentioned in section 6.5.3 that minimum voidage in a monosize spherical system is about 0.26. Figure 6.38 shows that sample S3 has a narrow drop size distribution. Therefore, with a water fraction of about 0.26, the small drops must be packed to their closest possible structure.

This particular property of the emulsion polymer stabilised by copolymerisable carboxylic acid does not, generally, exist in aqueous PU ionomer colloidal system stabilised by carboxylic acid such as DMPA. This is because in the later case, the acidic molecules are generally isolated from each other; hence, ionisation and de-ionisation of any acidic groups tends to happen independently and the transition from fully ionised to un-ionised acid groups occur over a narrow pH range. The conclusion drawn by Satguru and his co-workers is true for most, if not all, work involving the production of aqueous PU ionomer colloids (Dieterich et al. (1970); Kim and Kim (1991); Zeneca Resins). In those cases, the water-continuous emulsions are “diluted” to accommodate the chain extension process.

In a RIIW emulsions, ionised carboxylic acid groups surrounding any particles will be isolated from each other due to the low overall ionic group content. However, at the phase inversion point, the polymer content is extremely high (about 74 wt.-%). Therefore, apparent ionic-centre-rich environments can exist around any isolated ionised carboxylic acid groups on a particle surface. This apparent ionic-centre-rich environment is provided by other isolated ionised groups from adjacent particles. As a result, any ionisation at one acid group affects acid groups from neighbouring particles. In other word, the potential loss of colloid stability by de-ionising any single acid group is minimised; this is because de-ionisation of any ionised acid groups also affect others ionised acid groups from neighbouring particles. Similarly, the apparent ionic-centre-rich environment strengthens the repulsive force between particles to provide extra stability even though the overall ionic group content is lower than the reported minimum requirement. Put it in another way, the potential loss of colloid stability between two particles, threatened by the lower repulsive force between them, is minimised due to the apparent ionic-centre-rich environment.

Formation of the pseudo-drops

The production of these pseudo-drops is a vital step towards the formation of a mixture of “matured” drop structures following subsequent additions of water. Since water additions take place at 10 minutes intervals, the pseudo-drops must form simultaneously with the small PUp ionomer drops. In essence, the formation of the pseudo-drops would be a kinetically driven event during the dynamic PWCPI process. The formation of these structures is illustrated using the following examples:

- (1) The formation of the pseudo-simple P_1/W_C drops (figure 6.43): Figure 6.43a shows a scenario whereby some water drops are fully surrounded by ionic centres before phase inversion takes place. During inversion, the small P_1/W_C drops start to form at the ionic-centre-rich PUp-water interface and extend towards the bulk of the polymer matrix. As a result, polymer matrix surrounding the water drops will form PUp droplets with high ionic strength. Further into the bulk, the PUp drops possess lesser ionic strength as they contain less ionised groups. This process causes a net attractive force from the highly ionised small drops towards the poorly ionised small drops. As this happens, spherical pseudo-simple drops will form, with the poorly ionised small drops in their cores. Coalescence between the pseudo-drops is prevented through repulsive force provided by the highly ionised small P_1/W_C drops that occupy their surface (figure 6.43b). All these happen in the absence of any coalescence between the small P_1/W_C drops that are stabilised by the aforementioned mechanism.
- (2) The formation of the pseudo- $W_1/P_1/W_C$ drops (figure 6.44): Figure 6.44a shows a scenario whereby, before phase inversion, some water drops that are fully surrounded by ionic centres coexist with a water drop that is not surrounded by any ionic centre. During the inversion, similar events that occurred during the formation of pseudo-simple drops would happen. The only difference is that the PUp-water interface of the water drop that is not surrounded by any ionic centre would not initiate the formation of small P_1/W_C drops. Small drops will only start to form at the ionic-centre-rich interface and extend towards the isolated water drops. Eventually, poorly ionised small PUp drops will build up around the isolated water drops. Water movement from this isolated water drop is hindered by the poorly ionised drops, which are closely packed around it. This process produces the pseudo- $W_1/P_1/W_C$ drops (figure 6.44b).
- (3) The formation of the pseudo- $P_2/W_1/P_1/W_C$ drops (figure 6.45): Figure 6.45a shows a scenario whereby, before phase inversion, water drops fully surrounded by ionic centres coexists with water drops partially surrounded by ionic centres. Again, the ionic-centre-rich PUp-water interface initiates the formation of the small P_1/W_C drops at the inversion point. For the partially isolated water drops, restructuring of their PUp-water interface starts at the surfaces covered with ionic centres. As this happened, the partially isolated drops might joint with the now continuous water

phase (as drop 'i' of figure 6.45a). However, if the partially isolated water drops are close to each other (as drops 'ii', 'iii' and 'iv' of figure 6.45a), a local water-continuous region can be created. Pseudo-drops formed inside this local water-continuous region in a similar way to the previously mentioned method (figure 6.45b). Depending on the ionic strength of small P_1/W_C drops surrounding the isolated water continuous region, more pseudo-simple drops might be produced; otherwise, isolated water drops with entrained pseudo-simple drops can be found inside a larger pseudo-drop to form the pseudo- $P_2/W_1/P_1/W_C$ drop (figure 6.45c).

The above suggestions might have oversimplified the events that lead to the formation of various pseudo-drops. In practice, the number of possible combinations is large. Considerations of such cases, however, make it possible to demonstrate the basic mechanisms that are responsible for the production of the pseudo drops and the stability of the small drops.

6.6.4 Zone 3 (Z3)

Figure 6.34 shows that torque value, and hence the viscosity of the emulsion reduces following further addition of water due to the dilution effect. As a result, the apparent ionic-centre-rich environment surrounding any isolated ionised carboxylic acid groups on a particle surface has now been destroyed. Therefore, the repulsive force provided by the ionic centres on the particle surface will determine the colloid stability between any two particles, and hence the stability of the emulsion as a whole.

As mentioned earlier, the ionic group content in RIIW emulsions alone is insufficient to prevent coalescence between particles. Therefore, coalescence of small drops takes place within the pseudo-drops to create the matured drops. The matured drops are identifiable easily due to the absence of the small P_1/W_C drops (as for samples S4 and S5 in figures 6.39 and 6.40). It was mentioned in section 6.3.3 that droplets in the RIIW emulsions are stable. This stability can be attributed to the similar distribution of ionic centres within the matured drops as in the pseudo-drops. Similar to the pseudo-drops, the surface of the matured drops is rich in ionic centres; while the core of the drops contains little, or no, ionic centres. Consequently, coalescence between any two drops is prevented by the repulsive force provided by the ionic-centre-rich PUp droplets' surface.

6.6.5 Nomenclature for multiple emulsions

Myers (1988) suggested a system of nomenclature to describe multiple emulsions based on the production sequence of various phases. This system works for multiple emulsions produced through a multiple-step emulsification process, especially a two-step emulsification process. During a two-step emulsification process (Matsumoto et al. (1976); Davis and Burbage (1977); Florence and Whitehill (1981)), primary emulsion containing simple W/O (or O/W) drops was firstly created. This emulsion was then emulsified into the final aqueous (or oil) phase to create the multiple-phase emulsions containing W/O/W (or O/W/O) drops. In those cases, Myers use numbers as subscripts to describe the emulsions. For example, in a W/O/W system, the aqueous phase of the primary emulsion is denoted as W_1 and the primary emulsion as W_1/O . After the second emulsification process, the complete system is denoted $W_1/O/W_2$. W_2 is referred to as the secondary aqueous phase. A similar method of nomenclature was used for O/W/O emulsions, in which case the notation would be $O_1/W/O_2$.

Various researchers have shown that multiple-phase emulsions can also be created before or after a catastrophic phase inversion process (Brooks and Richmond (1991); Pacek et al. (1994a)). For a dispersion process starting with oil as the continuous phase, two possible conditions may occur upon water addition (Zerfa et al. (1999 and 2000); Further details has been discussed in section 2.9.2):

1. Only W/O_m drops are formed before the inversion. $W/O_m/W$ drops are formed after the 'stable' catastrophic phase inversion has taken place;
2. $O/W_m/O$ drops are formed before the inversion. O/W_m drops are formed after the 'unstable' catastrophic phase inversion has taken place.

They used subscript 'm' to represent the micelle-containing phase. The aforementioned nomenclature method can also be used to describe the multiple drops formed through the stable catastrophic phase inversion process. One can say that the primary W_1/O_m emulsions are created before water becomes the continuous phase to form $W_1/O_m/W_2$ drops. However, the shortfalls of the nomenclature method suggested by Myers are apparent when it is applied to describe the multiple drops in the unstable catastrophic inversion process. In those cases, the multiple $O/W_m/O$ drops can only be formed after the production of W_m/O drops. In terms of the sequence of appearance,

the multiple drops would have to be identified as $O_2/W_m/O_1$ drops. As a result, direct comparison between various multiple emulsions would require prior knowledge of the production methods. A slightly different nomenclature system reviewed by Florence and Whitehill (1982) also had the same problem as the method suggested by Myers.

In this work, the sequence of the formation of various phases is very complicated. As shown in previous sub-sections, both inner and outer polymer drops might be created at the same time, specifically at the phase inversion point. It becomes impossible to use the nomenclature system suggested by Myers. Therefore, a new method of nomenclature is required. An alternative method based on the "location" of the different phases in the emulsions is suggested here. Continuous phases can be represented by subscript 'C'. The dispersed phase, which is in direct contact with the continuous phase is identified using subscript '1', and is called a primary phase. For example, notation for simple polymer-in-water drops would be P_1/W_C . Water droplet in direct contact with the P_1 phase can be denoted as W_1 , the multiple drops in concern would be a $W_1/P_1/W_C$ drops. Other W/P drops dispersed inside this multiple $W_1/P_1/W_C$ drops can carry numbers, in increasing orders, as their subscript. For example, $W_2/P_2/W_1/P_1/W_C$ or $W_2/P_1/W_1/P_C$ drops. It should also be noted that the word 'primary' used in this nomenclature method describes the location of the phases. They carry different meanings to those used by Myers to describe the sequence of appearance of the phases. This alternative method of nomenclature is independent of the production method and should leads to clearer and more consistent description of multiple emulsions. This alternative nomenclature method is employed throughout this thesis.

6.6.6 Drop size studies

Droplet sizes from SEM images of the emulsions were calculated and analysed using the C⁺⁺ programmes mentioned in section 5.3.6. The number of simple drops used for the analysis is larger than N_{crit} (i.e., reliable results are obtained) for all samples. However, it is not always possible to count enough multiple drops and W_1 drops to ensure that N_{crit} , or even N_{lim} , is achieved. This section aims to discuss some of the results obtained from the drop size analysis.

Results

Figure 6.46a shows the effect of water content on P_1/W_C drops, and pseudo P_1/W_C drops (for S3). Figure 6.46b shows the effect of water content on W_1/P_C drops before phase inversion and $W_1/P_1/W_C$ drops after phase inversion. Results of emulsion sample S8, which were analysed after 1¼ years are also shown in figure 6.46a. Figure 6.47 and 6.48 are the SEM images of emulsion sample S8 and S3 analysed using freeze fracture technique 1¼ years after these emulsions were produced.

Table 6.6 shows the total calculated interfacial area per unit volume, a , of various emulsion samples. For S4, S5, S8 and S11, the a values are the total interfaces between simple P_1/W_C drops and the continuous water phase; and both the external and internal multiple $W_1/P_1/W_C$ interfaces. For S3 (pseudo-drops), the a value is the total PUP-W interface of the pseudo-drops. For S2, the a value is the interface between the W_1 drops and the polymer continuous phase. For S3 (small drops), the a value is only calculated from the interface of the small P_1/W_C drops. Table 6.7 shows the effect of storage time on the emulsion withdrawn at the phase inversion point. The variables shown include volume fraction of pseudo- P_1/W_C drops ($f_{P/W}$) and mean diameters of both pseudo- P_1/W_C drops and small P_1/W_C drops.

Table 6.6. Total interfacial area per unit volume, in m^2/m^3 , of the emulsion samples,

Sample	a (m^2/m^3) $\times 10^{-6}$	Sample	a (m^2/m^3) $\times 10^{-6}$
S3 (pseudo-drops)	1.95	S11	1.09
S4	1.58	S2	0.21
S5	1.78	S3 (small drops)	29.6
S8	1.62		

Table 6.7. Effect of time on the emulsion withdrawn at the phase inversion point,

	$f_{P/W}$	Pseudo- P_1/W_C drops		Small P_1/W_C drops	
		d_{10} (μm)	d_{32} (μm)	d_{10} (μm)	d_{32} (μm)
Immediate	0.4189	1.29 (± 0.01)	1.82 (± 0.01)	0.14	0.15
After 3 months	0.4324	1.20 (± 0.01)	1.60 (± 0.01)	N/A	N/A
After 1¼ years	1.00	2.26 (± 0.03)	2.95 (± 0.05)	0.13	0.13

Effect of water content

The size of P_1/W_C drops increases slightly with the amount of water present in the emulsions (as shown in figure 6.46a). d_{10} of S3 does not match this result possibly due to the difficulties in measuring the small pseudo- P_1/W_C drops. It is worth pointing out that although sample S8 is analysed 1¼ years after its production, the mean diameters of its P_1/W_C drops still follow the same trend. As in figure 6.46b, the size of the W_1 drops also increases after the phase inversion has taken place. These results show that some coalescence between P_1 drops takes place following dilution of the water-continuous emulsions. The increase in the size of W_1 drops is likely to be caused by the coalescence of W_1 drops inside type-B multiple drops (i.e., drops containing more than one water drop).

The W_1/P_C drops in sample S2 before PWCPI has taken place are at least 2 times larger, in diameter, than W_1 drops obtained after the inversion has taken place. Therefore, the larger W_1/P_C drops are likely to have participated in the phase inversion, leaving behind the small water drops to form the primary water drops in the multiple emulsions.

From table 6.6, it is seen that the total interfacial area per unit volume before phase inversion is about $0.2 \times 10^6 \text{ m}^2/\text{m}^3$. After the phase inversion, the a value increases by 5 to 10 times. The amount of water presence in the multiple emulsions appears to have little effect on the a value. This shows that the emulsions are quite stable irrespective of the amount of water present. At the phase inversion point, the interfacial area can actually increase by up to 30 times due to the existence of the small P_1/W_C drops. The a values of these emulsions are comparable to those mentioned in section 6.5.2.

Effect of storage time on emulsion sample S8

As mentioned earlier, emulsion sample S8 was examined 1¼ years after its production. From figure 6.47, it is noticeable that very few multiple drops are left after 1¼ years. At the same time, it is seen in figure 6.46a and table 6.6 that the mean diameters of its simple P_1/W_C drops and total interfacial area per unit volume show little deviation from the expected values if it was analysed instantly. The exact mechanism of the breakdown of the W_1 drops is unknown. However, judging by the

small changes in mean diameters and total a values, the emulsions as a whole are stable over time. This result agrees with the early observation in section 6.3.3.

Effect of storage time on emulsions withdrawn at the phase inversion point

As seen in figure 6.48, the small P_1/W_C drops still exist 1¼ years after emulsion S3 has been produced. However, all the entrapped water drops have gone into the water-continuous phase, leaving behind emulsions containing only pseudo- P_1/W_C drops. In table 6.7, it can also be seen that the size of the small P_1/W_C drops only reduces slightly after 1¼ years.

From table 6.7, there appear to be little change over a 3-month period in terms of the volume fraction of pseudo- P_1/W_C drops (at about 42 %), and the mean pseudo- P_1/W_C drop size. However, the differences are noticeable between samples analysed after 3 months and after 1¼ years. These results shows that the emulsion withdrawn at the phase inversion point is quite stable since any losses in its identity happens over a period of few months rather than a few weeks or days.

Conclusions

The existing literatures on catastrophic phase inversion mechanism of PU-W dispersions can only describe the existence of the RI and RIII regions of the phase inversion map. A modified mechanism is proposed to describe the events that occurred during the PWCPI process carried out in the RII regions of the phase inversion map. Before phase inversion, initial water addition leads to the hydration of ionic groups. The hydrated portions gradually enlarge with further addition of water and start forming water drops; water drops also start to form independently in the hydrophobic portions of the polymer matrix. The moderate ionic group content in the PUP ionomer leads to uneven distribution of ionic centres around the W_1/P_C drops.

At the phase inversion point, the PUP-W interface restructures and PUP ionomer disintegrates into a dispersion of spherical particles enclosed by a continuous aqueous phase. This restructuring process starts at the ionic-centre-rich PUP-W interface and extends towards the bulk of the polymer matrix and PUP-W interfaces without any ionic centres. Although the ionic group content in a RII PUP-W mixture is insufficient to stabilise the small P_1/W_C particles, results show that there must be a mechanism that only stabilises closely packed emulsions containing small PUP

ionomer particles. It is believed that the additional stability is provided by the apparent ionic-centre-rich environment surrounding any isolated ionic groups on the particle surface. It is also suggested that pseudo-drop structures are formed simultaneously during the production of the small P_1/W_C drops. Essentially, the formation of the pseudo-drops is a kinetically driven event during the dynamic catastrophic phase inversion process. Some simplified events that may lead to the formation of various pseudo-drops were also described to demonstrate the proposed modified catastrophic phase inversion mechanism.

After phase inversion, water addition dilutes the emulsion and destroys the apparent ionic-centre-rich environment surrounding any isolated ionic groups on a particle surface. This leads to the collapse of the pseudo-drop structures to create emulsions containing matured multiple drop structures. The resultant emulsions are stable because the matured drops have a similar distribution of ionic centres to the pseudo-drops, i.e., ionic-centres-rich surface and a core containing little, or no, ionic centres. Coalescence between any two matured drops is prevented by the repulsive force provided by the ionic-centre-rich PUp droplet surface.

The problems of using existing nomenclature systems to describe multiple emulsions are also tackled in this section. An alternative nomenclature system based on the “location” of the different phases in the emulsions is suggested and is used throughout this thesis. This alternative method should lead to a clearer and more consistent description of multiple emulsions. In the last sub-section, it is shown that some coalescence of W_1 and P_1 drops took place when more water is present in the emulsions. It is also shown that most water drops would disappear from the multiple drops after a period of 1¼ years. However, the emulsions as a whole are quite stable upon dilution and over time. Lastly, it is shown that aqueous PUp ionomer emulsions with moderate ionic group contents can have high interfacial area per unit volume at the phase inversion point. This is due to the presence of the small P_1/W_C drops of about 0.14 μm . At the same time, this emulsion is stable over a period of a few months rather than weeks or days.

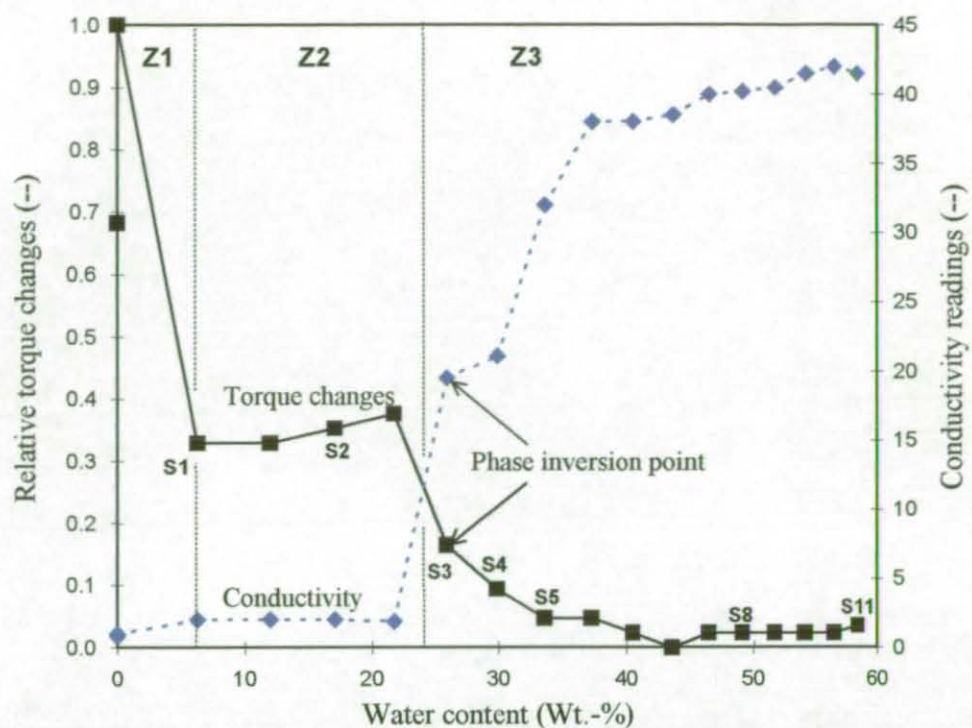


Figure 6.34. Torque changes and conductivity graphs of experiment EX58



Figure 6.35. SEM image of sample EX58/S1

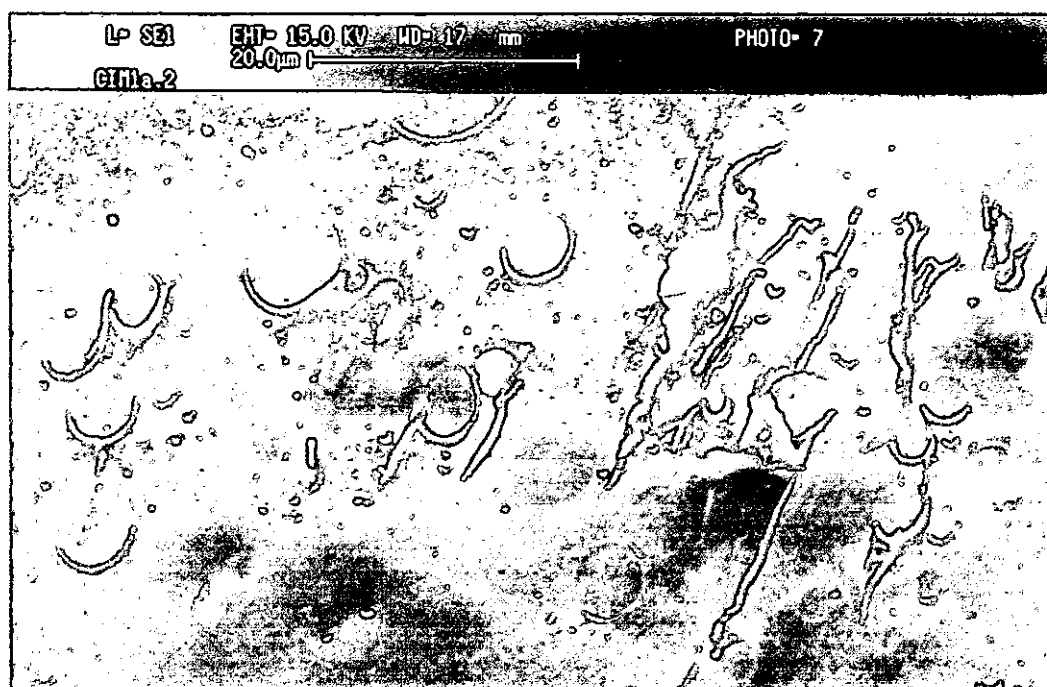


Figure 6.36. SEM image of sample EX58/S2

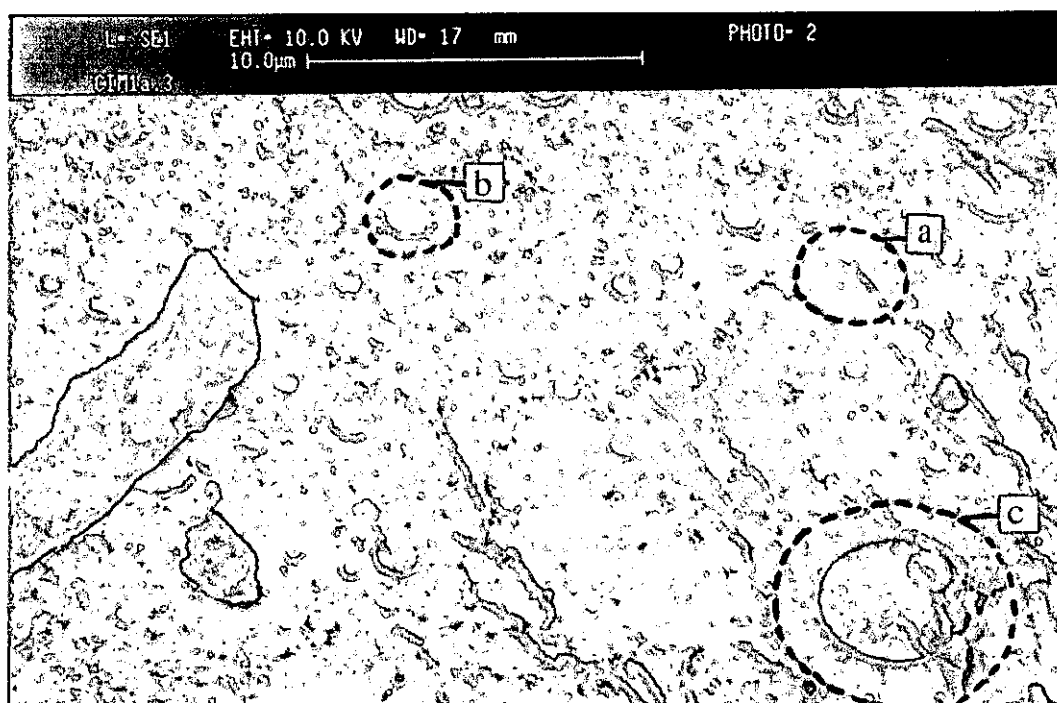


Figure 6.37. SEM image of sample EX58/S3: (a) pseudo- P_1/W_C drop; (b) pseudo- $W_1/P_1/W_C$ drop; and (c) pseudo- $P_2/W_1/P_1/W_C$ drop

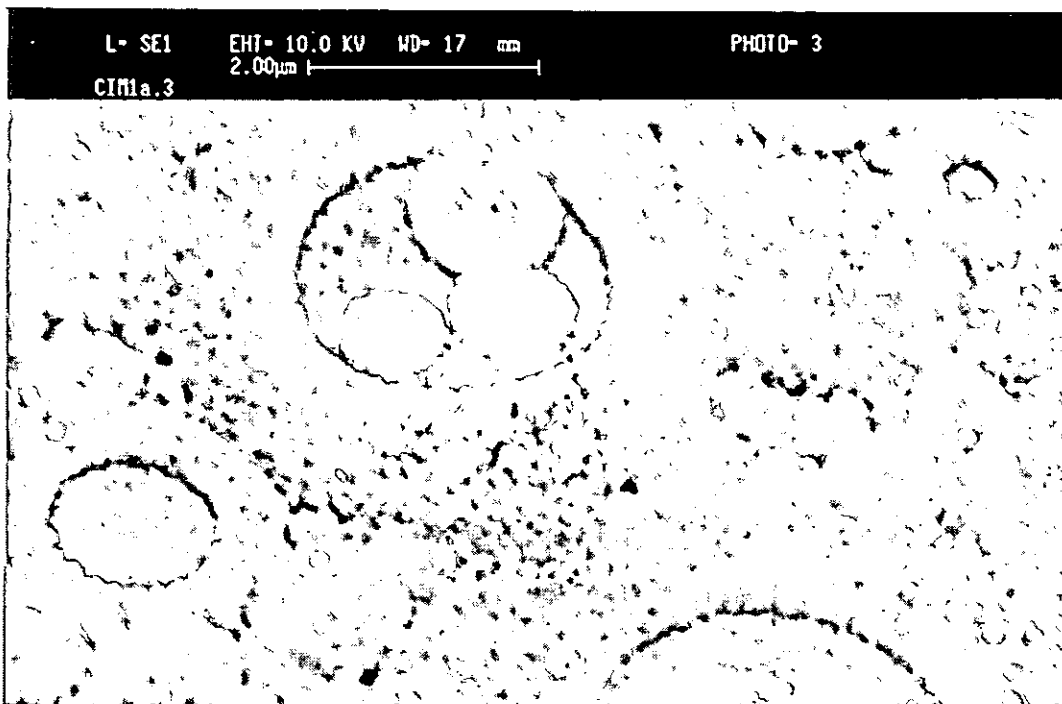


Figure 6.38. Enlarged SEM image of sample EX58/S3

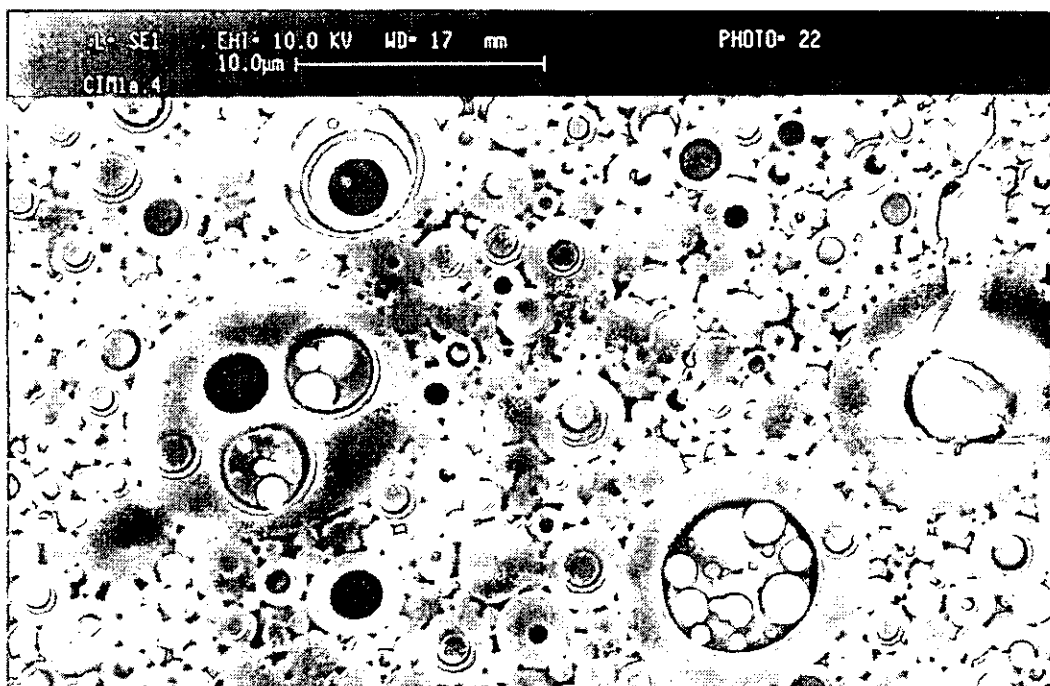


Figure 6.39. SEM image of sample EX58/S4

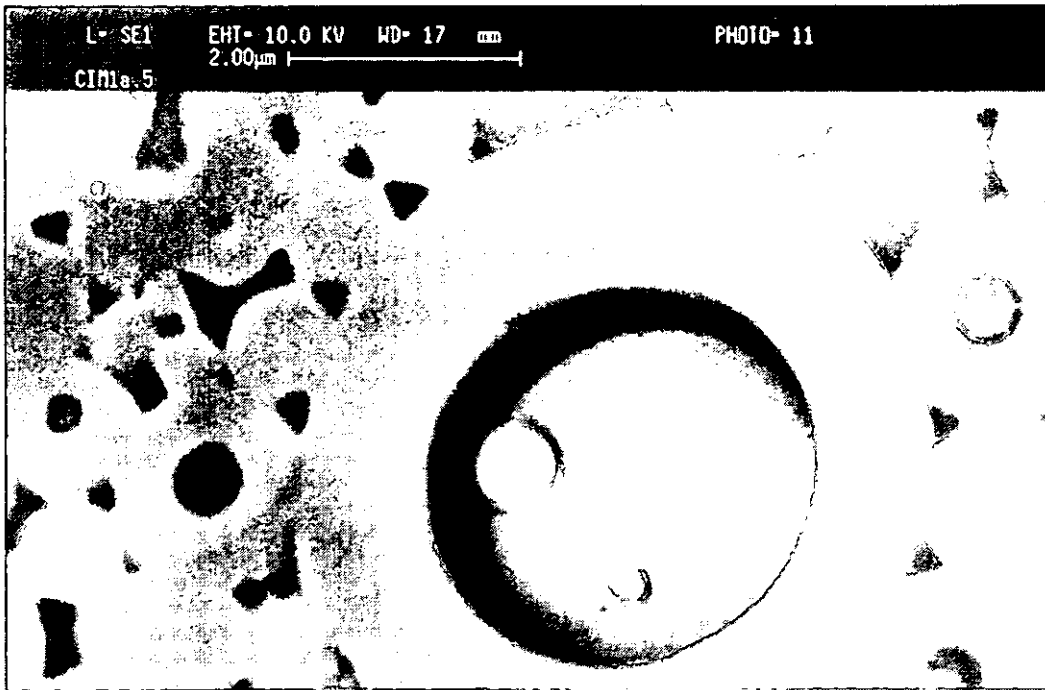


Figure 6.40. SEM image of sample EX58/S5

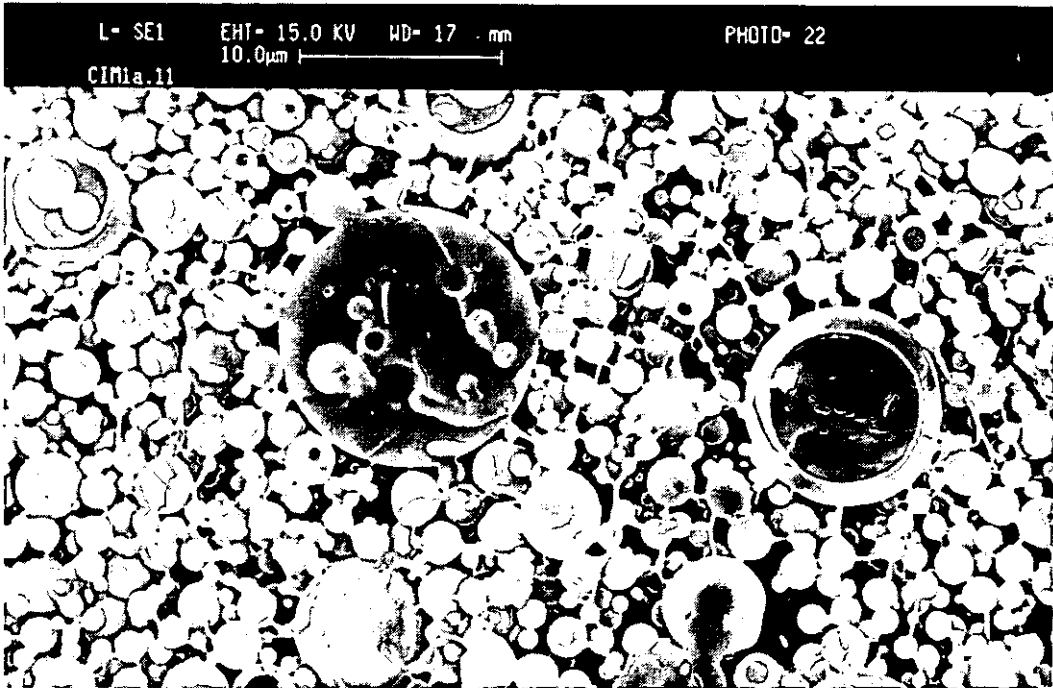


Figure 6.41. SEM image of sample EX58/S11

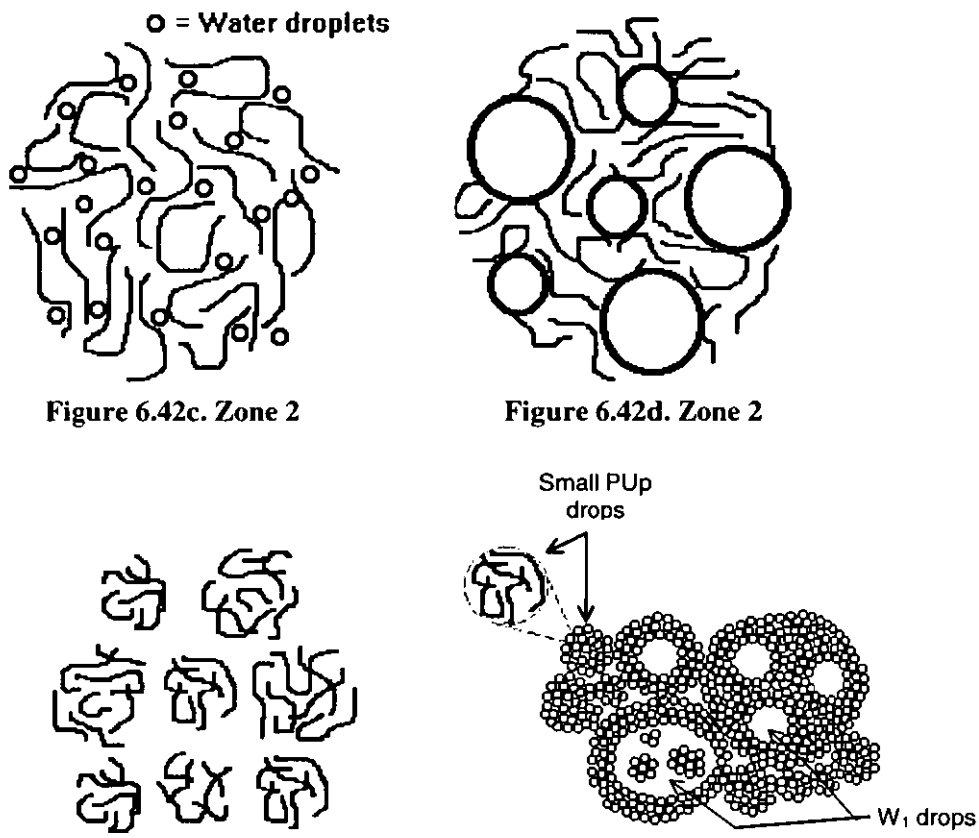
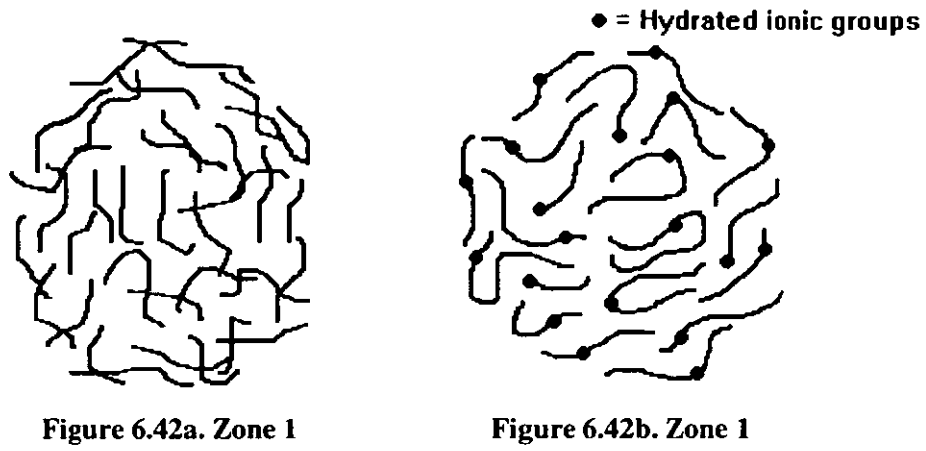


Figure 6.42e. Phase inversion point

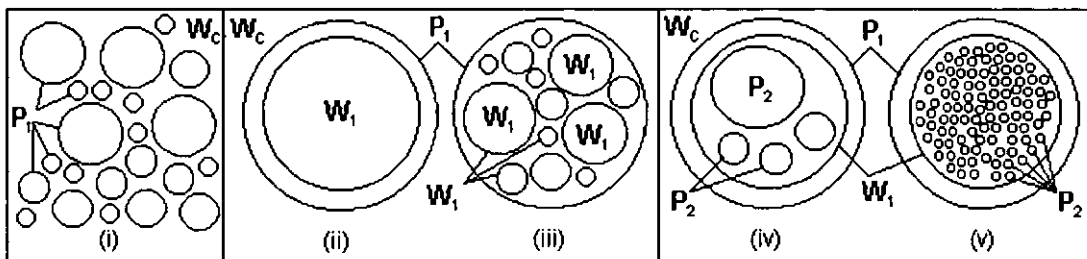
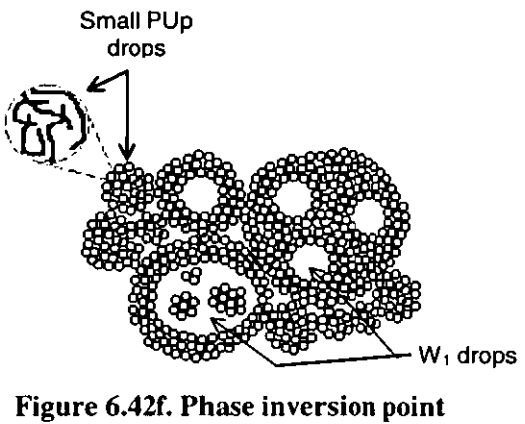
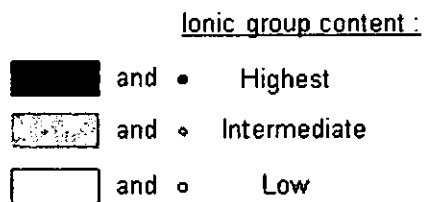


Figure 6.42. Events occurring during the PWCPI process in the RII region

For figure 6.43 to figure 6.45, the small PU₁ drops as shown in figures 6.42e and 6.42f can have different ionic group content. They are represented as:



Notation:

‘W’ stands for water drops.

‘PC’ stands for polymer-continuous system.

‘WC’ stands for water-continuous system.

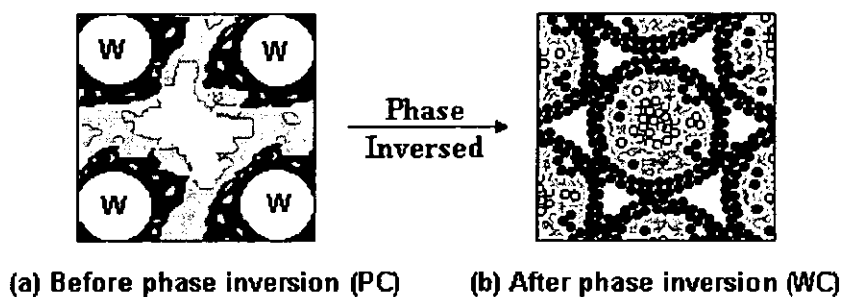


Figure 6.43. The formation of pseudo-simple P₁/W_C drops

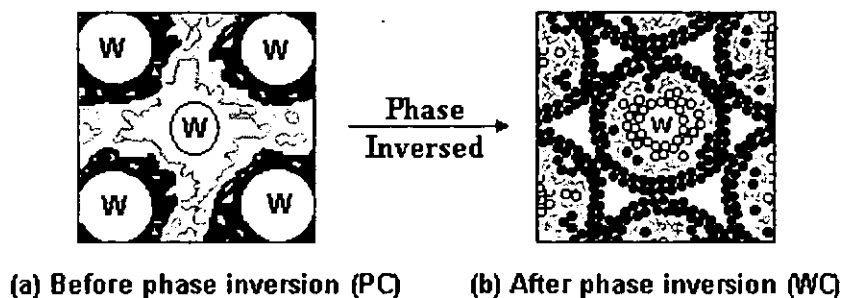


Figure 6.44. The formation of a pseudo-W₁/P₁/W_C drop

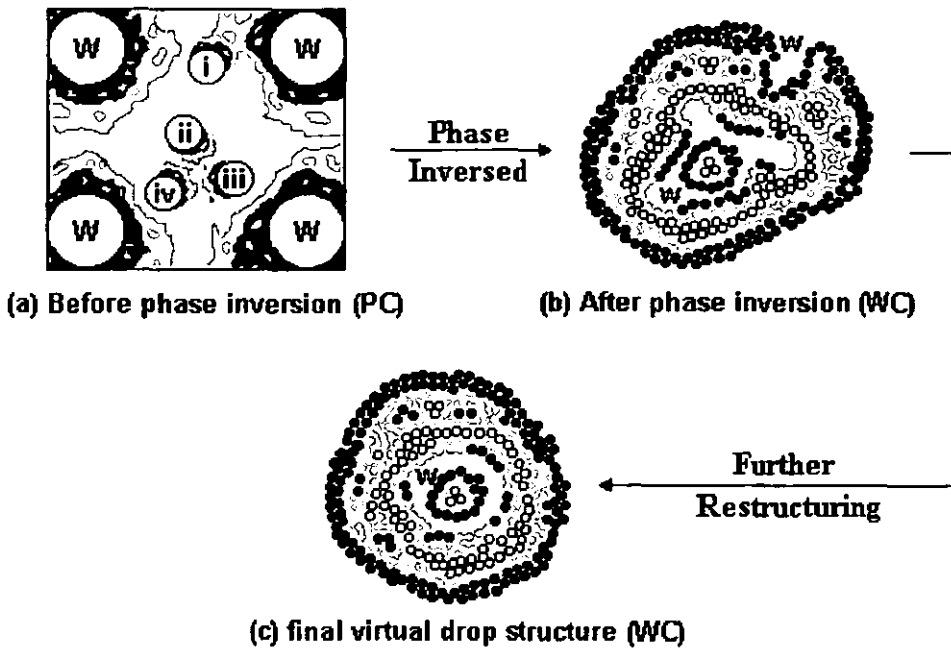
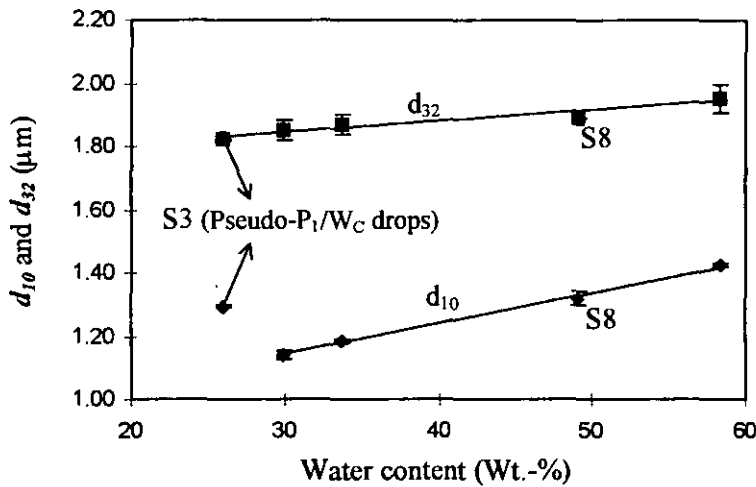
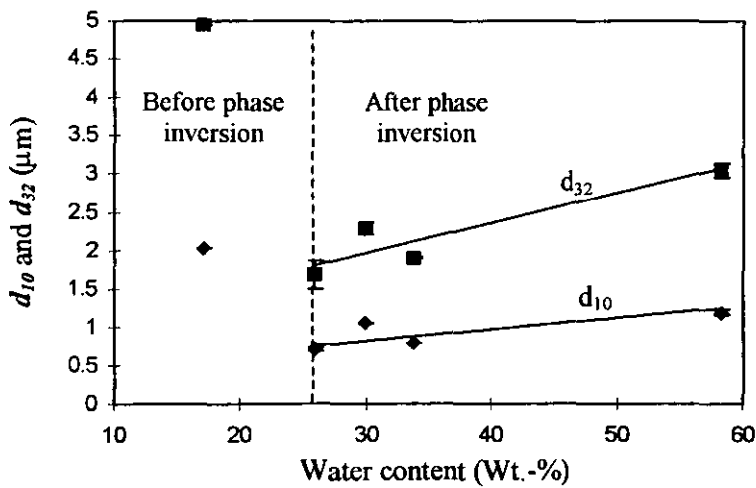


Figure 6.45. The formation of a pseudo- $P_2/W_1/P_1/W_C$ drop



(a) P_1/W_C drops



(b) W_1 drops

Figure 6.46. Effect of water content on mean diameters of (a) P_1/W_C and (b) W_1 drops

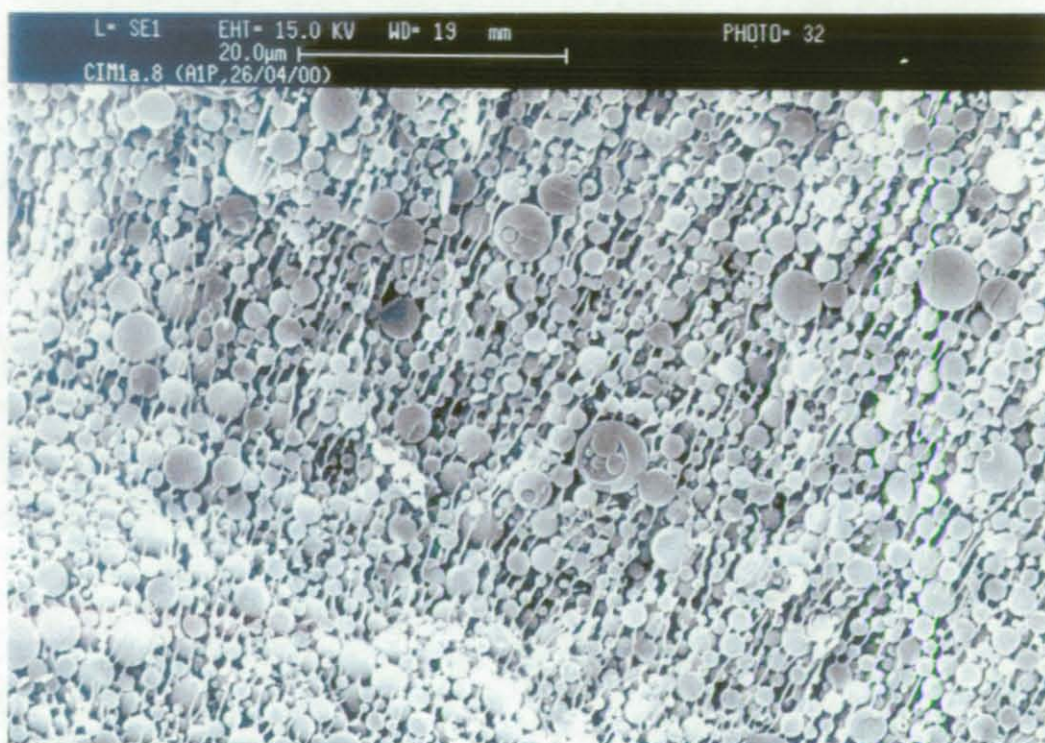


Figure 6.47. SEM image of emulsion sample EX58/S8 analysed 1¼ years later

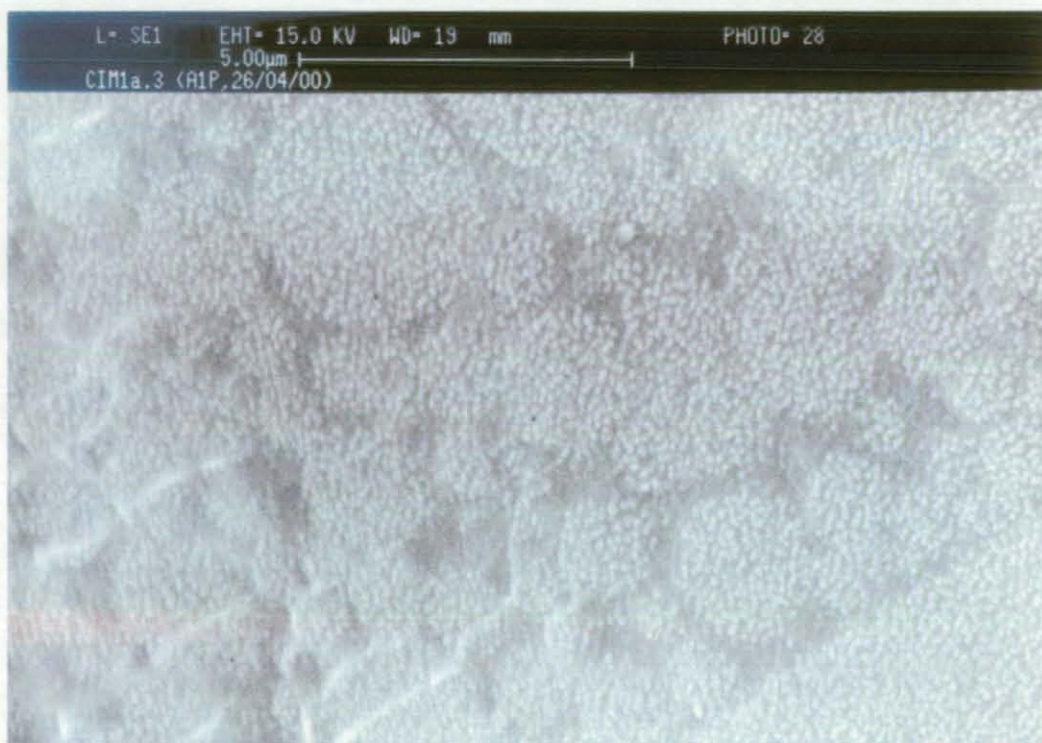


Figure 6.48. SEM image of emulsion sample EX58/S3 analysed 1¼ years later

6.7 Effect of stabilising groups

PUp-W dispersions stabilised using TEA-neutralised PUp ionomers have been studied in previous sections. The stabilising groups in those dispersions are a mixture of free carboxylic acid groups, $-\text{COOH}$, and carboxylate groups ionised by TEA cations, $\text{COO}^-\text{HN}^+(\text{CH}_2\text{CH}_3)_3$. This section aims to study the effect of other stabilising groups including carboxylate groups ionised by sodium cations, $-\text{COO}^-\text{Na}^+$, and free carboxylic acid groups, $-\text{COOH}$. The sodium cations are obtained by neutralising the PUp ionomer using NaOH solution. The effect of free carboxylic acid groups is studied by comparing results of previous sections with fully TEA-neutralised PUp ionomers, which have low $-\text{COOH}$ concentrations. Two types of PUp ionomers, both having low $-\text{COOH}$ concentrations, are used: (1) Pure PUp ionomers that contain low DMPA concentration (i.e., PUp2-3.75 and PUp2-1.5) and (2) blends of high DMPA content-PUp ionomer with PUp without any DMPA (i.e., the 'PUpB' series). The following discussions focus on the effect of stabilising groups on phase inversion loci and some droplet characteristics of various emulsions produced.

6.7.1 Carboxylate groups ionised by sodium cations

EX59/1 to EX59/5 and EX59/12 to EX59/14, mentioned in section 5.9, provide the necessary results for this study. Torque changes and conductivity graphs of these PWCPi and RIITI experiments are similar to those obtained from TEA-neutralised PUp-W dispersions. The phase inversion map of the new system studied is produced using the same method mentioned in previous sections.

Figure 6.49 compares the phase inversion maps of NaOH-neutralised PUp-W dispersions with that of TEA-neutralised PUp-W dispersions. Only the RI and RII regions are shown in figure 6.49. The RIII region has been neglected because stable emulsions can not be produced in that region. Aqueous emulsions produced from EX59/12, after the RIITI has taken place, were withdrawn, diluted instantly and drop sizes were measured using the Malvern Mastersizer on the same day as their production. The measured mean diameters were plotted against the ionic group content in figure 6.50. A similar relationship, between mean drop size and ionic group content, for TEA-neutralised emulsions produced through the RIITI process was already studied in section 6.5.2. The line notified as "same day" in figure 6.27a was reproduced in figure 6.50 for ease of comparison.

Phase inversion map

Figure 6.49 shows that the catastrophic phase inversion points (of the PWCPI process) in both RI and RII regions have been displaced when NaOH is employed as the neutralising agent. Chen and Chen (1992) shows that the alkali metal cations (as for NaOH-neutralised dispersions) are more easily hydrated in the aqueous phase than are the ammonia cations (as for TEA-neutralised dispersions). This is because the presence of hydrophobic alkyl substituent in the ammonium cation reduces its hydration ability when it is in contact with the aqueous phase. The observed results suggest that more water can be dispersed into (and/or absorbed by) the alkali metal-neutralised PUp ionomer matrix due to its improved hydration ability.

On the other hand, the transitional phase inversion loci for NaOH-neutralised PUp-W dispersions are only slightly lower than that of TEA neutralised PUp-W dispersions during the RIITI process. This result seems to support earlier findings in section 6.5, which shows that transitional phase inversion of the RIITI process takes place when a certain amount of ionic groups has occupied the PUp-W interface. In other words, locations of the transitional phase inversion loci of the RIITI process depend mainly on the concentration of ionic groups and, to a lesser extent, on their hydration ability during the production of PUp-W dispersions.

Drop size studies

Drop sizes of NaOH-neutralised PUp-W dispersions decrease with ionic group content, as shown in figure 6.50. This behaviour is similar to the TEA-neutralised dispersions, although the asymptotic decrease in drop size is not significant in the case of NaOH-neutralised dispersions. It is also obvious that the mean droplet diameter of the NaOH-neutralised dispersions is smaller than that of TEA-neutralised dispersions.

Chen and Chen (1992) observed similar results to this work. They attributed the result to the higher hydration ability of the alkali metal cations, comparing with the ammonia cations. The better hydration ability results in a higher Zeta potential on the particles' surface for dispersions containing alkali metal cations. Rosthauser and Nachtkamp (1986) mentioned that aqueous PU ionomer dispersions are stabilised by the well-known phenomenon of diffuse double layer (details are already mentioned in section 2.3.4). The same model should also accounts for the necessary stability of the aqueous PUp ionomer dispersions produced in this work. For the diffuse double layer,

the repulsive force of the Zeta potential between particles is responsible for the overall stability of the dispersions (Hunter (1985)). Therefore, the result indicates that the particle size is determined by the stability of the dispersed PUp ionomers. Stable dispersions prevent coagulation during the dispersion process and result in finer particles.

6.7.2 Effect of free carboxylic acid groups

Table 6.8 shows the phase inversion points of PWCPI experiments using 98% neutralised PUp2-1.5 (EX59/6) and PUp2-3.75 (EX59/7), 98% neutralised blends containing equivalent amount of ionic groups (EX59/8 and EX59/10) and PUp2-7.5 neutralised to the same ionic group contents (EX55/6 and EX55/4). TEA was used as the neutralising agent for all these experiments.

Table 6.8. Water content at the catastrophic phase inversion points of different PUp ionomer-W dispersions containing same ionic group content,

Ionic group content	0.280 mmole/g (RI region)		0.112 mmole/g (RII region)	
	PUp with low DMPA content	98% DN PUp2-3.75	23.16 (\pm 1.98) wt.-%	98% DN PUp2-1.5
PUp blends	98% DN PUpB-50/50	23.20 (\pm 1.98) wt.-%	98% DN PUpB-20/80	18.96 (\pm 2.2) wt.-%
PUp2-7.5 with low DN	49.9 % DN	23.07 (\pm 1.97) wt.-%	20.05 % DN	26.88 (\pm 1.79) wt.-%

Some emulsion samples produced from PWCPI experiments using PUpB-20/80 (EX59/8) and PUp2-1.5 (EX59/6) were withdrawn for analysis using the SEM-freeze fracture technique. Figure 6.51 is the SEM image of aqueous PUpB-20/80 emulsions containing 38.55 wt.-% of water. Figure 6.52 and 6.53 are the SEM images of an aqueous PUp2-1.5 emulsion containing 41.17 wt.-% of water.

The catastrophic phase inversion map of the TEA-neutralised PUpB-W dispersions is plotted in figure 6.54, together with the phase inversion map of the TEA-neutralised PUp2-7.5-W dispersions. Again, only the RI and RII regions are studied. The RIII region has been neglected because stable emulsions can not be

produced in that region. Table 6.9 compares the droplet characteristic of multiple drop emulsions produced from EX59/8 and EX59/9. The variables shown in table 6.9 include the amount of ionic groups, the water content of the emulsions, the volume fraction of simple P_1/W_C drops ($f_{P/W}$), Sauter mean diameter (d_{32}) of the simple P_1/W_C drops ($d_{32,PW}$), d_{32} of the multiple drops ($d_{32,WPW}$) and total calculated interfacial area per unit volume, a . The a value is the total contact surfaces of various P_1 and water interfaces.

Table 6.9. Droplet characteristics of the emulsions produced from experiments EX59/8 and EX59/9,

Experiment code	EX59/8	EX59/9
Ionic group content	0.111 mmole/g	0.175 mmole/g
Water content	50.74 wt.-%	50.17 wt.-%
$f_{P/W}$	0.204	0.280
$d_{32,PW}$	4.56 (\pm 0.08) μm	3.39 (\pm 0.07) μm
$d_{32,WPW}$	7.09 (\pm 0.07) μm	5.27 (\pm 0.04) μm
$a \times 10^{-6}$	0.5814 m^2/m^3	0.8379 m^2/m^3

Different forms of PUp ionomers

In the RI region (\sim 0.28 mmole/g of ionic groups), phase inversion takes place at similar water content regardless of the forms of the PUp ionomers (Table 6.8). For the PWCPI process, this characteristic can be extended to the rest of the RI region since the catastrophic phase inversion loci of the blend are similar to PUp2-7.5 with high DN (as shown in figure 6.54). This result suggests that the ionic group content in the RI region is high enough to suppress the effect of the free carboxylic acid groups.

In the RII region (\sim 0.112 mmole/g of ionic groups), however, the PUpB-20/80 blend and PUp2-1.5 have similar inversion points, but they are different from that of PUp2-7.5 with moderate DN (Table 6.8). This results is best explained by exploring the two main differences amongst the three forms of PUp ionomers, namely different starting phase viscosity and the existence of free carboxylic acid groups.

The viscosity of all three types of PUp ionomers can be calculated using equation (4-4) and the constants shown in tables 4.4 and 4.7. At the operating temperature of 60 °C, the viscosities of PUp2-7.5, PUp2-1.5 and PUpB-20/80 are

27,000 (± 27) cPs, 5,100 (± 95) cPs and 3,300 (± 37) cPs respectively. Although viscosity changes after neutralisations and upon water additions, it is not unreasonable to assume that dispersions using PUp2-7.5 would still have significantly higher viscosity compared with the other two PUp ionomers throughout the PWCPI process. Selker and Sleicher (1965) and Brooks and Richmond (1994e) observed that “as the viscosity of an organic phase increases, its tendency to be dispersed increases”. Based on this prediction, one would expect the PUp2-7.5-W system to phase-invert at lower water content. However, the results contradict this prediction and therefore viscosity is unlikely to be a suitable explanation for the findings.

One other possible explanation left is the existence of free carboxylic acid groups in PUp2-7.5. It is probable that the remaining free carboxylic acid groups in the poorly neutralised PUp2-7.5 makes the system more hydrophobic than the other two fully neutralised PUp ionomers (PUp2-1.5 and PUpB-20/80). As a result, the partially neutralised PUp2-7.5-W mixture could favour polymer-continuous dispersions and delay the phase inversion to higher water content. More extensive data are needed to verify and extend these statements.

Based on above arguments, blends (of PUp ionomer with high DMPA content with PUp without any DMPA) would behave similarly to PUp ionomer containing an equivalent amount of DMPA groups in both RI and RII regions of the phase inversion map. This should be true as far as the locations of the phase inversion boundaries are concerned. For the PWCPI process, figure 6.54 confirms that the catastrophic phase inversion loci of PUpB-W dispersions have lower water content compared with those of PUp2-7.5-W dispersions in the RII region.

Droplet characteristics

Aqueous PUpB-20/80 emulsions consist of mainly multiple $W_1/P_1/W_C$ drops, with very few simple P_1/W_C drops or $W_2/P_2/W_1/P_1/W_C$ drops. The W_1 drop diameters in emulsions containing about 39 wt.-% of water are between 0.4 to 10.61 μm and P_1 drop diameters are between 1.63 to 18.88 μm (as shown in figure 6.51). Drop structures of aqueous PUp2-1.5 emulsions are very different from the aqueous PUpB-20/80 emulsions. The most obvious difference is the “rigid” and spherical appearance of the PUpB-20/80 drops compared to the “soft” and slightly irregular appearance of the PUp2-1.5 drops (as shown in figures 6.52 and 6.53). Also, more

$W_2/P_2/W_1/P_1/W_C$ drops such as those shown in figure 6.53 are found in the aqueous PUp2-1.5 emulsions. The size of P_1 drops in the aqueous PUp2-1.5 emulsions ($< 6.5 \mu\text{m}$) is about 35 % of the size of P_1 drops in PUpB-20/80 emulsions. At the same time, W_1 drops (with diameter up to $6 \mu\text{m}$) are almost half the size of W_1 drops in the PUpB-20/80 emulsions.

The reasons for the existence of different drop structures in the two emulsions are unclear. However, the differences are very obvious. Therefore, although it is possible to use the blend to simulate the phase inversion behaviour of PUp-W dispersions containing intermediate ionic group content, the emulsions produced are not necessarily the same. It can be said that the two PUp-W systems are macroscopically similar but microscopically different. Same differences were also observed in samples with different polymer-to-water ratios.

From table 6.9, one can deduce that more simple P_1/W_C drops are produced in RII emulsions containing more ionic groups. It contains smaller simple and multiple drops, as the d_{32} values suggest. The emulsion with higher ionic group content also has higher total interfacial area per unit volume. These results agree with the characteristics of RI emulsions in that drop size reduces and a value increases as ionic group content increases.

Conclusions

The transitional phase inversion loci of the RII process depend mainly on the concentration of ionic groups. The hydration ability of the ionic groups, however, determines the location of the catastrophic phase inversion loci of the PWCPI process. The usage of the alkali metal cations results in displaced catastrophic phase inversion points because they are more easily hydrated in the aqueous phase (and have higher Zeta potentials) than are the ammonia cations. PUp ionomer dispersions are stabilised by the diffuse double layer, in which the overall stability depends on the repulsive force between particles. Therefore, droplets of NaOH-neutralised PUp-W dispersions are also smaller than droplets of TEA-neutralised PUp-W dispersions.

Ionic group content in the RI region is high enough to suppress the effect of the free carboxylic acid groups. However, the existence of free carboxylic acids is responsible for the increased hydrophobicity (and hence delayed catastrophic phase

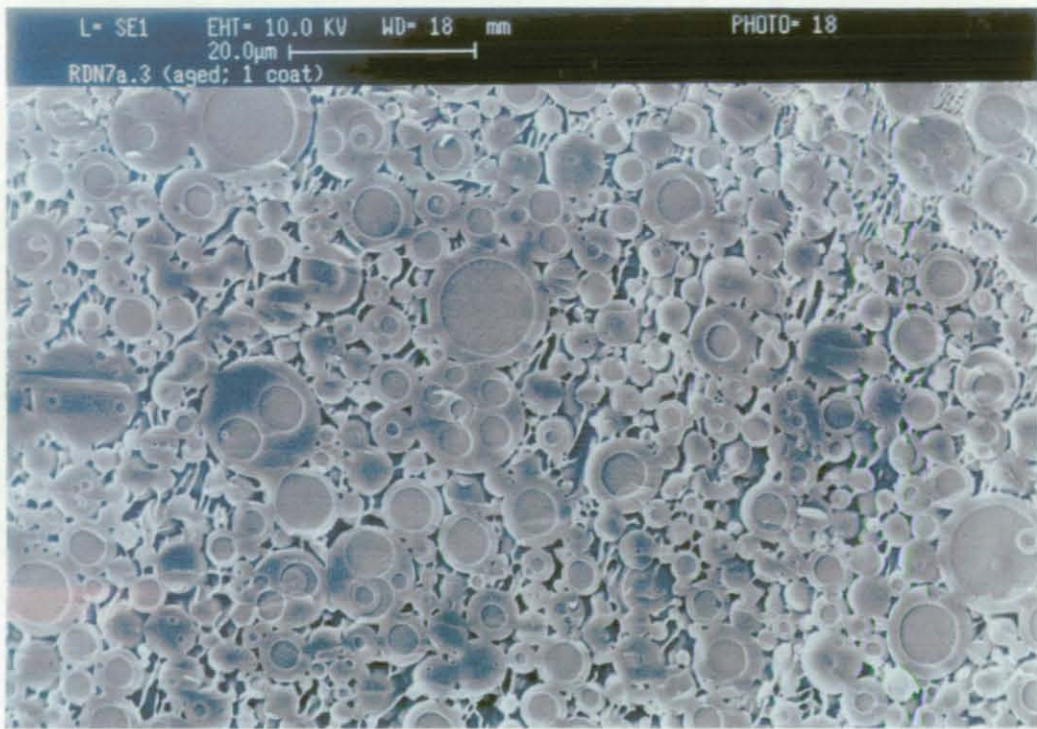


Figure 6.51. SEM image of aqueous PUpB-20/80 emulsions

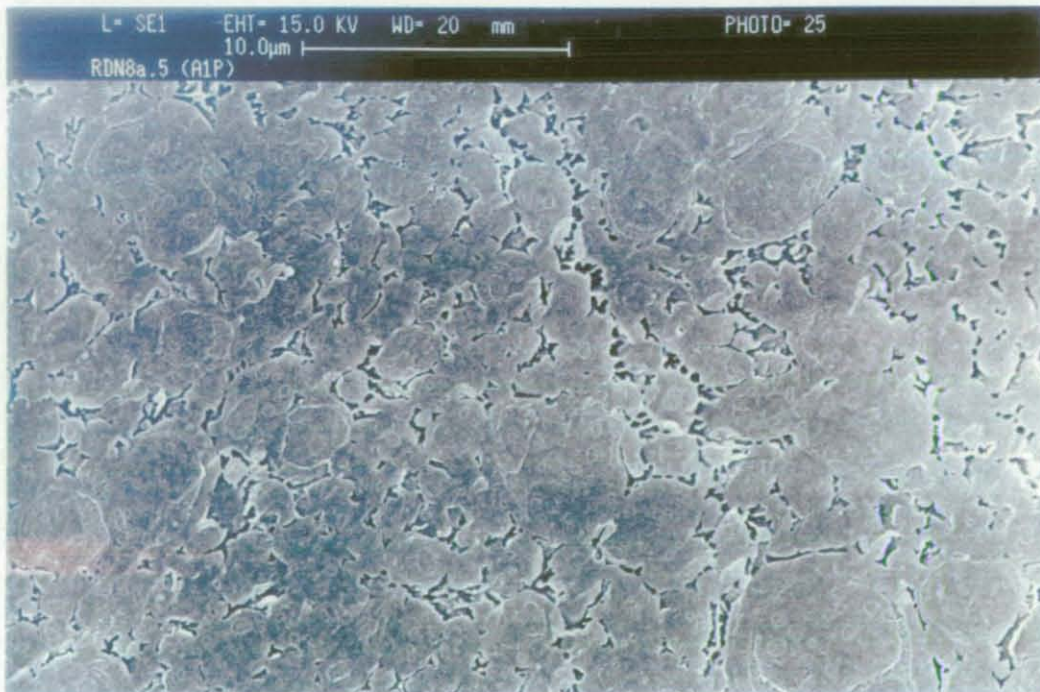


Figure 6.52. SEM image of aqueous PUp2-1.5 emulsions

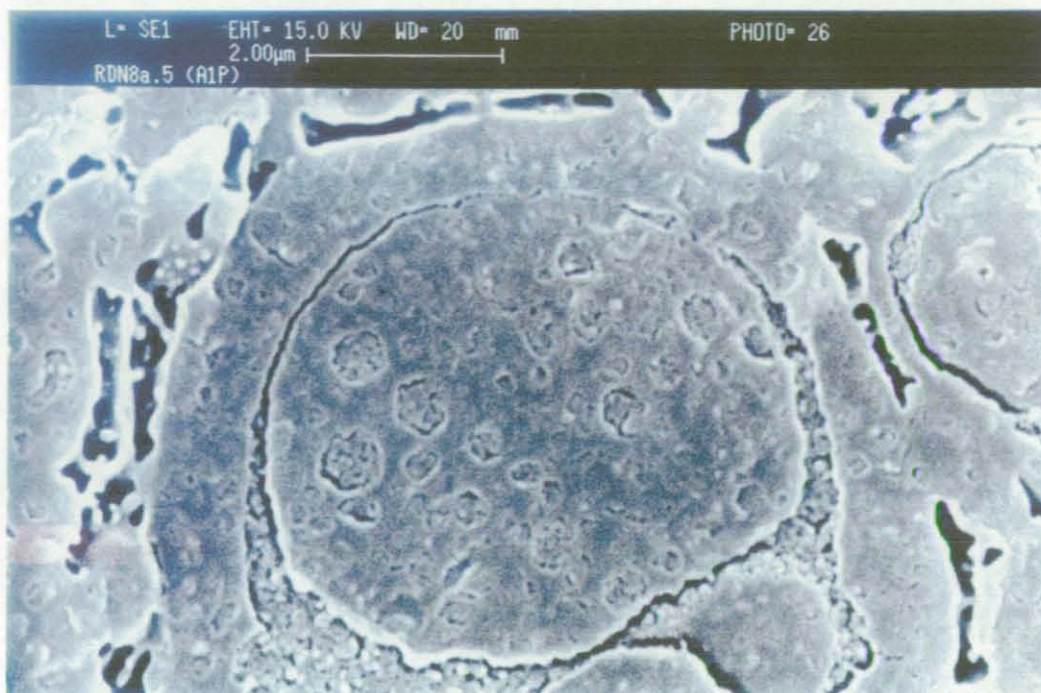


Figure 6.53. Enlarged image of figure 6.52

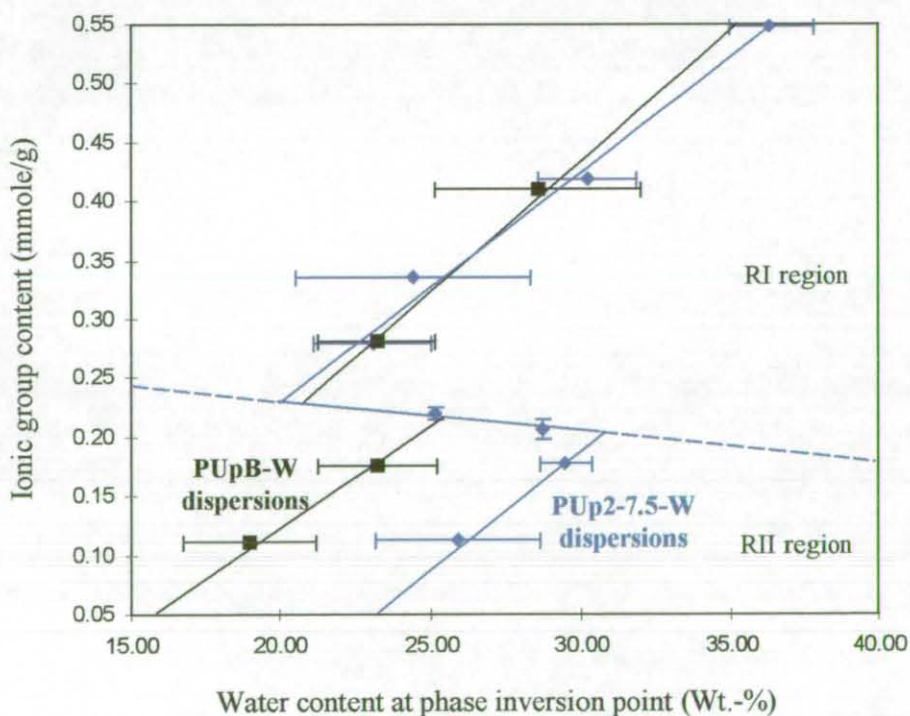


Figure 6.54. Phase inversion maps of PUpB-W and PUp2-7.5-W dispersions

6.8 Effect of some processing factors

Studies in this section are based on experiments mentioned in section 5.10. Figure 6.55 shows the catastrophic phase inversion maps at different operating temperatures, and hence different viscosity of the initial continuous phase. Figure 6.56 compares the catastrophic phase inversion maps obtained from different configurations of the dispersion vessel. Figure 6.57 shows the Sauter mean diameter of emulsions obtained from EX510/15 and EX59/12 after transitional phase inversion has taken place during the RIITI process.

6.8.1 Changing viscosity

It is shown in figure 6.55 that viscosity has a more significant effect on the RII region than on the RI region of the phase inversion map. It is also noticeable that catastrophic phase inversions are delayed to higher water content, in both the RI and RII regions, as viscosity of the initial continuous phase decreases. This finding is consistent with the earlier argument in previous section, which states that an organic phase with higher viscosity is more likely to become the disperse phase than one with lower viscosity.

6.8.2 Configuration of the dispersion vessel

The diameters of the turbine and baffle used in the dispersion vessel do not affect the location of the phase inversion loci, for both PWCPI and RIITI processes (figure 6.56). The aqueous emulsions produced from the RIITI process are also found to have a similar Sauter mean diameter regardless of the diameters of the turbine and baffle in used (figure 6.57). It is unclear, however, whether other agitators such as a U-type agitator or a propeller would have any significant effect on the phase inversion process during the production of PUp ionomer-W dispersions.

Conclusions

The PUp ionomer is more likely to become the dispersed phase when its viscosity is higher. The diameter of the four-bladed turbine and the width of the baffle have no significant effect on either the phase inversion loci (of PWCPI and RIITI processes) or drop size of the aqueous emulsions produced from the RIITI process.

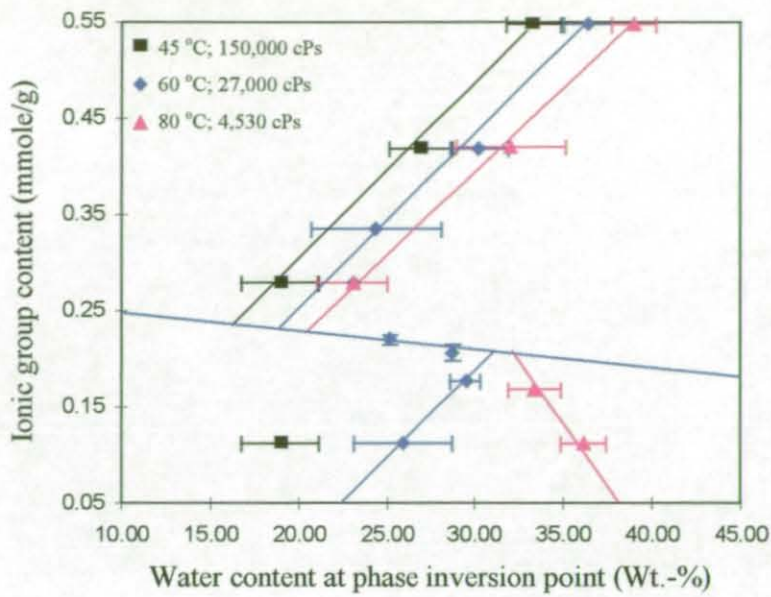


Figure 6.55. Phase inversion maps at different operating temperatures

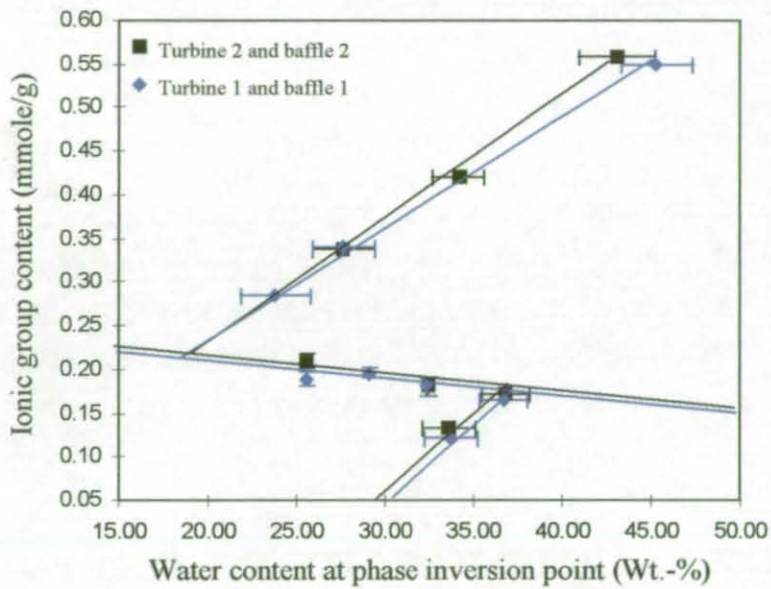


Figure 6.56. Phase inversion maps at different configurations of the dispersion vessel

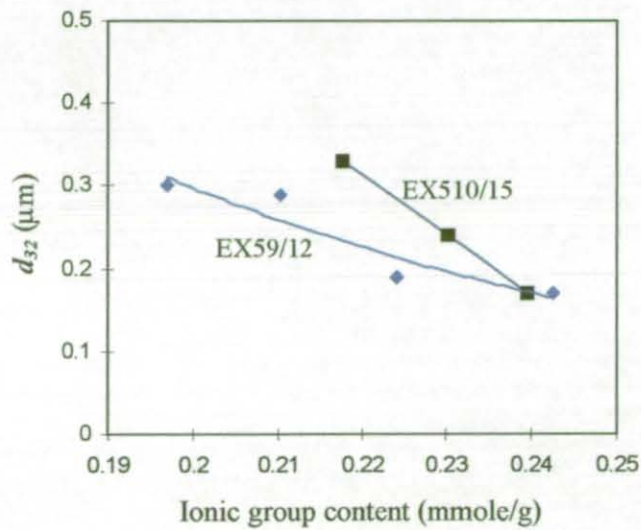


Figure 6.57. d_{32} of aqueous emulsions withdrawn from experiments EX510/15 and EX59/12

6.9 External surfactants-related PUp-W dispersions

Some external surfactants-related studies, as mentioned in section 5.11, have been conducted using PUp2-0 (PUp without any DMPA). These studies include the effect of HLB number and operating temperature for the usage of non-ionic surfactants, and the usage of anionic surfactant alone in producing PUp-W dispersions. The intention of these studies is to establish some preliminary comparisons between the usage of external surfactants and internal stabilising groups in producing PUp-W dispersions, via a PWCPI process.

6.9.1 Non-ionic surfactant – Changing HLB number

The operating temperature was maintained at 30 °C for the purpose of this study (EX511/2, EX511/4 and EX511/7).

Phase inversion map for production of non-ionic SPUp-W dispersions

Table 6.10 shows the types of surfactant used, their HLB numbers at 25 °C, the catastrophic phase inversion route taken and its detection method, the state of the final emulsion and the equivalent regions on the phase inversion map of PUp ionomer-W dispersions. Figure 6.58 is a proposed phase inversion “map” for SPUp-W system plotted using HLB number (at 25 °C) as its ordinate and water content at the phase inversion point as its abscissa.

The 3 experimental points located on figure 6.58, each having a different dispersion behaviour, can be used to represent 3 different regions separated by two lines (Line ‘A’ and ‘B’). By doing this, it is not difficult to see that the phase inversion map for SPUp-W dispersions is similar to that of internally stabilised PUp-W dispersions (or PUp ionomer-W dispersions, first shown in figure 6.11). The similarities between the SPUp-W system and the PUp ionomer-W system are not restricted to the phase inversion map produced. By comparing table 6.10 with table 6.3, it can also be seen that the appearance of the drop structures and the inversion routes are similar between the two systems of concern. These similarities provide scope for applying some established knowledge, about dispersions stabilised using external surfactants, to understand the PUp-ionomer dispersions.

The above mentioned similarities between the two systems strengthen the suggestion that the transitional phase inversion line ‘A’ represents a condition when

SAD is equal to 0. At the same time, the RI region represents a condition when SAD is smaller than 0 and both RII and RIII regions represent a condition when SAD is larger than 0.

Table 6.10. Summaries of experimental results when three different Igepal-CO type non-ionic surfactants were used to produce SPU_p-W dispersions at 30 °C,

Surfactant	Igepal CO-720	Igepal CO-520	Igepal CO-210
HLB number (at 25°C)	14.2	10	4.2
Phase inversion route*	$W_1/P_C \rightarrow P_1/W_C$	$W_1/P_C \rightarrow W_1/P_1/W_C$ + P_1/W_C	$W_1/P_C \rightarrow$ (W_1/P_1)/ W_C
Detection method	T and C	T and C	T (and possibly C)
Dispersion behaviour	Stable emulsion (Type 5 emulsion)	Semi-stable coarse emulsion (Type 3 and 4 emulsion)	Temporary dispersion (Type 2 emulsion)
Drop structure	Stable, small P_1/W_C drops ($d_{32} = 1.1 \mu\text{m}^\dagger$).	Different sizes of multiple drops coexist with small P_1/W_C drops.	Undispersed W_1/P_1 lumps in the water continuous phase.
Equivalent regions	RI	RII	RIII

Different phase inversion mechanism

Despite the similarities mentioned above, it is vital to notice that the phase inversion mechanism for a PU_p ionomer-W system is different from that for a SPU_p-W system. This difference in phase inversion mechanism is particularly obvious in the RII region of both systems.

Figure 6.59 shows the cinematography of events leading to the formation of smaller multiple drops in the RII region of the SPU_p-W system. A large multiple drop was seen stretching in two directions in figures 6.59a and 6.59b. Figure 6.59c shows how the large multiple drop over-stretched and eventually broke-up into two smaller

* Nomenclatures are same as table 6.3.

† Mean diameter is determined using Malvern Mastersizer and is confirmed using the optical microscopic image of the same emulsion.

multiple drops. In general, this mechanism for the formation of smaller multiple drops will be applicable to the formation of multiple drops in the whole RII region of the SPU_p-W system. In this case, the multiple drops are produced because the supplied external force is not enough to break-up the viscous W_1/P_1 phase at the phase inversion point. In other words, the $W_1/P_1/W_C$ drops are formed at the phase inversion point. This is different from the formation of multiple drops in the RII region of a PU_p ionomer-W system. In that case, multiple drops are formed after the phase inversion point, through coalescence of small P_1/W_C drops within the pseudo-multiple drops that are produced at the phase inversion point.

6.9.2 Non-ionic surfactant – Effect of temperature

Shinoda and Friberg (1986) noticed that the HLB number is not a characteristic property of an emulsion, but rather a property of a surfactant molecule in isolation. As a result, the HLB number required for the production of a specific emulsion changes with the oil type, the operating temperature, other additives in the two phases, etc. They suggested the use of HLB temperature (or phase inversion temperature (PIT)) as an alternative way to represent the hydrophile-lipophile property of an emulsion. According to Shinoda and Arai (1964), HLB temperature is a characteristic property of an emulsion for which the hydrophile-lipophile property of non-ionic surfactant is just balanced. The effect of additives, mixed emulsifiers, mixed oils, etc. are all reflected in the PIT and automatically adjusted in its determination. Their works show that temperature has a profound effect on the characteristic of a non-ionic surfactant-related system.

Igepal CO-720 at different operating temperatures

Table 6.11 shows how the types of emulsions produced and the routes leading to their production changed with changing operating temperatures. Igepal CO-720 was used for this study (EX511/5 to EX511/7).

It is interesting to notice that a specific SPU_p-W system changes from RI behaviour to RII behaviour as temperature increases. The size of the polymer drop in a $W_1/P_1/W_C$ drop also increases with increasing operating temperature. This work confirms the temperature effect and provides scope for plotting the phase inversion map by changing the operating temperature of a specific non-ionic SPU_p-W system.

The effect of temperature on catastrophic phase inversion behaviour can be understood by, firstly, understanding effect of temperature on the dissolution states of non-ionic surfactants. Shinoda and Friberg (1986) discussed the effect of temperature on the dissolution states of non-ionic surfactants containing polar parts, e.g. the "Igepal CO" surfactants that contain oxyethylene chains. According to Shinoda and Friberg, the non-ionic surfactants usually dissolve in water phase at low temperature; and in oil or the organic phase at high temperature. This is because the hydration force between the hydrophilic moiety of the surfactant and water is stronger at low temperature. As a result, the adsorbed surfactant monolayer tends to form a convex surface towards water. This in turns favours the formation of water-continuous dispersions or emulsions.

Table 6.11. Summaries of experimental results at different operating temperatures,

Temperature	30 °C	45 °C	60 °C
Phase inversion route*	$W_1/P_C \rightarrow P_1/W_C$	$W_1/P_C \rightarrow$ $W_1/P_1/W_C$	$W_1/P_C \rightarrow$ $W_1/P_1/W_C$
Detection method	T and C	T and C	T and C
Water content at the phase inversion (wt.-%)	11.74 (\pm 2.6)	13.09 (\pm 1.26)	14.17 (\pm 2.44)
Dispersion behaviour	Stable emulsion (Type 5 emulsion)	Semi-stable coarse emulsion (Type 3 and 4 emulsion)	Unstable coarse emulsion (Type 3 emulsion)
Drop structure	Stable, small P_1/W_C drops	$W_1/P_1/W_C$ drops of different sizes.	Mainly large $W_1/P_1/W_C$ drops.
Equivalent regions [†]	RI	RII	RII

Having understood the effect of temperature on the dissolution states of non-ionic surfactants, it is not difficult to explain the results shown in table 6.11. At low temperature, the non-ionic surfactant favours the formation of water-continuous dispersions. Therefore, a SAD^- condition exists in the non-ionic SPU_p-W mixture.

* Nomenclatures are same as table 6.3.

† Regions equivalent to the PUP ionomer-W system and the SPU_p-W system obtained by changing HLB number.

This type of mixture favours the RI catastrophic phase inversion as mentioned in sections 6.3 and 6.5.

As temperature increases, the adsorbed surfactant monolayer becomes concave towards the water. Following this change, a SAD⁺ condition exists in the SPU_p-W mixture. This would in turn favour the RII, and even RIII region, catastrophic phase inversion.

Changing HLB number at high operating temperature

Operating temperature was maintained at 60 °C and Igepal-CO surfactants were used as the external stabilisers for the purpose of this study (EX511/1, EX511/3, EX511/5, EX511/8 and EX511/9). Figure 6.60 shows a phase inversion map of the non-ionic SPU_p-W system at 60 °C.

It can be seen from figure 6.60 that the ranges of both the RII and RIII regions have increased. At the same time, the RI region does not exist within the range of HLB numbers studied. In the RII region, it was noticed that the size of the P₁ drops increases as HLB number approaches the line separating RII region from RIII region. In some cases, the polymer drops are so large that coalescence between them takes place very quickly and separation occurred when agitation was stopped. As a result of the coalescence between the big multiple drops, the separated emulsions can not be recreated by simply hand-shaking the sample bottle. This shows the difference between the RII region of the SPU_p-W system and that of the PU_p ionomer-W system. In the RII region of the PU_p ionomer-W dispersions, all multiple drops in the emulsions are stable and separated emulsions can be recreated with little energy input. The transitions of the emulsion characteristics from RII to RIII region (and vice versa) are also more distinct for the PU_p ionomer-W dispersions, comparing to the SPU_p-W system.

6.9.3 Different HLB number – operating temperature zone

It becomes clear that, HLB number of the non-ionic surfactant alone can not represent the type of emulsion produced for a specific SPU_p-W system. Also, the locations of various regions on the phase inversion map are likely to depend on the thermodynamic condition of the specific non-ionic SPU_p-W mixtures. Therefore, a location map that takes account of both the HLB number and operating temperature

will be useful. Figure 6.61 shows a proposed location map that can be used to identify the thermodynamic condition necessary for the production of a specific type of emulsion. Although the exact locations of various lines (especially that of line 'A' and 'B') have not yet been identified, figure 6.61 shows a map that can potentially be used to identify various regions of the phase inversion map for non-ionic SPU_p-W systems.

The two solid lines (Line 'A' and 'B') of figure 6.61 are analogous to lines 'A' and 'B' of figure 6.58. Above line 'A', a RI region will exist; between line 'A' and 'B', a RII region will exist; and below line 'B', a RIII region will exist. The broken lines, 'C' and 'D', which lie between line 'A' and 'B' help to locate what type of multiple drop emulsion can be produced. Below line 'C' (but above line 'B'), the multiple drops emulsion will consist of mainly large $W_1/P_1/W_C$ drops. As a result, coalescence between the drops will take place very quickly. Between line 'C' and 'D', multiple drops with a mixture of sizes can be found. The large multiple drops will coalesce and settle, leaving the small multiple drops suspended in the water. Above line 'D' (but below line 'A'), small multiple drops are produced. The resultant emulsion is very stable and any separated emulsion can be reproduced with little energy input. Emulsion produced from EX511/9 lies within this zone. Figure 6.62 is the SEM image of this emulsion containing about 50 wt.-% of water. The measured Sauter mean diameter of the emulsion is between 11.04 to 11.75 μm (analysed using the Malvern Mastersizer).

6.9.4 Anionic surfactant

Table 6.12 summarises the experimental results of works involving the use of anionic surfactants, specifically Lauric acid and Stearic acid (EX511/10 to EX511/12). From table 6.12, it is noticeable that only stable coarse emulsions (Type 4 emulsions), which contain stable $W_1/P_1/W_C$ drops, have been successfully produced in all experiments. This finding is surprising in that:

1. The neutralised anionic surfactants would possess high HLB numbers (Larger than 17, which is the HLB number of their non-neutralised counterpart). It is surprising that the anionic SPU_p-W dispersions can not generate a stable small drop emulsion under this condition. This result seems to suggest that some stearic

Table 6.12. Summaries of experimental results of work involving anionic surfactants,

Experiment code	EX511/10	EX511/11	EX511/12
Anionic surfactant	Lauric acid	Lauric acid	Stearic acid
Concentration (mmole -COOH/g of blend)	0.559	1.116	0.553
DN	98.1 %	98.2 %	99.0%
Phase inversion route	$W_1/P_C \rightarrow$ $W_1/P_1/W_C$	$W_1/P_C \rightarrow$ $W_1/P_1/W_C$	$W_1/P_C \rightarrow$ $W_1/P_1/W_C$
Water content at the phase inversion point	19.09 (\pm 2.21) wt.-%	21.05 (\pm 4.13) wt.-%	36.17 (\pm 1.35) wt.-%
Dispersion behaviour	Type 4 emulsion	Type 4 emulsion	Type 4 emulsion
Drop structure and size of P_1 drops *	$W_1/P_1/W_C$ drops ($d_{32} = 9.34 \mu\text{m}$).	$W_1/P_1/W_C$ drops ($d_{32} = 1.34 \mu\text{m}$).	$W_1/P_1/W_C$ drops ($d_{32} = 24.43 \mu\text{m}$).
Equivalent regions [†]	RII	RII	RII

stabilisation (normally provided by water-soluble component of non-ionic surfactant) is necessary for the production of stable SPU_p-W dispersions.

- When the concentrations of the free acid groups are double the amount contained in PUP2-7.5, no simple drop emulsion can be produced. Also, this increase in concentration does not change the type of emulsion produced or the catastrophic phase inversion point; increase in the surfactant concentration only seems to change the size of the drops produced. (Comparing EX511/10 with EX511/11).
- Traditionally, it was believed that multiple drops exist due to the presence of a mixture of molecules in the commercial surfactant or through the usage of a mixture of surfactants (Florence and Whitehill (1982)). Due to the presence of a mixture of surfactant molecules, the hydrophilic molecules and lipophilic molecules will stabilise the external P_1 - W_C and internal W_1 - P_1 interfaces of the multiple $W_1/P_1/W_C$ drops respectively (and vice versa for polymer-continuous emulsions). However, this work shows that this is not necessary the case. This is

* The Sauter mean diameters of these emulsions are determined using the Malvern Mastersizer. The emulsion samples contain about 50 wt.-% of water before being diluted using distilled water.

† Regions equivalent to the PUP ionomer-W system and the non-ionic SPU_p-W system obtained by changing HLB number.

because both anionic surfactants used contained only one type of molecule and surfactant molecules would not partition between different surfaces. However, it is unclear what causes the formation of multiple drops in these cases.

Conclusions

All three dispersion regions that exist during the production of internally stabilised PUp-W dispersions have been produced successfully using non-ionic surfactants to stabilise the PUp-W dispersions. This can be done by using non-ionic surfactants with different HLB numbers at a fixed operating temperature. A similar phase inversion “map”, which contains all three dispersion regions, is proposed and plotted using HLB number as its ordinate and water content as its abscissa. Line ‘A’ of this map is the “true” transitional phase inversion line that is observed in other surfactant-oil-water dispersions. This line corresponds to a condition when SAD is equal to 0. The RI region represents a condition when SAD is smaller than 0; the RII and RIII regions represent conditions when SAD is larger than 0. Despite the similarities of the different dispersion regions, it is shown that the catastrophic phase inversion mechanism during the production of externally stabilised PUp-W dispersions is different from that of internally stabilised PUp-W dispersions.

It is confirmed in this work that HLB number is not a characteristic property of an emulsion. Operating temperatures are found to have a significant effect on the characteristics of the non-ionic SPUp-W dispersions. At low temperature, the non-ionic SPUp-W mixtures favour the formation of water-continuous emulsions; at high temperature, the mixtures favour the formation of polymer-continuous emulsions. This is because the hydration force between hydrophilic moiety of the non-ionic surfactant and water is stronger at low temperature. As a result of this observation, a location map that takes account of both the HLB number and operating temperature is introduced. This map allows easy identification of the various regions that exist in the phase inversion map of a non-ionic SPUp-W system.

It is also shown that anionic surfactants alone (specifically Lauric acid and Stearic acid) cannot be used to create stable SPUp-W emulsions containing small P_1/W_C drops. It is therefore believed that some stearic stabilisation is needed to create any stable SPUp-W dispersions. Lastly, this work reveals that multiple emulsions do not necessarily have to be created using more than one type of surfactant.

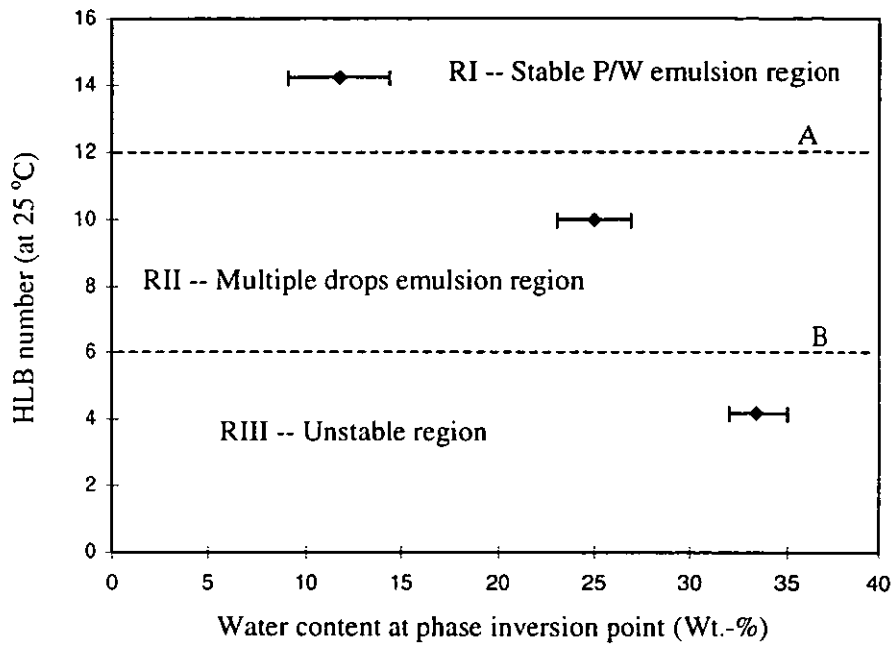


Figure 6.58. Phase inversion map for a non-ionic SPU_p-W system at 30 °C

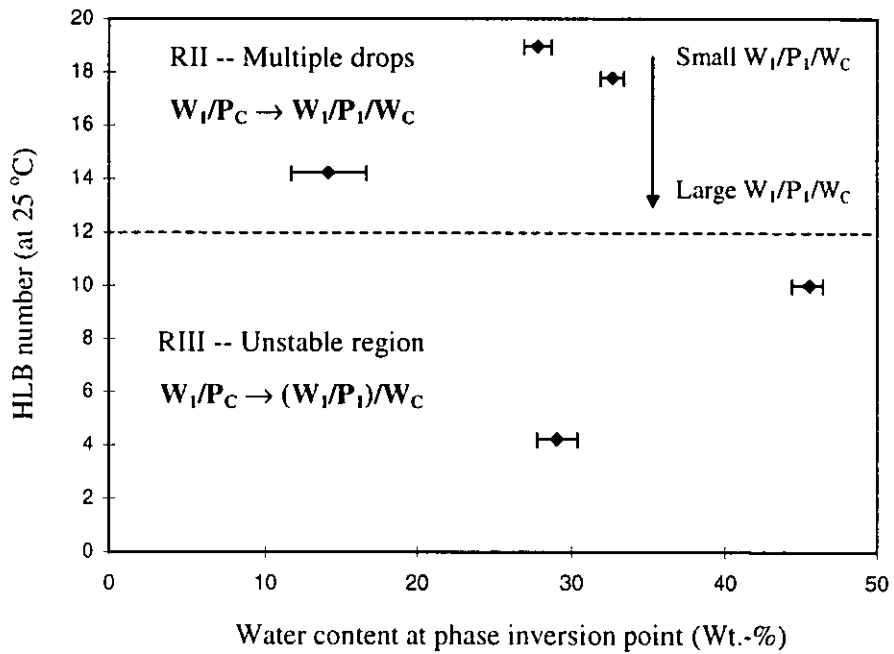
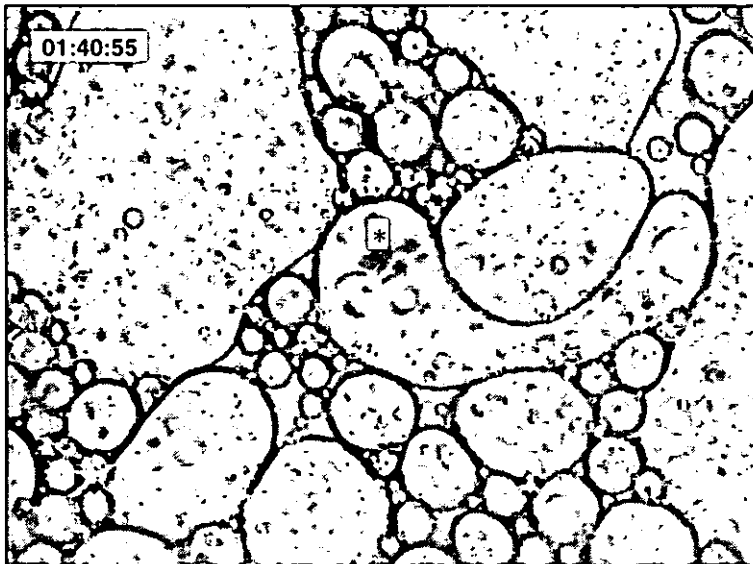
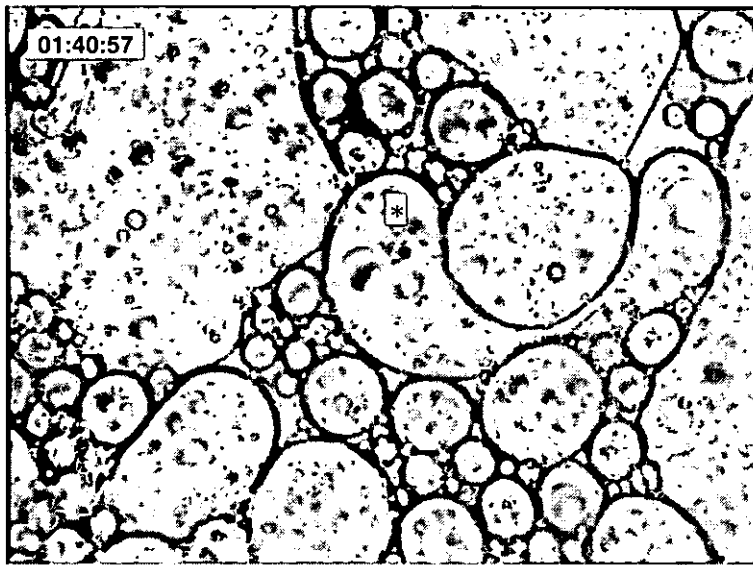


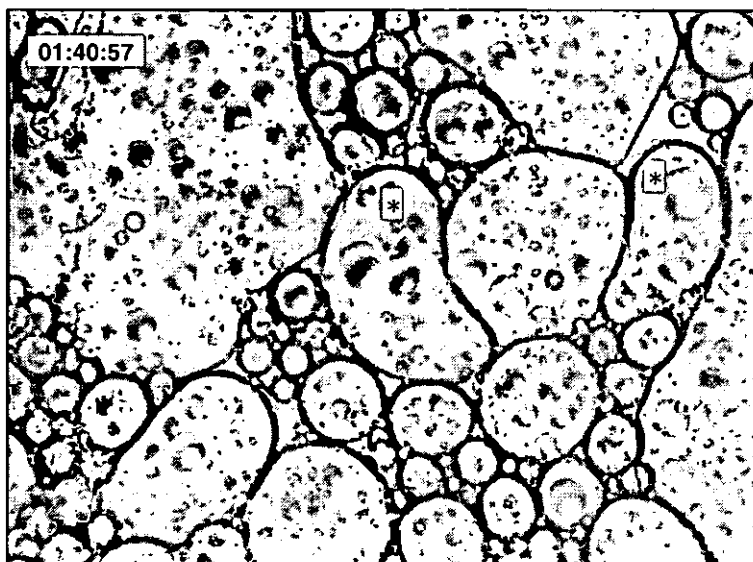
Figure 6.60. Phase inversion map for a non-ionic SPU_p-W system at 60 °C



(a) Before stretching



(b) Drop start stretching



(c) Break-up completed

Figure 6.59. Cinematography of events leading to the formation of smaller multiple drops in the RII region of the SPU_p-W system (* is the multiple drop of concern)

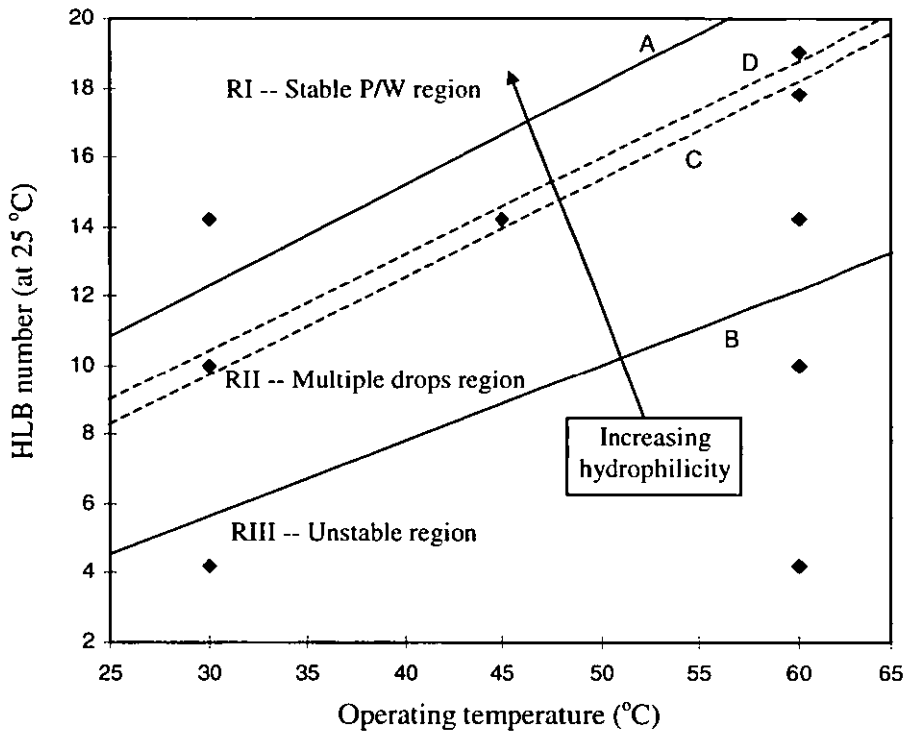


Figure 6.61. Different types of emulsions produced at different HLB number – operating temperature zones

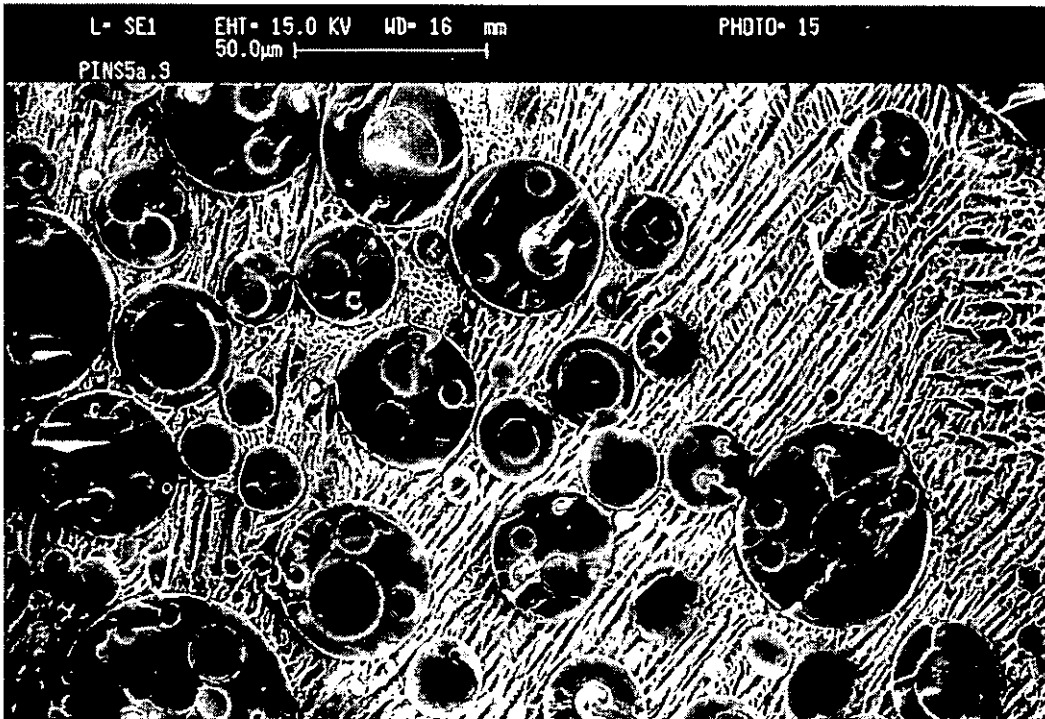


Figure 6.62. SEM image of emulsion produced from EX511/9

CHAPTER 7

General conclusions

Various aspects of phase inversion in the production of PUp-W dispersions have been studied in this thesis. Suitable drop size characterisation techniques have been developed to analyse droplet data of PUp-W dispersions produced in this work. Valid phase inversion detection methods, based on the combined usage of torque and conductivity measurements, have also been developed for the detection of phase inversion points during the production of PUp-W dispersions. Some conclusions have been drawn in each of the nine sections mentioned in chapter 6. The principal conclusions drawn from this research are as follows:

- During the production of PUp-W dispersions, three different dispersion regions have been identified by changing the ionic group content of the PUp-W mixtures. There are:

Region I: PUp contains more than ~ 0.2 mmole/g of ionic groups. Stable emulsions consisting of small simple polymer drops are produced in this region.

Region II: PUp contains between ~ 0.05 to 0.2 mmole/g of ionic groups. Stable coarse emulsions consisting of a mixture of simple and multiple drops are produced in this region.

Region III: PUp contains less than ~ 0.05 mmole/g of ionic groups. Only temporary emulsions can be produced in this region. Emulsions separated as soon as agitation has stopped.

- A modified phase inversion map, plotted using water content as the abscissa and ionic group content as the ordinate, can be used to describe the existence of all three dispersions regions.
- There are rheological changes during the catastrophic phase inversion process in the production of a PUp-W dispersion. At low dispersed phase content, the PUp-W mixture behaves as a Newtonian fluid. The PUp-W mixture becomes a power-law pseudo-plastic fluid as the dispersed phase content increases. The pseudo-plastic behaviour is most significant in the vicinity of the phase inversion point. After phase inversion has occurred, pseudo-plastic behaviour of the PUp-W dispersion diminishes until the inverted emulsion was diluted enough to behave as a Newtonian fluid again.
- Different transitional phase inversion processes, RIITI process and RIITI process, can be utilised for the production of PUp-W dispersions. Inversion of the RIITI process might take place at a condition when $SAD = 0$. During the RIITI process, less ionic groups are needed to induce the transitional phase inversion as initial water content increases. Also, it is more effective to induce the transitional phase inversion of the RIITI process by adding counterions instead of highly neutralised PUp ionomers.
- Drop size of emulsions produced through the RIITI process is controlled by the dual effects of ionic centres and the “effectiveness” of ionic groups. The latter is negligible at equilibrium.
- There are only two inversions during a RIITI process. The first polymer-to-water continuous inversion is a mass-transfer-controlled process and the second water-to-polymer continuous inversion is a reaction-controlled process.
- A modified catastrophic phase inversion mechanism has been proposed to describe the occurrence of all three dispersion regions, particularly that of RII region. Key features of this mechanism include: (1) Uneven distributions of ionic centres in the RII mixtures lead to the formation of isolated W_1 drops in the inverted multiple $W_1/P_1/W_C$ emulsions. (2) Apparent ionic-centre-rich environment provides additional stability to the small P_1/W_C drops that are produced at the phase inversion point. Therefore, these small P_1/W_C drops can only be obtained at, or near to, the catastrophic phase inversion point. (3) The

formation of pseudo-drops, at the phase inversion point, is a kinetically driven event. These pseudo-drops lead to the formation of stable multiple drops when the aqueous RII emulsions are being diluted.

- In the phase inversion map, the transitional phase inversion loci of the RIITI process are mainly governed by the concentration of ionic groups. On the other hand, the catastrophic phase inversion loci of the PWCPI process are mainly governed by the hydration ability of the ionic groups.
- Drop size of emulsion is influenced by the hydration ability of the ionic groups. Increased hydration ability of the ionic group leads to higher Zeta potential at the particle surface and hence smaller PUp drops. This is because PUp drops are stabilised by the phenomenon of diffuse double layer. The increasing ionic group content is also responsible for the decreasing drop size and increasing interfacial area of emulsions produced in both RI and RII regions.
- The effect of free carboxylic acids is suppressed by that of ionised groups in the RI region. However, free carboxylic acids can increase the hydrophobicity of RII mixtures and delay the catastrophic phase inversion to higher water content in the RII region.
- Blends (of PUp with high DMPA content with PUp without any DMPA) are shown to be macroscopically similar to, but microscopically different from, PUp containing equivalent amount of DMPA.
- The higher the viscosity of an organic PUp ionomer, the easier it is to become the disperse phase.
- The diameter of a flat-bladed turbine and the width of baffle have little effect on both catastrophic and transitional phase inversion loci, and drop size of emulsions produced from the RIITI process.
- All three dispersion regions have also been produced using different non-ionic surfactants as the external stabilisers. Both HLB number and operating temperature are incorporated into a location map to help identify the thermodynamic conditions suitable for the production of these dispersions. Stearic stabilisation is needed for the production of stable SPUp-W dispersions.

CHAPTER 8

Future work

The present research has increased understanding about the role of phase inversion processes during the production of PUp-W dispersions. The following suggestions for future work may provide more insights into the development of new routes to produce high performance, and stable, polymer colloids and extend the usage of the phase inversion processes.

1. The effect of other process variables and polymer types:

This thesis has, and could, only studied some of the vast number of variables that affect the properties and phase inversion characteristics during the production of polymer latices. It is believed that the techniques developed in this work, particularly the plotting of the phase inversion maps, can be extended to study other variables mentioned in table 2.3. It is also vital to extend knowledge developed from this work to the production of other types of polymer latices. Some polymer latices may be produced through similar routes to those for aqueous PU colloids. These include some hydrophilically-modified water-insoluble polymers (e.g., epoxy resin, polyacrylate and polyester) and possibly some copolymers (e.g., poly(styrene-*co*-maleic acid) and poly(ethylene-*co*-acrylic acid)).

2. The effect of chain extension:

Most, if not all, previous researches have neglected the importance of the dispersion stage. This leads to the belief that the minimum ionic group content required for the production of stable aqueous PU colloids is about 0.2 mmole/g. By using short chain pre-polymers to study the phase inversion process independently,

this work has revealed that stable colloids containing small polymer drops may be produced using less ionic group content (i.e., in the RII region, with about 0.05 ~ 0.2 mmole/g of ionic groups). It may also be possible to produce emulsions containing up to 75 wt.-% of solids (i.e., at the catastrophic phase inversion loci of the PWCPI process, as shown in the phase inversion map). However, in order to produce industrially and commercially favourable products, it is vital to understand how the chain-extension process affects the phase inversion characteristics (and the stability) of the (pre-)polymer-W dispersions in both the RI and RII regions of the phase inversion map.

3. WPCPI process:

Typical phase inversion maps for nSOW systems (as shown in figure 2.8) include catastrophic phase inversion loci from two directions, i.e., oil-continuous to water-continuous inversion and water-continuous to oil-continuous inversion. This work focussed on the production of aqueous PUp dispersions and hence only the PWCPI process has been studied. As a result, only the catastrophic phase inversion loci of the PWCPI process are included in the modified phase inversion map proposed in this thesis. Preliminary study of the WPCPI process (described in Brooks and Saw (2000)) reveals some interesting findings to be followed up in future researches. These include:

- Water content at the catastrophic phase inversion points of the WPCPI process seems to decrease as polymer addition rate increases.
- At high polymer addition rate, the catastrophic phase inversion loci of the WPCPI process do not necessary “overlap” with the catastrophic phase inversion loci of the PWCPI process. The term “not overlap” means that the catastrophic phase inversion of the WPCPI process may take place at higher water content than that of PWCPI process.
- The WPCPI process seems to follow the same inversion mechanism as the PWCPI process, albeit in a reverse direction. During a RII WPCPI process, small P_1/W_C drops and pseudo-drops are produced just before the phase inversion and disappear after the phase inversion has taken place.

4. Direct dispersion process:

By using a dispersion vessel similar to that in this work, Phongikaroon and Calabrese (1999) showed that fully TEA-neutralised PUp2-7.5 (containing about 0.559 mmole/g of ionic groups) can be dispersed directly into water. This result agrees with the findings in this work in that RI mixture favours the production of stable PUp-in-Water dispersions. However, direct dispersion of a RII mixture will result in unstable emulsions containing large multiple drops. Brooks and Saw (2000) described an interesting production route involving the use of a direct dispersion process to produce stable emulsions of RII mixture. The production route of concern involved dispersing PUp with moderate ionic group content directly into water until the water-continuous emulsion is close to its catastrophic phase inversion point. Before any phase inversion takes place, water was added to dilute the water-continuous emulsion again. Upon dilution, the final water-continuous emulsion product was found to be stable for more than half a year. This result is attributed to the formation of small W_1/P_C drops and pseudo-drops in the vicinity of the catastrophic phase inversion point of the WPCPI process, which allows ionic groups to be redistributed effectively. Further researches can be conducted to follow up this preliminary study.

5. Producing multiple emulsions using a one-step process:

The advantage of a two-step emulsification process is that it enables the production of stable and reproducible multiple emulsions (Matsumoto et al. (1976)). However, a two-step process always has the disadvantage of additional process requirements when compared to a one-step process. As mentioned in sub-section 2.10.2, multiple emulsions can be produced during a catastrophic phase inversion process, albeit the products can not be controlled easily. A probable one-step emulsification process that may lead to the production of stable and reproducible multiple emulsions is proposed here. This suggestion is based on the PWCPI mechanism of RII PUp-W dispersions presented in this work. Consider a case when two different aqueous phases, W' and W'' , are to be included into a multiple $W'_1/P_1/W''_C$ emulsion. The first W' phase may initially be dispersed into a polymer phase directly until the W'_1/P_C emulsion is close to or at the catastrophic phase

inversion point of the PWCPI process. The second W'' phase may then be added to induce the catastrophic phase inversion or to dilute the inverted emulsion respectively. Provided that the catastrophic phase inversion process follows the same PWCPI mechanism of the RII PUp-W dispersions, most W' will be trapped inside the multiple drops and most W'' will become the continuous phase. However, in order for this process to become viable, more researches in this area are needed. These include estimating the amount of internal drops that are entrapped in the emulsions and understanding how the internal drops may “escape” during the emulsification process.

6. The use of external surfactants:

Only a little work involving the use of external surfactants has been included in this thesis. More researches can be carried out to produce phase inversion maps and location maps, for various external surfactant-polymer-W systems, similar to those presented in section 6.9. More profound comparisons between internal functional groups and external functional groups can subsequently be carried out.

Bibliography

Akay, G. (1998) “**Flow-induced phase inversion in the intensive processing of concentrated emulsions**”, *Chemical Engineering Science*, **53**(2), 203-223.

Alberty, R.A. (1987) *Physical Chemistry*, Singapore: John Wiley and Sons, 7th edition.

Alberty, R.A. and Silbey, R.J. (1995) *Physical Chemistry*, New York: John Wiley and Sons, 2nd edition.

Allemann, E., Gurny, R. and Doelker, E. (1992) “**Preparation of aqueous polymeric nanodispersions by a reversible salting-out process: influence of process parameters on particle size**”, *International Journal of Pharmaceutics*, **87**(1-3), 247-253.

Annable, T. (1999) *SRF Project 269 – Internal Communication*.

Arashmid, M. and Jeffrey, G.V. (1980) “**Analysis of the phase inversion characteristics of liquid-liquid dispersions**”, *AIChE Journal*, **26**(1), 51-55.

Arnoldus, R. (1990) “**Water-based urethane dispersions**”, in *Surface Coatings*, London: Wilson Elsevier.

Ash, M. and Ash, I. (1989) *The Condensed Encyclopaedia of Surfactants*, Bristol: Edward Arnold.

Berkman, P.P. and Calabrese, R.V. (1988) “**Dispersion of viscous liquids by turbulent flow in a static mixer**”, *AIChE Journal*, **34**(4), 602-609.

Billmeyer, F.W. (1984) *Textbook of Polymer Science*, Singapore: John Wiley and sons, 3rd edition.

Brookfield Engineering Laboratories (1971) *Brookfield Synchro-Lectric viscometer instruction manual*, Massachusetts: Manufacturer instruction booklet.

Brookfield Engineering Laboratories, *Solution to Sticky Problems*, Massachusetts: Manufacturer instruction booklet.

Brooks, B.W. (1996) “**New technology for manufacture of aqueous polymer colloids**”, *Case for Support Part 2: Description of the Proposed Research*.

Brooks, B.W. and Richmond, H.N. (1991) **“Dynamics of liquid-liquid phase inversion using non-ionic surfactants”**, *Colloid and Surface*, **58**, 131-148.

Brooks, B.W. and Richmond, H.N. (1994a) **“The application of a mixed nonionic surfactant theory to transitional emulsion phase inversion: 1. Derivation of a mixed surfactant partitioning model”**, *Journal of Colloid and Interface Science*, **162**(1), 59-66.

Brooks, B.W. and Richmond, H.N. (1994b) **“The application of a mixed nonionic surfactant theory to transitional emulsion phase inversion: 2. The relationship between surfactant partitioning and transitional inversion – A thermodynamic treatment”**, *Journal of Colloid and Interface Science*, **162**(1), 67-74.

Brooks, B.W. and Richmond, H.N. (1994c) **“Phase inversion in non-ionic surfactant-oil-water systems: I. The effect of transitional inversion on emulsion drop sizes”**, *Chemical Engineering Science*, **49**(7), 1053-1064.

Brooks, B.W. and Richmond, H.N. (1994d) **“Phase inversion in non-ionic surfactant-oil-water systems: II. Drop size studies in catastrophic inversion with turbulent mixing”**, *Chemical Engineering Science*, **49**(7), 1065-1075.

Brooks, B.W. and Richmond, H.N. (1994e) **“Phase inversion in non-ionic surfactant-oil-water systems: III. The effect of oil-phase viscosity on catastrophic inversion and the relationship between the drop size present before and after catastrophic inversion”**, *Chemical Engineering Science*, **49**(11), 1843-1853.

Brooks, B.W. and Saw, L.K. (1999) **“Catastrophic phase inversion of an ionically modified polyurethane ionomer prepolymer (PUIp)-water (PUIp/W) system”**, *Abstract for the 6th Meeting of the UK Polymer Colloids Forum*.

Brooks, B.W. and Saw, L.K. (2000) **“Novel technology for the manufacture of aqueous polymer colloids”**, *SRF Project 269 – Progress Report*.

Calabrese, R.V., Chang, T.P.K. and Dang, P.T. (1986a) **“Drop breakup in turbulent stirred-tank contactors: Part I: Effect of dispersed-phase viscosity”**, *AIChE Journal*, **32**(4), 657-666.

Calabrese, R.V., Wang, C.Y. and Bryner, N.P. (1986b) **“Drop breakup in turbulent stirred-tank contactors: Part III: Correlations for mean size and drop size distribution”**, *AIChE Journal*, **32**(4), 677-681.

Chen, H.T. and Middleman, S. (1967) **“Drop size distribution in agitated liquid-liquid systems”**, *AIChE Journal*, **13**(5), 989-995.

Chen, S.A. and Chan, W.C. (1990) **“Polyurethane cationomers. 2. Phase inversion and its effect on physical properties”**, *Journal of Polymer Science: Part A- Polymer Physics*, **28**(9), 1515-1532.

Chen, Y. and Chen, Y.L. (1992) **“Aqueous dispersions of polyurethane anionomers: Effects of countercation”**, *Journal of Applied Polymer Science*, **46**, 435-443.

Church, J.M. and Shinnar, R. (1961) **“Stabilizing liquid-liquid dispersions by agitation”**, *Industrial and Engineering Chemistry*, **53**(6), 479-484.

Coulson, J.M., Richardson, J.F., Backhurst, J.R. and Harker, J.H. (1993) *Coulson and Richardson' Chemical Engineering Volume 2: Particle Technology and Separation Processes*, Oxford: Pergamon Press Ltd., 4th edition.

Davies, J.T. (1985) **“Drop sizes of emulsions related to turbulent energy dissipation rates”**, *Chemical Engineering Science*, **40**(5), 839-842.

Davies, J.T. (1987) **“A physical interpretation of drop sizes in homogenizers and agitated tanks, including the dispersion of viscous oils”**, *Chemical Engineering Science*, **42**(7), 1671-1676.

Davis, S.S. and Burbage, A.S. (1977) **“Electron micrography of water-in-oil-in-water emulsions”**, *Journal of Colloid and Interface Science*, **62**(2), 361-363.

Dickinson, E. (1981) **“Interpretation of emulsion phase inversion as a cusp catastrophe”**, *Journal of Colloid and Interface Science*, **84**(1), 284-287.

Dieterich D. (1981) **“Aqueous emulsions, dispersions and solutions of polyurethanes; sythesis and properties”**, *Progress in Organic Coatings*, **9**(3), 281-340.

Dieterich, D., Keberle, W. and Witt, H. (1970) **“Polyurethane ionomers, a new class of block polymers”**, *Angew. Chem. Internat. Edit.*, **9**(1), 40-50.

Ellis, B. (1992) *Chemistry and Technology of Epoxy Resins*, London: Blackie Academic and Professional.

Fitch, R.M. (1997) *Polymer Colloids: A Comprehensive Introduction*, London: Academic Press.

Florence, A.T. and Whitehill, D. (1981) **“Some features of breakdown in water-in-oil-in-water multiple emulsions”**, *Journal of Colloid and Interface Science*, **79**(1), 243-256.

Florence, A.T. and Whitehill, D. (1982) **“The formulation and stability of multiple emulsions”**, *International Journal of Pharmaceutics*, **11**(4), 277-308.

Gao, Z.S., Varshney, S.K., Wong, S. and Eisenberg, A. (1994) **“Block copolymer “crew-cut” micelles in water”**, *Macromolecules*, **27**(26), 7923-7927.

Gilchrist, A., Dyster, K.N., Moore, I.P.T., Nienow, A.W. and Carpenter, K.J. (1989) **“Delayed phase inversion in stirred liquid-liquid dispersions”**, *Chemical Engineering Science*, **44**(10), 2381-2384.

Goodwin, J.W., Hearn, J., Ho, C.C. and Ottewill, R.H., (1973) **“The preparation and characterisation of polymer latices formed in the absence of surface active agents”**, *British Polymer Journal*, **5**, 347-362.

Groeneweg, F., Agterof, W.G.M., Jaeger, P., Janssen, J.J.M., Wieringa, J.A. and Klahn, J. (1998) **“On the mechanism of the inversion of emulsions”**, *Trans. IChemE*, **26**(Part A), 55-63.

Gu, Y.X., Huang, Y.H., Liao, B., Cong G.M. and Xu, M. (2000) **“Studies on the characterization of phase inversion during emulsification process and the particle sizes of water-borne microemulsion of poly(phenylene oxide) ionomer”**, *Journal of Applied Polymer Science*, **76**, 690-694.

Hinze, J.O. (1955) **“Fundamentals of the hydrodynamic mechanism of splitting in dispersion processes”**, *AIChE Journal*, **1**(3), 289-295.

Hourston, D.J., Williams, G., Satguru, R., Padget, J.C., and Pears, D. (1997) **“Structure-property study of polyurethane anionomers base on various polyols and diisocyanates”**, *Journal of Applied Polymer Science*, **66**, 2035-2042.

Hourston, D.J., Williams, G., Satguru, R., Padget, J.C., and Pears, D. (1998) **“A structure-property study of IPDI-based polyurethane anionomers”**, *Journal of Applied Polymer Science*, **67**, 1437-1448.

Hunter, R.J. (1985) *Zeta Potential in Colloid Science: Principles and Applications*, London: Academic Press.

Kay, D.H. (1965) *Techniques for Electron Microscopy*, Oxford: Blackwell Scientific Publications.

Kim T.K. and Kim, B.K. (1991b) **“Preparation and properties of polyurethane aqueous dispersion from uncatalyzed system of H₁₂MDI, PTAd/bisphenol A polyol, and DMPA”**, *Colloid and Polymer Science*, **269**, 889-894.

Kim, B.K. and Kim, T.K. (1991c) **“Aqueous dispersion of polyurethane from H₁₂MDI, PTAd/PPG, and DMPA: Particle size of dispersion and physical properties of emulsion cast film”**, *Journal of Applied Polymer Science*, **43**, 393-398.

Kim, B.K. and Lee, J.C. (1996) **“Polyurethane ionomer dispersions from poly(neopentylene phthalate) glycol and isophorone diisocyanate”**, *Polymer*, **37**(3), 469-475.

Kim, B.K., Lee, J.C. and Lee, K.H. (1994) **“Polyurethane anionomer dispersion from ether-type polyols and isophorone diisocyanate”**, *Journal of Macromolecular Science – Pure and Applied Chemistry*, **A31**(9), 1241-1257.

Kim, C.K. and Kim, B.K. (1991a) **“IPDI-based polyurethane ionomer dispersions: Effects of ionic, noionic hydrophilic segments, and extender on particle size and physical properties of emulsion cast film”**, *Journal of Applied Polymer Science*, **43**, 2295-2301.

Kim, C.K., Kim, B.K. and Jeong, H.M. (1991) **“Aqueous dispersion of polyurethane ionomers from hexamethylene diisocyanate and trimellitic anhydride”**, *Colloid and Polymer Science*, **269**, 895-900.

Kotera, N. and Takahashi, K. (1990) **“Studies of aqueous resins. I – Water-dispersed polyesters containing polar groups”**, *Bulletin of the chemical society of Japan*, **63**(8), 2288-2291.

Kumar, S. Kumar, R. and Gandhi, K.S. (1991) **“Influence of the wetting characteristics of the impeller on phase inversion”**, *Chemical Engineering Science*, **46**(9), 2365-2367.

- Lee, D.Y. and Kim, J.H. (1997) **“Emulsion polymerisation using alkali-soluble random copolymer as a polymeric emulsifier”**, *Polymer Preprints - Division of Polymer Chemistry*, **38**(2), 418-419.
- Lee, J.C. and Kim, B.K. (1994) **“Basic structure - Property behaviour of polyurethane cationomers”**, *Journal of Polymer Science: Part A - Polymer Chemistry*, **32**, 1983-1989.
- Lee, J.S. and Kim, B.K. (1995) **“Poly(urethane) cationomers from poly(propylene)glycol and isophorone diisocyanate: Emulsion characteristics and tensile properties of cast films”**, *Progress in Organic Coatings*, **25**, 311-318.
- Lee, L.T. and Yang, C.D. (1992) **“Synthesis and properties of cationic resins derived from polyether/polyester-modified Epoxy resins”**, *Journal of Applied Polymer Science*, **46**, 991-1000.
- Lee, S.Y., Lee, J.S. and Kim, B.K. (1997) **“Preparation and properties of water-borne polyurethanes”**, *Polymer International*, **42**, 67-76.
- Lewis, G.N. and Randall, M. (1961) *Thermodynamics*, Singapore: McGraw-Hill Inc., 2nd edition.
- Li, M., Jiang, M., Zhu, L. and Wu, C. (1997) **“Novel surfactant-free stable colloidal nanoparticles made of randomly carboxylated polystyrene ionomers”**, *Macromolecules*, **30**(7), 2201-2203.
- Li, M., Liu, L. and Jiang, M. (1995) **“Fluorospectroscopy monitoring aggregation of block ionomers in aqueous media”**, *Macromolecular Rapid Communication*, **16**(11), 831-836.
- Malvern instruments, *Sample Dispersion and Refractive Index Guide*, Worcestershire: Manufacturer instruction booklet.
- Matsumoto, S., Kita, Y. and Yonezawa, D. (1976) **“An attempt at preparing water-in-oil-in-water multiple-phase emulsions”**, *Journal of Colloid and Interface Science*, **57**(2), 353-361.
- McCabe, W.L., Smith, J.C. and Harriott, P. (1993) *Unit Operations of Chemical Engineering*, Singapore: McGraw-Hill Inc., 5th edition.
- Myers, D. (1988) *Surfactant Science and Technology*, USA: VCH Publishers, 1st edition.

- Norato, M.A., Tsouris, C. and Tavlarides, L.L. (1998) **“Phase inversion studies in liquid-liquid dispersions”**, *The Canadian Journal of Chemical Engineering*, **76**, 486-494.
- Oertel, G. (1994) *Polyurethane Handbook*, New York: Hanser Publishers, 2nd edition.
- Orr, D. (1983) **“Emulsion droplet size data”**, in Becher, P. (Ed.), *Encyclopedia of Emulsion Technology: Volume 1 – Basic Theory*, New York: Marcel Dekker.
- Pacek, A.W., Man, C.C. and Nienow, A.W. (1998) **“On the Sauter mean diameter and size distribution in turbulent liquid/liquid dispersions in a stirred vessel”**, *Chemical Engineering Science*, **53**(11), 2005-2011.
- Pacek, A.W., Nienow, A.W. and Moore, I.P.T. (1994a) **“On the structure of turbulent liquid-liquid dispersed flows in an agitated vessel”**, *Chemical Engineering Science*, **49**(20), 3485-3498.
- Pacek, A.W., Nienow, A.W., Moore, I.P.T. and Calabrese, R.V. (1994b) **“Video technique for measuring dynamics of liquid-liquid dispersion during phase inversion”**, *AIChE Journal*, **40**(12), 1940-1949.
- Padget, J.C. (1994) **“Polymers for water-based coatings - A systematic overview”**, *Journal of Coatings Technology*, **66**(839), 84-105.
- Paine, A.I. (1993) **“Error estimates in the sampling from particle size distributions”**, *Particle and Particle System Characterization*, **10**, 23-32.
- Perry, R.H. and Green, D. (1984) *Perry's Chemical Engineers' Handbook*, Malaysia: McGraw-Hill International Edition, 6th edition.
- Phongikaroon, S. and Calabrese, R.V. (1998) **“Defining bin size for discrete characterization of particle size distribution”**, *SRF Project 269 – Progress Report*.
- Phongikaroon, S. and Calabrese, R.V. (1999) **“Direct dispersion of urethane prepolymers”**, *SRF Project 269 – Progress Report*.
- Phongikaroon, S. and Calabrese, R.V. (2000) **“Interfacial tension measurement via pendant drop method: Part II”**, *SRF Project 269 – Progress Report*.
- Pinfield, R.K. (1996) *Aqueous Dispersion of Polyurethane Polymers*, PhD Thesis in Manchester University.

- Poston, T. and Stewart, I. (1978) *Catastrophe Theory and Its Applications*, London: Pitman publishers.
- Puig, J.E., Corona-Galvan, S. and Kaler, E.W. (1990) “**Microemulsion copolymerisation of styrene and acrylic acid**”, *Journal Colloid and Interface Science*, **137**(1), 308-310.
- Rosthauser, J.W. and Nachtkamp, K. (1986) “**Waterborne polyurethanes**”, *Journal of Coated Fabrics*, **16**, 39-79.
- Rumpf, H. (Translated by Bull, F.A. and Nat, R.). (1990) *Particle Technology*, London: Chapman and Hall.
- Sakiadis, B.C. (1984) “**Fluid and particle mechanics**”, in Perry, R.H. and Green, D. (Ed.), *Perry's Chemical Engineers' Handbook*, Malaysia: McGraw-Hill International Edition, 6th edition.
- Salager, J.L. (1985) “**Phase behavior of amphiphile-oil-water systems related to the butterfly catastrophe**”, *Journal of Colloid and Interface Science*, **105**(1), 21-26.
- Salager, J.L. (1988) “**Phase transformation and emulsion inversion on the basis of catastrophe theory**”, in Becher, P. (Ed.), *Encyclopedia of Emulsion technology: Volume 3 – Basic Theory · Measurement · Applications*, New York: Marcel Dekker.
- Satguru, R., McMahon, J., Padget, J.C. and Coogan, R.G. (1994) “**Aqueous polyurethanes - Polymer colloids with unusual colloidal, morphological, and application characteristics**”, *Journal of Coatings Technology*, **66**(830), 47-55.
- Schlarb, B., Gyopar Rau, M. and Haremze, S. (1995a) “**Hydroresin dispersions: new emulsifier free binders for aqueous coatings**”, *Progress in Organic Coatings*, **26**, 207-215.
- Schlarb, B., Haremze, S., Heckmann, W., Morrison, B., Muller-Mall, R. and Gyopar Rau, M. (1995b) “**Hydroresin dispersions: Tailoring morphology of latex particles and films**”, *Progress in Organic Coatings*, **29**, 201-208.
- Selker, A.H. and Sleicher, C.A. Jr. (1965) “**Factors affecting which phase will disperse when immiscible liquids are stirred together**”, *The Canadian Journal of Chemical Engineering*, **43**, 298-305.

Shaw, D.J. (1992) *Colloid and Surface Chemistry*, Oxford: Butterworth-Heinemann Ltd., 4th edition.

Shinnar, R. (1961) "On the behaviour of liquid dispersions in mixing vessels", *Journal of Fluid Mechanics*, **10**, 259-275.

Shinnar, R. and Church, J.M. (1960) "Predicting particle size in agitated dispersions", *Industrial and Engineering Chemistry*, **52**(3), 253-256.

Shinoda, K. and Arai, H. (1964) "The correlation between phase inversion temperature in emulsion and cloud point in solution of nonionic emulsifier", *Journal of Physical Chemistry*, **68**(12), 3485-3490.

Shinoda, K. and Friberg, S. (1986) *Emulsion and Solubilization*, Singapore: John Wiley and Sons, 1st edition.

Sinnott, R.K. (1993) *Coulson and Richardson' Chemical Engineering Volume 6: Design*, Oxford: Pergamon Press Ltd., 2nd edition.

Sprow, F.B. (1967a) "Distribution of drop size produced in turbulent liquid-liquid dispersion", *Chemical Engineering Science*, **22**, 435-442.

Sprow, F.B. (1967b) "Drop size distribution in strongly coalescing agitated liquid-liquid systems", *AIChE Journal*, **13**(5), 995-998.

Tharanikkarasu, K. and Kim, B.K. (1997) "Aqueous dispersions of polyurethane ionomers", *Progress in Rubber and Plastics Technology*, **13**(1), 26-55.

Vijayendran, B.R. (1979) "Effect of carboxylic monomers on acid distribution in carboxylated polystyrene latices", *Journal of Applied Polymer Science*, **23**, 893-901.

Wang, C.Y. and Calabrese, R.V. (1986) "Drop breakup in turbulent stirred-tank contactors: Part II: Relative influence of viscosity and interfacial tensions", *AIChE Journal*, **32**(4), 667-676.

Weast, R.C. (1973) *Handbook of Chemistry and Physics*, USA: CRC Press, 54th edition.

Wischnitzer, S. (1981) *Introduction to Electron Microscopy*, Oxford: Pergamon Press Ltd., 3rd edition.

Yang, C.H., Lin, S.M. and Wen, T.C. (1995) **“Application of statistical experimental strategies to the process optimization of waterborne polyurethane”**, *Polymer Engineering and Science*, **35**(8), 722-730.

Yang, Z.Z., Xu, Y.Z., Wang, S.J., Yu, H. and Cai, W.Z. (1997a) **“Preparation of waterborne ultrafine particles of epoxy resin by phase inversion technique”**, *Chinese Journal of Polymer Science*, **15**(1), 92-96.

Yang, Z.Z., Zhao, D.L. Xu, Y.Z., and Xu, M. (1997b) **“Determination of phase inversion point in the emulsification of polymers”**, *Chinese Journal of Polymer Science*, **15**(4), 373-378.

Zeneca (1998) *SRF project 269 – Internal Communication*.

Zeneca Resins, **“Zeneca resin urethanes”**, literature for customers.

Zerfa, M. (1994) *Vinyl Chloride Drop Behaviour in Suspension Polymerisation Reactors*”, PhD Thesis in Loughborough University.

Zerfa, M. And Brooks, B.W. (1996) **“Prediction of vinyl chloride drop sizes in stabilised liquid-liquid agitated dispersions”**, *Chemical Engineering Science*, **51**(12), 3223-3233.

Zerfa, M. Sajjadi, S. and Brooks, B.W. (1999) **“Phase behaviour of non-ionic surfactant-p-xylene-water systems during the phase inversion process”**, *Colloids and Surfaces – A. Physicochemical and Engineering Aspects*, **155**(2), 323-337.

Zerfa, M. Sajjadi, S. and Brooks, B.W. (2000) **“Phase behaviour of polymer emulsions during the phase inversion process in the presence of non-ionic surfactants”**, to be published in ”, *Colloids and Surfaces – A. Physicochemical and Engineering Aspects*.

Zhou, G.W. and Kresta, S.M. (1998a) **“Correlation of mean drop size and minimum drop size with the turbulence energy dissipation and the flow in an agitated tank”**, *Chemical Engineering Science*, **53**(11), 2063-2079.

Zhou, G.W. and Kresta, S.M. (1998b) **“Evolution of drop size distribution in liquid-liquid dispersions for various impellers”**, *Chemical Engineering Science*, **53**(11), 2099-2113.

Appendixes

Appendix I - Viscosity measurements

- AI.1 Theory
- AI.2 Experiments
- AI.3 Results

Appendix II – Example calculations

- AII.1 Amount of functionalised PUp molecules (for section 4.1.2)
- AII.2 Amount of TEA required (for chapter 5)
- AII.3 Actual DN (for chapter 5)

Appendix III – Supplement for drop size characterisation

- AIII.1 Derivations of equations
- AIII.2 Computer program for simple drop system
- AIII.3 Computer program for multiple drop system
- AIII.4 Analysis report from Malvern mastersizer

Appendix I

Viscosity measurements

Viscosities of the PUp samples were measured using a “falling ball” method. This method utilises the idea of particle motions in the Stokes’ law region. Theoretical considerations of the falling ball method are described in this appendix. This is followed by descriptions of the relevant experiment and results obtained.

AI.1 Theory

When a spherical particle is settling freely in a continuous fluid under the gravitational force, its velocity will increase until the accelerating force is balanced by the resistance force. After this, the spherical particle will continue to fall at a constant velocity known as the terminal (or free-settling) velocity, u_t .

AI.1.1 Force balance

Consider a particle of mass, M_p , moving through a continuous fluid at a relative velocity of u_p . Forces acting on this particle are the external force, F_E , the buoyant force, F_B , and the drag force, F_D . The resultant force acting on the particle will be $F_E - F_B - F_D$ and causing the acceleration of the particle to be du_p/dt . Therefore, the force balance can be written as,

$$M_p \frac{du_p}{dt} = F_E - F_B - F_D \quad [\text{AI-1}]$$

For a settling particle affected solely by the gravitational force, the external force acted on this particle can be defined as:

$$F_E = M_p \cdot a_e = M_p \cdot g \quad [\text{AI-2}]$$

where a_e is the acceleration of the particle due to the external force (in m/s^2). In this case, $a_e = g$, where g is the acceleration due to gravity (in m/s^2). According to the Archimedes' principle, the product of the mass of fluid displaced by the particle and the acceleration from external force is equivalent to the buoyant force. For a particle with a volume of $\frac{M_p}{\rho_p}$ (where ρ_p is the density of the particle, in kg/m^3), the mass of fluid displaced is $\left(\frac{M_p}{\rho_p}\right)\rho_l$ (where ρ_l is the density of the continuous fluid, in kg/m^3).

The buoyant force can then be defined as,

$$F_B = \frac{M_p \cdot \rho_l \cdot a_e}{\rho_p} = \frac{M_p \cdot \rho_l \cdot g}{\rho_p} \quad [\text{AI-3}]$$

A fluid will exert drag upon a particle whenever relative motion exists between the particle and its surrounding fluid. This drag force on the particle is,

$$F_D = \frac{C_D}{2} \times A_p \cdot \rho_l \cdot u_p^2 \quad [\text{AI-4}]$$

where C_D is the dimensionless fanning drag coefficient and A_p is the projected particle area in the direction of motion (in m^2). By substituting equations (AI-2), (AI-3) and (AI-4) into equation (AI-1), the following equation can be obtained:

$$\frac{du_p}{dt} = g \frac{\rho_p - \rho_l}{\rho_p} - \frac{C_D \cdot u_p^2 \cdot \rho_l \cdot A_p}{2 \cdot M_p} \quad [\text{AI-5}]$$

AI.1.2 Terminal velocity in the Stokes' law region

When a free falling spherical particle has attained its terminal velocity, $u_p = u_t$ and du_p/dt is equal to 0. Therefore, equation (AI-5) becomes,

$$u_t^2 = \frac{2 \cdot g \cdot (\rho_p - \rho_l) \cdot M_p}{\rho_p \cdot C_D \cdot \rho_l \cdot A_p} \quad [\text{AI-6}]$$

According to McCabe et al. (1993), the fanning drag coefficient in the Stokes' law region can be expressed as,

$$C_D = \frac{24}{\text{Re}} \quad [\text{AI-7}]$$

This Stokes' law region exists when $Re < 0.2$ (Coulson et al. (1991)). By substituting equation (AI-7) into equation (AI-6), the terminal velocity in the Stokes' law region can be express as,

$$u_t = \frac{g \cdot (\rho_p - \rho_f) \cdot d_p^2}{18 \cdot \mu_f} \quad [\text{AI-8}]$$

where d_p is the diameter of the particle (in m). The distance travelled by a particle before reaching its terminal velocity can be calculated using methods that will be mentioned in section AI.1.4.

AI.1.3 Correction factors

For the above "free settling" condition to be valid, the particles have to be travelling through a relatively large cross section within a relatively dilute fluid. According to Sakiadis (1984), the "hindered settling" effect is insignificant when the solids volumetric concentration is below 0.1 percent. As will become clear later, this effect is negligible for the falling ball experiment. The effect of the wall has to be taken into account when particle diameter to vessel diameter (d_v) ratio, β , is larger than 0.01. When $\beta > 0.01$, the vessel wall will exert an additional retarding effect to the particle and thereby reduced the terminal velocity. In order to take account of the wall effect, the actual terminal velocity (u_t') can be correlated to the u_t calculated from equation (AI-8) by the following equation,

$$u_t' = u_t \times k_w \quad [\text{AI-9}]$$

where k_w is a dimensionless correction factors. For free settling particles, Sakiadis (1984) presented some values of k_w at different β values. These values are reproduced in table AI.1. For values of $\beta < 0.05$, k_w can be calculated using the Ladenburg correction as,

$$k_w = 1 / (1 + 2.1 \beta) \quad [\text{AI-10}]$$

Table AI.1. Wall correction factors [reproduced from Sakiadis (1984)],

β	k_w	β	k_w
0.0	1.000	0.2	0.596
0.05	0.885	0.4	0.279
0.1	0.792	0.8	0.0205

AI.1.4 Vertical accelerating motion of a particle

In the Stokes' law region, vertical accelerating motion of a particle in a gravitational field can be represented by the equation (Coulson et al. (1991)),

$$\frac{d^2y}{dt^2} = -\frac{18 \cdot \mu_l}{d_p^2 \cdot \rho_p} \frac{dy}{dt} + g \left(1 - \frac{\rho_l}{\rho_s} \right) = -a \frac{dy}{dt} + b \quad [\text{AI-11}]$$

where dy/dt and d^2y/dt^2 are the first and second derivatives of the vertical displacement y with respect to time t . By integrating equation (AI-11) with respect to

$$t, \quad \frac{dy}{dt} = -ay + bt + \text{constant} \quad [\text{AI-12}]$$

At time $t = 0$, the vertical displacement is at the origin, i.e. $y = 0$. Let the initial velocity of the particle in the vertical direction be u_o and substitute these boundary conditions into equation (AI-12), constant of equation (AI-12) is equal to u_o . Therefore, the equation can be rewritten as,

$$\frac{dy}{dt} = -ay + bt + u_o \quad [\text{AI-13}]$$

Multiplying the equation by e^{at} :

$$\begin{aligned} e^{at} \frac{dy}{dt} + e^{at} ay &= (bt + u_o) \cdot e^{at} \\ \Rightarrow e^{at} y &= \int (bt + u_o) e^{at} dt + \text{constant} \end{aligned}$$

and integrate the right-hand side using the relation $\int u dv = uv - \int v du$,

$$\begin{aligned} \Rightarrow e^{at} y &= (bt + u_o) \frac{e^{at}}{a} - \int b \frac{e^{at}}{a} dt + \text{constant} \\ \Rightarrow e^{at} y &= (bt + u_o) \frac{e^{at}}{a} - \frac{b}{a^2} e^{at} + \text{constant} \quad [\text{AI-14}] \end{aligned}$$

Again, when time $t = 0$, then $y = 0$. At this boundary condition, constant of equation (AI-14) is equal to $b/a^2 - u_o/a$. Therefore,

$$y = \frac{b}{a} t + \frac{u_o}{a} - \frac{b}{a^2} + \left(\frac{b}{a^2} - \frac{u_o}{a} \right) \cdot e^{-at} \quad [\text{AI-15}]$$

where
$$a = \frac{18 \cdot \mu_l}{d_p^2 \cdot \rho_p} \quad [\text{AI-16a}]$$

and
$$b = \left(1 - \frac{\rho_l}{\rho_p}\right) \cdot g \quad [\text{AI-16b}]$$

It should also be noted that $\frac{b}{a} = \frac{g \cdot (\rho_p - \rho_l) \cdot d_p^2}{18 \cdot \mu_l} = u_t$. Equation (AI-15)

enables the vertical displacement of the particle to be calculated at any time t .

AI.2 Experiments

AI.2.1 Design of equipment

The equipment and experimental set-up used for the falling ball experiments have already been mentioned in section 3.3.1. The most important calculation, to determine the suitability of the glass tube, is the distance travelled by the stainless steel ball before reaching its terminal velocity. To estimate this, the following values were used: $d_p = 1.6 \text{ mm} = 1.6 \times 10^{-3} \text{ m}$; $d_v = 1.6 \text{ cm} = 1.6 \times 10^{-2} \text{ m}$; $\rho_p = 7,572 \text{ kg/m}^3$; and $g = 9.81 \text{ m/s}^2$. In addition to this, two assumptions were also made. They are $\rho_l = 1000 \text{ kg/m}^3$ and $\mu_l = 500 \text{ cPs} = 0.5 \text{ kg/ms}$.

By substituting these values into equation (AI-8), the calculated u_t is equal to $1.83 \times 10^{-2} \text{ m/s}$. This value was used to estimate the Reynolds number. The wall effect was neglected because taking account of it will only result in reduced u_t value, and hence reduced calculated vertical displacement distance. Reynolds number

$\left(\text{Re} = \frac{\rho_l u_t d_p}{\mu_l}\right)$ is about 0.059. Since $\text{Re} < 0.2$, equations (AI-8), (AI-15) and

(AI-16), which were derived for calculations in the Stokes' law region, can be applied for this purpose. The longest distance travelled by the ball before reaching its terminal velocity can be calculated by taking $u_n = 0 \text{ m/s}$. Therefore, equation (AI-15) can be

simplified as,
$$y = \frac{b}{a}t - \frac{b}{a^2} + \frac{b}{a^2}e^{-at} \quad [\text{AI-17}]$$

in which $a = 464.29/\text{s}$ and $b = 8.51 \text{ m/s}^2$. Differentiating equation (A-17) with respect to time, then

$$\frac{dy}{dt} = \frac{b}{a}(1 - e^{-at}) = u_t(1 - e^{-at}) \quad [\text{AI-18}]$$

It is impossible to solve for t when dy/dt is equal to u_t . Hence, dy/dt was taken as $0.9999 u_t$. Substitute dy/dt and a into equation (AI-18) and the time for the steel ball to approach its terminal velocity in the fluid medium is calculated to be about 0.02 second. The calculated a , b and t values can then be substituted into equation (AI-17) and the vertical distance travelled by the steel ball before reaching its terminal velocity in the fluid medium can be solved. This distance is about 3.27×10^{-2} cm, which is far shorter than the length of the glass tube (18 cm) used for this experiment. Hence, the experimental set-up mentioned in section 3.3.1 can be used to measure fluid with viscosity higher than 500 cPs.

AI2.2.2 Experimental procedure

Before the experiment, the PUP sample was poured into the glass tube. It was then left untouched for a few days until all entrapped air bubbles had escaped. During the experiment, a ruler was strapped to the glass tube. Both of them were then immersed into a water bath that was maintained at a constant temperature. A thermocouple was immersed into the PUP samples to measure its temperature. After the PUP sample was heated up to the measuring temperature, the thermocouple was removed. This was followed by carefully resting a steel ball at the central of the fluid surface. The steel ball was allowed to settle freely and its movement was monitored to ensure that the glass tube was placed parallel to the gravitational field. Suitable adjustments were subsequently made until any steel ball, which was placed at the central of the fluid surface, will travel in the central of the glass tube through to its bottom.

During the measurements, steel balls were firstly rested at the central of the fluid surface. Again, they were allowed to fall freely in the PUP sample. The steel balls were allowed to travel for 5 to 7 cm to attain their terminal velocity. After that, the times for the steel balls to travel a further 5 to 7 cm were recorded. Five measurements were made for each of five measuring temperatures, ranging from 35 °C to 80 °C. The average u_t' values were calculated by dividing the average

distance travelled by the steel balls against the average time they take to complete the “journey”. The wall effect was accounted for using equation (AI-9).

The corrected terminal velocity (u_t) was substituted into equation (AI-8) to obtain the actual viscosity of the PUp samples. It is worth pointing out that the actual densities of the PUp samples were measured using the modified densitometer mentioned in section 3.3.3. It should also be noticed that the actual Reynolds numbers were re-calculated using the measured values to ensure that the experiments were carried out in the Stokes’ law region.

AI.3 Results

The measured density and viscosity, at different temperatures, of some PUp samples were shown in figure AI.1. As mentioned in section 4.1.3, the density-temperature and viscosity-temperature relationships of these samples can be represented by equations (4-3) and (4-4). These relationships of the PUp samples are also plotted in figure AI.1 using constants A, B and C shown in section 4.1.3. From figure AI.1, it is obvious that reasonably good matching between the measured and predicted density and viscosity values has been obtained. Although figure AI.1 is plotted using density and viscosity of PUp2-0 and PUpB-50/50, the good agreement between measured and predicted values is also found in other PUp samples.

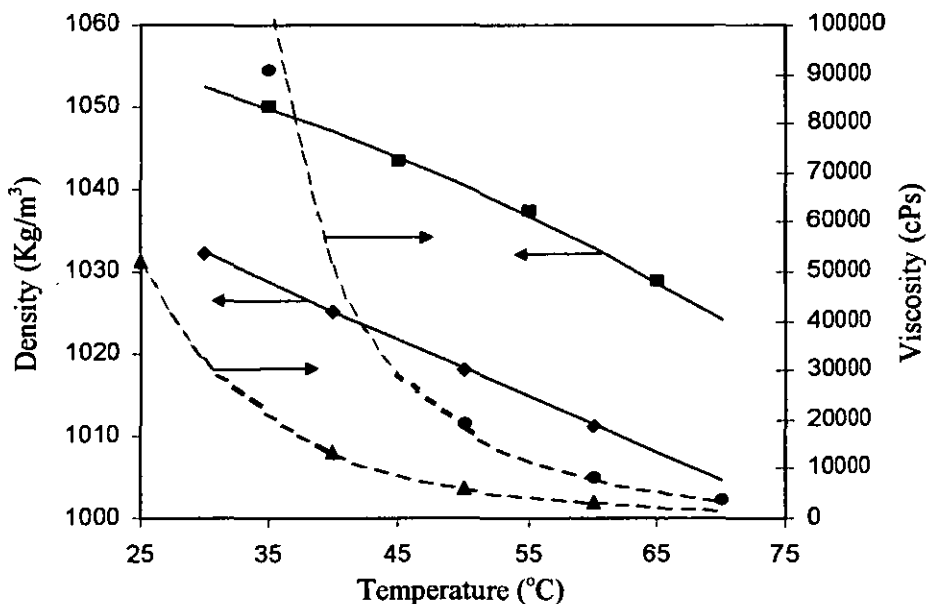


Figure AI.1. Comparison of measured density and viscosity (dots) to values predicted using equations (lines) (Black colour is for PUp2-0 and blue colour is for PUpB-50/50)

Appendix II

Example calculations

AII.1 Amount of functionalised PUp molecules (for section 4.1.2)

As mentioned in section 4.1.2, PUp samples used in this work are likely to be a mixture of functionalised PUp molecules and non-functionalised PUp molecules. Based on the samples' NCO/OH ratio and DMPA content, the amount of functionalised PUp molecules in the samples can be calculated. The calculations involved are shown in this appendix.

Two assumptions are made in these calculations. They are:

1. Reaction times are long enough for diols to be used up completely. In other words, extent of reaction, p , approaches 1. Therefore, equation (4-2) can be used.
2. No pre-polymer chains will contain more than one DMPA group unless all the pre-polymer molecules have already possessed one DMPA group.

A detailed calculation is shown based upon sample PUp2-7.5: -

AII.1.1 Values used

Amount of DMPA in the reactant mixtures	=	7.5 wt.-%
NCO/OH ratio	=	2
Molecular weight of DMPA, $(MW)_{DMPA}$	=	134.13 g/mole
Molecular weight of TXDI, $(MW)_{TXDI}$	=	244.3 g/mole
Molecular weight of PTHF, $(MW)_{PTHF}$	=	1,000 g/mole

AII.1.2 Mole-% of DMPA in reactant mixtures

Basis: - 100 g of reactant mixtures

$$\text{Amount of DMPA} = 7.5 \text{ g} = 0.0559 \text{ moles}$$

$$\text{Amount of TXDI} = a \text{ g} = A \text{ moles}$$

$$\text{Amount of PTHF} = b \text{ g} = B \text{ moles}$$

Since $\text{NCO/OH} = 2$,

$$\frac{A}{(B + 0.0559)} = 2$$

$$\Rightarrow A = 2 \times (B + 0.0559) \quad [\text{AII-1}]$$

$$\text{Also, } a + b + 7.5 = 100$$

$$\Rightarrow a + b = 92.5$$

$$\Rightarrow (MW)_{\text{TXDI}} \times A + (MW)_{\text{PTHF}} \times B = 92.5$$

$$\Rightarrow A = 0.3786 - 4.0933 \times B \quad [\text{AII-2}]$$

Solving equations (AII-1) and (AII-2),

$$B = \underline{0.0438} \text{ mole}$$

and substitute into equation (AII-1),

$$A = \underline{0.1994} \text{ mole}$$

$$\text{total moles in 100 g of reactant mixtures} = 0.0559 + A + B = \underline{0.2991} \text{ moles}$$

Therefore,

$$\text{mole-\% of DMPA groups, } [DMPA] = \frac{0.0559}{0.2991} \times 100\% = \underline{18.69} \%$$

AII.1.3 Amount of each type of monomer

$$\text{Let, Amount of TXDI molecules} = N_{\text{TXDI}}$$

$$\text{Total amount of diol molecules} = N_{\text{diol.T}}$$

Basis: - 100 mole of monomer molecules

$$N_{\text{TXDI}} + N_{\text{diol.T}} = 100$$

Since NCO/OH ratio = 2,

$$N_{TXDI} = \underline{66.67} \text{ moles} \quad \text{and} \quad N_{diol,T} = \underline{33.33} \text{ moles}$$

Also, $[DMPA] = 18.69$ mole-%, therefore

$$\text{Amount of DMPA molecules, } N_{DMPA} = \underline{18.69} \text{ moles}$$

$$\text{Amount of PTHF molecules, } N_{PTHF} = N_{diol,T} - N_{DMPA} = \underline{14.64} \text{ moles}$$

II.1.4 PUp molecules produced

$$\text{Functional group ratio, } r = \frac{N_{diol,T}}{N_{TXDI}} = 0.5.$$

Substitute $r = 0.5$ into equation (4-2), then $\overline{X}_n = 3$ (as mentioned in section 4.1.2)

Therefore, an average PUp molecule contains just 1 diol monomer. In other words, total amount of PUp molecules produced ($N_{PUp,T}$) is equal to total number of diol monomers,

$$N_{PUp,T} = N_{diol,T} = \underline{33.33} \text{ moles}$$

$$\text{Amount of functionalised PUp molecules, } N_{PUp,DMPA} = N_{DMPA} = \underline{18.69} \text{ moles}$$

$$\text{Amount of non-functionalised PUp molecules, } N_{PUp,PTHF} = N_{PTHF} = \underline{14.64} \text{ moles}$$

Therefore, mole-% of functionalised PUp molecules,

$$[PUp_{DMPA}] = \frac{18.69}{33.33} \times 100\% = \underline{56.08} \%$$

II.1.5 Spreadsheet for calculations with different DMPA contents

<i>DMPA</i>	<i>B</i>	<i>A</i>	N_{DMPA}	$[PUp_{DMPA}]$
7.5	0.0438	0.1994	18.69	56.08
3.75	0.0555	0.1669	11.17	33.51
2.5	0.0594	0.1560	7.96	23.89
1.5	0.0625	0.1474	5.06	15.18
0	0.0672	0.1344	0.00	0.00

AII.2 Amount of TEA required (for chapter 5)

This section shows the calculation of the amount of TEA required in order to neutralise a fixed amount of PUP ionomer based on the nominal DN.

AII.2.1 Constants

Molecular weight of DMPA, $(MW)_{DMPA}$ = 134.13 g/mole

Molecular weight of TEA, $(MW)_{TEA}$ = 101.19 g/mole

Nominal DN, $(DN)_{nom}$ = 98 %

AII.2.2 TEA solution (99 % pure) required

Basis: - 100 g of PUp2-7.5

$$\text{Amount of DMPA, } N_{DMPA} = \frac{7.5}{100} \cdot \frac{100}{(MW)_{DMPA}} = \underline{0.0559} \text{ moles}$$

Amount of TEA to obtain the nominal DN,

$$\begin{aligned} N_{TEA,req} &= N_{DMPA} \times (DN)_{nom} \times (MW)_{TEA} \\ &= 0.0559 \times 0.98 \times 101.19 \\ &= \underline{5.54} \text{ g} \end{aligned}$$

TEA solution is 99 % pure, therefore the amount of TEA solution required is $N_{TEA,req}/0.99 = \underline{5.60}$ g.

AII.3 Actual DN (for chapter 5)

The actual DN is calculated based on the amount of TEA and PUP added.

Basis: - 100 g of PUp2-7.5

Amount of TEA solution added = 5.5 g

Therefore,

$$\text{Actual DN, } (DN)_{act} = \frac{5.5 \times 0.99}{(MW)_{TEA} \times N_{DMPA}} \times 100 \% = \underline{96.26} \%$$

Appendix III

Supplement for drop size characterisation

The first section of this appendix includes derivations of some equations for drop size characterisations. The following sections show both C⁺⁺ programmes in full and the last section shows a typical analysis report from Malvern Mastersizer.

AIII.1 Derivations of equations

This section shows derivations of equations used in section 5.3.

AIII.1.1 $D_{L,i}$ and $D_{H,i}$ for the arithmetic progression method

For the arithmetic progression method, ΔD_i is constant for every bin. Define N_{bin} and use the known D_{min} and D_{max} values, ΔD_i can be expressed as equation (5-1).

Then, Lower drop diameter limit of bin 1, $D_{L,1} = D_{min}$;

Upper drop diameter limit of bin 1, $D_{H,1} = D_{L,1} + \Delta D_i = D_{min} + \Delta D_i$;

Lower drop diameter limit of bin 2, $D_{L,2} = D_{H,1} = D_{min} + \Delta D_i$;

Upper drop diameter limit of bin 2, $D_{H,2} = D_{L,2} + \Delta D_i = D_{min} + 2 \cdot \Delta D_i$.

By analogy,

Lower drop diameter limit of bin i , $D_{L,i} = D_{min} + (i-1) \cdot \Delta D_i$ [i.e., (5-2)]

Upper drop diameter limit of bin i , $D_{H,i} = D_{min} + i \cdot \Delta D_i$ [i.e., (5-3)]

AIII.1.2 $D_{L,i}$ and $D_{H,i}$ for the geometric progression method

For the geometric progression method, bin size is defined by equal differences between the logarithms of the upper and lower drop diameter limits of the bins.

Assume that only two bins exist in the analysis; $D_{L,1}$, $D_{H,1}$, $D_{L,2}$, and $D_{H,2}$ stand for the lower and upper drop diameter limits of bins 1 and 2 respectively. For the geometric progress method,

$$\log D_{H,i} - \log D_{L,i} = \text{Constant} = \log \frac{D_{H,1}}{D_{L,1}} = \log \frac{D_{H,2}}{D_{L,2}} \quad [\text{AIII-1}]$$

Rearranging equation (AIII-1), and substitute $D_{L,2}$ with $D_{H,1}$. The upper drop diameter limit of bin 1, $D_{H,1}$, can then be expressed as,

$$D_{H,1}^2 = D_{L,1} \cdot D_{H,2} \quad [\text{AIII-2}]$$

Since $D_{L,1} = D_{\min}$ and $D_{H,2} = D_{\max}$, $D_{H,1}$ can also be expressed as,

$$D_{H,1}^2 = D_{\min} \cdot D_{\max} \quad [\text{AIII-3}]$$

The same expressions can be derived by taking $\Delta D_i / D_{\text{avg},i}$ as a constant for every bin. In which case,

$$\frac{\Delta D_i}{D_{\text{avg},i}} = \text{Constant} = \frac{\Delta D_1}{D_{\text{avg},1}} = \frac{\Delta D_2}{D_{\text{avg},2}}$$

Similar derivations can be carried out for the analysis where more bins are used. When doing so, equation (AIII-1) is used to relate the first bin with the last bin. Also, the lower drop diameter limit of bin i is assumed to be equal to upper drop diameter limit of the previous bin, $(i-1)$, i.e., $D_{L,i} = D_{H,(i-1)}$. By extending these derivations to cover other bins, the upper drop diameter limit of each bin can be represented in terms of $D_{H,1}$ and $D_{L,1} (= D_{\min})$, as follows,

$$\text{Upper drop diameter limit of bin 2, } D_{H,2} = \frac{D_{H,1}^2}{D_{L,1}} = \frac{D_{H,1}^2}{D_{\min}} ;$$

$$\text{Upper drop diameter limit of bin 3, } D_{H,3} = \frac{D_{H,1}^3}{D_{L,1}^2} = \frac{D_{H,1}^3}{D_{\min}^2} .$$

By analogy, the upper drop diameter limit of bin i , $D_{H,i}$, can be expressed as,

$$D_{H,i} = \frac{D_{H,1}^i}{D_{L,1}^{i-1}} = \frac{D_{H,1}^i}{D_{\min}^{i-1}} \quad [\text{AIII-4}]$$

Also, when an analysis includes more than 2 bins, the upper drop diameter limit of the first bin, $D_{H,1}$, can be related to D_{min} and D_{max} as follows,

$$\text{For analysis with 3 bins, } D_{H,1}^3 = D_{min}^2 \cdot D_{max};$$

$$\text{For analysis with 4 bins, } D_{H,1}^4 = D_{min}^3 \cdot D_{max}.$$

By analogy, when an analysis contains N_{bin} , the upper drop diameter limit of the first bin, $D_{H,1}$, can be related to D_{min} and D_{max} by,

$$D_{H,1}^{N_{bin}} = D_{min}^{(N_{bin}-1)} \cdot D_{max} \quad [\text{AIII-5}]$$

Combining equations (AIII-4) and (AIII-5), one gets the following expression,

$$D_{H,i} = D_{min}^{(1-i/N_{bin})} \cdot D_{max}^{(i/N_{bin})} \quad [\text{i.e., (5-5)}]$$

If $i = N_{bin}$, then $D_{H,i} = D_{max}$. Since $D_{L,i} = D_{H,(i-1)}$, equation (5-5) can be extended to express the lower drop diameter limit in terms of D_{min} , D_{max} , i and N_{bin} ,

$$D_{L,i} = D_{min}^{(1-(i-1)/N_{bin})} \cdot D_{max}^{((i-1)/N_{bin})} \quad [\text{i.e., (5-4)}]$$

When $i = 1$, $D_{L,1} = D_{min}$.

AIII.1.3 Expressing $P_{A,i}$ and $P_{V,i}$ in terms of $P_{N,i}$ and $D_{avg,i}$

Area percentage $P_{A,i}$

$$\text{Surface area of a droplet with diameter } d_{avg,i}, A_{avg,i} = \pi D_{avg,i}^2 \quad ;$$

$$\text{Total surface area in bin } i, A_{T,avg,i} = N_i (\pi D_{avg,i}^2) \quad ;$$

$$\text{Total surface area of all calculated drops, } A_T = \sum_1^i N_i (\pi D_{avg,i}^2) \quad .$$

Therefore, surface area percentage $P_{A,i}$ of bin i can be expressed as,

$$P_{A,i} = \frac{A_{T,avg,i}}{A_T} \times 100 \% = \frac{N_i \cdot D_{avg,i}^2}{\sum_1^i N_i \cdot D_{avg,i}^2} \times 100 \%$$

$$\Rightarrow P_{A,i} = \frac{P_{N,i} \cdot D_{avg,i}^2}{\sum_1^i P_{N,i} \cdot D_{avg,i}^2} \times 100 \% \quad [\text{i.e., (5-7)}]$$

Volumetric percentage $P_{V,i}$

$$\text{Volume of a droplet with diameter } d_{avg,i}, V_{avg,i} = \frac{\pi}{6} D_{avg,i}^3 \quad ;$$

$$\text{Total volume in bin } i, V_{T,avg,i} = N_i \left(\frac{\pi}{6} D_{avg,i}^3 \right) \quad ;$$

$$\text{Total volume of all calculated drops, } V_T = \sum_1^i N_i \left(\frac{\pi}{6} D_{avg,i}^3 \right) \quad .$$

Therefore, volume percentage $P_{V,i}$ of bin i can be expressed as,

$$P_{V,i} = \frac{V_{T,avg,i}}{V_T} \times 100 \% = \frac{P_{N,i} \cdot D_{avg,i}^3}{\sum_1^i P_{N,i} \cdot D_{avg,i}^3} \times 100 \%$$

$$\Rightarrow P_{V,i} = \frac{P_{N,i} \cdot D_{avg,i}^3}{\sum_1^i P_{N,i} \cdot D_{avg,i}^3} \times 100 \% \quad [\text{i.e., (5-8)}]$$

AIII.1.4 Mean diameters

Recalling equation (5-9), by dividing numerator and denominator by N_T , the mean diameter can be expressed as,

$$d_{mn} = \left[\frac{\sum_i P_{N,i} \cdot D_{avg,i}^m}{\sum_i P_{N,i} \cdot D_{avg,i}^n} \right]^{1/(m-n)}$$

d_{10} is derived by substituting $m = 1$ and $n = 0$; and d_{32} is derived by substituting $m = 3$ and $n = 2$.

AIII.2 Computer program for simple drop system

This section shows the whole C++ programme written to characterise droplet information for emulsions consisting of mainly simple P/W or W/P drops:

```
/*1. Library connection*/
#include <stdio.h>
#include <stdlib.h>
#include <math.h>
#include <ctype.h>
#include <conio.h>
```

```

#define TRUE 1
#define FALSE 0
#define ARRAYS 35

/*2. Declare functions */
FILE *open_file(int);
void display1(float,float,int);
float setting_new_maximum(float);
float setting_new_minimum(float);
int drops_to_count(int);
int bin_number(void);
void display2(float,float,int,int,float,float,int);
int continue_or_not(void);
int bins_classification_method (void);
int comparison(float,float[]);
float sum_percentage(int,int,float[],float[]);
void display3(int,float[],float[],float[],int[],float[],float[],float[]);
void display4 (int,int,float[],float[],float[],float[]);
void mean_diameter(float[]);
float geometric_std (float [],float [],int);
void error_estimation (float,int);
void write_data(int,int,int,int,int[],float,float,float,float,float[],float[],float[],float[],float[],float[],float[],float[],float[],float[],float[]);

/*3. Main function*/
int main(void)
{
    /* Global variables */
    int number_of_drops,new_number_of_drops,number_of_bins,i, confirmation=TRUE,
        drops_in_bin[ARRAYS] = {0}, classification_method;
    float drop_data,min,max,oldmax,oldmin,bin_difference,j,lower_limit_of_bin[ARRAYS],
        upper_limit_of_bin[ARRAYS],average_diameter_of_bin[ARRAYS],sum_PN = 0,
        PN[ARRAYS] = {0},PA[ARRAYS],PV[ARRAYS],sum_PD[4] = {0},
        cumulative_PN[ARRAYS], cumulative_PA[ARRAYS], cumulative_PV[ARRAYS],
        std_sum = 0,GSD,std;
    double d10;
    FILE *data_file_input;

    /*Main programme */
    /*(a) open file*/
    data_file_input = open_file(1);

    /*(b) determine maximum, minimum and number of drops in data bank*/
    fscanf(data_file_input,"%f",&drop_data);
    oldmax = drop_data;
    oldmin = oldmax;
    number_of_drops = 1;
    while (fscanf(data_file_input,"%f",&drop_data)!= EOF)
    {
        if ((drop_data - oldmax) > 0.0001)
            oldmax = drop_data;
        if ((oldmin - drop_data) > 0.0001)
            oldmin = drop_data;
        number_of_drops++;
    }
    display1(oldmax,oldmin,number_of_drops);

    /*(c) Setting new maximum, minimum, number of drops to count and bin numbers*/
    confirmation = TRUE;
    do
    {
        max = setting_new_maximum(oldmax);

```

```

min = setting_new_minimum(oldmin);
while (max <= min)
{
printf("\nMaximum diameter must be larger than the minimum diameter!\n");
printf("Please re-set the maximum and minimum drop diameter.\n");
max = setting_new_maximum(oldmax);
min = setting_new_minimum(oldmin);
}
new_number_of_drops = drops_to_count(number_of_drops);
number_of_bins = bin_number();
display2(max,min,new_number_of_drops,number_of_bins,oldmax,oldmin,number_of_drops);
confirmation = continue_or_not ();
}
while (confirmation);

/*(d) Creating bins*/
if ((classification_method = bins_classification_method ())== 1)
{
bin_difference = (max-min)/number_of_bins;
for (i=0; i<number_of_bins; i++)
{
lower_limit_of_bin[i] = min + i*bin_difference;
upper_limit_of_bin[i] = min + (i+1)*bin_difference;
average_diameter_of_bin[i] =(lower_limit_of_bin[i]+upper_limit_of_bin[i])/2;
}
}
else
{
j=0.0;
for (i=0; i<number_of_bins; i++)
{
lower_limit_of_bin[i] = pow(min,1-j/number_of_bins)*
pow(max,j/number_of_bins);
upper_limit_of_bin[i] = pow(min,1-(j+1)/number_of_bins)*
pow(max,(j+1)/number_of_bins);
average_diameter_of_bin[i] = pow(lower_limit_of_bin[i]*upper_limit_of_bin[i] ,0.5);
j++;
}
}

/*(e) Locating datas into bins*/
rewind(data_file_input);
while (fscanf(data_file_input,"%f",&drop_data)!= EOF && sum_PN < new_number_of_drops)
{
drops_in_bin[comparison(drop_data,upper_limit_of_bin)]++;
sum_PN++;
}
fclose(data_file_input);

/*(f) datas for curve plotting, include: (1) number distribution; (2) area distribution;
(3) volumetric distribution; and (4) cumulative data*/
for (i=0; i<number_of_bins; i++)
PN[i] = drops_in_bin[i]/sum_PN;
for (i=0; i<=3; i++)
sum_PD[i] = sum_percentage (i,number_of_bins,PN,average_diameter_of_bin);
for (i=0; i<number_of_bins; i++)
{
PA[i] = (PN[i]*pow(average_diameter_of_bin[i],2.00))/sum_PD[2];
PV[i] = (PN[i]*pow(average_diameter_of_bin[i],3.00))/sum_PD[3];
}
display3(number_of_bins,lower_limit_of_bin,upper_limit_of_bin,average_diameter_of_bin,

```

```

        drops_in_bin,PN,PA,PV);
cumulative_PN[0] = PN[0];
cumulative_PA[0] = PA[0];
cumulative_PV[0] = PV[0];
for (i=1; i<number_of_bins; i++)
    {
        cumulative_PN[i] = cumulative_PN[i-1] + PN[i];
        cumulative_PA[i] = cumulative_PA[i-1] + PA[i];
        cumulative_PV[i] = cumulative_PV[i-1] + PV[i];
    }
display4(1,number_of_bins,upper_limit_of_bin,cumulative_PN,cumulative_PA,cumulative_PV);
display4(2,number_of_bins,lower_limit_of_bin,cumulative_PN,cumulative_PA,cumulative_PV);

/*(g) others drop size characterisation data: (1) all mean diameters; (2) standard deviations and
(3) Error estimation (two methods)*/
mean_diameter(sum_PD);
d10 = sum_PD[1]/sum_PD[0];
if (classification_method == 1)
    {
        /*STD of arithmetic method = SUM(Pni*(Di-D10)^2)*/
        for (i=0; i<number_of_bins; i++)
            std_sum += PN[i]*pow((average_diameter_of_bin[i]-d10),2.00);
        std = pow(std_sum,0.50);
        printf("\nstandard deviation = %5.3f\n", std);
    }
else
    {
        /*STD of geometric method: STD=ln(GSD)*/
        GSD = geometric_std (cumulative_PV,upper_limit_of_bin,number_of_bins);
        printf("\nGSD = %6.3f\n",GSD);
        std=log(GSD);
        printf("std = %6.3f\n",std);
        getch();
        error_estimation(std,new_number_of_drops);
    }

/*(h) write datas into a text file for further data processing*/
write_data(classification_method,number_of_drops,new_number_of_drops,number_of_bins,
    drops_in_bin,min,max,oldmax,oldmin,lower_limit_of_bin,upper_limit_of_bin,
    average_diameter_of_bin,PN,PA,PV,sum_PD,cumulative_PN,cumulative_PA,
    cumulative_PV,GSD,std);

printf("\nEnd\n");
getch();
return 0;
}

/*Sub-functions*/
/*Open a file for calculation*/
FILE *open_file(int x)
{
    FILE *file;
    char file_name[13],answer = 'a';
    int cont = TRUE;

    switch (x)
    {
        case 1:
            while (cont)
                {
                    printf("Enter a file name: ");
                    gets(file_name);
                    if ((file = fopen(file_name,"r")) == NULL)        /* open file*/

```

```

        {
            printf("Failed to open the data file.\n\n");
            printf("Re-");
        }
    else
    {
        printf("File opened successfully.\n\n");
        cont = FALSE;
    }
}

break;
case 2:
    while (cont)
    {
        printf("Enter a file name: ");
        gets(file_name);
        if ((file = fopen(file_name,"r")) != NULL) /*check existence of file*/
        {
            do
            {
                printf("\n%s already exist.\nRe-write the file(Y/N)?",file_name);
                answer = getche();
                answer = tolower(answer);
            }
            while (answer != 'y' && answer != 'n');
            fclose (file);
            if (answer == 'y')
            {
                if ((file = fopen(file_name,"w")) == NULL) /* open file*/
                {
                    printf("\nFailed to open the data file.\n\n");
                    printf("Re-");
                }
                else
                {
                    printf("\nFile opened successfully.\n\n");
                    cont = FALSE;
                }
            }
            else
            {
                printf("\nRe-");
            }
        }
        else
        {
            fclose (file);
            if ((file = fopen(file_name,"w")) == NULL) /* open file*/
            {
                printf("\nFailed to open the data file.\n\n");
                printf("Re-");
            }
            else
            {
                printf("\nFile opened successfully.\n\n");
                cont = FALSE;
            }
        }
    }

break;
}
getch();
return (file);

```

```

}

/*display detected values*/
void display1 (float maximum, float minimum, int number )
{
    printf("Total number of drops in the data bank are %d;\n",number);
    printf("The maximum drop diameter is %5.2f;\n",maximum);
    printf("The minimum drop diameter is %5.2f.\n",minimum);
}

/*Setting new maximum drop diameter*/
float setting_new_maximum (float oldmax1)
{
    float max1;
    char answer = 'a';

    do
    {
        printf("\nSetting new maximum (Y/N)?");
        answer = getche();
        answer = tolower(answer);
    }
    while (answer != 'y' && answer != 'n');
    max1 = oldmax1;
    while (answer == 'y')
    {
        printf("\n\nWhat is the new maximum drop diameter? ");
        scanf("%f",&max1);
        answer = '\n';
        if (max1 <= 0)
        {
            printf("\nDrop diameter must be a positive value!\n");
            do
            {
                printf("\nDo you want to re-enter the maximum drop diameter(Y/N)?");
                answer = getche();
                answer = tolower(answer);
            }
            while (answer != 'y' && answer != 'n');
            if (answer == '\n')
                {max1 = oldmax1; printf("\n");}
        }
    }
    printf("\nThe maximum drop diameter is %5.2f.\n",max1);
    return (max1);
}

/*Setting new minimum drop diameter*/
float setting_new_minimum (float oldmin1)
{
    float min1;
    char answer = 'y';

    do
    {
        printf("\nSetting new minimum (Y/N)?");
        answer = getche();
        answer = tolower(answer);
    }
    while (answer != 'y' && answer != 'n');
    min1 = oldmin1;
}

```

```

while (answer == 'y')
{
    printf("\n\nWhat is the new minimum drop diameter? ");
    scanf("%f",&min1);
    answer = 'n';
    if (min1 < 0)
    {
        printf("\nDrop diameter must be a positive value!!\n");
        do
        {
            printf("\nDo you want to re-enter the minimum drop diameter(Y/N)?");
            answer = getche();
            answer = tolower(answer);
        }
        while (answer != 'y' && answer != 'n');
        if (answer == 'n')
            {min1 = oldmin1; printf("\n");}
    }
}
printf("\nThe minimum drop diameter is %5.2f.\n",min1);
return (min1);
}
/*Total number of drops to count*/
int drops_to_count (int number)
{
    int new_number;
    int cont = TRUE;
    char answer;

    printf("\n\n\t Enter the amount of drops to count\n");
    printf("\t -----\n");
    printf("\t(NB: 0 for all the drops in the data bank;\n");
    printf("\t or 1 to %d for other amount.          )\n\n",number);
    do
    {
        printf("Enter the amount of drops to count: ");
        scanf("%d",&new_number);
        if (new_number < 0 || new_number > number)
        {
            printf("\nThe amount of drops to be counted is out of range\n");
            answer = 'a';
            do
            {
                printf("\nAll the drops will be counted instead.\n");
                printf("Is that alright? (Y/N) ");
                answer = getche();
                answer = tolower(answer);
            }
            while (answer != 'y' && answer != 'n');
            if (answer == 'y')
            {
                new_number = number;
                cont = FALSE;
            }
            else printf("\nRe-");
        }
        else
        {
            if (new_number == 0)
                new_number = number;
            cont = FALSE;
        }
    }
}

```



```

        }
    }
    while (cont);
    printf("\nthe amount of drops to be counted is %d.\n\n", new_number);
    return (new_number);
}

/*Total number of bins to be used*/
int bin_number (void)
{
    int new_number;
    int cont = TRUE;

    do
    {
        printf("Enter the number of bins to be used (2-%d): ", ARRAYS);
        scanf("%d",&new_number);
        if (new_number < 2)
            printf("\nAt least 2 bins are needed in the calculation.\nRe-");
        else if (new_number > ARRAYS)
            printf("\nNot more than %d bins can be created.\nRe-", ARRAYS);
        else cont = FALSE;
    }
    while (cont);
    printf("\nthe amount of bins to be used are %d.\n\n", new_number);
    return (new_number);
}

/*display values for calculation*/
void display2 (float maximum1, float minimum1, int number1, int number2, float maximum2,
              float minimum2, int number3)
{
    printf("\nThese are the original values in the data bank\n");
    printf("-----\n");
    display1 (maximum2,minimum2,number3);
    printf("\nThe following datas will be used for the rest of the calculation\n");
    printf("-----\n");
    printf("Total number of drops to be counted are %d;\n",number1);
    printf("The new maximum drop diameter setting is %5.2f;\n",maximum1);
    printf("The new minimum drop diameter setting is %5.2f;\n",minimum1);
    printf("The number of bins to be used are %d.\n",number2);
}

/*confirmation of the usage of data values*/
int continue_or_not (void)
{
    char confirm = 'a';
    int true_false = TRUE;

    do
    {
        printf("\n\tConfirmed ? (Y/N) ");
        confirm = getche();
        confirm = tolower(confirm);
    }
    while (confirm != 'y' && confirm != 'n');
    printf("\n");
    if (confirm == 'y')
        true_false = FALSE;
    return (true_false);
}

```

```

/* Choosing the suitable bins classification method */
int bins_classification_method (void)
{
    int method.true_false = TRUE;

    do
    {
        printf("\n\nSelect method for bins classification:\n");
        printf("\t-----\n");
        printf("\t 1. Arithmetic progression method  \n");
        printf("\t 2. Geometric progression method  \n");
        printf("\t-----\n");
        printf("\n\nMethod 1 or 2? ");
        scanf("%d",&method);
        switch (method)
        {
            case 1:
                printf("\nArithmetic progression method has been selected\n\n");
                true_false = FALSE;
                break;
            case 2:
                printf("\nGeometric progression method has been selected\n\n");
                true_false = FALSE;
                break;
            default:
                printf("\nSelect 1 or 2 only.\n");
        }
    }
    while (true_false);
    return (method);
}

/*Locating data into bins*/
int comparison (float data, float upper_bin[])
{
    int x = 0;

    while ((data - upper_bin[x]) >= 0.0001) /*drops above .0001 if for next bin*/
        x++;
    return (x);
}

/*Summation of Pni*davgi^n for various distribution data*/
float sum_percentage (int x, int bins, float number[], float average_diameter[])
{
    float sum = 0;
    int y;

    switch (x)
    {
        case 0:
            for (y=0; y<bins; y++)
                sum += number[y]*pow(average_diameter[y],0.00);
            break;
        case 1:
            for (y=0; y<bins; y++)
                sum += number[y]*average_diameter[y];
            break;
        case 2:
            for (y=0; y<bins; y++)

```

```

        sum += number[y]*pow(average_diameter[y],2.00);
    break;
case 3:
    for (y=0; y<bins; y++)
        sum += number[y]*pow(average_diameter[y],3.00);
    break;
}
return (sum);
}

/*Display number,area and volumetric distribution datas*/
void display3(int number,float lower_bin[],float upper_bin[],float average_bin[],int drop_number[],float pni[],
float pai[],float pvi[])
{
    int x;

    printf("Bin\tlower\tupper\tavg.\tdrops\n");
    printf("no.\tlimit\tlimit\tdia.\tcount\tPN,i \tPA,i \tPV,i \n");
    printf("----\t----\t----\t----\t----\t----\t----\t----\t----\n");
    for (x=0; x<number; x++)
        printf("%d \t%5.2f\t%5.2f\t%5.2f\t %d \t%5.2f\t%5.2f\t%5.2f\n",x+1,lower_bin[x],
            upper_bin[x],average_bin[x],drop_number[x],100*pni[x],100*pai[x],100*pvi[x]);
    getch();
}

/*Display cumulative datas*/
void display4 (int x,int number,float limit_bin[],float lgPN[],float lgPA[],float lgPV[])
{
    int y;

    switch (x)
    {
        case 1:
            printf("\nPercentage of droplets <= upper limit of bin\n");
            printf("=====\n");
            printf("Bin\tupper\t PN,i \t PA,i \t PV,i \n");
            printf("no.\tlimit\t <=(%) \t <=(%) \t <=(%) \n");
            printf("----\t----\t----\t----\t----\n");
            for (y=0; y<number; y++)
                printf("%d \t%5.2f\t%6.2f\t%6.2f\t%6.2f\n",y+1,
                    limit_bin[y],100*lgPN[y],100*lgPA[y],100*lgPV[y]);
            getch();
            break;
        case 2:
            printf("\nPercentage of droplets >= lower limit of bin\n");
            printf("=====\n");
            printf("Bin\tlower\t PN,i \t PA,i \t PV,i \n");
            printf("no.\tlimit\t >=(%) \t >=(%) \t >=(%) \n");
            printf("----\t----\t----\t----\t----\n");
            for (y=0; y<number; y++)
                printf("%d \t%5.2f\t%6.2f\t%6.2f\t%6.2f\n",y+1,limit_bin[y],
                    100-100*lgPN[y-1],100-100*lgPA[y-1],100-100*lgPV[y-1]);
            getch();
            break;
    }
}

/*Displaying mean diameter values*/
void mean_diameter(float summation[])
{
    int x,y;

```

```

float z;

for (x=0; x<=3; x++)
    printf("summation of PNi* Davgi^%d is %6.2f.\n",x,100*summation[x]);
printf("\n\t n \t 0 \t 1 \t 2 \n");
printf("\t---\t-----\t-----\t-----\n");
for (x=1; x<=3; x++)
    {
        printf("\td%dn",x);
        z=0;
        for (y=0; y<x; y++)
            {
                printf("\t%5.2f",pow(summation[x]/summation[y],(1/(x-z))));
                z++;
            }
        printf("\n");
    }
}

/*Calculate Geometric Standard Deviation (GSD) = (d3,84/d3,16)^0.5*/
float geometric_std (float cum_PV[], float upper_bin[],int number)
{
    int x;
    float P1,P2,D1,D2,D316,D384;

    x = 0;
    while ((0.16-cum_PV[x])>0.0001)
        x++;
    P1=cum_PV[x-1];
    D1=upper_bin[x-1];
    P2=cum_PV[x];
    D2=upper_bin[x];
    D316=exp(log(D2)-(P2-0.16)*(log(D2)-log(D1))/(P2-P1));

    x=number-1;
    while ((0.84-cum_PV[x])<0.0001)
        x--;
    P1=cum_PV[x];
    D1=upper_bin[x];
    P2=cum_PV[x+1];
    D2=upper_bin[x+1];
    D384=exp(log(D2)-(P2-0.84)*(log(D2)-log(D1))/(P2-P1));
    return (pow(D384/D316,0.50));
}

/*Error estimation using equation from Paine(1993)*/
void error_estimation (float std_for_ee, int number)
{
    int critical_number,limiting_number;

    critical_number = exp(1.5 + 5.5*std_for_ee + 7.5*pow(std_for_ee,2.00));
    limiting_number = exp(0.5 + 7*std_for_ee + 3.5*pow(std_for_ee,2.00));

    printf("\n\tUnreliable <-- %d --> Marginal <-- %d --> reliable\n",
        limiting_number,critical_number);
    printf("\n\tThe amount of droplet counted are %d.\n",number);
    if (number < limiting_number)
        printf("Results are unreliable. More droplets need to be counted!\n");
    else if (number >= limiting_number && number < critical_number)
        printf("Acceptable results; More drops can improve the reliability\n");
    else

```

```

        printf("Results are very reliable\n");
    }

/*Output data to an external file*/
void write_data(int method,int drop_number,int new_drop_number,int bin_number,int bin_count[],
    float minimum,float maximum,float oldmaximum,float oldminimum,float lower_bin[],
    float upper_bin[],float average_of_bin[],float pni[],float pai[],float pvi[],float pd_sum[],float lgPN[],
    float lgPA[],float lgPV[], float gsd,float std_dev)
{
    FILE *output;
    char description[40];
    int x,y,critical_number,limiting_number;
    float z;

    printf("\nProgramme will continue to write all results to an external file.");
    if (continue_or_not() == FALSE)
    {
        output = open_file(2);
        printf("\nShort description of the file (<40 words): ");
        gets(description);
        fprintf(output,"%s.\n",description);
        /*(a) Universal data*/
        fprintf(output,"\n(a)Universal data:\n");
        fprintf(output,"\t\tdata\tfor\n");
        fprintf(output,"\t\tbank\tcalc.\n");
        fprintf(output,"\tNdrops\t%d\t%d\n",drop_number,new_drop_number);
        fprintf(output,"\tMax\t%5.2f\t%5.2f\n",oldmaximum,maximum);
        fprintf(output,"\tMin\t%5.2f\t%5.2f\n",oldminimum,minimum);
        fprintf(output,"\tNbin\tNIL\t%d\n",bin_number);

        /*(b) Distribution data*/
        fprintf(output,"\n(b)drop size distribution:\n");
        fprintf(output,"Bin\tLower\tUpper\tAvg.\tDrops\tNumber\tArea\tVolume\n");
        fprintf(output,"no.\tlimit\tlimit\tdia.\tcount\tdis.\tdis.\tdis.\n");
        fprintf(output,"i\tDL,i\tDH,i\tDavg,i\tNi\tPN,i(\%)\tPA,i(\%)\tPV,i(\%)\n");
        for (x=0; x<bin_number; x++)
            fprintf(output,"%d\t%6.4f\t%6.4f\t%6.4f\t%d\t%5.2f\t%5.2f\t%5.2f\n",x+1,lower_bin[x],
                upper_bin[x],average_of_bin[x],bin_count[x],100*pni[x],100*pai[x],100*pvi[x]);

        /*(c) Cumulative datas*/
        fprintf(output,"\n(c)Cumulative distribution data:\n");
        fprintf(output,"(i)Percentage of droplets <= upper limit of bin\n");
        fprintf(output,"Bin\tupper\tNumber\tArea\tVolume\n");
        fprintf(output,"no.\tlimit\tbasis\tbasis\tbasis\n");
        fprintf(output,"i\t<=DH,i\t(\%)\t(\%)\t(\%)\n");
        for (x=0; x<bin_number; x++)
            fprintf(output,"%d\t%6.4f\t%5.2f\t%5.2f\t%5.2f\n",x+1,upper_bin[x],
                100*lgPN[x],100*lgPA[x],100*lgPV[x]);
        fprintf(output,"\n(ii)Percentage of droplets >= lower limit of bin\n");
        fprintf(output,"Bin\tlower\tNumber\tArea\tVolume\n");
        fprintf(output,"no.\tlimit\tbasis\tbasis\tbasis\n");
        fprintf(output,"i\t>=DL,i\t(\%)\t(\%)\t(\%)\n");
        for (x=0; x<bin_number; x++)
            fprintf(output,"%d\t%6.4f\t%5.2f\t%5.2f\t%5.2f\n",x+1,lower_bin[x],
                100-100*lgPN[x-1],100-100*lgPA[x-1],100-100*lgPV[x-1]);
        for (x=0; x<=3; x++)
            fprintf(output,"\nsummation of PNi*Davgi=\t\t\t%6.2f",x,100*pd_sum[x]);

        /*(d) Mean diameters*/
        fprintf(output,"\n\n(d)Mean diameters (dmn):");
        fprintf(output,"\n\t\tdmn\t=0\t=1\t=2");
    }
}

```

```

for (x=1; x<=3; x++)
{
    fprintf(output, "\n\m=%d", x);
    z=0;
    for (y=0; y<x; y++)
    {
        fprintf(output, "\t%5.2f", pow(pd_sum[x]/pd_sum[y], (1/(x-z))));
        z++;
    }
}

/*(e) Standard deviation and error estimation*/
fprintf(output, "\n\n(e)standard deviation:\n");
switch (method)
{
    case 1:
        fprintf(output, "\tArithmetic std =\t\t%6.3f\n", std_dev);
        break;
    case 2:
        fprintf(output, "\tGeometrical std =\t\t%6.3f\n", std_dev);
        fprintf(output, "\t\tGSD =\t\t%6.3f\n\n", gsd);
        critical_number = exp(1.5 + 5.5*std_dev + 7.5*pow(std_dev, 2.00));
        limiting_number = exp(0.5 + 7*std_dev + 3.5*pow(std_dev, 2.00));
        fprintf(output, "Unreliable <-- %d --> Marginal <-- %d --> reliable",
                limiting_number, critical_number);
        fprintf(output, "\n\tDroplet counted =\t\t%d\n", new_drop_number);
        if (new_drop_number < limiting_number)
            fprintf(output, "Unreliable results, more droplets data needed!\n");
        else if (new_drop_number >= limiting_number &&
                new_drop_number < critical_number)
            fprintf(output, "Acceptable results.\n");
        else
            fprintf(output, "Results are very reliable!\n");
        break;
}
fclose(output);
printf("\nExternal file has been created successfully.\n");
}
else
    printf("\nNo external file created.\n");
getch();
}
/*END*/

```

AIII.3 Computer program for multiple drop system

This section shows the whole C++ programme written to characterise droplet information for emulsions containing a mixture of drop structures:

```

/*1. Library connection*/
#include <stdio.h>
#include <stdlib.h>
#include <math.h>
#include <ctype.h>
#include <conio.h>

```

```

#define TRUE 1
#define FALSE 0
#define ARRAYS 30
#define PI 3.141592654

/*2. Declare functions */
FILE *open_file(int);
void preliminary_calculation(FILE *,float *,int *,int *,int *,int *,int *,float *,
                             float *,float *,float *,float *,float *,float *,float *);
float determine_maximum (float,float);
float determine_minimum (float,float);
float equivalent_WPW(float,float);
void display1(FILE*,float,int,int,int,int,int,int,float,float,float,float,float,float,float);
int calculation_method(void);
void display1(float,float,int);
float setting_new_maximum(float);
float setting_new_minimum(float);
int drops_to_count(int);
int bin_number(void);
void display2(float,float,int,int,float,float,int);
int continue_or_not(void);
int bins_classification_method (void);
int comparison(float,float[]);
float sum_percentage(int,int,float[],float[]);
void display3(int,float[],float[],float[],int[],float[],float[],float[]);
void display4 (int,int,float[],float[],float[],float[]);
void mean_diameter(float[]);
float geometric_std (float [],float [],int);
void error_estimation (float,int);
void write_data(FILE *,int,int,int,int,int[],float,float,float,float,float[],float[],float[],float[],
                float[],float[],float[],float[],float[],float[],float,float);
void DSC_mtd1(int,FILE *,FILE *,int,float,float,float *,float *,float *,float *,int *);
void vol_frac_analysis(FILE *,float,float,float,float,float,float,float,float,float,float,
                       float *,float *,float *);
void interfacial_area(FILE *,float,float,float,float,float,float);
void WPW_W2_relationship(FILE *,FILE *,float,float,float);

/*3. Main function*/
int main(void)
{
/* Global variables */
int number_of_PW=0,number_of_WPW=0,number_of_WPWA=0,number_of_WPWB=0,
    number_of_WPWC=0,number_of_W2=0,choice,no_counted_PW,no_counted_WPW,
    no_counted_eq_WPW,no_counted_W2,no_counted_PW_eq_WPW,
    no_counted_PW_WPW,no_counted_W2_eq_WPW,number_for_calculation;
float pol_vol_frac,oldmax_PW=0,oldmax_WPW=0,oldmax_eq_WPW=0,oldmax_W2=0,
    oldmin_PW=0,oldmin_WPW=0,oldmin_eq_WPW=0,oldmin_W2=0,d10_PW=0,
    d31_PW=0,d32_PW=0,GSD_PW=0,d10_WPW=0,d31_WPW=0,d32_WPW=0,
    GSD_WPW=0,d10_eq_WPW=0,d31_eq_WPW=0,d32_eq_WPW=0,
    GSD_eq_WPW=0,d10_PW_eq_WPW=0,d31_PW_eq_WPW=0,
    d32_PW_eq_WPW=0,GSD_PW_eq_WPW=0,d10_W2=0,d31_W2=0,d32_W2=0,
    GSD_W2=0,d10_W2_eq_WPW=0,d31_W2_eq_WPW=0,d32_W2_eq_WPW=0,
    GSD_W2_eq_WPW=0,d10_PW_WPW=0,d31_PW_WPW=0,d32_PW_WPW=0,
    GSD_PW_WPW=0,W2_vol_frac=0,PW_vol_frac=0,WPW_vol_frac=0,
    max_for_calculation,min_for_calculation;

```

```

FILE *data_file_input;
FILE *data_file_output;

/*Main programme */
/*(a) open file*/
data_file_input = open_file(1);
data_file_output = open_file(2);

/*(b) Determine volume fraction of the dispersed phase, the maximum, minimum and number of drops
for each drop types in data bank*/
preliminary_calculation(data_file_input,&pol_vol_frac,&number_of_PW,
&number_of_WPW,&number_of_WPW_A,&number_of_WPWB,
&number_of_WPWC,&number_of_W2,&oldmax_PW,&oldmax_WPW,
&oldmax_eq_WPW,&oldmax_W2,&oldmin_PW,&oldmin_WPW,
&oldmin_eq_WPW,&oldmin_W2);
display1(data_file_output,pol_vol_frac,number_of_PW,number_of_WPW_A,
number_of_WPWB,number_of_WPWC,number_of_W2,oldmax_PW,
oldmax_WPW,oldmax_eq_WPW,oldmax_W2,oldmin_PW,oldmin_WPW,
oldmin_eq_WPW,oldmin_W2);

/*(c) choice of different calculation*/
while ((choice = calculation_method()) != 11)
{
switch (choice)
{
case 1:
d10_PW=0;d31_PW=0;d32_PW=0;GSD_PW=0;no_counted_PW=0;

DSC_mtd1(choice,data_file_input,data_file_output,number_of_PW,
oldmax_PW,oldmin_PW,&d10_PW,&d31_PW,&d32_PW,
&GSD_PW,&no_counted_PW);

break;
case 2:
d10_WPW=0;d31_WPW=0;d32_WPW=0;GSD_WPW=0;no_counted_WPW=0;

DSC_mtd1(choice,data_file_input,data_file_output,number_of_WPW,
oldmax_WPW,oldmin_WPW,&d10_WPW,&d31_WPW,
&d32_WPW,&GSD_WPW,&no_counted_WPW);

break;
case 3:
d10_eq_WPW=0;d31_eq_WPW=0;d32_eq_WPW=0;GSD_eq_WPW=0;
no_counted_eq_WPW=0;

DSC_mtd1(choice,data_file_input,data_file_output,number_of_WPW,
oldmax_eq_WPW,oldmin_eq_WPW,&d10_eq_WPW,
&d31_eq_WPW,&d32_eq_WPW,&GSD_eq_WPW,&no_counted_eq_WPW);
break;
case 4:
d10_W2=0;d31_W2=0;d32_W2=0;GSD_W2=0;no_counted_W2=0;

DSC_mtd1(choice,data_file_input,data_file_output,number_of_W2,
oldmax_W2,oldmin_W2,&d10_W2,&d31_W2,&d32_W2,
&GSD_W2,&no_counted_W2);

break;
case 5:
d10_PW_eq_WPW=0;d31_PW_eq_WPW=0;d32_PW_eq_WPW=0;

```



```

GSD_PW_eq_WPW=0;no_counted_PW_eq_WPW=0;

if ((oldmax_eq_WPW - oldmax_PW)>0.0001)
    max_for_calculation = oldmax_eq_WPW;
else
    max_for_calculation = oldmax_PW;
if ((oldmin_eq_WPW - oldmin_PW)>0.0001)
    min_for_calculation = oldmin_PW;
else
    min_for_calculation = oldmin_eq_WPW;
    number_for_calculation = number_of_PW + number_of_WPW;
DSC_mtd1(choice,data_file_input,data_file_output,number_for_calculation,
    max_for_calculation,min_for_calculation,&d10_PW_eq_WPW,
    &d31_PW_eq_WPW,&d32_PW_eq_WPW,
    &GSD_PW_eq_WPW,&no_counted_PW_eq_WPW);

break;
case 6:
d10_W2_eq_WPW=0;d31_W2_eq_WPW=0;d32_W2_eq_WPW=0;
GSD_W2_eq_WPW=0;no_counted_W2_eq_WPW=0;

if ((oldmax_eq_WPW - oldmax_W2)>0.0001)
    max_for_calculation = oldmax_eq_WPW;
else
    max_for_calculation = oldmax_W2;
if ((oldmin_eq_WPW - oldmin_W2)>0.0001)
    min_for_calculation = oldmin_W2;
else
    min_for_calculation = oldmin_eq_WPW;
DSC_mtd1(choice,data_file_input,data_file_output,number_of_WPW,
    max_for_calculation,min_for_calculation,&d10_W2_eq_WPW,
    &d31_W2_eq_WPW,&d32_W2_eq_WPW,&GSD_W2_eq_WPW,
    &no_counted_W2_eq_WPW);

break;
case 7:
d10_PW_WPW=0;d31_PW_WPW=0;d32_PW_WPW=0;
GSD_PW_WPW=0;no_counted_PW_WPW=0;

if ((oldmax_WPW - oldmax_PW)>0.0001)
    max_for_calculation = oldmax_WPW;
else
    max_for_calculation = oldmax_PW;
if ((oldmin_WPW - oldmin_PW)>0.0001)
    min_for_calculation = oldmin_PW;
else
    min_for_calculation = oldmin_WPW;
    number_for_calculation = number_of_PW + number_of_WPW;
DSC_mtd1(choice,data_file_input,data_file_output,number_for_calculation,
    max_for_calculation,min_for_calculation,&d10_PW_WPW,
    &d31_PW_WPW,&d32_PW_WPW,&GSD_PW_WPW,
    &no_counted_PW_WPW);

break;
case 8:
WPW_W2_relationship(data_file_input,data_file_output,number_of_WPW,
    oldmax_WPW,oldmin_WPW);

break;

```

```

        case 9:
            W2_vol_frac=0;PW_vol_frac=0;WPW_vol_frac=0;

            vol_frac_analysis(data_file_output,d10_PW,d10_PW_eq_WPW,
                d10_eq_WPW,d10_W2,d10_W2_eq_WPW,d31_PW,
                d31_PW_eq_WPW,d31_eq_WPW,d31_W2,d31_W2_eq_WPW,
                pol_vol_frac,&PW_vol_frac,&WPW_vol_frac,&W2_vol_frac);

        break;
        case 10:
            interfacial_area(data_file_output,PW_vol_frac,WPW_vol_frac,
                W2_vol_frac,d32_PW,d32_WPW,d32_W2);

        break;
    }
    printf("\n\n\t\t***Calculation completed***\n\n");
    getch();
}

printf("\n\n\n\t\t***Thanks for using this programme***\n\n\n");
fclose(data_file_output);
fclose(data_file_input);
return(0);
}

/*Sub-functions*/
/*Open a file for calculation*/
FILE *open_file(int x)
{
    FILE *file;
    char file_name[13],description[81],answer = 'a';
    int cont = TRUE;

    switch (x)
    {
        case 1:
            while (cont)
            {
                printf("Enter the file name of the data bank: ");
                gets(file_name);
                if ((file = fopen(file_name,"r")) == NULL) /* open file*/
                {
                    printf("Failed to open the data file.\n\n");
                    printf("Re-");
                }
                else
                {
                    printf("File opened successfully.\n\n");
                    cont = FALSE;
                }
            }

        break;
        case 2:
            while (cont)
            {
                printf("Enter a file name to record results: ");
                gets(file_name);
                if ((file = fopen(file_name,"r")) != NULL) /*check existence of file*/

```

```

    {
    do
        {
        printf("\n%s already exist.\nRe-write the file(Y/N)?",file_name);
            answer = getche();
            answer = tolower(answer);
        }
        while (answer != 'y' && answer != 'n');
        fclose (file);
        if (answer == 'y')
            {
            if ((file = fopen(file_name,"w")) == NULL) /* open file*/
                {
                printf("\nFailed to open the data file.\n\n");
                printf("Re-");
                }
            else
                {
                printf("\nFile opened successfully.\n\n");
                cont = FALSE;
                }
            }
        else
            printf("\nRe-");
    }
else
    {
    fclose (file);
    if ((file = fopen(file_name,"w")) == NULL) /* open file*/
        {
        printf("\nFailed to open the data file.\n\n");
        printf("Re-");
        }
    else
        {
        printf("\nFile opened successfully.\n\n");
        cont = FALSE;
        }
    }
}
printf("\nShort description of this section (<80 words):\n");
gets(description);
fprintf(file,"%t%s",description);

break;
}
return (file);
}

/*Preliminary determination of values in the data bank*/
void preliminary_calculation (FILE *input,float *vol_frac,int *pwnumber,int *wpwnumber,
int *wpwanumber,int *wpwbnumber,int *wpwcnumber,int *w2number,float *pwmax,
float *wpwmax,float *eqwpwmax,float *w2max,float *pwmin,float *wpwmin,
float *eqwpwmin,float *w2min)
{
int W2_in_WPW;

```

```

float drop_data,water_drop,polymer_drop,diameter_of_eq_WPW=0,oldmax_PW1=0,
oldmax_WP1=0,oldmax_eq_WPW1=0,oldmax_W21=0,oldmin_PW1=0,
oldmin_WP1=0,oldmin_eq_WPW1=0,oldmin_W21=0;

fscanf(input,"%f",&drop_data);
*vol_frac = drop_data;
while (fscanf(input,"%f",&drop_data)!=EOF)
{
polymer_drop=drop_data;
if (polymer_drop != 0)
{
fscanf(input,"%f",&drop_data);
water_drop=drop_data;
if (water_drop == 0) /*Simple PW drops*/
{
*pwnumber += 1;
oldmax_PW1 = determine_maximum(polymer_drop,oldmax_PW1);
*pwmax = oldmax_PW1;
oldmin_PW1 = determine_minimum(polymer_drop,oldmin_PW1);
*pwmin = oldmin_PW1;
}
else
/*Multiple WPW drops*/
{
*wpwanumber += 1;
oldmax_WP1 = determine_maximum(polymer_drop,oldmax_WP1);
*wpwmax = oldmax_WP1;
oldmin_WP1 = determine_minimum(polymer_drop,oldmin_WP1);
*wpwmin = oldmin_WP1;
if (diameter_of_eq_WPW != 0)
{
/*One loop late of Eq_wpw calculation*/
oldmax_eq_WPW1 = determine_maximum(diameter_of_eq_WPW,oldmax_eq_WPW1);
*eqwpwmax = oldmax_eq_WPW1;
oldmin_eq_WPW1 = determine_minimum(diameter_of_eq_WPW,oldmin_eq_WPW1);
*eqwpwmin = oldmin_eq_WPW1;
}
diameter_of_eq_WPW = equivalent_WPW(water_drop,polymer_drop);
W2_in_WPW=1;
}
}
else
{
W2_in_WPW += 1;
fscanf(input,"%f",&drop_data);
water_drop=drop_data;
diameter_of_eq_WPW = equivalent_WPW(water_drop,diameter_of_eq_WPW);
if (W2_in_WPW == 2) /*WPWB for 2-15 W2 drops*/
{
*wpwanumber -= 1;
*wpwbnnumber += 1;
}
else if (W2_in_WPW == 16) /*>15 W2 drops, must be WPWC*/
{
wpwbnumber -= 1;
wpwcnumber += 1;
}
}
}

```

```

        }
    }
    if (water_drop != 0)
    {
        *w2number += 1;
        oldmax_W21 = determine_maximum(water_drop,oldmax_W21);
        *w2max = oldmax_W21;
        oldmin_W21 = determine_minimum(water_drop,oldmin_W21);
        *w2min = oldmin_W21;
    }
}
/*Last eq_WPW calculation*/
oldmax_eq_WPW1 = determine_maximum(diameter_of_eq_WPW,oldmax_eq_WPW1);
*eqwpwmax = oldmax_eq_WPW1;
oldmin_eq_WPW1 = determine_minimum(diameter_of_eq_WPW,oldmin_eq_WPW1);
*eqwpwmin = oldmin_eq_WPW1;
*wpwnumber = *wpwanumber + *wpwbnumber + *wpwcnumber;
}

/*Calculate equivalent WPW diameter*/
float equivalent_WPW(float w, float eq_wpw)
{
    double temporary,eq_wpw1;

    temporary = pow(eq_wpw,3.00)-pow(w,3.00);
    eq_wpw1 = pow(temporary,1.00/3.00);
    return (eq_wpw1);
}

/*Determine maximum drops*/
float determine_maximum (float drop_diameter,float maximum)
{
    if (maximum == 0)
        maximum = drop_diameter;
    else
    {
        if ((drop_diameter - maximum)>0.0001)
            maximum = drop_diameter;
    }
    return (maximum);
}

/*Determine minimum drops*/
float determine_minimum (float drop_diameter,float minimum)
{
    if (minimum == 0)
        minimum = drop_diameter;
    else
    {
        if ((minimum - drop_diameter)>0.0001)
            minimum = drop_diameter;
    }
    return (minimum);
}

```

```

/*display detected values*/
void display1(FILE *output,float vol_frac,int pwnumber,int wpwanumber,int wpwbnumber,
int wpwcnnumber,int w2number,float pwmax,float wpwmax,float eqwpwmax,
float w2max,float pwmin,float wpwmin,float eqwpwmin,float w2min)
{
float total;

printf("\nVolume fraction of polymer phase is %5.2f;\n",vol_frac);
printf("%d PW drop;\n", pwnumber);
printf("%d WPW type A drop;\n", wpwanumber);
printf("%d WPW type B drop;\n", wpwbnumber);
printf("%d WPW type C drop;\n", wpwcnnumber);
printf("%d W2 drop;\n", w2number);
printf("Maximum PW drop is %5.2f;\n",pwmax);
printf("Maximum WPW drop is %5.2f;\n",wpwmax);
printf("Maximum eq_WPW drop is %5.2f;\n",eqwpwmax);
printf("Maximum W2 drop is %5.2f;\n",w2max);
printf("Minimum PW drop is %5.2f;\n",pwmin);
printf("Minimum WPW drop is %5.2f;\n",wpwmin);
printf("Minimum eq_WPW drop is %5.2f;\n",eqwpwmin);
printf("Minimum W2 drop is %5.2f;\n",w2min);
total = pwnumber + wpwanumber + wpwbnumber + wpwcnnumber;
getch();

fprintf(output,"\nfp,t =\t%5.2f\n",vol_frac);
fprintf(output,"(a) Data detected from source file:\n");
fprintf(output,"(i) Number percentage of each type of drops:\n");
fprintf(output,"\t Drop \t number \t num. \t\n");
fprintf(output,"\t type \tof drop\t % \t\n");
fprintf(output,"\t PW \t%d\t%5.2f\n",pwnumber,(pwnumber/total)*100);
fprintf(output,"\t WPWA \t%d\t%5.2f\n",wpwanumber,wpwanumber*100/total);
fprintf(output,"\t WPWB \t%d\t%5.2f\n",wpwbnumber,wpwbnumber*100/total);
fprintf(output,"\t WPWC \t%d\t%5.2f\n",wpwcnnumber,wpwcnnumber*100/total);
fprintf(output,"\t total \t%3.0f\n",total);
fprintf(output,"\t W2 \t%d\n",w2number);
fprintf(output,"(ii) Maximum and minimum values:\n");
fprintf(output,"\t\t max. \t min. \t\n");
fprintf(output,"\t\t dia. \t dia. \t\n");
fprintf(output,"\t Dpw \t%5.2f\t%5.2f\n",pwmax,pwmin);
fprintf(output,"\t Dwpw \t%5.2f\t%5.2f\n",wpwmax,wpwmin);
fprintf(output,"\t Dwpw' \t%5.2f\t%5.2f\n",eqwpwmax,eqwpwmin);
fprintf(output,"\t Dw2 \t%5.2f\t%5.2f\n",w2max,w2min);
printf("\nThese datas have been written onto the output file.\n");
getch();
}

/*Display the choice of calculation method*/
int calculation_method(void)
{
int ans;

printf("\nThe following are different data that can be calculated:\n");
printf("-----\n");
printf(" 1. Simple polymer drop size characterisation (DSC)\n");
printf(" 2. Multiple polymer drops DSC\n");
}

```

```

printf(" 3. Equivalent multiple polymer drops DSC\n");
printf(" 4. Water drops DSC\n");
printf(" 5. Combine DSC of 1 + 3\n");
printf(" 6. Combine DSC of 3 + 4\n");
printf(" 7. Combine DSC of 1 + 2\n");
printf(" 8. Relationship of WPW drops and the contained W2 drops\n");
printf(" 9. Calculation for the volume fraction of simple polymer\n");
printf("    drops, multiple polymer drops and water drops(required\n");
printf("    data from calculation 1, 3, 4, 5 and 6)\n");
printf(" 10. Calculate various interfacial area / unit volume value\n");
printf("    (required data from calculation 9)\n");
printf(" 11. No further calculation\n");
do
    {
        printf("\nSelect the calculation mehod (1-11): ");
        scanf("%d",&ans);
    }
while (ans < 1 || ans > 11);
printf("\n");
return (ans);
}
/*display detected values*/
void display1 (float maximum, float minimum, int number )
{
    printf("Total number of drops in the data bank are %d;\n",number);
    printf("The maximum drop diameter is %5.2f;\n",maximum);
    printf("The minimum drop diameter is %5.2f.\n",minimum);
}

/*Setting new maximum drop diameter*/
float setting_new_maximum (float oldmax1)
{
    float max1;
    char answer = 'a';

    do
        {
            printf("\nSetting new maximum (Y/N)?");
            answer = getche();
            answer = tolower(answer);
        }
while (answer != 'y' && answer != 'n');
max1 = oldmax1;
while (answer == 'y')
    {
        printf("\n\nWhat is the new maximum drop diameter? ");
        scanf("%f",&max1);
        answer = 'n';
        if (max1 <= 0)
            {
                printf("\nDrop diameter must be a positive value!\n");
                do
                    {
                        printf("\nDo you want to re-enter the maximum drop diameter(Y/N)?");
                        answer = getche();
                    }
            }
    }
}

```

```

        answer = tolower(answer);
    }
    while (answer != 'y' && answer != 'n');
    if (answer == 'n')
        { max1 = oldmax1; printf("\n");}
    }
    printf("\nThe maximum drop diameter is %5.2f.\n",max1);
    return (max1);
}

/*Setting new minimum drop diameter*/
float setting_new_minimum (float oldmin1)
{
    float min1;
    char answer = 'y';

    do
        {
            printf("\nSetting new minimum (Y/N)?");
            answer = getche();
            answer = tolower(answer);
        }
    while (answer != 'y' && answer != 'n');
    min1 = oldmin1;
    while (answer == 'y')
        {
            printf("\n\nWhat is the new minimum drop diameter? ");
            scanf("%f",&min1);
            answer = 'n';
            if (min1 < 0)
                {
                    printf("\nDrop diameter must be a positive value!!\n");
                    do
                        {
                            printf("\nDo you want to re-enter the minimum drop diameter(Y/N)?");
                            answer = getche();
                            answer = tolower(answer);
                        }
                    while (answer != 'y' && answer != 'n');
                    if (answer == 'n')
                        { min1 = oldmin1; printf("\n");}
                }
        }
    printf("\nThe minimum drop diameter is %5.2f.\n",min1);
    return (min1);
}

/*Total number of drops to count*/
int drops_to_count (int number)
{
    int new_number;
    int cont = TRUE;
    char answer;

    printf("\n\n\t Enter the amount of drops to count\n");

```



```

printf("\t -----\n");
printf("\t(NB: 0 for all the drops in the data bank;\n");
printf("\t or 1 to %d for other amount. )\n\n",number);
do
{
printf("Enter the amount of drops to count: ");
scanf("%d",&new_number);
if (new_number < 0 || new_number > number)
{
printf("\n\nThe amount of drops to be counted is out of range\n");
answer = 'a';
do
{
printf("\n\nAll the drops will be counted instead.\n");
printf("Is that alright? (Y/N) ");
answer = getch();
answer = tolower(answer);
}
while (answer != 'y' && answer != 'n');
if (answer == 'y')
{
new_number = number;
cont = FALSE;
}
else printf("\nRe-");
}
else
{
if (new_number == 0)
new_number = number;
cont = FALSE;
}
}
while (cont);
printf("\n\nthe amount of drops to be counted is %d.\n\n", new_number);
return (new_number);
}

/*Total number of bins to be used*/
int bin_number (void)
{
int new_number;
int cont = TRUE;

do
{
printf("Enter the number of bins to be used (2-%d): ", ARRAYS);
scanf("%d",&new_number);
if (new_number < 2)
printf("\n\nAt least 2 bins are needed in the calculation.\n\nRe-");
else if (new_number > ARRAYS)
printf("\n\nNot more than %d bins can be created.\n\nRe-", ARRAYS);
else cont = FALSE;
}
while (cont);
}

```

```

    printf("\nthe amount of bins to be used are %d.\n", new_number);
    return (new_number);
}

/*display values for calculation*/
void display2 (float maximum1, float minimum1, int number1, int number2,float maximum2,
              float minimum2, int number3)
{
    printf("\nThese are the original values in the data bank\n");
    printf("-----\n");
    display1(maximum2,minimum2,number3);
    printf("\nThe following datas will be used for the rest of the calculation\n");
    printf("-----\n ");
    printf("Total number of drops to be counted are %d;\n",number1);
    printf("The new maximum drop diameter setting is %5.2f;\n",maximum1);
    printf("The new minimum drop diameter setting is %5.2f;\n",minimum1);
    printf("The number of bins to be used are %d.\n",number2);
}

/*confirmation of the usage of data values*/
int continue_or_not (void)
{
    char confirm = 'a';
    int true_false = TRUE;

    do
    {
        printf("\n\tConfirmed ? (Y/N) ");
        confirm = getche();
        confirm = tolower(confirm);
    }
    while (confirm != 'y' && confirm != 'n');
    printf("\n");
    if (confirm == 'y')
        true_false = FALSE;
    return (true_false);
}

/* Choosing the suitable bins classification method */
int bins_classification_method (void)
{
    int method,true_false = TRUE;

    do
    {
        printf("\n\tSelect method for bins classification:\n");
        printf("\t-----\n");
        printf("\t 1. Arithmetic progression method  \n");
        printf("\t 2. Geometric progression method  \n");
        printf("\t-----\n");
        printf("\t\tMethod 1 or 2? ");
        scanf("%d",&method);
        switch (method)
        {
            case 1:

```

```

                printf("\nArithmetic progression method has been selected\n\n");
                true_false = FALSE;
                break;
            case 2:
                printf("\nGeometric progression method has been selected\n\n");
                true_false = FALSE;
                break;
            default:
                printf("\nSelect 1 or 2 only.\n");
        }
    }
    while (true_false);
    return (method);
}

/*Locating data into bins*/
int comparison (float data, float upper_bin[])
{
    int x = 0;

    while ((data - upper_bin[x]) >= 0.0001) /*drops above .0001 if for next bin*/
        x++;
    return (x);
}

/*Summation of Pni*davgi^n for various distribution data*/
float sum_percentage (int x, int bins, float number[], float average_diameter[])
{
    float sum = 0;
    int y;

    switch (x)
    {
        case 0:
            for (y=0; y<bins; y++)
                sum += number[y]*pow(average_diameter[y],0.00);
            break;
        case 1:
            for (y=0; y<bins; y++)
                sum += number[y]*average_diameter[y];
            break;
        case 2:
            for (y=0; y<bins; y++)
                sum += number[y]*pow(average_diameter[y],2.00);
            break;
        case 3:
            for (y=0; y<bins; y++)
                sum += number[y]*pow(average_diameter[y],3.00);
            break;
    }
    return (sum);
}

/*Display number,area and volumetric distribution datas*/
void display3(int number,float lower_bin[],float upper_bin[],float average_bin[],

```

```

        int drop_number[],float pni[],float pai[],float pvi[])
    {
        int x;

        printf("Bin\tlower\tupper\tavg.\tdrops\n");
        printf("no.\tlimit\tlimit\tdia.\tcount\tPN,i \tPA,i \tPV,i \n");
        printf("----\t----\t----\t----\t----\t----\t----\t----\t----\n");
        for (x=0; x<number; x++)
            printf("%d \t%5.2f\t%5.2f\t%5.2f\t %d \t%5.2f\t%5.2f\t%5.2f\n",x+1,lower_bin[x],
                upper_bin[x],average_bin[x],drop_number[x],100*pni[x],100*pai[x],100*pvi[x]);
        getch();
    }

```

/*Display cumulative datas*/

```

void display4 (int x,int number,float limit_bin[],float lgPN[],float lgPA[],float lgPV[])
{
    int y;

    switch (x)
    {
        case 1:
            printf("\nPercentage of droplets <= upper limit of bin\n");
            printf("=====\n");
            printf("Bin\tupper\t PN,i \t PA,i \t PV,i \n");
            printf("no.\tlimit\t <=(%) \t <=(%) \t <=(%) \n");
            printf("----\t----\t----\t----\t----\t----\n");
            for (y=0; y<number; y++)
                printf(" %d \t%5.2f\t%6.2f\t%6.2f\t%6.2f\n",y+1,
                    limit_bin[y],100*lgPN[y],100*lgPA[y],100*lgPV[y]);
            getch();
            break;

        case 2:
            printf("\nPercentage of droplets >= lower limit of bin\n");
            printf("=====\n");
            printf("Bin\tlower\t PN,i \t PA,i \t PV,i \n");
            printf("no.\tlimit\t >=(%) \t >=(%) \t >=(%) \n");
            printf("----\t----\t----\t----\t----\t----\n");
            printf(" 1 \t%5.2f\t100.00\t100.00\t100.00\n",limit_bin[0]);
            for (y=1; y<number; y++)
                printf(" %d \t%5.2f\t%6.2f\t%6.2f\t%6.2f\n",y+1,
                    limit_bin[y],100-100*lgPN[y-1],100-100*lgPA[y-1],100-100*lgPV[y-1]);
            getch();
            break;
    }
}

```

/*Displaying mean diameter values*/

```

void mean_diameter(float summation[])
{
    int x,y;
    float z;

    for (x=0; x<=3; x++)
        printf("summation of PNi*Davgi is %6.2f\n",x,100*summation[x]);
    printf("\n\t n \t 0 \t 1 \t 2 \n");
}

```

```

printf("\t---\t----\t-----\t-----\n");
for (x=1; x<=3; x++)
{
    printf("\td%dn",x);
    z=0;
    for (y=0; y<x; y++)
    {
        printf("\t%5.2f",pow(summation[x]/summation[y],(1/(x-z))));
        z++;
    }
    printf("\n");
}
}
/*Calculate Geometric Standard Deviation (GSD) = (d3,84/d3,16)^0.5*/
float geometric_std (float cum_PV[], float upper_bin[],int number)
{
    int x;
    float P1,P2,D1,D2,D316,D384;

    x = 0;
    while ((0.16-cum_PV[x])>0.0001)
        x++;
    P1=cum_PV[x-1];
    D1=upper_bin[x-1];
    P2=cum_PV[x];
    D2=upper_bin[x];
    D316=exp((log(D2)-(P2-0.16)*(log(D2)-log(D1)))/(P2-P1));

    x=number-1;
    while ((0.84-cum_PV[x])<0.0001)
        x--;
    P1=cum_PV[x];
    D1=upper_bin[x];
    P2=cum_PV[x+1];
    D2=upper_bin[x+1];
    D384=exp((log(D2)-(P2-0.84)*(log(D2)-log(D1)))/(P2-P1));
    return (pow(D384/D316,0.50));
}
/*Error estimation using equation from Paine(1993)*/
void error_estimation (float std_for_ee, int number)
{
    int critical_number,limiting_number;

    critical_number = exp(1.5 + 5.5*std_for_ee + 7.5*pow(std_for_ee,2.00));
    limiting_number = exp(0.5 + 7*std_for_ee + 3.5*pow(std_for_ee,2.00));

    printf("\n\tUnreliable <-- %d --> Marginal <-- %d --> reliable\n",
        limiting_number,critical_number);
    printf("\n\tThe amount of droplet counted are %d.\n",number);
    if (number < limiting_number)
        printf("Results are unreliable. More droplets need to be counted!!\n");
    else if (number >= limiting_number && number < critical_number)
        printf("Acceptable results: More drops can improve the reliability\n");
    else
        printf("Results are very reliable\n");
}

```

```

}
/*Output data to an external file*/
void write_data(FILE *output1,int method,int drop_number,int new_drop_number,int bin_number,
int bin_count[],float minimum,float maximum,float oldmaximum,float oldminimum,
float lower_bin[],float upper_bin[],float average_of_bin[],float pni[],float pai[],float pvi[],
float pd_sum[],float lgPN[],float lgPA[],float lgPV[],float gsd,float std_dev)
{
char a[1],description[40];
int x,y,critical_number,limiting_number;
float z;

printf("\nShort description of this section (<40 words): ");
gets(a);
gets(description);
fprintf(output1,"%s",description);
/*(a) Universal data*/
fprintf(output1,"\n(a)Universal data:\n");
fprintf(output1,"\t\tdata\tfor\n");
fprintf(output1,"\t\tbank\tcalc.\n");
fprintf(output1,"\tNdrops\t%d\t%d\n",drop_number,new_drop_number);
fprintf(output1,"\tMax\t%.2f\t%.2f\n",oldmaximum,maximum);
fprintf(output1,"\tMin\t%.2f\t%.2f\n",oldminimum,minimum);
fprintf(output1,"\tNbin\tNIL\t%d\n",bin_number);
/*(b) Distribution data*/
fprintf(output1,"\n(b)drop size distribution:\n");
fprintf(output1,"Bin\tLower\tUpper\tAvg.\tDrops\tNumber\tArea\tVolume\n");
fprintf(output1,"no.\tlimit\tlimit\tDia.\tcount\tDis.\tDis.\tDis.\n");
fprintf(output1,"i\tDL,i\tDH,i\tDavg,i\tNi\tPN,i(%)tPA,i(%)tPV,i(%)n");
for (x=0; x<bin_number; x++)
    fprintf(output1,"%d\t%.6f\t%.6f\t%.6f\t%.5f\t%.5f\t%.5f\n",x+1,
lower_bin[x],upper_bin[x],average_of_bin[x],bin_count[x],100*pni[x],100*pai[x],
100*pvi[x]);

/*(c) Cumulative datas*/
fprintf(output1,"\n(c)Cumulative distribution data:\n");
fprintf(output1,"(i)Percentage of droplets <= upper limit of bin\n");
fprintf(output1,"Bin\tupper\tNumber\tArea\tVolume\n");
fprintf(output1,"no.\tlimit\tbasis\tbasis\tbasis\n");
fprintf(output1,"i\t<=DH,i\t(%)t(%)t(%)n");
for (x=0; x<bin_number; x++)
    fprintf(output1,"%d\t%.6f\t%.5f\t%.5f\t%.5f\n",x+1,upper_bin[x],100*lgPN[x],
100*lgPA[x],100*lgPV[x]);
    fprintf(output1,"\n(ii)Percentage of droplets >= lower limit of bin\n");
    fprintf(output1,"Bin\tlower\tNumber\tArea\tVolume\n");
    fprintf(output1,"no.\tlimit\tbasis\tbasis\tbasis\n");
    fprintf(output1,"i\t>=DL,i\t(%)t(%)t(%)n");
    fprintf(output1,"1\t%.6f\t100.00\t100.00\t100.00\n",lower_bin[0]);
for (x=1; x<bin_number; x++)
    fprintf(output1,"%d\t%.6f\t%.5f\t%.5f\t%.5f\n",x+1,lower_bin[x],
100-100*lgPN[x-1],100-100*lgPA[x-1],100-100*lgPV[x-1]);
for (x=0; x<=3; x++)
    fprintf(output1,"\nsummation of PNi*Davgid =\t\t%.2f",x,100*pd_sum[x]);

/*(d) Mean diameters*/
fprintf(output1,"\n\n(d)Mean diameters (dmn):");

```

```

fprintf(output1, "\n\tdmn\tn=0\tn=1\tn=2");
for (x=1; x<=3; x++)
{
    fprintf(output1, "\n\tn=%d", x);
    z=0;
    for (y=0; y<x; y++)
    {
        fprintf(output1, "\t%5.2f", pow(pd_sum[x]/pd_sum[y], (1/(x-z))));
        z++;
    }
}

/*(e) Standard deviation and error estimation*/
fprintf(output1, "\n\n(e)standard deviation:\n");
switch (method)
{
    case 1:
        fprintf(output1, "\tArithmetic std =\t\t%6.3f\n", std_dev);
        break;
    case 2:
        fprintf(output1, "\tGeometrical std =\t\t%6.3f\n", std_dev);
        fprintf(output1, "\t\tGSD =\t\t%6.3f\n", gsd);
        critical_number = exp(1.5 + 5.5*std_dev + 7.5*pow(std_dev, 2.00));
        limiting_number = exp(0.5 + 7*std_dev + 3.5*pow(std_dev, 2.00));
        fprintf(output1, "Unreliable <-- %d --> Marginal <-- %d --> reliable",
            limiting_number, critical_number);
        fprintf(output1, "\n\tDroplet counted =\t\t%d\n", new_drop_number);
        if (new_drop_number < limiting_number)
            fprintf(output1, "Unreliable results, more droplets data needed!\n");
        else if (new_drop_number >= limiting_number &&
            new_drop_number < critical_number)
            fprintf(output1, "Acceptable results.\n");
        else
            fprintf(output1, "Results are very reliable\n");

        break;
}
printf("\nExternal file has been created successfully.\n");
}
/*Method 1: DSC of simple PW drops*/
void DSC_mtd1(int mtd, FILE *input, FILE *output, int oldnumber, float oldmaximum,
    float oldminimum, float *d10, float *d31, float *d32, float *GSD, int *newnumber)
{
    int confirmation, number_of_bins, newnumber1, classification_method, s; b_sum = 0,
        i, drops_in_bin[ARRAYS] = {0}, sum_PN1;
    float drop_data, polymer_drop, water_drop, newmaximum, newminimum, bin_difference,
        lower_limit_of_bin[ARRAYS], upper_limit_of_bin[ARRAYS], j, sum_PN = 0,
        average_diameter_of_bin[ARRAYS], PN[ARRAYS] = {0}, PA[ARRAYS],
        PV[ARRAYS], sum_PD[4] = {0}, cumulative_PN[ARRAYS],
        cumulative_PA[ARRAYS], cumulative_PV[ARRAYS], std_sum = 0, GSD1, std,
        diameter_of_eq_WPW=0;

        /*Setting max, min, number of drops and bins for calculation*/
    switch (mtd)
    {
        case 1:

```

```

        printf("Simple polymer drops drop size characterisation:\n");
    break;
    case 2:
        printf("Multiple polymer drops drop size characterisation:\n");
    break;
    case 3:
        printf("Equivalent multiple polymer drops drop size characterisation:\n");
    break;
    case 4:
        printf("Water drops drop size characterisation:\n");
    break;
    case 5:
        printf("Simple PW and equivalent WPW drop size characterisation:\n");
    break;
    case 6:
        printf("Equivalent WPW and water drops drop size characterisation:\n");
    break;
    case 7:
        printf("Simple PW and WPW drop size characterisation:\n");
    break;
}
printf("-----\n");
display1(oldmaximum,oldminimum,oldnumber);
confirmation = TRUE;
do
    {
    newmaximum = setting_new_maximum(oldmaximum);
    newminimum = setting_new_minimum(oldminimum);
    while (newmaximum <= newminimum)
        {
        printf("\nMaximum diameter must be larger than the minimum diameter!!\n");
        printf("Please re-set the maximum and minimum drop diameter.\n");
        newmaximum = setting_new_maximum(oldmaximum);
        newminimum = setting_new_minimum(oldminimum);
        }
    *newnumber = drops_to_count(oldnumber);
    newnumber1 = *newnumber;
    number_of_bins = bin_number();
    display2(newmaximum,newminimum,newnumber1,number_of_bins,
            oldmaximum,oldminimum,oldnumber);
    confirmation = continue_or_not ();
    }
while (confirmation);

/*Creating bins*/
if ((classification_method = bins_classification_method ())== 1)
    {
    bin_difference = (newmaximum-newminimum)/number_of_bins;
    for (i=0; i<number_of_bins; i++)
        {
        lower_limit_of_bin[i] = newminimum + i*bin_difference;
        upper_limit_of_bin[i] = newminimum + (i+1)*bin_difference;
        average_diameter_of_bin[i] =(lower_limit_of_bin[i]+upper_limit_of_bin[i])/2;
        }
    }

```



```

else
{
j=0.0;
for (i=0; i<number_of_bins; i++)
{
lower_limit_of_bin[i] = pow(newminimum,1-j/number_of_bins)*
pow(newmaximum,j/number_of_bins);
upper_limit_of_bin[i] = pow(newminimum,1-(j+1)/number_of_bins)*
pow(newmaximum,(j+1)/number_of_bins);
average_diameter_of_bin[i] = pow(lower_limit_of_bin[i]*
upper_limit_of_bin[i],0.5);
j++;
}
}

/*Locate data into bins*/

rewind(input);
fscanf(input,"%f",&drop_data);
switch (mtd)
{
case 1:
while ((fscanf(input,"%f",&drop_data)!=EOF) && sum_PN < newnumber1)
{
polymer_drop=drop_data;
if (polymer_drop != 0)
{
fscanf(input,"%f",&drop_data);
water_drop=drop_data;
if (water_drop == 0) /*Diameter of simple PW drops*/
{
drops_in_bin[comparison(polymer_drop,upper_limit_of_bin)]++;
sum_PN++;
}
}
else
fscanf(input,"%f",&drop_data);
}
break;
case 2:
while ((fscanf(input,"%f",&drop_data)!=EOF) && sum_PN < newnumber1)
{
polymer_drop=drop_data;
if (polymer_drop != 0)
{
fscanf(input,"%f",&drop_data);
water_drop=drop_data;
if (water_drop != 0) /*Diameter of WPW drops*/
{
drops_in_bin[comparison(polymer_drop,upper_limit_of_bin)]++;
sum_PN++;
}
}
else
fscanf(input,"%f",&drop_data);
}
break;

```

case 3:

```

while ((fscanf(input,"%f",&drop_data)!=EOF) && sum_PN < newnumber1)
{
    polymer_drop=drop_data;
    if (polymer_drop != 0)
    {
        fscanf(input,"%f",&drop_data);
        water_drop=drop_data;
        if (water_drop != 0)          /*Multiple WPW drops*/
        {                            /*One loop late of Eq_wpw calculation*/
            if (diameter_of_eq_WPW != 0)
            drops_in_bin[comparison(diameter_of_eq_WPW,upper_limit_of_bin)]++;
            sum_PN++;
            diameter_of_eq_WPW = equivalent_WPW(water_drop,polymer_drop);
        }
    }
    else
    {
        fscanf(input,"%f",&drop_data);
        water_drop=drop_data;
        diameter_of_eq_WPW = equivalent_WPW(water_drop,diameter_of_eq_WPW);
    }
    /*Last eq_WPW calculation*/
    drops_in_bin[comparison(diameter_of_eq_WPW,upper_limit_of_bin)]++;
}

```

break;

case 4:

```

while ((fscanf(input,"%f",&drop_data)!=EOF) && sum_PN < newnumber1)
{
    fscanf(input,"%f",&drop_data);
    water_drop=drop_data;
    if (water_drop != 0)
    {
        drops_in_bin[comparison(water_drop,upper_limit_of_bin)]++;
        sum_PN++;
    }
}

```

break;

case 5:

```

while ((fscanf(input,"%f",&drop_data)!=EOF) && sum_PN < newnumber1)
{
    polymer_drop=drop_data;
    if (polymer_drop != 0)
    {
        fscanf(input,"%f",&drop_data);
        water_drop=drop_data;
        if (water_drop != 0)          /*Multiple WPW drops*/
        {                            /*One loop late of Eq_wpw calculation*/
            if (diameter_of_eq_WPW != 0)

            drops_in_bin[comparison(diameter_of_eq_WPW,upper_limit_of_bin)]++;
            diameter_of_eq_WPW = equivalent_WPW(water_drop,polymer_drop);
        }
        if (water_drop == 0)          /*Diameter of simple PW drops*/
            drops_in_bin[comparison(polymer_drop,upper_limit_of_bin)]++;
        sum_PN++;
    }
}

```

```

    }
else
    {
        fscanf(input,"%f",&drop_data);
        water_drop=drop_data;
diameter_of_eq_WPW = equivalent_WPW(water_drop,diameter_of_eq_WPW);
    }
    /*Last eq_WPW calculation*/
    drops_in_bin[comparison(diameter_of_eq_WPW,upper_limit_of_bin)]++;
break;
case 6:
while ((fscanf(input,"%f",&drop_data)!=EOF) && sum_PN < newnumber1)
    {
    polymer_drop=drop_data;
    if (polymer_drop != 0)
        {
            fscanf(input,"%f",&drop_data);
            water_drop=drop_data;
            if (water_drop != 0)                /*Multiple WPW drops*/
                {                    /*One loop late of Eq_wpw calculation*/
                    drops_in_bin[comparison(water_drop,upper_limit_of_bin)]++;
                    sub_sum++;
                    if (diameter_of_eq_WPW != 0)
                        {
                            drops_in_bin[comparison(diameter_of_eq_WPW,upper_limit_of_bin)]++;
                            sum_PN++;
                        }
                    diameter_of_eq_WPW = equivalent_WPW(water_drop,polymer_drop);
                }
            else
                {
                    fscanf(input,"%f",&drop_data);
                    water_drop=drop_data;
diameter_of_eq_WPW = equivalent_WPW(water_drop,diameter_of_eq_WPW);
                    drops_in_bin[comparison(water_drop,upper_limit_of_bin)]++;
                    sub_sum++;
                }
            /*Last eq_WPW calculation*/
        }
    if (water_drop !=0)
        {
            drops_in_bin[comparison(water_drop,upper_limit_of_bin)]--;
            sub_sum--;
            sum_PN1 = sum_PN + 1;
            if (sum_PN1 == newnumber1)
                {
                    drops_in_bin[comparison(diameter_of_eq_WPW,upper_limit_of_bin)]++;
                    sum_PN++;
                    drops_in_bin[comparison(water_drop,upper_limit_of_bin)]++;
                    sub_sum++;
                }
        }
    }
    *newnumber = sum_PN + sub_sum;
    newnumber1 = *newnumber;
    printf("Number of WPW drops counted = %3.0f; W2 drops counted = %d.\n",

```

```

        sum_PN,sub_sum);
    getch();
break;
case 7:
    while ((fscanf(input,"%f",&drop_data)!=EOF) && sum_PN < newnumber1)
        {
        polymer_drop=drop_data;
        if (polymer_drop != 0)
            {
            drops_in_bin[comparison(polymer_drop,upper_limit_of_bin)]++;
            sum_PN++;
            }
        fscanf(input,"%f",&drop_data);
        }
    break;
}
/* datas for curve plotting, include: (1) number distribution; (2) area distribution;
(3) volumetric distribution; and (4) cumulative data*/
for (i=0; i<number_of_bins; i++)
    PN[i] = drops_in_bin[i]/sum_PN;
for (i=0; i<=3; i++)
    sum_PD[i] = sum_percentage(i,number_of_bins,PN,average_diameter_of_bin);
for (i=0; i<number_of_bins; i++)
    {
    PA[i] = (PN[i]*pow(average_diameter_of_bin[i],2.00))/sum_PD[2];
    PV[i] = (PN[i]*pow(average_diameter_of_bin[i],3.00))/sum_PD[3];
    }
display3(number_of_bins,lower_limit_of_bin,upper_limit_of_bin,average_diameter_of_bin,
        drops_in_bin,PN,PA,PV);
cumulative_PN[0] = PN[0];
cumulative_PA[0] = PA[0];
cumulative_PV[0] = PV[0];
for (i=1; i<number_of_bins; i++)
    {
    cumulative_PN[i] = cumulative_PN[i-1] + PN[i];
    cumulative_PA[i] = cumulative_PA[i-1] + PA[i];
    cumulative_PV[i] = cumulative_PV[i-1] + PV[i];
    }
display4(1,number_of_bins,upper_limit_of_bin,cumulative_PN,cumulative_PA,cumulative_PV);
display4(2,number_of_bins,lower_limit_of_bin,cumulative_PN,cumulative_PA,cumulative_PV);

/* others drop size characterisation datas: (1) all mean diameters; (2) standard deviations and
(3) Error estimation (two methods)*/
mean_diameter(sum_PD);
*d10 = sum_PD[1]/sum_PD[0];
*d31 = pow(sum_PD[3]/sum_PD[1],0.50);
*d32 = sum_PD[3]/sum_PD[2];
if (classification_method == 1)
    {
        /*STD of arithmetic method = SUM(Pni*(Di-D10)^2)*/
        for (i=0; i<number_of_bins; i++)
            std_sum += PN[i]*pow((average_diameter_of_bin[i]-*d10),2.00);
        std = pow(std_sum,0.50);
        printf("\nstandard deviation = %5.3f\n", std);
    }
else

```

```

        {
            /*STD of geometric method: STD=ln(GSD)*/
            *GSD = geometric_std (cumulative_PV,upper_limit_of_bin,number_of_bins);
            GSD1 = *GSD;
            printf("\nGSD = %6.3f\n",GSD1);
            std=log(GSD1);
            printf("std = %6.3f\n",std);
            getch();
            error_estimation(std,newnumber1);
        }

        /*write datas into a text file for further data processing*/
        printf("\nProgramme will continue to write all results to an external file.");
        if (continue_or_not() == FALSE)
        {
            switch (mtd)
            {
                case 1:
                    fprintf(output,"\nSimple polymer drop size characterisation:\n");
                    break;
                case 2:
                    fprintf(output,"\nMultiple polymer drop size characterisation:\n");
                    break;
                case 3:
                    fprintf(output,"\nEquivalent multiple polymer drop size ");
                    fprintf(output,"characterisation:\n");
                    break;
                case 4:
                    fprintf(output,"\nWater drops drop size characterisation:\n");
                    break;
                case 5:
                    fprintf(output,"\nSimple PW and equivalent WPW drop size ");
                    fprintf(output,"characterisation:\n");
                    break;
                case 6:
                    fprintf(output,"\nEquivalent WPW and W2 drops drop size ");
                    fprintf(output,"characterisation:\n");
                    break;
                case 7:
                    fprintf(output,"\nSimple PW and WPW drop size characterisation:\n");
                    break;
            }
            write_data(output,classification_method,oldnumber,newnumber1,number_of_bins,
                drops_in_bin,newminimum,newmaximum,oldmaximum,oldminimum,
                lower_limit_of_bin,upper_limit_of_bin,average_diameter_of_bin,PN,PA,PV,
                sum_PD,cumulative_PN,cumulative_PA,cumulative_PV,GSD1,std);
        }
        else
            printf("\nResults have not been written to the external file.\n");
        getch();
    }
    /* Volumer fraction of different phases */
    void vol_frac_analysis(FILE *output,float d10_pw,float d10_pw_eq_wpw,float d10_eq_wpw,
        float d10_w2,float d10_w2_eq_wpw,float d31_pw,float d31_pw_eq_wpw,float d31_eq_wpw,
        float d31_w2,float d31_w2_eq_wpw,float p_vol_frac,float *pw_vol_frac,
        float *wpw_vol_frac,float *w2_vol_frac)

```

```

float w_vol_frac,wc_vol_frac;

printf("Volume fraction of various phases:\n");
printf("-----\n");
if (d10_pw == 0 || d31_pw == 0)
    printf("Make sure that calculation 1 has been done");
else if (d10_eq_wpw == 0 || d31_eq_wpw == 0)
    printf("Make sure that calculation 3 has been done");
else if (d10_w2 == 0 || d31_w2 == 0)
    printf("Make sure that calculation 4 has been done");
else if (d10_pw_eq_wpw == 0 || d31_pw_eq_wpw == 0)
    printf("Make sure that calculation 5 has been done");
else if (d10_w2_eq_wpw == 0 || d31_w2_eq_wpw == 0)
    printf("Make sure that calculation 6 has been done");
else
{
printf("fp = %5.2f\n", p_vol_frac);
printf("drop type\t d10 \t d31 \n");
printf("-----\t-----\t-----\n");
printf(" WPW' \t%5.2f\t%5.2f\n",d10_eq_wpw,d31_eq_wpw);
printf(" PW \t%5.2f\t%5.2f\n",d10_pw,d31_pw);
printf(" PW_WPW' \t%5.2f\t%5.2f\n",d10_pw_eq_wpw,d31_pw_eq_wpw);
printf(" W2 \t%5.2f\t%5.2f\n",d10_w2,d31_w2);
printf(" W2_wpw' \t%5.2f\t%5.2f\n",d10_w2_eq_wpw,d31_w2_eq_wpw);
getch();
*pw_vol_frac = p_vol_frac * ((d10_pw_eq_wpw - d10_eq_wpw)/(d10_pw - d10_eq_wpw)) *
    (d10_pw/d10_pw_eq_wpw) * pow((d31_pw/d31_pw_eq_wpw),2.00);
*wpw_vol_frac = p_vol_frac - *pw_vol_frac;
*w2_vol_frac = *wpw_vol_frac *
    ((d10_w2_eq_wpw - d10_eq_wpw)/(d10_w2 - d10_eq_wpw)) *
    (d10_w2/d10_w2_eq_wpw) * pow((d31_w2/d31_w2_eq_wpw),2.00);
w_vol_frac = 1 - p_vol_frac;
wc_vol_frac = w_vol_frac - *w2_vol_frac;
printf("fp = %5.2f;\tfw = %5.2f\n",p_vol_frac,w_vol_frac);
printf("fpw = %5.2f;\twpw = %5.2f\n",*pw_vol_frac,*wpw_vol_frac);
printf("fw2 = %5.2f;\tffc = %5.2f\n",*w2_vol_frac,wc_vol_frac);
getch();
printf("\nProgramme will continue to write all results to an external file.");
if (continue_or_not() == FALSE)
{
fprintf(output,"Volume fraction of various phases:\n");
fprintf(output,"\tdrop type\t d10 \t d31 \n");
fprintf(output,"\t WPW' \t%5.2f\t%5.2f\n",d10_eq_wpw,d31_eq_wpw);
fprintf(output,"\t PW \t%5.2f\t%5.2f\n",d10_pw,d31_pw);
fprintf(output,"\t PW_WPW' \t%5.2f\t%5.2f\n",d10_pw_eq_wpw,d31_pw_eq_wpw);
fprintf(output,"\t W2 \t%5.2f\t%5.2f\n",d10_w2,d31_w2);
fprintf(output,"\t W2_wpw' \t%5.2f\t%5.2f\n",d10_w2_eq_wpw,d31_w2_eq_wpw);
fprintf(output,"\n\tfp =\t%5.2f\tfw =\t%5.2f\n",p_vol_frac,w_vol_frac);
fprintf(output,"\tfpw =\t%5.2f\twpw =\t%5.2f\n",*pw_vol_frac,*wpw_vol_frac);
fprintf(output,"\tfw2 =\t%5.2f\tffc =\t%5.2f\n",*w2_vol_frac,wc_vol_frac);
printf("\nExternal file has been created successfully.\n");
}
else
printf("\nResults have not been written to the external file.\n");

```

```

    }
    getch();
}
/*Interfacial area/unit volume of various contacting surfaces*/
void interfacial_area(FILE *output,float pw_vol_frac,float wpw_vol_frac,float w2_vol_frac,
    float d32_pw,float d32_wpw,float d32_w2)
{
    float pw_area,wpw_area,w2_area,outer_p_w_area,total_area;

    if (d32_pw == 0)
        printf("Make sure that calculation 1 has been done!\n");
    else if (d32_wpw == 0)
        printf("Make sure that calculation 2 has been done!\n");
    else if (d32_w2 == 0)
        printf("Make sure that calculation 4 has been done!\n");
    else if (pw_vol_frac == 0 || wpw_vol_frac == 0 || w2_vol_frac == 0)
        printf("Make sure that calculation 9 has been done!\n");
    else
    {
        printf("Interfacial area/unit volume (SA) of various contacting surfaces:\n");
        printf("-----\n");
        pw_area = 6*pw_vol_frac/d32_pw;
        wpw_area = 6*wpw_vol_frac/d32_wpw;
        w2_area = 6*w2_vol_frac/d32_w2;
        outer_p_w_area = pw_area + wpw_area;
        total_area = pw_area + wpw_area + w2_area;
        printf("P/W surface\vol. frac.\td,32 \t SA \n");
        printf("-----\t-----\t----\t-----\n");
        printf(" PW/W \t %6.4f \t%5.2f\t%6.4f\n",pw_vol_frac,d32_pw,pw_area);
        printf("Outer WPW/W\t %6.4f \t%5.2f\t%6.4f\n",wpw_vol_frac,d32_wpw,wpw_area);
        printf("Inner WPW/W\t %6.4f \t%5.2f\t%6.4f\n",w2_vol_frac,d32_w2,w2_area);
        printf(" Outer P/W \t N/A \t N/A \t%6.4f\n",outer_p_w_area);
        printf(" Total P/W \t N/A \t N/A \t%6.4f\n",total_area);
        printf("\nProgramme will continue to write all results to an external file.");
        if (continue_or_not() == FALSE)
        {
            fprintf(output,"Interfacial area/unit volume (SA) of various ");
            fprintf(output,"contacting surfaces:\n");
            fprintf(output,"P/W surface\vol. frac.\td,32 \t SA \n");
            fprintf(output," PW/W \t %6.4f \t%5.2f\t%6.4f\n", pw_vol_frac,d32_pw,pw_area);
            fprintf(output,"Outer WPW/W\t %6.4f \t%5.2f\t%6.4f\n", wpw_vol_frac,
                d32_wpw,wpw_area);
            fprintf(output,"Inner WPW/W\t %6.4f \t%5.2f\t%6.4f\n", w2_vol_frac,d32_w2,w2_area);
            fprintf(output," Outer P/W \t Nil \t Nil \t%6.4f\n",outer_p_w_area);
            fprintf(output," Total P/W \t Nil \t Nil \t%6.4f\n",total_area);
            printf("\nExternal file has been created successfully.\n");
        }
        else
            printf("\nResults have not been written to the external file.\n");
    }
    getch();
}
/*Calculate volume of WPW and W2 occupies them*/
void WPW_W2_relationship(FILE *input,FILE *output,float oldnumber,float oldmax,float oldmin)
{

```

```

int confirmation,newnumber,number_of_bins,sum = 0,i;
float newmaximum,newminimum,bin_difference,lower_limit_of_bin[ARRAYS],j,
    upper_limit_of_bin[ARRAYS],average_diameter_of_bin[ARRAYS],drop_data,
    polymer_drop,water_drop,volume_of_wpw[ARRAYS] = {0},
    volume_of_w2[ARRAYS] = {0},volume_of_wpw_left[ARRAYS] = {0};

    /*Setting max,min,number of drops and bins for calculation*/
printf("Relationship of multiple polymer drops and the contained water");
printf(" drops\n");
printf("-----");
printf("-----\n");
display1(oldmax,oldmin,oldnumber);
confirmation = TRUE;
do
    {
        newmaximum = setting_new_maximum(oldmax);
        newminimum = setting_new_minimum(oldmin);
        while (newmaximum <= newminimum)
            {
                printf("\nMaximum diameter must be larger than the minimum diameter!!\n");
                printf("Please re-set the maximum and minimum drop diameter.\n");
                newmaximum = setting_new_maximum(oldmax);
                newminimum = setting_new_minimum(oldmin);
            }
        newnumber = drops_to_count(oldnumber);
        number_of_bins = bin_number();
display2(newmaximum,newminimum,newnumber,number_of_bins,oldmax,oldmin,oldnumber);
        confirmation = continue_or_not ();
    }
while (confirmation);

    /*Creating bins*/
if (bins_classification_method () == 1)
    {
        bin_difference = (newmaximum-newminimum)/number_of_bins;
        for (i=0; i<number_of_bins; i++)
            {
                lower_limit_of_bin[i] = newminimum + i*bin_difference;
                upper_limit_of_bin[i] = newminimum + (i+1)*bin_difference;
                average_diameter_of_bin[i] =(lower_limit_of_bin[i]+upper_limit_of_bin[i])/2;
            }
    }
else
    {
        j=0.0;
        for (i=0; i<number_of_bins; i++)
            {
                lower_limit_of_bin[i] = pow(newminimum,1-j/number_of_bins)*
                    pow(newmaximum,j/number_of_bins);
                upper_limit_of_bin[i] = pow(newminimum,1-(j+1)/number_of_bins)*
                    pow(newmaximum,(j+1)/number_of_bins);
                average_diameter_of_bin[i] = pow(lower_limit_of_bin[i]*
                    upper_limit_of_bin[i],0.5);
                j++;
            }
    }

```



```

                                                                    /*Locate data into bins*/
rewind(input);
fscanf(input,"%f",&drop_data);
while ((fscanf(input,"%f",&drop_data)!=EOF) && sum <= newnumber)
{
    polymer_drop=drop_data;
    if (polymer_drop != 0)
    {
        fscanf(input,"%f",&drop_data);
        water_drop=drop_data;
        if (water_drop != 0)                                /*Multiple WPW drops*/
        {
            i = comparison(polymer_drop,upper_limit_of_bin);
            volume_of_wpw[i] = volume_of_wpw[i] + (PI/6)*pow(polymer_drop,3.00);
            volume_of_w2[i] = volume_of_w2[i] + (PI/6)*pow(water_drop,3.00);
            sum++;
        }
    }
    else
    {
        fscanf(input,"%f",&drop_data);
        water_drop = drop_data;
        volume_of_w2[i] = volume_of_w2[i] + (PI/6)*pow(water_drop,3.00);
    }
}
if (water_drop != 0)
{
    volume_of_wpw[i] = volume_of_wpw[i] - (PI/6)*pow(polymer_drop,3.00);
    volume_of_w2[i] = volume_of_w2[i] - (PI/6)*pow(water_drop,3.00);
    if (sum == newnumber)
    {
        volume_of_wpw[i] = volume_of_wpw[i] + (PI/6)*pow(polymer_drop,3.00);
        volume_of_w2[i] = volume_of_w2[i] + (PI/6)*pow(water_drop,3.00);
    }
}
for (i=0; i<number_of_bins; i++)
{
    volume_of_wpw_left[i] = volume_of_wpw[i] - volume_of_w2[i];
    printf("%d\t%.2f\t%.2f\t%.2f\n",i+1,volume_of_wpw[i],volume_of_w2[i],
        volume_of_wpw_left[i]);
}
printf("\nProgramme will continue to write all results to an external file.");
if (continue_or_not() == FALSE)
{
    fprintf(output,"Relationship of WPW drops and the contained W2 drops\n");
    fprintf(output,"Bin\tLower\tUpper\tAvg.\tWPW\tW2\t(WPW)\n");
    fprintf(output,"no.\tlimit\tlimit\tdia.\tvol.\tvol.\tvol.\n");
    fprintf(output,"i\tDL,i\tDH,i\tDavg,i\tVwpw\tVw2\tV(wpw)\n");
    for (i=0; i<number_of_bins; i++)
        fprintf(output,"%d\t%.2f\t%.2f\t%.2f\t%.2f\t%.2f\t%.2f\n",i+1,
            lower_limit_of_bin[i],upper_limit_of_bin[i],
            average_diameter_of_bin[i],volume_of_wpw[i],volume_of_w2[i],
            volume_of_wpw_left[i]);
    printf("\nExternal file has been created successfully.\n");
}

```

```

else
    printf("\nResults have not been written to the external file.\n");
getch();
}
    
```

AIII.4 Analysis report from Malvern Mastersizer

A typical analysis report from Malvern Mastersizer is as follows:

